IN TWO SECTIONS—SECTION ONE

Transactions

of the

ASME

JANUARY, 1950

VOL. 72, NO. 1

Transactions

of The American Society of Mechanical Engineers

Published on the tenth of every month, except March, June, September, and December

---

Published monthly by The American Society of Mechanical Engineers. Publication office at 20th and Northampton Streets, Easton, Pa. The editorial department is located at the headquarters of the Society, 29 West Thirty-Ninth Street, New York 18, N. Y. Cable address, "Dynamic," New York. Price $1.50 a copy, $12.00 a year for Transactions and the *Journal of Applied Mechanics;* to members and affiliates, $1.00 a copy, $6.00 a year. Changes of address must be received at Society headquarters three weeks before they are to be effective on the mailing list. Please send old as well as new address.... By-Law: The Society shall not be responsible for statements or opinions advanced in papers or ... printed in its publications (B13, Par. 4).... Entered as second-class matter March 2, 1928, at the Post Office at Easton, Pa., under the Act of August 24, 1912....

Solid-Type Journal Bearings in High-Speed Freight Service

By E. S. PEARCE,[1] R. J. SHOEMAKER,[2] and I. E. COX[3]

This paper encompasses the operating conditions involved in the selection of the bearing equipment used in high-speed freight service. Consideration is given to the performance of the solid-type bearing, as well as the potentials of future development, and the superior adaptability of the solid-type bearing to the economics of railroad operation.

Introduction

The term "high-speed freight" implies the shortening of elapsed time between terminals. This would require higher top speeds and more rapid acceleration.

The public has been led to picture freight equipment operating continuously at sustained speeds of 50, 60, 80, and 100 mph. To achieve this result, it would be necessary to have less gross tons per train; less resistance per train; or more power per train; or a combination of all three.

In the final analysis, high-speed freight must be obtained within the practical limits of cost and over-all economies of railroad operation. If high-speed freight is not to be restricted as to interchange, special equipment, and special movements, then all freight equipment must be equally adaptable to high-speed operation as and when the occasion arises.

For high-speed freight, bearings are involved in the elements of the following:

(*a*) Less resistance per train.
(*b*) Dependability and safety.
(*c*) Economy in first cost, maintenance, and weight.

There are listed, for freight-train service operation, 1,902,265 cars under railroad ownership, and 263,747 cars under private-line ownership.[4] There are, therefore, in excess of 17,000,000 journals with companionate bearings in operation today. The investment in these journals and bearings, and the operation and maintenance of them are the common responsibility of all interchanging rolling-stock operators.

Six railroads have been selected as representing a cross section of certain operating conditions upon which an analysis of the over-all bearing problem for high-speed freight must be predicated. These six roads represent an operating ownership of 25 per cent of all freight equipment. Basic data are given in Table 1[5] for the year 1947.

TABLE 1 AVERAGE NUMBER OF CARS IN EACH 100 CARS OPERATED BY EACH RESPECTIVE ROAD WHICH ARE OF OWNERSHIP OTHER THAN ITS OWN[a]

Road	No. foreign cars per 100 cars operated
A	55.2
B	68.7
C	72.8
D	83.8
E	72.2
F	69.0

The basic elements of facility and economy of maintenance, repair, and replacement must be recognized as the first requirement of the bearing equipment.

Gross tons per train in high-speed freight will be made up in units of weights given in Table 2.[5] It is the rolling resistance of units of these weights that will determine train resistance. It is units of these weights that will determine the required bearing-load carrying capacity. It is under such bearing loads at the contemplated operating speeds, that bearing resistance in pounds per ton, in relation to total resistance, must be determined as a relative factor in high-speed freight.

TABLE 2 AVERAGE GROSS TONS PER LOADED CAR

Road	Gross tons per car: Average	Minimum	Maximum
A	58.4	57.0	59.1
B	55.6	54.9	57.8
C	55.5	54.1	56.3
D	52.8	52.2	54.0
E	53.7	52.7	54.2
F	69.7	69.0	70.4

Table 3[5] gives the distance that the average car on line, which was in movement or subject to movement, traveled per day. It is only in movement that the function of the journal bearing assumes any relative and significant importance. It is in this distance that the functional advantages of the bearing are utilized and the investment justified.

TABLE 3 AVERAGE DISTANCE IN MILES PER DAY OF ALL CARS IN MOVEMENT OR SUBJECT TO MOVEMENT

Road	Distance per day, miles: Average	Minimum	Maximum
A	34.5	32.1	37.2
B	30.0	26.9	33.2
C	40.6	37.2	44.0
D	61.9	56.2	67.6
E	47.7	42.1	52.3
F	48.4	39.1	59.6

Table 4 reflects the factor of dependability under the operating conditions as obtained in 1947.

TABLE 4 AVERAGE JOURNAL BEARINGS IN SERVICE PER DAY ON ALL CARS IN MOVEMENT OR SUBJECT TO MOVEMENT PER BEARING FAILURE

Road	Number of bearings for one failure: Yearly avg	Minimum	Maximum
A	37432	20288	113480
B	86648	48464	204984
C	32304	15992	97104
D	19424	9376	55304
E	33624	17576	69856
F	45560	20968	147072

[1] President, Railway Service and Supply Corporation, Indianapolis, Ind. Fellow ASME.
[2] Chief Engineer, Magnus Metal Division, National Lead Company, Chicago, Ill. Fellow ASME.
[3] Vice-President in Charge of Engineering, National Bearing Division, American Brake Shoe Company, St. Louis, Mo.
[4] "The Pocket List," Third Quarter 1948, published by The Railway Equipment and Publication Company, New York, N. Y.
[5] "Freight Operating Statistics of Large Steam Railways," data compiled monthly by the Bureau of Transport Economic and Statistics, Interstate Commerce Commission.

Contributed by the Railroad Division and presented at the Annual Meeting, New York, N. Y., November 27–December 2, 1948, of The American Society of Mechanical Engineers.
Note: The authors constitute the Research Advisory Committee for Railroad Journal Bearing Manufacturers.

Paper No. 48—A-128.

A minimum average of one failure for 9376 bearings to a maximum of one failure for 204,984 bearings is equivalent to one failure for 526,931 bearing-miles as a minimum to 6,805,469 bearing-miles as a maximum. Since this reflects the actual performance of the solid unit-type bearing under existing operating conditions, this measure of dependability is an outstanding factor to consider.

Unit Solid-Type-Bearing Tests

To determine the potential possibilities of the unit solid-type bearing under the more accelerated rate of operation of high-speed freight, it is necessary to turn to the laboratory test plant. Such tests are required since there are no road-test data available; nor is there ever likely to be, due to the inability to separate journal resistance from other elements which go to make up total car resistance. Likewise, extended operation under high speeds, effect of temperature, and other factors to give controlled conditions so that journal-bearing operation alone may be evaluated, are available only in the laboratory test plant.

In evaluating laboratory bearing-performance data, it must be recognized that laboratory operation is purposely "controlled accelerated service experience." Failure is the objective in order that the cause and effect may be determined and improvement devised and evaluated. A construction which may operate successfully on the railroad may fail under the adverse conditions in the test plant. These adverse test-plant factors are as follows:

1 Laboratory tests are conducted in still air, as against a high-velocity flow of air around journal-box contained parts in service.

2 The load on a journal bearing in a laboratory test is a maximum "dead" static load; whereas, in service, the load is "alive" and varying.

3 In a laboratory test there is no benefit of lateral motion of the axle in distribution of lubricant between the journal and the bearing; whereas, in actual service, the axle is constantly moving laterally, enhancing distribution of lubricant.

4 Speeds can be high and for extended periods of time not obtainable in practice. Rates of acceleration and deceleration, to and from high speeds, are attained that are not obtainable in practice.

Fig. 1 represents the data obtained with a $5^1/_2$-in. × 10-in. conventional solid-type journal-box assembly operated under the foregoing conditions, augmented by subzero temperatures. The total bearing load was 16,375 lb, equivalent to a 70-ton car. The bearing, being nonfitted to the journal, had a crown area of only 22.5 sq in. The resulting unit loading was 735 psi. With a full or fitted bearing area of 45.7 sq in., the unit loading would have been reduced to 358 psi. The operation was one of constant speed at 50 mph for 66 hr. The run started in an atmosphere of +80 F, with temperature reducing, as the run progressed, to a minimum of —12 F. The operation was equivalent to a continuous run of 3300 miles. Ambient temperature, journal temperature, and journal resistance in pounds per ton are shown in Fig. 1.

To evaluate these results properly, some comparison should be made with total car resistance under like conditions of load, speed, and ambient temperature. This is true also for bearing resistance only of other types of bearings, such as those of multiple-unit design, of which type the roller bearing is a sample. However, such data apparently have not been developed.

As some measure of relative comparison, it is interesting to note that the distance of 3300 miles is 3 times the distance from New York to Chicago. The speed of 50 mph is 10 miles under the average speed of the 20th Century Limited.

Fig. 2 represents data obtained from tests using the same journal-box assembly and loading as used in the test covered in

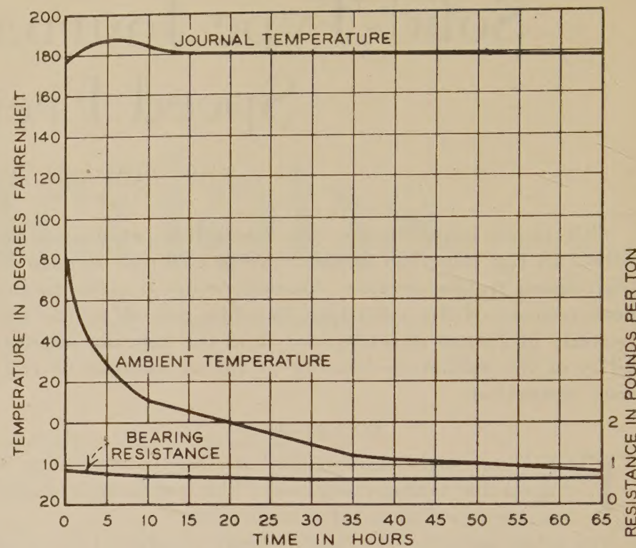

Fig. 1 Test Data With $5^1/_2$-In. × 10-In. Conventional Solid-Type Journal-Box Assembly

Fig. 1, but operating in an atmosphere of —14 F to —10 F at speeds of 20, 60, 80, and 100 mph. On the speed-cycle curve are reflected acceleration, sustained speeds, deceleration, reversal of movement, ambient temperature, journal temperature, and resistance in pounds per ton.

Significance of Journal Resistance

It is in order to explore the potential significance of journal resistance in high-speed freight. For this purpose we have such basic data as shown in Figs. 1 and 2; and for available drawbar pull, motive power of the characteristics shown in Fig. 3.[6] It is assumed that operation will take place on tangent level track with trains made up of 70-ton cars, at speeds of 50 and 80 mph.

Total car resistance for 70-ton cars at 80 mph is 10.5 lb per ton; at 50 mph, 6.7 lb per ton.[7] Journal resistance only at 50 mph, Fig. 2, is 0.71 lb per ton. From Fig. 3, journal resistance after accelerating to 80 mph is 0.96 and 0.86 lb per ton. After running at 80 mph, it is 0.69 and 0.73 lb per ton. The average of these is 0.81 lb per ton. Drawbar pull of the S-1 locomotive at 50 mph is 36,000 lb and at 80 mph, 22,000 lb.

With bearing resistance entirely eliminated, the resistance of the 70-ton car at 50 mph is 5.99 lb per ton, and at 80 mph, 9.69 lb per ton on tangent level track. At 50 mph the available drawbar pull of the S-1 locomotive is equivalent to 86 cars of 70 tons each per train, and at 80 mph 32 cars of 70 tons each per train.

Speed has been increased 60 per cent to achieve high-speed freight at a sacrifice of 63.5 per cent in the number of cars per train for factors other than bearing resistance.

At 80 mph the bearing resistance for a train of 70-ton cars if entirely eliminated is the difference between a train of 30 cars as compared to 32 cars.

In freight service, under the prevailing conditions of railroad operation in the last 20 years, with the unit solid-type bearing, the average freight car has increased its average daily production as shown in Table 5.

Transportation service by the railroads, as required in this

[6] "Railroad Motive Power," by P. W. Kiefer, published by Steam Locomotive Research Institute, Inc., New York, N. Y., June, 1947, chart B, p. 52.

[7] "The Steam Locomotive," by R. P. Johnson, Simmons-Boardman Publishing Corporation, New York, N. Y., 1942, p. 188, table 31.

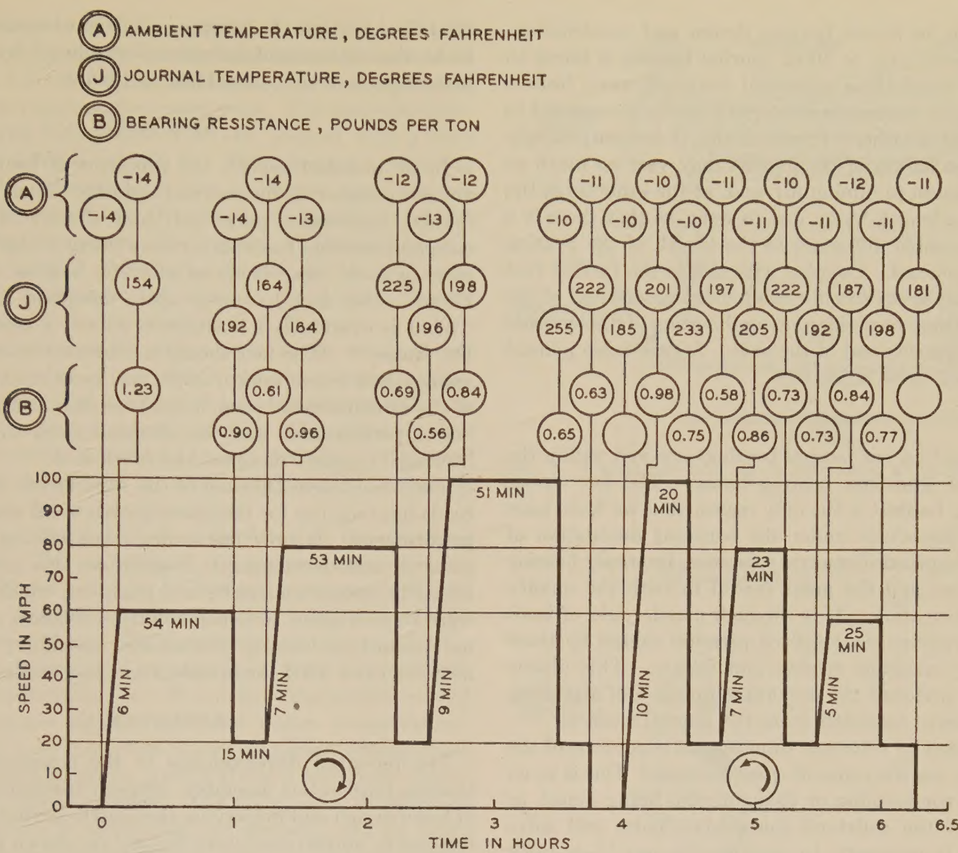

Fig. 2 Test Data With $5^1/_2$-In. × 10-In. Conventional Solid-Type Journal-Box Assembly Operating in Atmosphere of —14 F to —10 F

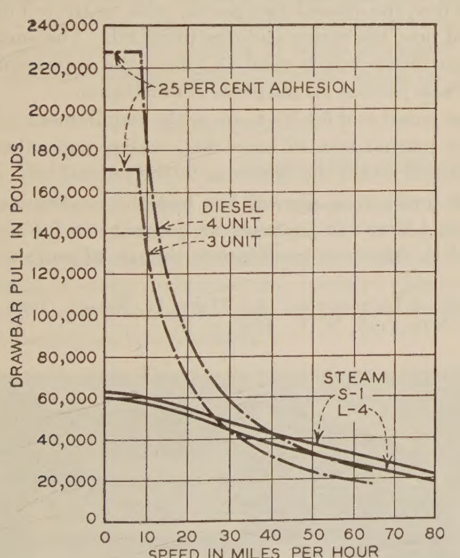

Fig. 3 Power Characteristic Curves for Reciprocating-Steam and Diesel-Electric Freight Locomotives

country, makes necessary the highest degree of unrestricted movement of equipment over the railroad mileage of the continent regardless of territorial extent and ownership of any one railroad. Obviously, uniform and universal facility of maintenance is a basic necessity; hence there has developed a high degree of standardization and interchange of parts. This imposes severe limitations on improvements in design, restricting changes to those not incompatible with maintaining standards.

TABLE 5 TWENTY-YEAR INCREASE IN DAILY FREIGHT-CAR PRODUCTION

	1926	1946	Per cent increase
Average car miles per day[a]	32.6	45.2	38.6
Average freight-car capacity, tons[b]	45.1	51.3	13.8
Average net ton-miles per car per day[a]	569	948	66.5

[a] "Year Book of Railroad Information," Eastern Railroad Presidents Conference, Committee of Public Relations, 1948, p. 72.
[b] Ibid., p. 12.

It is recognized that improvements in design, materials, and practice relating to the unit solid-type-journal bearing-box assembly, can be made within the confines of the foregoing limitations of standardization.

The Journal Box

There is general recognition of the necessity for a properly sealed and vented journal box to keep dirt, water, and other foreign matter out and to retain the lubricant in the journal box. Likewise, it is equally evident that lateral, in its ultimate reaction on lading and wear on mechanical parts, must be flexibly controlled and not rigidly opposed. These objectives are obtainable.

The Axle Journal

Journals are finished by roller-burnishing, a practice which is scarcely conducive to a geometrically perfect surface. It requires considerable bearing-lining life and many miles of running to lap a rolled car journal to a satisfactory bearing surface. The permissible tolerances of journals, both diametrically and axially, are not only limiting factors in performance, but greatly

restrict the latitude in future bearing design and construction.

To illustrate, the $5^1/_2$-in. × 10-in. journal bearing is bored to $5\ ^9/_{16}$-in., but it is applied to a journal that will vary from a minimum of 5 in. to a maximum of $5^1/_2$ in.; and it is expected to perform equally well on either. Paradoxically, it does surprisingly well. Likewise, the length of the journal may vary as much as $^{11}/_{16}$ in. from maximum to minimum; and, at the same time, the bearing can vary in length $^3/_8$ in. due to wear, so that there is a total of $1^1/_{16}$ in. possible difference in the length of the bearing and length of the journal. Coupled with this is the further fact that these variations apply to only one journal on one end of the axle, whereas there may be a different combination of dimensional tolerances on the opposite end of the axle. A renewable journal sleeve will overcome these objections.

Bearings

The loads imposed on car journal bearings are well within the safe load limits of lead-base bearing lining. The low elastic modulus of bearing babbitt is the only reason that we have been able to operate successfully under the constant fluctuation of alignment, the widespread diametral tolerance, improper bearing and journal surfaces, and the great spread in both the quality and quantity of lubrication. It is the high plastic yield of lead-base lining which relieves the localized pressure caused by these conditions, thereby avoiding seizure and failure. This plastic condition of lining performs the important function of absorbing and removing abrasive materials from the journal surface.

Shock loads, caused by improper dimensional conditions of the wedge and bearing, are the cause of spread linings. This is in no sense a reason for condemning or changing the lining metal, as closer tolerances of the collateral journal-box parts will solve this problem. It is necessary to continue to use $^1/_4$-in-thick bearing linings, as this dimension is controlled by the journal diametral tolerance. This journal-bearing clearance has made necessary the design of the present bearing designated as the "no clearance type." The present journal collar fixes the bearing arc at approximately 120 deg.

In considering improvements in design and materials of the present unit solid-type bearing per se, the low but widely fluctuating incidence of failure, shown in Table 4, presents an economic element for consideration. There is the question as to the relative improvement in performance that would accrue through proper maintenance practices, as compared to improved design and materials, although it is obvious that combination of both is the ultimate goal.

The economic value of relatively simple facilities of repair and maintenance of the solid-type bearing and journal-box assembly, wheels, and trucks must be recognized in considering improvements in design and materials. Likewise, changes in design and/or materials must be consistent with the economies of the present numerous sources of bearing supply with the added element of protection in time of national emergencies when railroad transportation is the backbone of defense.

The solid-type-bearing journal-box assembly, by virtue of its extreme simplicity, is victimized by unsubstantiated opinions and deprived of the benefits of facts. As an example, the derogatory misnomer, "friction bearing," established by advertising is now popularly accepted as descriptive of the standard AAR car journal bearing. The use of the term "friction type," applying to solid bearings, and the term "antifriction" to roller and ball bearings is erroneous and misleading, implying that friction is created in the operation of the solid type, and no friction in the operation of the roller and ball-bearing types. This is far from the true fact. Nonperformance in the proper functioning of any component parts of the journal-box assembly and truck manifests itself ultimately in a bearing failure. This results in promoting the false idea that the bearing is deficient because it fails to overcome the detrimental influences introduced by the other component parts of the journal box and truck.

Conclusion

In its broadest aspect, the problems of bearing performance are not peculiar to the railroad industry alone. A co-ordinated, factual, aggressive, persistent, and effective approach to their economic solution has been far less evident in the railroad industry than in such other fields as aircraft, marine, automotive, and Diesel. This fact has been aptly described as an example of "What is everybody's business is nobody's business." Quoting Dr. Hersey:[8] "The fact should not be overlooked, that in many applications where improvement has been reported as the result of the substitution of some novel type of bearing, equally good or better performance may be obtained from the simple oil-film bearing if properly designed and lubricated."

The Mechanical Division of the Association of American Railroads has facilities for the investigation of all elements of bearing performance. It now has under consideration an all-inclusive research and development program on this subject. Developments in design, materials, and practices, which are directed toward improvement in dependability, economy, and safety of the unit solid-type-bearing journal-box assembly, have been submitted to the AAR for investigation and evaluation.

APPENDIX A

The potential developments in the conventional solid-type-bearing journal-box assembly, without disturbing the standards of basic design and preserving the most essential facility of maintenance in unrestricted interchange, are shown by the composite illustration, Fig. 4.

The conventional journal box is cut away in section showing the axle journal, packing, bearing, and wedge, on the right or rear of the box, the oil-seal dust guard; and, on the left or front of the journal box, the water and dustproof lid. The small mirror in the front of the box is used to reflect the appearance of the end of the axle journal for purposes of illustration.

The dust guard and lid are to meet the requirement for a properly sealed journal box to keep dirt, water, and other foreign matter out and retain the lubricant in the journal box.

The axle journal, as shown, has had the conventional collar removed, and shows in place on the journal one form of sleeve. The use of the sleeve is to eliminate the use of journals varying

[8] "Theory of Lubrication," by Mayo D. Hersey, John Wiley & Sons, Inc., New York, N. Y., 1936, p. 13.

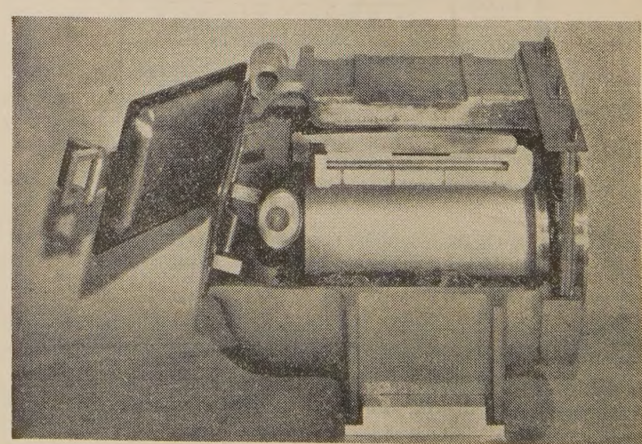

Fig. 4 Solid-Type-Bearing Journal-Box Assembly

$^1/_2$ in. in diam; and, as in the case of the illustration, a $5^1/_2$-in. × 10-in. journal, maintaining the diameter at $5^1/_2$ in. instead of a variation from 5 in. to $5^1/_2$ in. occasioned by the necessity for turning journals to repair surface conditions. The sleeve is $^1/_8$-in. straight-wall tubing fitting over a $5^1/_4$-in. journal with a very light shrink fit of 0.005 in. at 380 F. This provides a retaining force of 60,000 lb. Maintenance of axle-journal surface is accomplished by the renewal of the sleeve, no machining of the axle journal being necessary. To remove a damaged sleeve, simply split with a chisel and apply a new sleeve by heating to 380 F and rapidly slipping on the journal. The journal bearing is that described in a previous paper by E. S. Pearce.[9]

The journal-box wedge is the conventional wedge with a downwardly projecting ledge or lug welded to the existing wedge. This lug is to replace the function of the axle-journal collar to retain the journal bearing in place laterally. This eliminates the troublesome limitations introduced by the presence of the conventional journal collar, that is, service difficulties, as well as those pertaining to future bearing design.

The reflection of the end of the axle shows in the centering hole a plastic plug. This plug is made of a temperature-responsive material, whose liquid point and softening point are identical. The material can be made to respond within 2 deg F to any desired temperature. When the predetermined temperature is reached, the plug liquefies and by centrifugal force is spread over the end of the axles marking it a yellow color. The predetermined temperature is known as the "potential failure temperature." This temperature is an indication before a journal heating exists that attention should be given; and, if given, a road delay due to a journal heating will be avoided. The objective is to eliminate the personal equation in inspecting and servicing journal boxes by indicating positively those that need attention and, conversely, by the absence of the indication those that do not need attention.

Journal-box packing is of conventional material (waste and oil), applied, however, in the form of machine-made pads of oil-saturated waste. This insures uniform packing of boxes and prevents displacement of the packing in whole or in part from the normal position in contact with the bottom arc of the journal.

APPENDIX B

National Bearing Division—American Brake Shoe Company

The renewable axle sleeve and the compound bore bearing as hereinafter described, have been submitted to the Mechanical Division of the Association of American Railroads as two of our developments in design, material, and practice directed toward improvement in dependability, economy, and safety of the unit solid-type bearing and its assembly.

The Renewable Axle Sleeve. A renewable axle sleeve has been developed after several years of study and investigation, as illustrated in Figs. 5 and 6.

It consists of a rigid type of bushing made of high-carbon low-alloy steel, heat-treated to 480–520 Bhn, with ground journal and dust-guard-fit surfaces. This sleeve bushing is provided with a ground-finished taper bore $^1/_4$ in. to the foot, and is arranged to be locked in place by a nut screwed on the end of the axle.

Axle preparation for the use of this sleeve consists of turning either new or worn axles with a taper to fit the sleeve bore, and threading the end of the axle for the axle nut.

The renewable axle sleeve should be induction-heated or immersion-heated in oil to 200 F, and assembled on the axle, tightening the axle nut immediately so the sleeve will have a shrink fit in place.

[9] "Locomotive and Car Journal Lubrication," by E. S. Pearce, Trans. ASME, vol. 58, 1936, pp. 37–45.

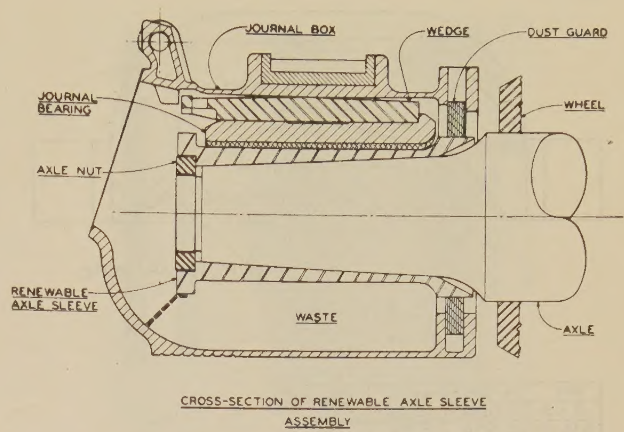

Fig. 5 Cross Section of Renewable Axle-Sleeve Assembly

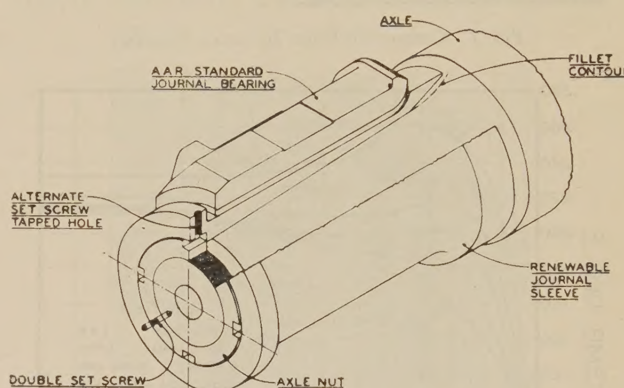

Fig. 6 Phantom View of Renewable Axle-Sleeve Assembly

It can be removed readily by use of a hydraulic jack mounted in a stirrup with lugs to fit over the renewable axle sleeve collar so the jacking pressure can be applied against the end of the axle. The axle nut should be unscrewed only a turn or two so it will act as an arrester when the shrink fit is broken. A thin coating of white lead and oil swabbed on the axle before driving the heated sleeve in place will prevent galling of the sleeve on the axle.

The advantages claimed for the renewable bearing-axle sleeve are as follows:

1 The provision of a hardened and accurately ground journal, journal collar, and journal fillet will eliminate excessive wear and enable the use of full-size journals throughout axle life.

2 The use of the renewable axle sleeve will enable the continued use of worn axles that would otherwise have to be scrapped.

3 Axle life will be limited only by fatigue defects that are detected by magnafluxing.

4 By maintenance of proper journal size, the tendency of forming waste grabs will be reduced greatly because of the reduction in clearance between the bearing and the journal, adjacent to the contact area.

5 Both starting and running friction will be reduced due to improved fit between axle and journal, and by better and harder journal surface.

6 Bearing failures due to spread and distorted lining will be reduced since, with full-sized journal, component contained parts of the journal box will not be displaced from their intended position. This displacement of parts which occurs on undersize journal, also causes interruption to lubrication and packing down of waste away from the journal, two troubles that will be greatly reduced.

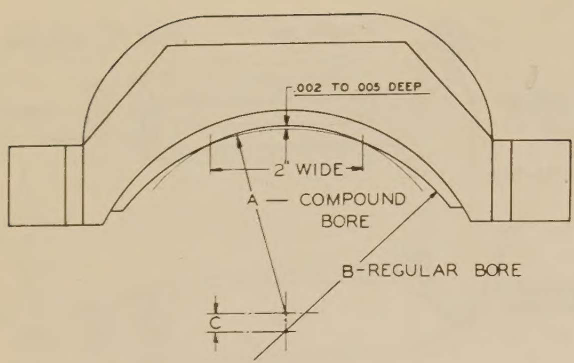

SIZE	A-DIA.	B-DIA.	C
5 x 9	5.004	5 1/16	1/32
5½ x 10	5.504	5 9/16	1/32
6 x 11	6.004	6 1/16	1/32
6½ x 12	6.504	6 9/16	1/32

Fig. 7 Compound-Bore Journal Bearing

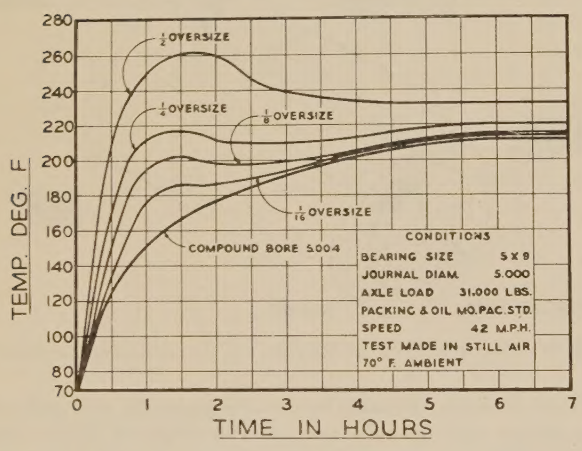

Fig. 8 Time-Temperature Curve for AAR Journal Bearing as Affected by Variation Between Journal Diameter and Bearing Bore

Compound-Bore Journal Bearing. The compound-bore journal bearing has a secondary bore superimposed on the standard or primary bore, providing a precision fit 0.004 in. in diam over the nominal axle diameter approximately 2 in. wide, parallel to and in the center of the standard bore, as shown in Fig. 7.

The compound-bore bearing provides the equivalent to precision hand-scraped fit on a full-size-axle. Where it is applied on undersized axles there is much less conformation of bearing required in initial operation. Comparative breaks in temperature characteristics are shown in Fig. 8.

The advantages claimed for the compound-bore car journal bearing are:

1 Possibility of waste grabs and lint burns is decreased during initial operation, which are invited by larger clearances adjacent to contact area between journal and a standard bore bearing.

2 Due to reduced conformation of bearing lining to journal surface, there is a reduction of pulling and cracking of the babbitt lining.

3 Hot boxes are reduced by the reduction of both the severity and duration of high-temperature "break-in" period experienced initially on all bearings applied.

4 Lubrication is improved by insurance of a larger initial contact area under load, reducing the initial fluid-film pressure per unit of area. Frequently, initial fluid-film pressures combined with high initial operating temperature, and relatively small initial contact areas causes oil film to fail, and in extreme cases fluid-film cannot even be established.

The compound-bore journal bearing is now in use by several leading railroads in both freight and passenger service.

The compound-bore journal bearing has been submitted to the AAR, requesting its approval as an alternate standard for interchange use and is on the test program. However, there will be no objection to its interchange use pending this approval since in no way does it conflict with specifications now in force, under which hand scraping of bearing bore is condoned and practiced.

APPENDIX C

Magnus Metal Corporation

Some of the improvements in designs and materials developed and recommended by the Magnus Metal Corporation in connection with the service of solid-type bearings and their assemblies in high-speed freight service, are herein described. These improved products have been developed as a result of many years research and they have a background of millions of miles of successful service in railroad operation.

Satco Bearing Metal. Satco bearing metal has been used very successfully for many years past as a lining for various types of railway bearings in place of lead and tin-base babbitts, antimonial lead, etc. This alloy was made an alternate for babbitt metal in linings of freight-car bearings by the Association of American Railroads.[10]

Satco metal is a lead-base alloy composed of approximately 95–98 per cent lead with balance calcium and other hardeners. The composition of the alloy is varied according to the service in which the bearings are used. One of the mixtures used by the railroads as a general-purpose bearing metal contains approximately 97–98 per cent lead, with balance calcium and other hardeners.

Graphs showing the physical properties of Satco metal at normal and elevated temperatures, as compared with AAR lead-base babbitt, tin-base babbitt, and antimonial lead are shown in Figs. 9 and 10.

Satco metal has a melting point approximately 150 deg F higher than that of babbitt metals with a correspondingly higher hardness at elevated temperatures. These are very important advantages as they are a measure of the heat resistance to spalling and melting of the bearing lining in service. This is particularly important in protecting the bearing against the effects of "waste grabs." Satco-lined bearings are said to function perfectly at temperatures where babbitt-lined bearings fail by melting.

Satco can be bonded firmly to brass, bronze, steel, and aluminum, the bond strength between lining and brass being 20–40 per cent greater than that obtained with babbitt-lined material. Consequently, bearings lined with Satco metal are more resistant to cracking and loosening of the lining and resist oil penetration to a much greater degree than with babbitt-lined bearings.

Illustrations showing some of the various types of bearings lined with Satco metal used by the railroads for passenger cars and locomotives are shown in Figs. 11, 12, and 13.

"Twinplex" Satco-Lined Alarm Journal Bearings. The "Twinplex" Satco-lined alarm journal bearing shown in Fig. 11 is an AAR emergency-type bearing equipped with two brass tubes, each having a small orifice sealed with fusible metal which melts at 350 F. If the temperature of the bearing reaches that point, one of the tubes releases a distinctive and penetrating odor and the other a large volume of dense white smoke. The discharge continues until both tubes are empty, which requires

[10] Circular DV-905, May 15, 1937.

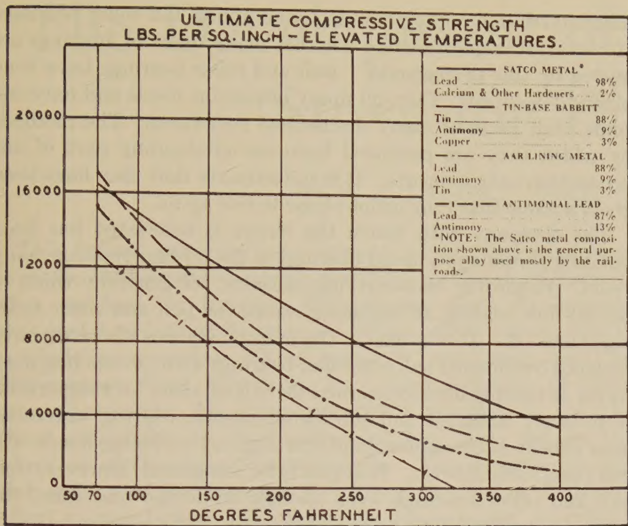

Fig. 9

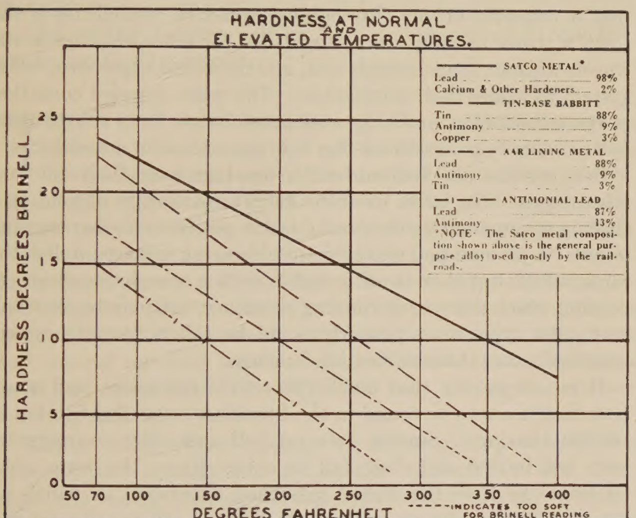

Fig. 10

about 8 min. This device has had wide application for several years past on main-line high-speed passenger cars and locomotives of an important Eastern trunk line railroad. Experience has shown that the odor can be detected in any car in a passenger train, regardless of whether it is a tightly sealed, air-conditioned car or not. This odor is noticeable in the train for from 4 to 8 min.

"Magsafe" Satco-Lined Journal Bearing. The Magsafe Satco-lined journal bearing shown in Fig. 12 is a standard AAR type bearing equipped with a special device to prevent lint wipers and "waste grabs."

This device consists of two T-section brass comb strips one on either side of the crown of the bearing, positioned in longitudinal grooves milled in the brass. In running position, the comb strips drop down of their own weight and contact the journal at all times, regardless of whether the journal is new or turned down to the limit of wear, thus preventing lint and strands of waste from climbing the journal.

The comb strips are stopped off 1 in. from the hub end of the bearing to prevent end leakage of oil and to maintain full bearing contact at the hub end of the wheel.

The comb and slots are T-shaped to prevent combs from falling out of the bearing when being applied or removed from the jour-

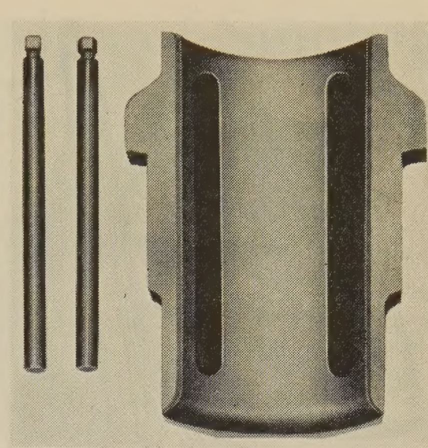

Fig. 11 Satco-Lined "Twinplex" Alarm Journal Bearing

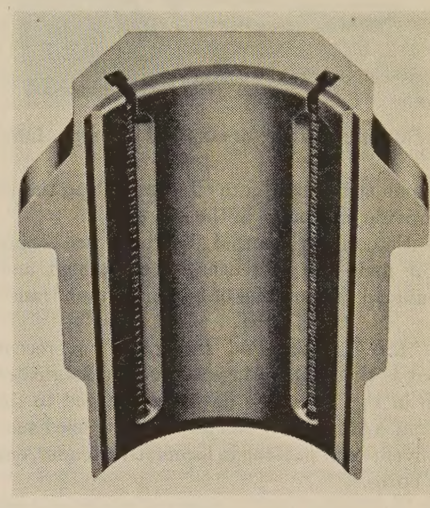

Fig. 12 "Magsafe" Satco-Lined Journal Bearing

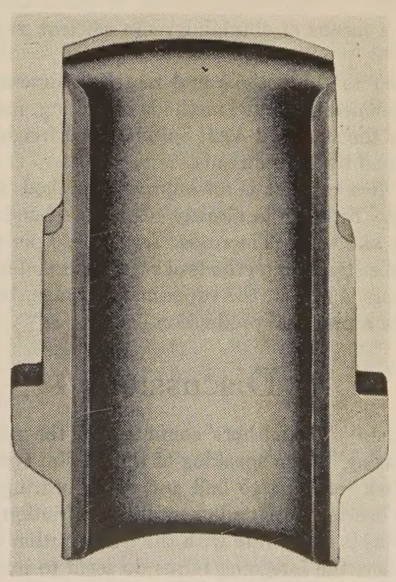

Fig. 13 Standard AAR Prewar or Emergency Satco-Lined Journal Bearing

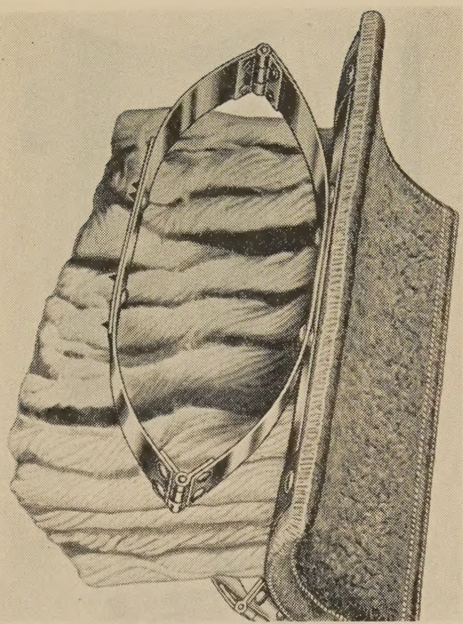

Fig. 14 Magnus "R.B." Spring-Pad Journal Lubricator

nal. The comb strips distribute oil evenly along the journal, and they also provide oil storage in the bearing.

Magsafe Satco-lined journal bearings are being used as standard for main-line passenger-car equipment and regularly assigned Pullman cars on one of our important transcontinental railroads.

Magnus "R.B." Spring-Pad Lubricator. A recent Magnus development is the R.B. spring-pad journal lubricator shown in photograph in Fig. 14. This device is adapted to the standard round-bottom AAR type of box and is being used successfully in place of conventional packing in locomotive-tender, engine-truck, and trailer boxes.

The R.B. lubricator pad is inserted easily or removed without being necessary to jack up the box or remove the bearing and wedge. It is recommended for use in journal boxes of freight-car equipment in high-speed service in place of conventional packing, as a means of obtaining more efficient and dependable lubrication.

In addition to the designs and materials described, Magnus has also developed improved methods of casting, machining, and broaching of the standard AAR babbitt-lined freight-car bearing now being used by the railroads.

One new development is an improved method of casting the lining metal. From tests already made, the bond strength between lining and brass is increased from 20–40 per cent, as compared with the standard methods of casting heretofore used. This special process is still in the experimental stage, but it is being developed on a practical production basis.

Discussion

S. J. Needs.[11] The authors' comments on the use of the terms "friction bearing" when speaking of the oil-film type, and "antifriction" when referring to ball and roller bearings, are indeed timely. All bearings are fundamentally antifriction, since one of their functions is to operate with the least friction possible; but taken together, the foregoing terms do seem to imply that some inherent friction miracle is to be found in ball and roller bearings. However, it is questionable whether many users of bearings are misled by this propaganda. Ball and roller bearings have been highly developed. They fill many important needs and have become vital parts of many mechanical structures. The methods by which they are produced form an outstanding part of our production achievements. It is unfortunate that they have been given a name that they cannot hope to live up to.

The company with which the writer is associated has been building thrust and journal bearings of the oil-film type for many years. Regarding load-carrying capacity, we generally think of the oil-film bearing as beginning where the ball and roller bearings leave off. This is seen in the many instances where we have replaced overloaded ball and roller bearings with oil-film bearings. As far as bearing life is concerned there is no room for comparison. A properly designed and lubricated oil-film bearing suffers no wear except at the moments of starting and stopping, hence will last practically forever. It is generally recognized, however, that ball and roller bearings, even though lubricated and cared for properly, are limited by an uncertain span of life.

There are instances where the two types are not in competition and fall into well-defined fields. For example it is almost certain that a majority of our automobiles would be stalled along the roads if sleeve bearings were substituted for roller bearings in the wheels without some complicated, and doubtless expensive, oiling system to insure their lubrication. The same crippled condition of the automobiles probably would also follow from substituting ball or roller bearings for oil-film bearings on motor crankshafts.

Both oil-film and ball and roller bearings have their inherent advantages. The latter have the definite advantage of holding a shaft in approximately the same relative position whether running or not. A pivoted-pad oil-film journal bearing will accomplish the same result, but that is not possible with a complete cylindrical bearing which must have running clearance. It may be that ball and roller types more properly could be called "anticlearance" bearings rather than antifriction bearings.

It is noteworthy that much theoretical treatment and many test results are to be found in the literature regarding friction in oil-film bearings. Similar data on ball and roller bearings are very few indeed and these fail to substantiate the term antifriction. In 1945 the writer published a paper,[12] in which an attempt was made to analyze friction in railway-car journal bearings of the oil-film type. Some tests were run later with roller bearings under similar conditions. These studies were sponsored by the Association of American Railroads. If the data on roller bearings were also published, they might throw some light on the relative frictions of the two types, and the quantitative value of the term antifriction could then be established for railway-car roller bearings.

Authors' Closure

To whatever extent or particular the operation of the conventional solid-type journal-box assembly per se may be factually deficient in meeting present-day requirements, it is evident that:

1 Economic improvement does not lie in replacement or substitution of the unit as a whole.

2 Improvement does lie in the proper evaluation of the nature, cause, and extent of presumed deficiencies.

3 With such factual evaluation available, the testing and selection of materials, practices, and designs of the elements of the journal-box assembly already developed will lead to the most dependable and economic operation.

[11] Service Manager, Kingsbury Machine Works, Inc., Philadelphia, Pa. Mem. ASME.

[12] "Tests of Oil-Film Journal Bearings for Railroad Cars," by S. J. Needs, Trans. ASME, vol. 68, 1946, pp. 337–353.

The Development of a Design of Smokeless Stove for Bituminous Coal

By B. A. Landry[1] and R. A. Sherman,[2] Columbus, Ohio

This paper presents an account of an extended systematic investigation which resulted in the development of a method for burning bituminous coals in nonmechanical hand-fired heaters or stoves with substantially smokeless operation. The research was sponsored by Bituminous Coal Research, Inc., and a group of stove manufacturers. An experimental investigation of the three principles of combustion in fuel beds led to the adoption of the cross-feed principle. The design of a special grate and the research to prevent puffing, a difficulty often encountered with magazine heaters, are described. The principles of a calorimeter room in which the output of a space heater can be directly measured are presented. Data given show the thermal efficiency of a manufacturer's model of the heater, which had an output of 41,000 Btu per hr, to be 65 per cent.

The United States leads the world in the number and proportion of residences that are heated from a central plant, and a high percentage of these use automatic firing of coal, oil, or gas. However, the Census of 1940 showed that 16,000,000, or about 47 per cent of the dwelling units of the country were being heated by some type of stove. Some 40 per cent of these dwellings use coal as a fuel. Because many dwellings use more than one stove, it can be estimated that there are probably about 8,000,000 coal-burning stoves in the United States today and several hundred thousand are sold each year. Estimates have been made that 25 to 30 million tons of coal are used annually in stoves.

Because these stoves operate on the simple surface-burning principle and because they are usually connected to low chimneys, the charge that stoves are important contributors to the smoke problem of cities where bituminous coal is used is probably not without some justification.

As a part of its program to develop improved equipment for the utilization of bituminous coal, Bituminous Coal Research, Inc. (BCR), the research agency of the bituminous-coal industry, initiated at Battelle late in 1940 a research project aimed at the development of stoves that would burn bituminous coal without the emission of objectionable smoke. In July, 1941, a group of manufacturers of stoves joined BCR in support of the program.

This paper presents an account of the steps that were followed in the investigation which has now culminated in the design of smokeless stoves which are in commercial production and are being sold and used. The design principles developed are applicable also to warm-air furnaces and residential boilers, and are now in process of being applied to these types of equipment.

---

[1] Supervisor, Fuels Research, Battelle Memorial Institute. Mem. ASME.

[2] Assistant Director, Battelle Memorial Institute. Mem. ASME.

Contributed by the Fuels Division and presented at the Annual Meeting, New York, N. Y., November 28–December 3, 1948, of The American Society of Mechanical Engineers.

Note: Statements and opinions advanced in papers are to be understood as individual expressions of their authors and not those of the Society. Paper No. 48—A-119.

General Principles of Combustion of Bituminous Coal

As do all other natural solid fuels, and some processed ones, bituminous coals, when heated, release gaseous products composed of water vapor, hydrocarbons, hydrogen, and sometimes carbon monoxide, and carbon dioxide. The weight of these products is approximately directly related to the volatile-matter content of the coal. Following the process of distillation or devolatilization of the coal, there still remains an appreciable portion of the fixed carbon to burn. Hence, the complete burning of bitumious coals involves, usually in two steps, the burning of gases and the burning of solids.

When bituminous coal is burned in pulverized form, the single process of mixing air with coal particles is effective in carrying out the burning requirements of both gases and solids. However, when the coal is burned in fuel beds other than exceptionally thin overfeed beds, two distinct processes are needed to burn satisfactorily the two fuel forms. One, of course, simply involves passing air through the fuel bed to burn the coke; the other, requires (1) that air be mixed thoroughly with the gases, as they are released from the portion of the bed where devolatilization takes place, and (2) that temperatures be maintained high enough for completion of the combustion reactions. Failure to satisfy these two requirements results in the formation of smoke.

If no air is provided for mixing with the gases, and temperatures in the furnace are low, smoke consists mainly of a tar fog which is condensed hydrocarbons. If air is supplied but mixing is incomplete, and furnace temperatures are high enough to cause ignition, there will be regions of intense burning wherever oxygen is available, and other regions where, because of the absence of oxygen, the hydrocarbons simply will be heated by radiation to temperatures high enough to cause cracking, with formation of carbon or soot which will appear as smoke. Actually, both tar and soot may be emitted simultaneously with the gases from different parts of the furnace.

In mechanically fired industrial furnaces with good control of the air/fuel ratio, streams of gases rich in hydrocarbons may arise from certain portions of the fuel bed while other streams of gases, in which excess air is present, may arise from other portions. The mixing of these two streams may take place rapidly enough to avoid smoke formation if mixing arches are provided or if a large furnace volume gives time for mixing by diffusion. With smaller furnace volumes or higher rates of operation, which decrease time available for diffusion, smoke is of common occurrence unless overfire jets are used to establish turbulence where stratification otherwise would prevail. Even overfire jets, however, may not be completely effective if furnace volumes are too small or control of the air/fuel ratio is lost as a result of large intermittent firings.

Smoke emission from hand-fired heating equipment results from causes similar to those described, with considerable exaggeration of some of them, particularly in regard to the relatively large intermittent firings that are made, as is necessitated by the impracticality of frequent attention, and in regard to the low furnace temperatures usually maintained, which are unfavorable for ignition of the mixture but which are required to prevent overheating. The palliative of overfire-airjets is not available

for this type of equipment because furnace conditions would render them ineffective. Elimination of smoke from hand-fired heating equipment must depend primarily, therefore, on the selection and application of such combustion principles that will be effective purely as a result of design arrangements. The difficulties associated with following such a course have long been considered as affording little chance of success.

Stages of Investigation

The stages followed in the investigation were as follows:

1 A test survey of all those commercially available heaters, for which differences could be recognized in the principles used for combustion, in order not to overlook any promising feature of design. This period was also of value in the development of methods of test, including the use of a light-sensitive smoke meter, to insure reproducibility of results and the drawing of assured conclusions.

2 The selection of the cross-feed principle of burning, so disposed that the fuel moved downward from a magazine toward a horizontal grate above which cross-feed air and gases moved horizontally across the bed, and the addition of an arch of special construction to provide for the intimate mixing of secondary air with the gases escaping from the bed for complete combustion.

3 The introduction of air above the fuel fired in the magazine in order to alter the caking properties of the fuel and convert strongly caking coals to a free-burning form for gravity feeding to the "hearth" or cross-feed burning portion of the bed.

4 The development of special grates to insure horizontal flow of air above them, without danger of short-circuiting through the ashpit, and to provide a dumping arrangement to dispose of larger pieces of ash, especially laminated material.

5 The translation from the laboratory type of construction to a commercial design.

6 The development of a calorimeter room to measure directly the output of heaters and to make possible the evaluation of the various heat losses including the saving in fuel from smoke elimination.

Results of Test Survey

Method of Test. The method of test used in making the survey, which remained essentially unchanged during the course of the investigation, consisted in placing the heater or stove on scales to observe the rate of weight loss during the burning, and providing flexible connections to the points where drafts were measured, temperatures taken by means of thermocouples, and gas samples obtained by means of water-cooled samplers. Imposed conditions to evaluate performance and to permit duplication of tests, to insure reproducibility of results, were either (1) to maintain constant flue-gas temperature, at some preassigned value, or (2) to maintain constant applied draft, again at some preassigned value. The first type of operation is valuable to show the frequency and type of attention required to maintain approximately constant output; the second type of operation serves to relate burning rate and output to applied draft to ascertain whether the burning process is under control. Both types of test were usually required for complete evaluation of the heaters.

Heaters Tested. Figs. 1 to 6, inclusive, show in diagrammatic form the burning principles of heaters on which tests were conducted during the survey stage preceding the development of the smokeless stove. In these diagrams the diagonally hatched areas represent solid fuel, whether freshly fired or at various degrees of devolatilization, except for Fig. 5 where the rectangular hatching represents freshly fired coal. Comments which follow refer to the performance of these heaters when burning bituminous coal.

Fig. 1 represents the conventional "surface-fired" heater with primary air admitted through the grates, and secondary air admitted either through the firing-door slots or through a "down-blast" pipe. This type of heater produces abundant smoke, because of poor mixing with secondary air, or low temperatures during devolatilization, or both; the period between attentions is short, but the average CO_2 is acceptable and draft requirements are well within the capacity of a small chimney.

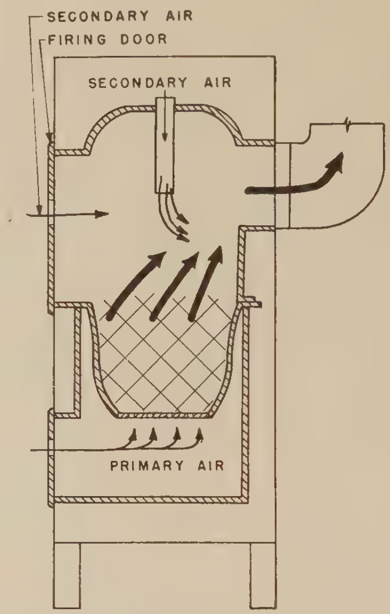

Fig. 1 Conventional Surface-Fired Stove With Two Alternate Forms of Secondary-Air Admission

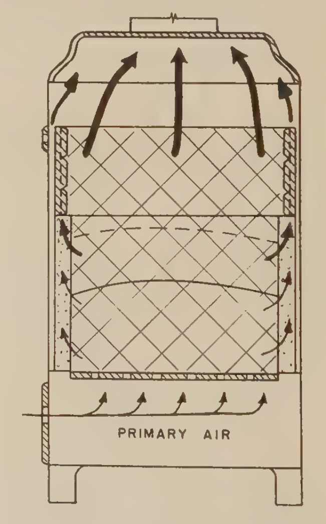

Fig. 2 "Magazine-Type" Heater With Deep Fire Pot

Fig. 2 represents a version of the so-called magazine-type heater having a deep fire pot, primary air passing through the grates and gases leaving the fuel bed at various heights through side channels or ducts, or at the top of the bed, the type of flow depending on the extent of caking in the fuel bed. The devolatilization of the charge is more rapid in this type of heater so that the smoking period, because of poor mixing with secondary air at low temperatures, is more intense although of relatively shorter duration than in the conventional heater, in view of the larger firing possible. The period between attentions is long, the

average CO_2 is acceptable, but the draft requirements are so low that the rate of burning may easily become excessive and control of heat output may be lost.

Fig. 3 represents a downdraft heater with part of the air supply passing through a rear slot to burn the gases at the outlet which is small in comparison with the size of heater. Because high temperatures are not maintained at the throat, owing to excessive air flow in comparison to the flow through the bed, smoke from this heater is abundant, rates of burning are low, and draft requirements high unless frequent poking is done to break the cake and prevent short-circuiting of primary air to the slot.

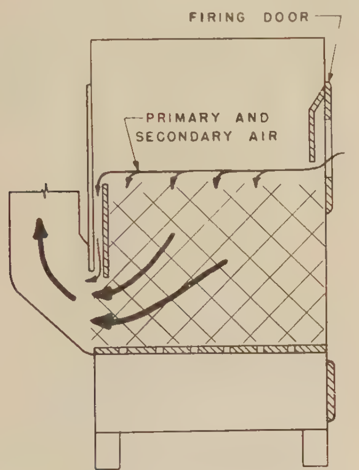

Fig. 3 Downdraft Heater

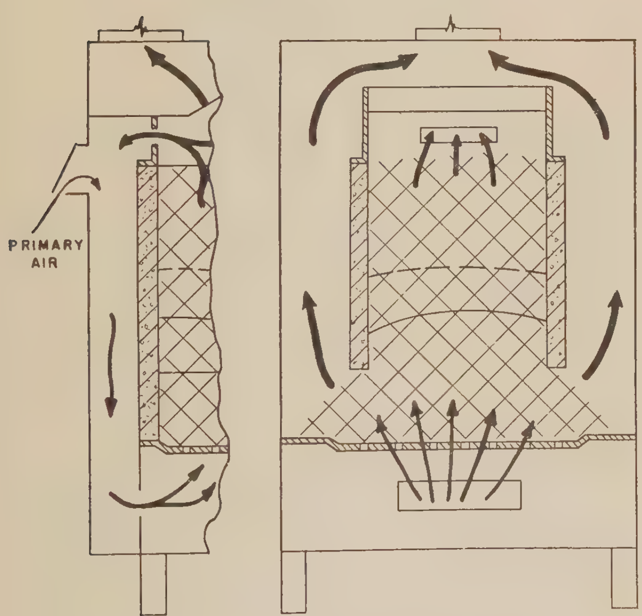

Fig. 4 Dual-Side Heater

Fig. 4 represents a dual-side heater in which devolatilization takes place, because of lateral heating, in the fuel magazine; the volatile gases escape at the top and are allowed to mix with primary air which serves also as secondary air when passing through the edges of the bed. Because of poor mixing, abundant smoke is produced, rates of burning are low, with low CO_2, unless frequent poking replenishes the fuel supply at the two sides, which also tend to burn at uneven rates.

Fig. 5 represents a divided heater with a half-circular lid which is pivoted on the partition. As the fuel in one half burns, the fuel in the other half devolatilizes by heat transfer, the gaseous products leaving through a hole in the partition to pass into the burning side; after refiring, the lid is rotated over the freshly fired side. Nearly smokeless operation can be obtained, with acceptable average CO_2 and low-draft requirements, if the heater is as small as a 14-in-diam cylinder. With a further increase in diameter, heat transfer is not high enough to devolatilize all of the fresh fuel during the burning of the residual fuel, and with increase in diameter of heater, progressively more abundant smoke is produced after rotation of the lid.

Fig. 6 represents a type of cross-feed unit in which air is admitted at two levels, at the side (1) at the lower level, to burn the residual coke, and (2) at the upper level, to act as secondary air for mixing with the gases leaving the bed. Air is admitted also at the top of the magazine to alter the caking properties of the fuel in the magazine. Because of the unequal flow of the lower air, owing to its tendency to make a short curvature bend immediately after entering the heater, and thus escape contact with the fuel, the rate of burning can be maintained only by frequent poking to fill cavities formed, and smoke is produced in objectionable

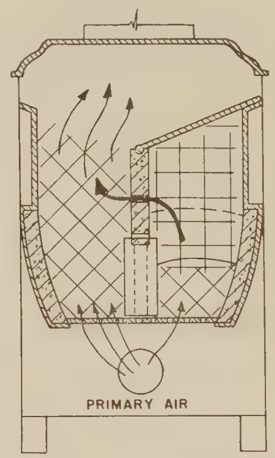

Fig. 5 Divided Heater With Pivoted Lid

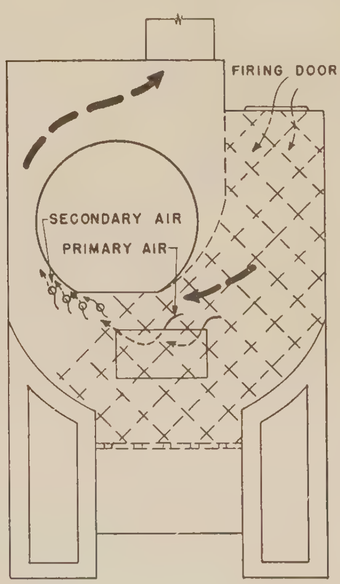

Fig. 6 Side-Feed Heater

quantity because of poor mixing of the secondary air with the gases for the same reason. With frequent poking, average CO_2 is acceptable and the draft required is low.

Discussion of Results of Survey. Consideration of the results obtained during the survey led to a number of conclusions. One of these was that if the products of combustion, as they emerge from the fuel bed, contain smoke-forming constituents, the casual introduction of secondary air into the combustion space will not eliminate smoke. This results from the stratification of the gas and air streams, owing to their low velocities, at all rates of operation, in addition to the impossibility of attainment of temperatures high enough for ignition at the lower rates. Hence, a positive means of insuring mixing of gases with air in a region of high temperature, at all rates of burning, was indicated as a requisite for smoke elimination. This conclusion made it appear that a bed fired from above with air admitted through the grates was not a promising principle for the smokeless heater.

Another conclusion was that burning by means of admission of air at the top of the charge, as attempted in the heater shown in Fig. 3, could not be depended upon to prevent caking of bituminous coals rapidly enough to maintain air flow at the higher burning rates, and hence offered little promise.

By elimination, therefore, only the cross-feed principle remained as one upon which further investigation appeared to be warranted. None of the heaters tested in the survey could be considered as embodying true cross-feed burning; however, to the extent that the heater shown in Fig. 6 represented an attempt at cross-feed burning, to the same extent it could be concluded that this type of burning was not one which would give smokeless burning purely by virtue of the relative directions of flow of air and fuel.

Basis for Selection of Cross-Feed Principle for Smokeless Heater

Although the cross-feed bed is used to advantage in so-called "underfeed-stoker" beds, yet, for this type of application, mechanical action is required to move the fuel from the retorts laterally across the tuyères. Thus, if cross-feed burning were to be used in heaters, in the absence of mechanical means of feeding, the motion of the fuel relative to the air stream could only be so directed as to result in a downward flow under the action of gravity, the air movement being at right angles, or in a horizontal direction. This arrangement provided for the following distinct advantages:

1 Horizontal flow of the gaseous products of combustion across the bed would require the use of a vertical arch descending to a level adjacent to the grate to confine the bed while permitting the outflow of gases under the edge of the structure. Admission of secondary air in this region was indicated because the gases would be at their maximum temperature at all times to favor sustained ignition.

2 Generation of heat over the entire volume of hearth subject to cross-feed burning would favor transfer of heat through the upper boundary of the hearth for devolatilization of the fresh fuel fired in the magazine space above, and thus insure eventual minimum release of hydrocarbons during the cross-feed burning.

3 Constancy in the thickness of bed between the arch and the opposite wall would favor sustained combustion efficiency during the burning cycle.

In carrying out the development of a smokeless stove using the cross-feed principle of burning, there were two main stages, namely (1) stoves that required poking to bring the caked fuel down from the magazine into the hearth, and (2) stoves for which the necessity to poke was eliminated by providing oxidizing conditions during devolatilization to prevent caking.

First Stage in Development of Smokeless Stove

Fig. 7 is a diagrammatic view of the heater that was built to test in a preliminary way whether the advantages described would accrue from cross-feed burning. All of the primary air was admitted through louvers set in a wall opening opposite to the arch. Secondary air was admitted at the bottom of the passage under the arch through similar louvers, and a combustion chamber was provided on the other side of the arch to give time for the completion of the reactions. Results showed that, as compared with smoke emission from conventional heaters, much improvement had been obtained; however, observation showed that the stream of products of combustion, usually containing combustible

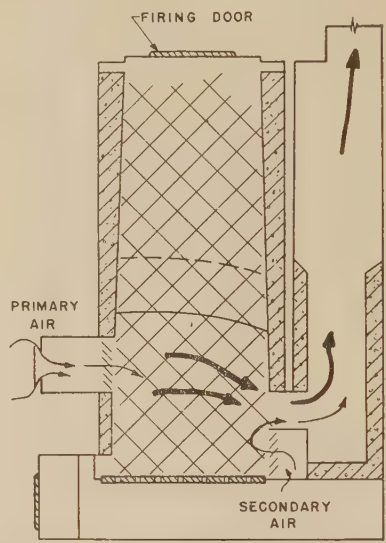

Fig. 7 Preliminary Cross-Feed Heater

gases, passed closely under the bottom of the arch as they left the fuel bed and did not mix well with the stream of secondary air coming from below, and that the stratification thus set up did not disappear in the combustion chamber.

Fig. 8 shows the next design in which provision was made for the admission of secondary air through a flattened metal pipe, approximately 3 in. wide, set above a 7-in. refractory-lined duct serving as gas outlet. A 1-in. pipe vent was also provided to relieve the gas pressure that otherwise would build up at the top of the magazine owing to the formation of a hard and impervious layer of coke at the lower boundary of the fresh charge. The vent was so disposed as to make the gases mix with primary air before passage through the fuel bed.

Results were immediately so promising from the point of view of smoke elimination that there was no doubt that the proper method of introduction of secondary air had been provided to give complete mixing of air and gases as both streams moved along the bottom of the arch, that is, the top of the gas outlet or throat. The heat-exchanger section, attached to the outlet, no longer served as combustion chamber, but solely to dissipate heat. In the form sketched in Fig. 8, the heater could be placed in one room, adjacently to a wall, and the heat exchanger placed in the adjoining room, the connection outlet passing through a hole in the wall. Operation of the heater disclosed, however, that the rate of burning was definitely limited to low values under the maximum allowable draft; it was reasoned that the restricted outlet limited the flow of air to a small cross section of the bed in addition to offering rather high resistance to the flow of gases.

Fig. 9 represents the next important development. For this heater, a generally rectangular construction was adopted to

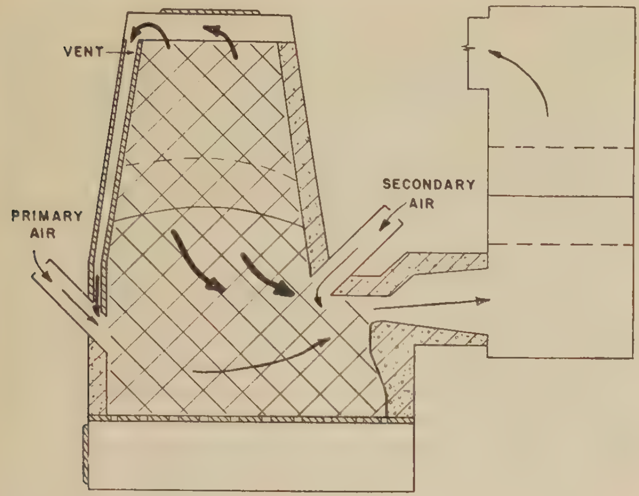

Fig. 8 Second Version of the Smokeless Heater

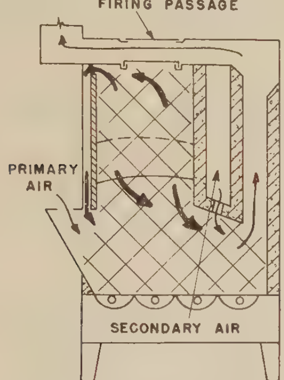

Fig. 9 A Third Version of the Smokeless Heater

provide a combustion-gas outlet as wide as the heater, and the heat exchanger was, so to speak, wrapped around the side and top of the heater for compactness. Secondary air, introduced through the ends of a refractory arch, was admitted above the gas passage, but the error was made of admitting the air through eight $^3/_4$-in. holes spaced about 2 in. apart, whereas in the heater of Fig. 8 the secondary-air slot had extended continuously over the gas outlet. It was found that smoke was not completely eliminated, and it was verified that lateral stratification of streams of gases occurred, owing to lack of side mixing with air. An investigation was carried out whereby the individual holes were first replaced by four 4-in. divided slots having 1-in. closed spacing between them, and then by a continuous slot extending over the entire length of arch.

Table 1 summarizes average results obtained from four successive tests under each of the conditions listed. The advantage of replacing individual holes by a continuous slot, to prevent lateral stratification, is shown by the decrease obtained in recorded durations of smoke, indicated by the inclusive minutes above each of the conventional Ringelmann numbers. The average percentage of carbon dioxide obtained in these tests was also of interest in showing that, by standards of low-duty, hand-fired heating equipment, acceptable and rather constant combustion efficiency was being obtained with decrease in smoke.

In this connection, tests made with the four 4-in-slot arrangement had shown a distinct relation between the area of opening

TABLE 1 COMPARISON OF RESULTS OF SMOKE EMISSION FROM USE OF HOLES, OF DIVIDED SLOTS, AND OF A CONTINUOUS SLOT IN SECONDARY-AIR ARCH. AVERAGE RESULTS FROM FOUR TESTS OF HEATER SHOWN IN FIG. 9

(Ohio No. 6 coal, size 2 in. × 1 in.)

Secondary-air openings in arch...	Eight, $^3/_4$-in. holes	Four, 4-in. slots	Continuous 20-in. slot
Average applied draft, in. water......	0.059	0.056	0.060
Combustible gasified, lb.............	19.25	19.10	23.75
Duration, hr........................	3.5	4.0	4.0
Combustible gasified, lb per hr......	5.5	4.8	6.0
Average flue-gas temperature, deg F..........................	875	850	880
Smoke, Ringelmann No., minutes (inclusive) in test period			
Above No. 1.......................	26	16	15
Above No. 2.......................	12	4	2
Above No. 3.......................	8	2	1
Above No. 4.......................	6	1	0
Average flue-gas composition, per cent			
CO_2..............................	9.6	9.2	10.0
O_2...............................	9.7	10.2	9.2
CO.................................	0.1	0.1	0.3

provided for the admission of secondary air to the interior plenum of the arch, the smoke emission, and the excess air. Table 2 illustrates the relation determined by the average of four tests in each series with the stated areas of opening. The table shows that with a small area the CO_2 was high at 13.5 per cent and also the smoke emission. With increase in area and, consequently,

TABLE 2 RELATION OF SMOKE EMISSION AND OF AVERAGE CO_2 TO AREA OF SECONDARY-AIR OPENING IN HEATER SHOWN IN FIG. 9

(Ohio No. 6 Coal, size 2 in. × 1 in.)

Area of opening for secondary air, sq in...	1.77	3.53	5.30
Average CO_2.........................	13.5	10.0	9.2
Smoke, Ringelmann No., minutes (inclusive) in test period of 4 hr			
Above No. 1...........................	89	18	16
Above No. 2...........................	62	5	4
Above No. 3...........................	37	3	2
Above No. 4...........................	6	2	1

increase of secondary air, both CO_2 and smoke decreased, but the reduction in smoke obtained with a CO_2 content as low as 9.2 per cent was not so large as that obtained by replacing the partial slots by a continuous slot, in further view of the fact that an average CO_2 of 10 per cent was obtained with the latter arrangement.

Discussion of Results of First Stage of Development. Although the evolution described in the design of the cross-feed heater properly could be considered to have solved the problems of smoke emission and of compactness of design, yet there remained the serious difficulty that the heater required poking to bring devolatilized fuel into the hearth. To minimize the labor of poking, successive heaters had been made smaller, with a firing door at the top, to permit more advantageous use of the poker in breaking the hard coke layer formed above the hearth section. Such small heaters had the disadvantage of a short interval between firings, of approximately 4 hr, as shown in Tables 1 and 2, and could not be construed as magazine heaters. This was confirmed in field trials of some twenty units of a jacketed heater based upon the heater shown in Fig. 9, for which the principal complaint was precisely the difficulty of poking. Hence, it was indicated that means had to be found to prevent caking in the magazine if a smokeless heater with true magazine feed was to be developed to give users the very tangible advantage of a long period between refirings, at rating, in addition to smokeless operation. This was the objective of the second stage.

Second Stage in the Development of the Smokeless Stove

One of the simplest ways to prevent the caking of bituminous coal is to provide oxidizing conditions around pieces, as tar exudes from them while the coal is being heated. Little air is required to prevent caking in this manner when the rate of heating is low but the reverse is true at higher rates. The application of this principle to the smokeless stove appeared promising enough that

trials were made in a deep-magazine heater built for this purpose. As soon as confirmation had been obtained that caking could be prevented, a number of units were built for field tests.

Fig. 10 is a diagrammatic cross section of this second field-test unit which embodied a means of admission of magazine air, under controlled conditions, for self-feeding. The air was admitted through an external duct and entered near the top of the firing space above the magazine charge. Flow of this air through the fresh charge of caking fuel induced upward travel of ignition of the tarry substances, against the flow of air. Meanwhile, cross-feed burning, in the hearth, maintained heat output and provided the heat source from which the upward travel of ignition could start; thus the time was provided that is required to convert the caking coal to the free-burning stage to permit its descent into the hearth. This combination of principles was found to correct, in the manner described, for the operating deficiencies of the heater shown in Fig. 3, which depended entirely on downdraft burning to sustain the burning rate. Because of air admission to the magazine, the vent formerly used to lead fumes from the magazine to the point of entry of cross-feed air was no longer required and was not provided in the heater shown in Fig. 10, and in other heaters subsequently built.

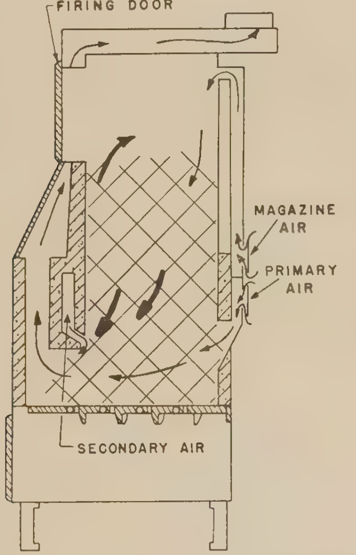

Fig. 10 Second Field-Test Model of Smokeless Heater

Occurrence and Cure of Puffing. At this stage of the development, laboratory and field experience showed that, as a result of the admission of air to the magazine, "puffing" was introduced during operation, particularly following an adjustment in the rate of air supply. The puffing was normally inaudible but manifested itself by the emission of visible smoke puffs at one or more of the various air inlets to the heater, the smoke having the characteristic odor of incompletely burned gases from bituminous coal. This occurrence led to a rather long investigation to obtain a cure; the fact that puffs might appear at any of the air openings made it difficult to understand their exact cause.

Final conclusions reached were that puffing could occur as a result of two types of actions, namely, (1) formation of an ignitible mixture within the fuel-bed voids, in the vicinity of the secondary-air arch, when these voids were large enough to yield appreciable kinetic effects upon ignition of the mixture, and (2) formation of an ignitible mixture of combustible gases and air in the firing space above the magazine charge, followed by ignition of the mixture, as a result of the upward travel of ignition to the top of the charge.

Fig. 11 shows the general design of three heaters used for the experimental work on which the first of these conclusions was based. In these heaters the magazine air was introduced within the charge rather than near the top of the firing space as in Fig. 10. The three heaters were similar in every respect, except that the dimension corresponding to the distance from the refractory arch to the opposite wall was only 11.75 in., as in the heater shown in Fig. 10, for the first heater; for the second heater, this dimension was 14.75 in. as in the heater shown in Fig. 11; and in the third heater this dimension was 18.25 in. When burning the weakly caking Illinois or Indiana coals in these heaters, under steady conditions, no puffing was observed. When burning the strongly caking Pittsburgh coal, however, puffs were observed, under steady operation, with the first of these heaters, but not with the other two having the longer dimensions from arch to wall.

The explanation for this behavior was that the residual-coke pieces formed with the more strongly caking coal were much larger than those formed with the weakly caking coals; hence the void spaces between pieces were also correspondingly larger, and appreciable kinetic effects could be developed, in the vicinity of the arch, provided there was enough residual oxygen brought into the void spaces to mix with the combustible gases also entering into them in their flow downward from the fresh fuel in the magazine. Since combustion efficiency would increase, with increase in the hearth dimension described, and also with decrease in size of coke pieces, it was apparent that only in the heater with the shortest hearth dimension were the two conditions both fulfilled, when burning a caking coal, of large voids and of enough residual oxygen to give an explosive mixture. This was confirmed by a flue-gas analysis which gave averages of 9.3 and 9.4 per cent CO_2, over an 8-hr period, for the two larger heaters, but only 6.7 per cent CO_2 for the smallest when burning Pittsburgh coal without smoke formation. The net result was that freedom from puffing from this cause required that the arch-to-wall dimension be at least 14 in., with little gain in combustion efficiency from any further increase in this dimension.

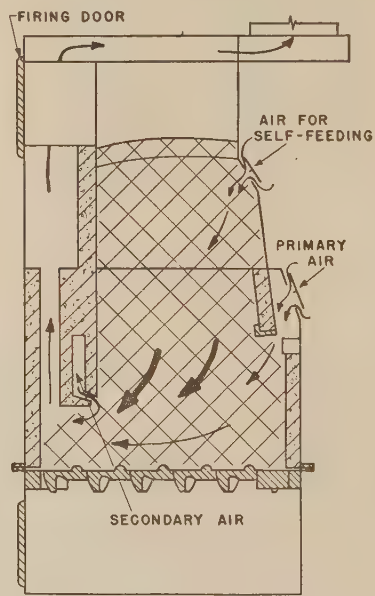

Fig. 11 Smokeless Heater With Admission of Magazine Air Below Top of Charge of Coal

The second process mentioned, in which a mixture of combustible gases and air could form in the space above the magazine fuel is illustrated in Fig. 10 by the arrow, showing the tendency for gases to leave the top of the charge in opposition to the downward flow of air. That such a process existed was demonstrated by the arrangement shown in Fig. 11 whereby the air required to induce self-feeding of the coal was introduced within the charge, through a narrow slot as wide as the heater, at a level some 2 in. below the top of the charge. Because little or none of the air passed to the space above, no puffing was experienced with this arrangement under steady or variable operation. However, a layer of hard coke was formed above the level of the air entry, and this layer remained in place even after the free-burning fuel below had fed down, thus giving a deceptive appraisal of the quantity of fuel in the magazine. Raising the level of self-feeding air admission to the level of the top of a normal firing was successful in avoiding the formation of the coke arch, but reintroduced occasional puffing following partial closure of the cross-feed air inlet to reduce heat output.

Fig. 12 illustrates how the change in level of air admission was carried out and shows also the next change made which was to provide a sloping roof in the magazine to halve, approximately, the volume available for the mixture and reduce the kinetic effects, following ignition.

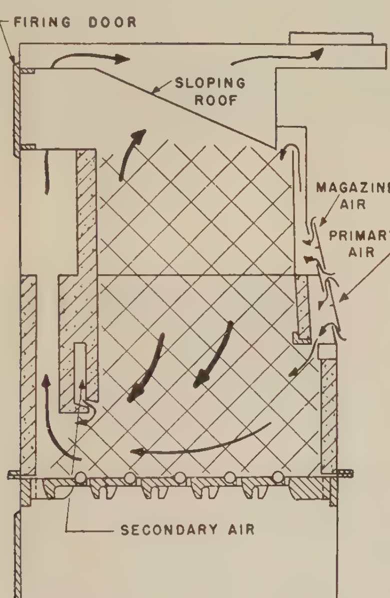

Fig. 12 Smokeless Heater With Sloping Roof of Magazine

The final arrangement designed to make it practically impossible for any slight puff to manifest itself outside of the heater was to provide a common plenum duct covering both the magazine-air and the cross-feed air inlets, and extending enough downwardly so that the duct opening would be approximately at the grate level.

Grates of the Smokeless Stove

Throughout the development of the smokeless stove, a great deal of attention had to be devoted to the development of a grate design that would (1) insure no short-circuiting of air through the ashpit in order to maintain the flow of cross-feed air above the grate, and (2) provide a dumping element for disposal of unburned refuse.

Fig. 13 shows the design of the final type of grate developed. The close-fitting fingered portion is intended to offer enough resistance to the flow of air to prevent short-circuiting while effectively serving to shake the bed and remove the fine ash released. Unburnable refuse is transferred by the motion of the grate into the troughlike end grate, under the vertical gas passage, for periodic removal by turning a crank attached to the trunnion support and thereby dumping the accumulation. The dump grate is counterbalanced to return automatically to a sealing position under the frame. A special re-entrant at the wall adja-

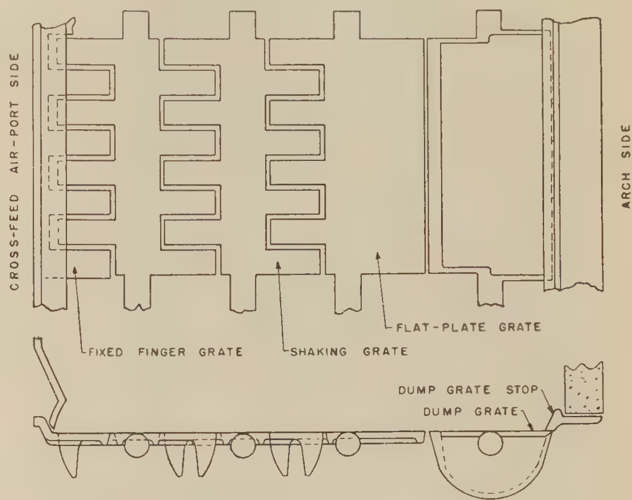

Fig. 13 Plan and Side View of Special Grate for Smokeless Stove

cent to the first rocking finger grate serves to prevent wedging of hard coke against this grate element.

Characteristics of Present Commercial Smokeless Heater

Fig. 14 shows in diagrammatic form the design of one of the present commercial smokeless stoves on which the plenum duct described earlier is visible. A feature of this design is the replacement by alloyed metal of the refractory portion of the arch, formerly on the fuel-bed side, to give longer life under existing

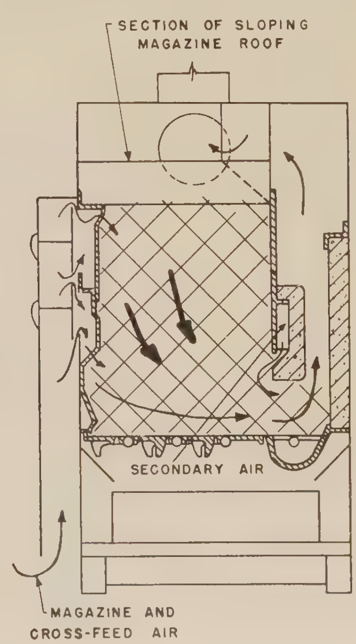

Fig. 14 Diagrammatic View of BCR Smokeless Stove

TABLE 3 TYPICAL TEST RESULTS, HEATER BCR-2A; CONSECUTIVE FIRING CYCLES

(Pittsburgh coal, size 2 in. × 1¼ in.)

Air openings:				
Magazine, position	4	4	4	4
Cross-feed, position	1 and 4	4	4	4
Secondary, in.	3/8	3/8	3/8	1/4
Average stack draft (natural), in. water	0.047	0.054	0.045	0.042
Weight of fuel fired, lb	43.5	47.0	43.0	45.0
Duration of test, hr	8.00	8.00	8.08	8.16
Average fuel gasified, lb per hr	3.94	5.13	4.46	4.04
Average flue-gas temperature, deg F	863	876	859	859
Flue-gas composition, per cent				
CO_2	9.1	8.2	8.3	8.8
O_2	9.5	10.9	10.7	10.5
CO	0.0	0.0	0.0	0.0
Smoke, Ringelmann No., min (inclusive) in 24 hr[a]				
Above No. 1	20[b]	7	5	11
Above No. 2	9[b]	5	0	6
Above No. 3	5[b]	3	0	0
Above No. 4	3[b]	0	0	0

[a] Smoke data include 8-hr burning test and 16-hr banking period.
[b] Smoke data include start of a new fire.

stresses. Table 3 summarizes typical test data obtained with this heater on a 24-hr firing cycle, 8 hr at rating and 16 under bank. The smoke-emission data are for 24 hr; those given in the first column include the start of a new fire, which by comparison even with the smoke normally emitted following a refiring, as shown in the other columns, would not be considered excessive.

The user of the smokeless stove regulates the heat output by adjustment of the cross-feed air damper only, except when chimney draft is excessive, when adjustment by means of a turn damper in the flue, or a barometric damper, may also be required. The magazine-air damper and the secondary-air dampers are adjusted by the coal dealer as follows: The magazine-air damper is set at the wide-open position for strongly caking coals (all Appalachian coals), at the mid-open point for mildly caking coals (Midwestern coals), and at the closed position for anthracite, coke, or the free-burning subbituminous coals and lignite. The secondary-air damper is set at the full opening for high-volatile coals, at the mid-opening for low-volatile coals, and at the closed position for anthracite and coke. A double-screened coal within the size range 3 to 1 in. is best-suited to the heater; smaller sizes have been found to give caking difficulty and larger sizes may contain impurities difficult to discharge through the dump grate. Run-of-mine coal is not recommended.

Calorimeter-Room Tests

A not inconsiderable part of the investigation for the development of the smokeless stove had to do with the design and construction of a calorimeter room in which the heat output of heaters could be measured directly. Fig. 15 is a cutaway view of the structure that was built for this purpose. On a simple stud-and-joist framework 12 ft × 12 ft × 8 ft, were attached sheets of ½-in. rigid fiber insulating board provided with differential thermocouples to indicate the average temperature difference between the inside and outside of the wall. Two blowers were mounted on the roof to force air in and withdraw air through constricted ducts for measurement of both (1) the quantity of air flow by means of Pitot tubes, and (2) the temperature of the air by means of thermocouple grids. A highly insulated floor was used. The room was calibrated by use of an electric heater, the unknown being the average thermal conductivity of the walls and ceiling which was obtained by subtracting from the known heat input the heat corresponding to the temperature rise of measured air flow and dividing by the indicated average temperature difference between the inside and outside wall and ceiling thermocouples.

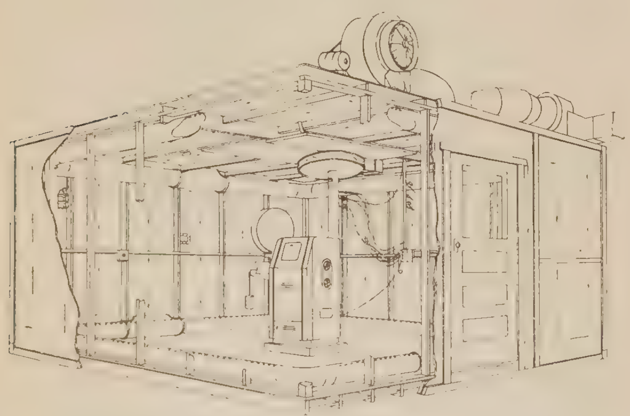

Fig. 15 Cutaway View of Calorimeter Room

Otherwise, the room was provided with all facilities for running burning tests of heaters from which heat losses in the dry flue gases, in the steam, and in the refuse could be determined directly. Knowledge of the heat input from the weight of coal burned and of the output as given by the room data thus made it possible to evaluate normally unaccountable heat losses due to tar and soot in the gases. By such tests it was shown that a conventional heater, such as shown in Fig. 1, gave a heat loss, due to smoke, of the order of 12 per cent of the heat input. By comparison, smokeless heater BCR-2 gave an unaccounted-for loss of less than 3 per cent.

Table 4 summarizes the heat-balance results from a typical test run in the calorimeter room on a 12-hr firing cycle with a commercial model of the BCR smokeless heater, using Illinois No. 6 coal. The rating output obtained of 41,000 Btu per hr with an applied draft of 0.05 in. of water and with firings every 12 hr, was also obtained with Island Creek and with Pittsburgh bed coals with this heater.

TABLE 4 SUMMARY HEAT-BALANCE RESULT, CALORIMETER ROOM TEST OF A COMMERCIAL MODEL OF THE BCR HEATER, 12-HR FIRING PERIOD

(Illinois No. 6 coal, size 2 in. × 1½ in.)

Measured heat output, Btu per hr:	
Heat gained by room air	32350
Heat loss through wall	11140
Heat from flue pipe	2560
Rating output of heater (12-hr basis)	40930

Heat balance

	Btu/lb	Per cent
Heat utilized (efficiency)	7649	64.6
Losses:		
Steam	656	5.5
Dry flue gas	2539	21.4
CO	70	0.6
Ashpit	591	5.0
Unaccounted for	335	2.9
Calorific value of fuel	11,840	100.0

For the 5 ft of pipe in the calorimeter room, Table 4 shows that 2560 Btu per hr corresponding to a 4 per cent gain in efficiency was transferred to the room. In a residential installation, additional recovery of heat and gain in efficiency may be realized from the flue pipe and chimney. However, because this is so variable with different installations and is uncontrollable after the installation is made, the efficiencies are reported here, as in usual practice, only on the output of the heater, including the first 20 in. of the metal flue pipe.

Under average winter-load conditions, firing would be expected to be required about once in 18 to 24 hr, and banking periods as long as 72 hr, followed by good pickup, have been obtained.

Fig. 16 is an exterior view of a circulator-type commercial version of the BCR smokeless heater. Fig. 17 is an exterior view of a radiant-type commercial version, the performance of which is similar to that of the circulator type.

A smaller-size radiant unit has also been developed and is in

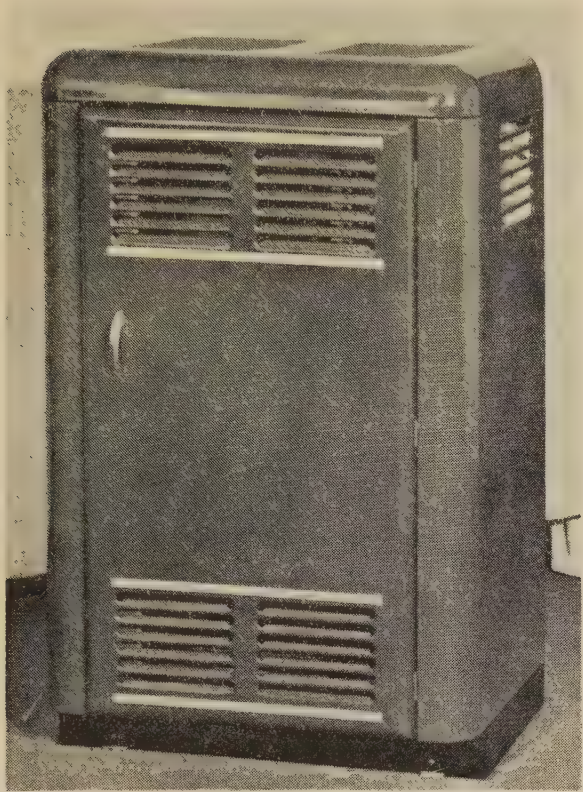

Fig. 16 Full-Size, Circulator Type, Commercial Version of BCR Smokeless Heater

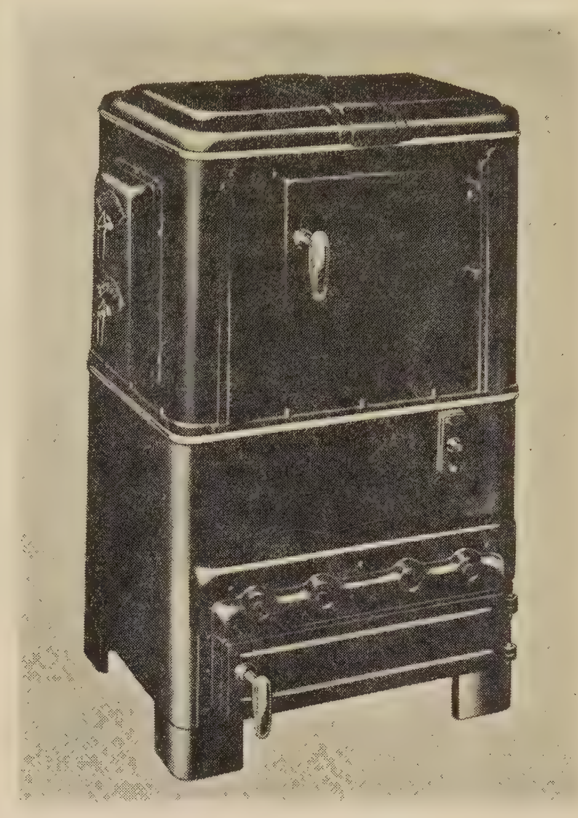

Fig. 17 Full-Size, Radiant Type, Commercial Version of BCR Smokeless Heater

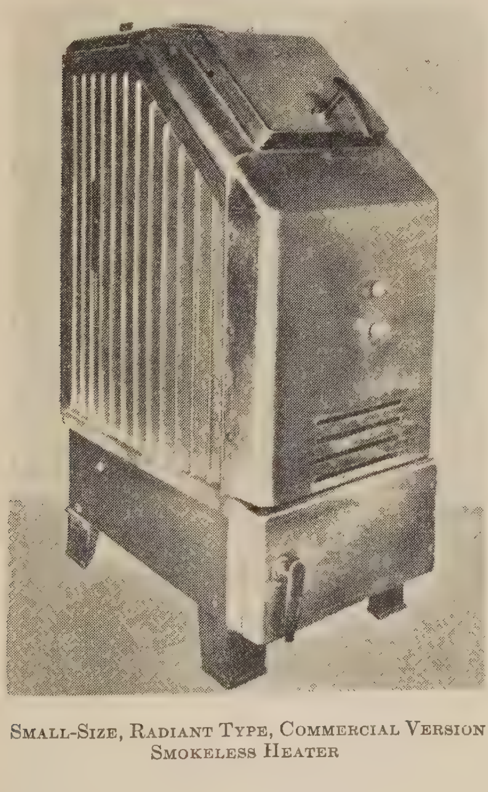

Fig. 18 Small-Size, Radiant Type, Commercial Version of BCR Smokeless Heater

commercial production. Fig. 18 illustrates this heater which has a rated output of 25,000 Btu per hr, under a 12-hr firing period, at an applied draft of 0.040 in. of water. The indicated efficiency of this unit is 67 per cent when burning bituminous coal.

Patent applications have been filed in the United States and Great Britain and various claims allowed for the developments described in this paper. A Canadian patent has been issued.

Acknowledgments

Acknowledgment is made of the significant contributions during the early stages of the work of Howard Limbacher, Henry Ostborg, and Robert Mattox; in the development of the calorimeter room, of the work of Paul Vyff; and of the contributions of Edward Erickson and John Tieman, all former or present research engineers at Battelle Memorial Institute.

Especial mention is made of the contributions of Elmer R. Kaiser, assistant director of research, and James R. Garvey, development engineer, Bituminous Coal Research, Inc., and of King Ehret, president, Oakland Foundry Company, Belleville, Ill., in the translation of laboratory design to finished commercial design.

Finally, thanks are due to H. J. Rose, vice-president and director of research, Bituminous Coal Research, Inc., to the Hand-Fired Heating Committee of the Technical Advisory Board of BCR, to other members of the Board, and to the members of the Stove Manufacturers Research Group, for their helpful suggestions and sustained interest and support during the long program.

Corrosion-Erosion of Boiler Feed Pumps and Regulating Valves at Marysville, Second Test Program

By J. M. DECKER,[1] H. A. WAGNER,[2] and J. C. MARSH,[3] DETROIT, MICH.

Corrosion-erosion tests at 320 and 385 F indicated that, at these temperatures, carbon steel is attacked to a lesser extent than at 250 F, whereas the reverse is true of the chromium-bearing steels. However, the rate of attack of the chromium steels is still only a fraction of that of carbon steels, so that use of the alloy steels for boiler-feed-pump parts is warranted at the higher temperatures also. Increasing the pH of the feedwater from 7.6 to 8.4 doubled the corrosion-erosion attack on carbon steel in the Marysville boiler feedwater at 250 F, as compared with previous tests at the lower pH. Of two bronzes tested, Navy M material appeared satisfactory at temperatures up to 320 F; a leaded bronze was unsatisfactory at all test temperatures in this program.

Introduction

In a previous paper,[4] the authors dealt with tests made at the Marysville plant of The Detroit Edison Company to determine the relative resistance of 18 different materials to the corrosion-erosion type of attack commonly experienced in boiler feed pumps and regulating valves. Feedwater at 250 F was used for these tests. Shortly after the paper was presented, plans were started for a 200-mw extension to the company's Trenton Channel plant. The plan adopted requires a cycle in which the feedwater temperature is 315 F at the boiler feed pumps. Initially, temperatures as high as 425 F were considered.

In order to obtain corrosion-erosion data for feedwater at the higher temperatures commonly found in newer power plants, a second test program was conducted at the Marysville plant. Temperatures of approximately 320 F and 385 F were chosen for the tests because they were within the range that was considered for the Trenton Channel and Connors Creek plant extensions, and because feedwater at those temperatures was available from the 7th and 4th stage heaters, respectively, of No. 7 turbogenerator. Since feedwater at 250 F from the boiler-feed-pump discharge of this same turbogenerator had been used in the earlier tests, the tests at higher temperatures should therefore evaluate the effect of the higher temperatures rather than some other variable.

Early in the test program it was noted that when the evaporator was taken from service, the pH of the feedwater increased from an average of about 7.3 to 8.3. Advantage was taken of this situation to determine in one series of tests the influence of pH in this range on the corrosion-erosion resistance of cast carbon steel. Included in this series of tests was one specimen each of 1.25 per cent chromium, 0.5 per cent molybdenum steel and leaded bronze.

The purpose of this paper is to present (1) the results obtained in the second test program; and (2) a comparison of the information thus obtained with corresponding data from the original tests.

Materials Tested

Nine different materials were tested. The materials, with their chemical compositions and physical properties, are listed in Table 1.

Six of the materials: Navy M (a bronze); 5 per cent Cr, 0.5 per cent Mo; 12 per cent Cr; 18 per cent Cr, 8 per cent Ni; Cr-Ni-Mo; and carbon steel, had been tested earlier at 250 F. With the exception of the carbon steel, which was used for control specimens, all of these materials had shown good corrosion-erosion resistance. They were selected, therefore, for testing at the higher temperatures. The other three materials were selected for the following reasons:

1 Leaded bronze had been suggested by a pump manufacturer for wearing-ring material in boiler feed pumps for the Trenton Channel plant extension.

2 An alloy steel containing 1.25 per cent chromium, 0.5 per cent molybdenum is being used frequently for high-temperature steam lines, and, if found to have good corrosion-erosion resistance, could be used advantageously for boiler-feedwater service because it is readily available. Previous tests also had indicated that steels of low chromium content would be satisfactory.

3 Chromium plating was included because it might be useful for protecting existing cast-carbon-steel equipment from attack, if it possessed the corrosion-erosion resistance common to iron-chromium alloys.

Four specimens of cast carbon steel were used in the test to determine the effect of increased pH on the corrosion-erosion rate. Cast carbon steel was chosen because any effect which changing the pH might have would be more readily observed on cast carbon steel than on the materials possessing greater corrosion-erosion resistance. This test was made at 250 F, as more data for comparative purposes were available for that test temperature than for other temperatures.

Specimens of 1.25 per cent chromium, 0.5 per cent molybdenum steel and of leaded bronze were included with the four cast-carbon-steel specimens because no tests of these materials had been made previously at 250 F.

Description of Test

The test method and equipment used for determining the corrosion-erosion resistance of the metals have been described in detail in the earlier paper[4] on this subject. Briefly it consists in exposing specimens of the material to be tested to the action of

[1] Research Department, The Detroit Edison Company. Jun. ASME.
[2] Engineering Department, The Detroit Edison Company. Mem. ASME.
[3] Production Department, The Detroit Edison Company.

[4] "Corrosion-Erosion of Boiler Feed Pumps and Regulating Valves," by H. A. Wagner, J. M. Decker, and J. C. Marsh, Trans. ASME, vol. 69, 1947, pp. 389–397.

Contributed by the Joint Research Committee on Boiler Feedwater Studies and the Power Division and presented at the Annual Meeting, New York, N. Y., November 29–December 3, 1948, of The American Society of Mechanical Engineers.

TABLE 1 CHEMICAL COMPOSITIONS AND PHYSICAL PROPERTIES OF TEST SPECIMENS

Chemical Composition, per cent

Specimen Designation	Material	Heat No.	C	Si	Mn	Cr	Ni	Mo	P	S	Cu	Sn	Fe	Zn	Pb	Sb
18, 18A, B, C, D, E and F	Carbon steel	3208	0.25	0.44	0.65				0.024	0.028						
1F†, 1G, 1H	" "	3191	0.24	0.45	0.69				0.028	0.027						
20, 20A,B,C	5% Cr, 0.5% Mo	W-6947	0.20	0.42	0.44	5.24		0.41								
3A,B,C,D,	12% Chromium	9121-AW	0.09	0.75	0.68	12.17	0.63	0.13								
5A,B,C,D	18% Chromium-8% Nickel	9122-AW	0.15	1.16	0.72	18.84	8.96									
21A,B,C,D	1-1/4% Chromium-1/2% Molybdenum		0.18	0.32	0.70	1.36	0.09	0.55	0.030	0.019	0.21					
9A	Cr-Ni-Mo	9120-AW	0.30	0.41	0.75	0.79	0.66	0.25								
13A,B,C,D,E	Navy M						0.49		0.01	0.03	87.58	5.30	0.06	4.14	1.64	0.15
19,19A,B,C	Leaded bronze										70.0	4.0			26.0	

Physical Properties

Specimen Designation	Material	Tensile Strength, psi	Yield Strength, psi	Elongation, per cent	Reduction of Area, per cent	Brinell§
18, 18A, B, C, D, E and F	Carbon steel	65,000‡	35,000	24	35	102
1F†, 1G, 1H	" "	65,000‡	35,000	24	35	102
20, 20A,B,C	5% Cr, 0.5% Mo	90,000□	60,000	18	30	224
3A,B,C,D,	12% Chromium	110,000□	85,000	24	55	241
5A,B,C,D	18% Chromium-8% Nickel	75,000□	36,000	45		144
21A,B,C,D	1-1/4% Chromium-1/2% Molybdenum	70,000□	45,000	22	35	169
9A	Cr-Ni-Mo	85,000□	53,000	22	35	185
13A,B,C,D,E	Navy M	40,000	22,000	30		52
19,19A,B,C	Leaded bronze	21,650		16		40

† Base metal of chromium-plated specimen. ‡ Approximate physical properties. § Brinell hardness mostly by test. □ Specified minimum.

high-velocity turbulent feedwater under conditions similar to those encountered in boiler feed pumps and regulating valves. The two parts of a test specimen with the mating faces upward are shown in Fig. 1.

During test, a weighed specimen is held in a corrosion-erosion tester as shown in Fig. 2. For 500 hr a differential pressure of 300 psi is maintained across the specimen. This pressure forces feedwater through the center hole in the bottom part of the specimen to impinge on the plain face of the top part, causing the flow of feedwater to change direction and leave the specimen at a velocity of about 200 fps through the slot openings in the lower part of the specimen.

At the end of the 500-hr period, the specimen is cleaned, reweighed, and the loss in weight calculated.

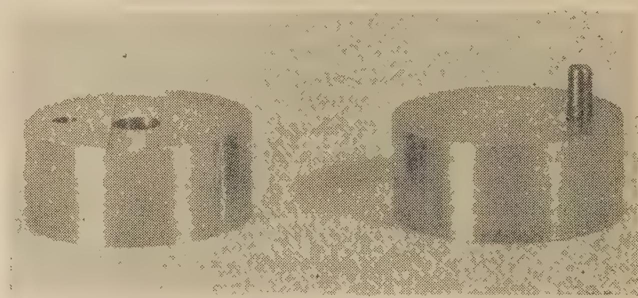

Fig. 1 Typical Corrosion-Erosion Test Specimen Before Test

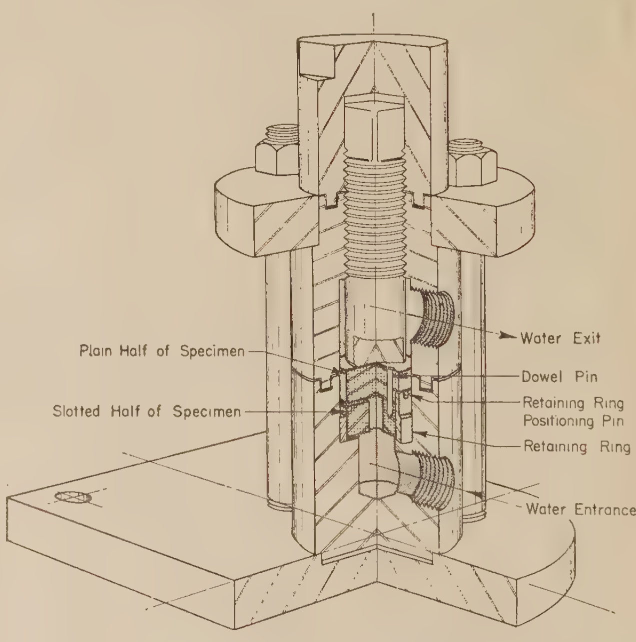

Fig. 2 Sectional View, Corrosion-Erosion Tester

Procedure and Results

At Marysville, six specimens were tested simultaneously. The six corrosion-erosion testers, pressure-measuring equipment, and pressure-regulating valves used are shown in Fig. 3.

Six series of 500-hr tests (tests No. 8 to 13, inclusive) were conducted in this program. As in previous tests, continuous records of pH, specific conductance, and dissolved oxygen concentration were made with recording instruments, and were supplemented by spot tests made with indicating instruments to check the accuracy of the recorded values.

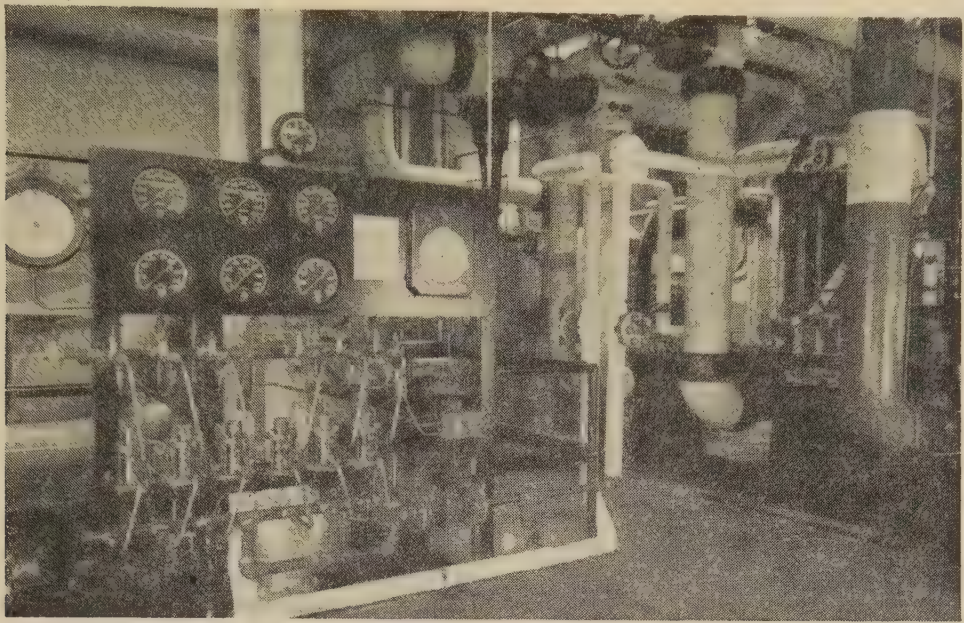

Fig. 3 General View of Test Setup

TABLE 2 BOILER FEEDWATER PRESSURE DIFFERENTIALS, TEMPERATURES, TEST RESULTS, AND WEIGHT LOSSES OF SPECIMENS

Test No.	Specimen & No.	Average Pressure Differential, psi	Average Water Temp. F	Avg. pH	Average Conductivity, Micromhos	Average Dissolved Oxygen, ppm	Total Weight Loss, 500 Hr, Grams
8	Carbon steel 18	299.7	381	7.3	0.43	0.008	0.6822
	5% Cr 20						0.0427
	12% Cr 3A						0.0447
	18-8 5A						0.0230
	Navy M 13A						0.0265
	Leaded bronze 19						0.2490
9	Carbon steel 18A	299.9	318	7.4	0.48	0.007	3.4673*
	5% Cr 20A						0.0641
	12% Cr 3B						0.0406
	18-8 5B						0.0348
	Navy M 13B						0.0473
	Leaded bronze 19A						0.2878
10	Carbon steel 18B	299.6	384	7.2	0.39	0.005	0.3915
	5% Cr 20B						0.0557
	12% 3C						0.0606
	Navy M 13C						0.2304
	Leaded bronze 19B						0.4699
	1-1/4 Cr--1/2 Mo 21A						0.0770
11	Carbon steel 18C	300.1	323	7.2	0.39	0.007	1.3638
	5% Cr 20C						0.0614
	12% Cr 3D						0.0953
	18-8 5C						0.0208
	Navy M 13D						0.0394
	1-1/4 Cr--1/2 Mo 21B						0.0870
12	Carbon steel 18D	299.9	388	7.5	0.41	0.004	0.1978
	Cr-Ni-Mo 9A						0.0609
	1-1/4 Cr--1/2 Mo 21C						0.0570
	18-8 5D						0.0171
	Navy M 13E						0.2678
	Cr Plated C steel 1F						0.3266
13	Carbon steel, 1G	297.8	255	8.4	0.66	0.007	4.6179
	" " 1H						5.2467**
	" " 18E						4.0695
	" " 18F						4.1204
	1-1/4 Cr--1/2 Mo, 21A						0.1678
	Leaded bronze, 19C						0.2822

* Loss corresponding to 447-hour test.
** Loss corresponding to 439-hour test.

In Table 2 the specimens are identified and averages of pressure differential, temperature, pH, specific conductance, and dissolved oxygen concentration, and specimen weight losses are given for each test. Weight losses are shown graphically in Figs. 5 and 6, along with data obtained in earlier tests at 250 F.

In Fig. 5 the weight losses obtained at 250, 320, and 385 F for each material are grouped together to show readily the effect of temperature on the corrosion-erosion rate of the various metals tested.

The weight losses obtained for cast carbon steel at 250 F are plotted in Fig. 6 to show the effect of the pH on the corrosion-erosion rate.

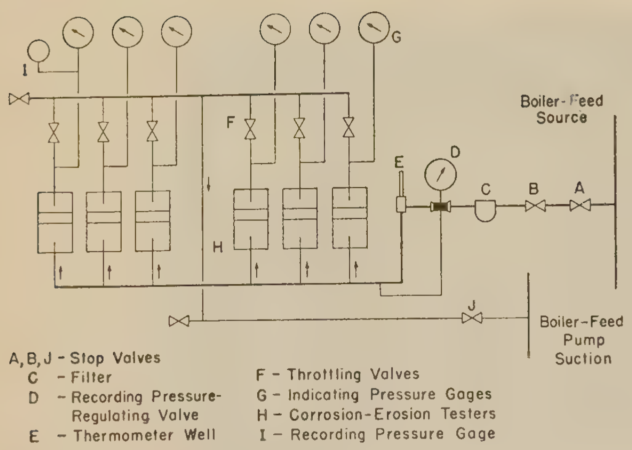

Fig. 4 Schematic Diagram, Corrosion-Erosion Test Setup

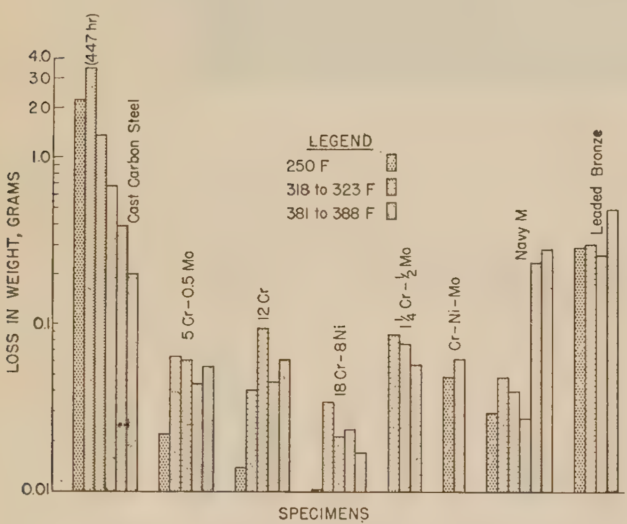

Fig. 5 Results of 500-Hr Corrosion-Erosion Tests of Cast-Metal Specimens at Various Temperatures

(Pressure differential 300 psi.)

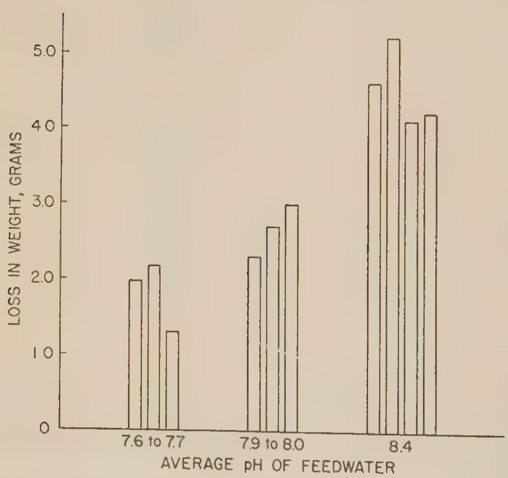

Fig. 6 Results of 500-Hr Corrosion-Erosion Tests of Cast-Carbon-Steel Specimens at Various pH Values

(Temperature 250 F, pressure differential 300 psi.)

Discussion of Results

In general, test results indicate that cast carbon steel is more resistant to corrosion-erosion attack at high temperatures than at low (See Table 2 and Fig. 5). At 388 F, for example, the loss in weight (0.1978 g) is less than $^1/_{10}$ that of the average (2.2582 g) of six specimens at 250 F. An exception to this generalization was observed, however. At 318 F, Specimen 18A (test No. 9) was attacked so extensively that the 300-psi differential across the specimen could not be maintained after 447 hr of test. A careful analysis of test and water conditions revealed no variations that would account for the accelerated attack. Specimen 18C, which was made from the same bar, lost much less weight under similar conditions. Microscopic examination of the metal structure of the two specimens revealed no significant differences that would account for the variation in weight losses. There may have been some slight variations in specimen dimensions or surface finish, although it is difficult on this basis to account for the great difference in attack.

The indication that cast carbon steel has higher corrosion-erosion resistance at 385 F than at 250 F is substantiated to some extent by actual experience at Marysville. Recently a check valve at the discharge of No. 7 boiler feed pump, where the feed-water temperature is 250 F, was found to be badly damaged. An identical valve located in the same line at the discharge of the 4th-stage heater, where the temperature is 385 F, however, showed little attack after the same number of service hours.

Inasmuch as water is more highly ionized at 320 F and 385 F than at 250 F (see Fig. 7), it would seem likely that metals would be more rapidly attacked at the higher temperatures. In the case of cast carbon steel, however, it seems that a more tenacious oxide coating forms on the surface of the metal at the high temperatures than at the low ones, and actually causes a reduction in rate of attack.

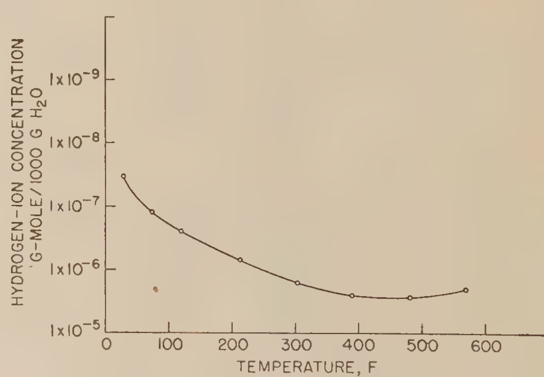

Fig. 7 Change of Hydrogen-Ion Concentration With Temperature in Pure Water

(From "Properties of Ordinary Water Substance," by N. E. Dorsey, Reinhold Publishing Corporation, New York, N. Y., 1940, Table 182, page 378.)

During the series of tests that composed this study, it was observed that the color of the coating on the specimens depended on the temperature at which they were tested. At 320 and 385 F the coatings were black, indicating them to be magnetic iron oxide, and at 250 F they were red, indicating ferric oxide. The black coatings were more tenaciously bonded to the specimens and were more difficult to remove than the red coatings.

In all cases the chromium-bearing steels were much more corrosion-erosion resistant than the carbon steel. As would be expected, the 18 per cent chromium-8 per cent nickel had the highest resistance. At 250 F the corrosion-erosion resistances of the chromium-bearing steels were roughly proportional to their chromium contents. At the higher temperatures, the relative

advantage of the high-chromium alloys was greatly reduced. For example, at 385 F the corrosion-erosion resistances of the Cr-Ni-Mo steel containing 0.79 per cent chromium, and of the 1.25 per cent chromium, 0.5 per cent molybdenum steel were about equal to that of 5 per cent and 12 per cent chromium steels.

The test results indicate that Navy M bronze should be satisfactory for service in feed pumps operating at temperatures up to 320 F. Two of three tests indicated that the rate of attack would be too high at 385 F for satisfactory service, the rate being about 10 times that found at 250 F. The rate of attack in the third test at 385 F was abnormally low, so much so that it was disregarded in evaluating this metal.

Test results obtained for leaded bronze indicated that it is not well suited for corrosion-erosion service at temperatures from 250 to 400 F. Experience with a coil-drains pump on an evaporator at the Trenton Channel plant corroborates these results. After operating for 6 months at approximately 400 F, the leaded-bronze wearing rings in the pump were badly damaged and had to be renewed, whereas other parts of the pump made of 12 per cent chromium steel were only slightly attacked.

Since even a small amount of chromium imparted a pronounced resistance to corrosion-erosion attack, it seemed that a thin chromium plate on the interior surface of carbon-steel pump casings might provide excellent protection for pumps already in service. It was determined that pumps could be plated at a reasonable cost. However, results of a test at 388 F of a chromium-plated (0.001-in. plate directly on steel[5]), cast carbon-steel specimen showed that the chromium plating was porous or cracked, which allowed the unprotected base metal to be attacked. The weight loss given for the specimen (see Table 2, test No. 12) is much too high as it includes part of the chromium plating which was stripped from the specimen during the cleaning treatment that preceded weighing. The view of the specimen, Fig. 8, shows that the chromium plating had broken down in spots and that the base metal had been attacked.

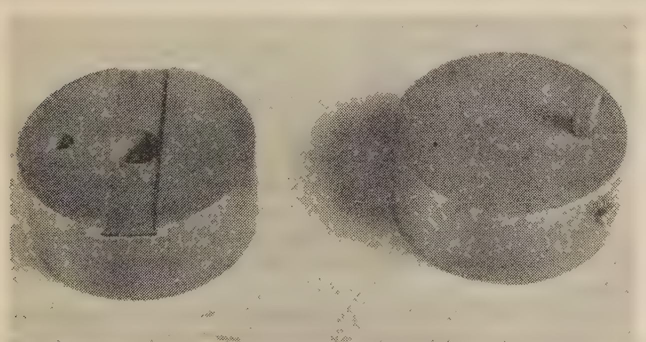

Fig. 8 Test Specimen No. 1F; Chromium-Plated Cast Carbon Steel After 500-Hr Test at 388 F

The results of the tests of cast carbon-steel specimens indicate that at 250 F the rate of corrosion-erosion attack increases with pH between 7.6 and 8.4, the rate at 8.4 being about double that at 7.6 (see Fig. 6). This is contrary to what is usually expected. However, in a different type of corrosion-erosion test, conducted at Ohio State University on similar material, using distilled water at 122 F, the rate at pH 8 was about 10 times that at pH 6, (see Fig. 9). These data tend to substantiate results obtained at Marysville, although no direct comparison is justified because of differences in test conditions. However, it is indicated that in-

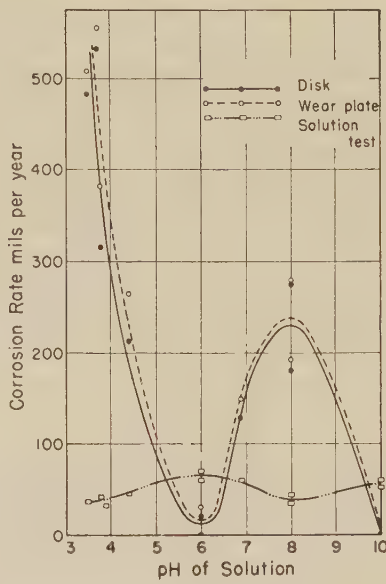

Fig. 9 Effect of pH on Corrosion-Erosion of Steel
(W. A. Luce, Engineering Experiment Station News, Ohio State University vol. 19, no. 5, pages 29–32.)

creases in feedwater pH for the purpose of reducing corrosion-erosion attack should be made with caution.

The attack on the 1.25 per cent chromium, 0.5 per cent molybdenum-steel specimen at 250 F and pH 8.4 (test No. 13, Table 2) was about twice that measured in the other tests at higher temperature and lower pH (test Nos. 10 and 11, Table 2). No direct comparison to show the effect of pH on this alloy could be made, however, as no tests had been made at 250 F and the lower pH. Although it seems that the higher pH had little effect on the corrosion-erosion resistance of the leaded bronze, here again comparable data were not available.

It was noted at the end of the test at 250 F and pH 8.4 (test No. 13), that the specimens were exceptionally clean. There was very little, if any, of the red iron oxide which formed heavy coatings on the specimens during earlier tests at 250 F and lower pH. This seemed to indicate that the higher pH retarded the formation of protective oxide films on the specimens, thereby promoting metal wastage.

Conclusions

The rate of corrosion-erosion attack on carbon steel decreased with increase in temperature of Marysville feedwater, whereas the rate of attack increased for chromium-iron alloys. There is some indication that attack of the chromium alloys is greatest at some point between 250 and 385 F. At all temperatures at which tests were made, the chromium alloys were much more resistant to corrosion-erosion attack than cast carbon steel, and therefore they are considered to be satisfactory for service in boiler feed pumps and regulating valves up to 400 F in all Detroit Edison plants where the feedwater has similar characteristics.

The 1.25 per cent chromium, 0.5 per cent molybdenum steel and the Cr-Ni-Mo steel were not attacked to a significantly greater extent than the 5 and 12 per cent chromium steels at the higher temperatures. Because of greater weldability and lower cost, it appears that the low-chromium alloys might be used advantageously in feedwaters having similar or less corrosive characteristics.

Leaded bronze is not a good material for use at 250 to 400 F under conditions where corrosion-erosion attack can be expected. Navy M bronze is satisfactory at temperatures up to about 320 F.

[5] Chrome-plating directly on the steel instead of on an intermediate plate of copper and nickel was recommended by the plater as a superior wear-resistant coating.

Chromium plating as a means of protecting existing carbon-steel pump casings is not satisfactory.

As in the previous tests,[4] the authors have not been able to deduce the underlying causes for corrosion-erosion attack, nor to determine which of the many variables is the most important. Increasing the pH of feedwater at Marysville from about 7.6 to 8.4, however, approximately doubled the rate at which cast carbon steel was attacked. This indicated that, for the Marysville feedwater, the lower pH is more desirable from the corrosion-erosion standpoint. While in some quarters higher pH values have been advocated as a panacea for all corrosion-erosion troubles, these results would seem to indicate that some caution should be exercised in increasing pH of feedwater indiscriminately.

Discussion

T. W. Bigger.[6] The Detroit Edison Company is to be warmly commended for making the investigation which is so ably reported in this and the original paper. The work has been carefully done and the information which is reported is usable and valuable to the industry.

Corrosion-erosion to an abnormal degree occurs only occasionally in a steam turbine, but is similar to that in feedwater pumps, in that it does not follow a set pattern as to the apparent conditions under which it does occur. Corrosion-erosion will be quite severe in a turbine in one plant, and an identical turbine in another with the same pressure and temperature conditions will be virtually free of damage. The erosion occurs principally on the low-carbon-steel parts, the high-chromium steels being but little affected by this type of attack.

Corrosion-erosion is not a serious problem in the superheat region of steam turbines, nor in the coldest stages at the exhaust end. However, it does occur in some machines in the so-called wet region, principally in the range where the steam contains up to about 5 per cent moisture. One turbine did not erode appreciably during the early months of operation when on base load, but corrosion-erosion became quite noticeable when the machine was changed to variable and intermittent operation. This can be construed as indicating that oxygen is a contributing factor.

Some time ago the writer's company studied the problem of determining the best method of making tests to solve the erosion problem. Moisture which is freshly formed within a turbine in a modern station is of a very high degree of purity, containing less impurities than the average distilled water. It was determined that the production of steam of sufficient purity in a laboratory would be extremely difficult and almost prohibitive in cost. It seemed that steam extracted from a turbine where erosion had occurred would be representative, and the Boston Edison Company kindly agreed to let us run the tests with steam extracted from such a turbine in its Mystic station.

About that time the original paper[4] by the present authors was published. Since the arrangement of specimens which they used simulated closely the condition of a leak between a turbine diaphragm and a shell ledge, and it seemed desirable for purposes of comparison to use a specimen which had been agreed upon in the industry, our specimens are dimensionally identical with theirs. To make possible a clean job of heat insulation we mounted our specimens in a recess in a solid block of steel and covered them with a small flange containing a jackscrew for clamping the specimens together.

Saturated steam for testing is taken from the 14th-stage extraction line and fed to eight specimens at 25 to 28 psig through a well-drained header. The supply laterals are short and receive steam from the top of the header. Several inches of each lateral are left bare to supply equal amounts of fresh moisture for the specimens. All inlet piping is stainless steel to minimize contamination. The exhaust goes to the main condenser where the pH of the condensate in the hot well is in the order of 6.5.

Tests of 1000 hr duration for a total of 16 specimens have been completed. Many of the specimens were of turbine materials commonly known as corrosion-resistant. They were run for purposes of comparison and of course stood up very well. A few specimens of cast low-carbon ferrous materials have been tried. From these essentially preliminary runs, we have been able to learn that 2 per cent chromium improves low-carbon cast steel for use under these conditions more than 4 to 1, a good check of the results reported in the paper under discussion. Cast iron was not benefited by the addition of up to 1.5 per cent nickel, but was improved nearly 50 per cent by the addition of 3 per cent nickel and 1 per cent silicon. Specimens of sprayed corrosion-resistant metals over cast iron are in test and in preparation.

A study is being made of the use of small amounts of alloying elements in carbon cast steel and cast iron with the object of producing useful low alloys at a reasonable cost. Samples of these alloys will be tested as rapidly as possible.

C. E. Brune.[7] Evidence from operating results in several stations of the American Gas and Electric System seems to indicate that plain carbon steel is subjected to greater attack under higher temperature or lower pH. Attack was evident sooner and more severe in stations with feed pumps handling water over 400 F than in a station where pumping temperature was less than 400 F. At one station a set of pumps with feedwater pH of 7.5 experienced severe attack while another set with feedwater pH of 8.5 experienced none. Feedwater temperature for both sets was 450 F. When the low pH was brought up to 8.5, the attack ceased.

Another phenomenon was experienced whereby deposits of corrosion products on sides of impellers, causing increase of motor horsepower, apparently, were reduced when feedwater temperature was reduced, by removing from service the last heater. In some instances, at least part of the deposit resulted from corrosion within the pumps. In one station the deposits started when ammonia content went down in the river from which evaporated make-up originates, and feedwater pH fell from above 8 progressively to as low as 6. When ammonia content of river water and feedwater pH rose to normal values, the deposits apparently disappeared. There may be a question whether lowered temperature and increased pH lessened the formation of corrosion products or whether these changes influenced only the deposition of those products.

From test No. 13, the authors incline to the belief that higher pH retards the formation of protective oxide film. The writer wonders whether the slightly more complete deaeration in test No. 13, as compared with earlier tests reported in the previous paper,[4] might not also have been a factor in retarding film formation.

While the authors consider the tests to justify use of the chromium alloys under test up to 400 F in deaerated feedwater, it is believed this limit can be raised, at least for some of those alloys, since no attack is evident on a 5.5 per cent chrome alloy in several stations on the A. G. & E. system after years of operation with deaerated feedwater at 450–460 F.

F. P. Fairchild.[8] This paper is a useful addition to the information presented by the authors in their first paper.[4] Our

[6] Development Engineer, General Electric Company, Schenectady, N. Y. Mem. ASME.

[7] Mechanical Engineering Division, American Gas and Electric Service Corporation, New York, N. Y.

[8] Chief Engineer, Electric Engineering Department, Public Service Electric and Gas Company, Newark, N. J. Mem. ASME.

corrosion-erosion tests on steel specimens with varying pH values indicate just the opposite of the findings of this paper, as reported in discussion of the paper on the first test program. We found that a higher pH results in less corrosion-erosion attack at both 90 and 205 F water temperatures.

Recently we made some corrosion-erosion tests in an attempt to determine why high-pressure boiler-feed-pump parts of nickel cast steel had a longer service life at Essex Station than similar parts under similar conditions at Marion Station. Detectors made from diffusers of the Essex and Marion pumps were tested side by side under similar conditions in the Marion feedwater. Contrary to expectations, the detector made from the shorter-lived Marion pump had the smaller weight loss in 500 hr by 12 per cent. Thus difference in materials was eliminated as an answer to the problem.

Having eliminated material as a cause of longer life, we next investigated the effect of condenser leakage, because the Essex condensate comes from condensers with packed tubes whereas the Marion condenser tubes are rolled at both ends. A tank and a variable-stroke proportioning pump were arranged to permit the injection of fluid from the tank into the line carrying feedwater to one of the detectors. Thus we were able to make concurrent corrosion-erosion tests comparing normal with polluted feedwater, using detectors of like material (cold-rolled steel).

Three tests simulating condenser leakage were run; two at Essex (4th and 5th) and one at Marion (11th), as shown in Fig. 10 of this discussion. In all of these tests a solution of condenser cir-

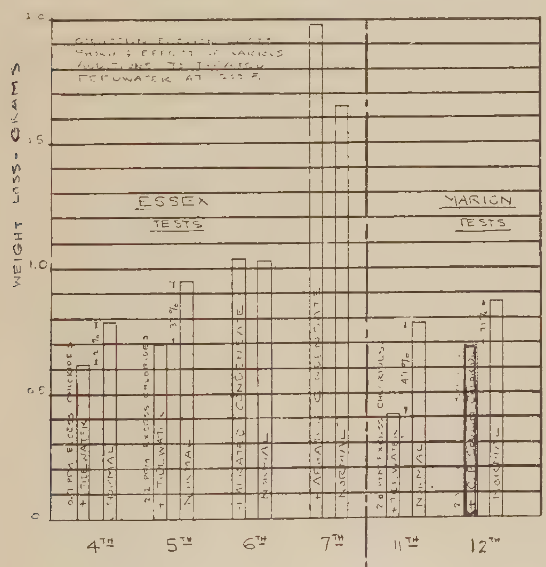

Fig. 10 Corrosion-Erosion Tests Showing Effect of Various Additions to Treated Feedwater at 200 F

culating water was injected into the line feeding one detector while normal feedwater flowed through the second detector. At Essex 0.7 ppm excess chlorides reduced the corrosion-erosion weight loss 21 per cent in 335 hr; and in the next run 2.2 ppm excess chlorides reduced the weight loss 37 per cent in 525 hr. At Marion the same test resulted in a reduction of weight loss of 47 per cent with 2 ppm excess chlorides in 500 hr.

Since the tank containing the injection water was an open tank, there was the possibility that oxygen in the water might be the cause of the unexpected results of pollution. Therefore, at Essex we repeated the test, polluting with undeaerated, pure condensate instead of raw water. The test shown as the 6th in Fig. 10, showed practically no effect of such pollution and very little difference in oxygen content of the two effluents. Another similar test (the 7th) was run in which air was bubbled through the condensate in order to increase the amount of oxygen in the injected condensate. In this case the corrosion-erosion of the polluted water was about 20 per cent greater than that of normal water. Thus oxygen was eliminated as a contributing factor.

The 12th test at Marion used a solution of chemically pure sodium chloride for pollution. In this case 2 ppm excess chlorides resulted in a reduction of corrosion-erosion weight loss of 21 per cent, about one half that resulting from the same excess chlorides with raw-water pollution.

In all of the foregoing tests, the degree of pollution was so small that there was no measurable difference between the pH of the normal and polluted water. This would seem to indicate that pH alone may not be the best criterion for controlling corrosion-erosion.

J. B. Godshall.[9] The reported unexpected effects of raising the pH value and the temperature of the feedwater are of considerable academic interest. The major consideration, however, is the confirmation of the earlier conclusions regarding the vast superiority of the chromium-bearing steels over carbon steels.

It is particularly interesting to note that 12 per cent chromium has virtually no advantage over 5 per cent chromium, 0.5 per cent molybdenum stainless steel. Furthermore, the lower-chromium steel has certain advantages. For example, it is less susceptible to galling in pump service.

Still lower-chromium steels, such as the 1.25 per cent chromium, 0.5 per cent molybdenum steel, may be practical for the feedwater at Marysville. Caution will be required if this material is considered for use in the many central-station feedwaters that are more aggressive toward carbon steel than the Marysville water appears to be.

These considerations, plus the impossibility of maintaining absolute control of the many variables affecting feedwater quality from a corrosion standpoint, indicate that the pump materials always should be selected for their ability to withstand any of the conditions likely to be encountered. Then, nominal fluctuation of the pH value or conductivity, or even a change in the water temperature, will be of no practical importance from the standpoint of corrosion-erosion.

The failure of the chromium-plated specimen probably was not unexpected. This failure, however, should not eliminate chromium plating from consideration for all feed-pump applications. Shaft sleeves are relatively easy to plate, and have very good resistance to corrosion-erosion by the feedwater. In addition, they provide an extremely hard, excellent wearing surface.

A. L. Penniman.[10] The writer believes there is a strong probability that some of the factors assumed to have been insignificant in effect as to rate of metal loss were perhaps actually significant. This comment applies particularly to the first paragraph under "Discussion of Results."

Since the average velocity is quite high and is accompanied by a sharp change in the direction of water flow, it is considered likely that there will be considerable variation in filament velocities with respect to both time and cross section which can result in some cavitation effect with material acceleration of metal loss, depending upon characteristics of metal and water. Under such conditions, it is believed that minor surface variations could influence the results materially.

[9] Metallurgist, Cameron Division, Ingersoll-Rand Company, Phillipsburg, N. J.

[10] General Superintendent, Electrical Operations, Consolidated Gas, Electric Light & Power Company of Baltimore, Md. Fellow ASME.

While it is recognized that maintenance of a constant differential pressure tends to maintain the average velocity of flow constant and thereby hinder large progressive changes in rate of loss, it is believed that the static pressure is also of importance and should be recorded since it, as well as temperature, affects cavitation.

It is noted that to obtain water at different temperatures, water was taken from different parts of the cycle. It is our opinion that such waters may differ in effect because of factors other than temperature which may have been assumed to be insignificant, e.g., suspended matter, metal and gas content. A filter is shown in Fig. 4 of the paper which obviously was intended to remove suspended matter. It would be of interest to learn the type and construction of this filter, since our experience in filtering-out suspended matter from boiler feedwater has not been considered satisfactory.

While the use of an evaporator may have been a convenient means of varying the pH content of the water, it is our opinion that there were influences other than pH which were brought into the picture, e.g., evaporator carry-over of solids and gases. Also, can we consider that it makes no difference whether or not the alkaline source is ammonia, ferrous hydroxide, or a solid like caustic soda?

Reference is made to Mr. Luce's work at Ohio State University, with Fig. 9 given as an illustration. While the statement is made that distilled water was used, the oxygen content was not mentioned. Since it is extremely difficult to obtain zero content of oxygen and other oxidizing influences, it is recommended that some statement be made about this. It would also be of interest to know about how the pH variation was obtained, and how the hydraulic conditions varied. Was only one point obtained at pH 10 where a negligible loss is shown?

If Mr. Luce's work is used as a criterion, it would appear that quite a number of plants in attempting to improve conditions have made them worse in maintaining the pH in the range of 8 to 9. However, maintenance of a pH of 6 does not fit in well with the use of sodium sulphite to react with remanent oxygen in the feedwater.

Authors' Closure

The work being done by the General Electric Company at the Boston Edison Company's Mystic station should produce some worth-while information. Inasmuch as the tests are being made with wet steam instead of water, information on a new phase of metal wastage will be obtained. It is interesting that results of tests of 2 per cent chromium cast steel obtained at Mystic station are similar to those obtained at Marysville with water. Information to be obtained on corrosion-resistant metals sprayed over cast carbon steel also will be valuable.

Experiences of the American Gas and Electric Company do not agree with the test results obtained at Marysville. The authors cannot explain this discrepancy. There is a possibility, however, that at 450 F corrosion-erosion might be much more severe than at 388 F, the maximum temperature used in the tests at Marysville. Because of the many variables involved, comparison of experiences on pumps operating on different feedwaters can be most misleading.

At the Detroit Edison Company's Connors Creek Plant where the feedwater temperature is approximately 250 F, severe corrosion-erosion of the feed pumps occurred when the pH of the feedwater was about 8.5. In this case, at least, the relatively high pH apparently did not protect the pumps.

A few years ago the source of feedwater for the evaporators producing make-up for the Connors Creek plant was changed. The new supply is practically free from ammonia whereas the old supply contained an appreciable amount. This caused a lowering of the pH from about 8.5 to about 8. Unfortunately, a change to corrosion-resistant metals for pump repairs was made at about the same time. This made it impossible accurately to gage the effect of the pH change. Results indicate, however, that the rate of corrosion-erosion is no higher than it was previously, and perhaps lower.

The experience of the American Gas and Electric Company indicates that the chromium alloys will give satisfactory service at temperatures 60 to 70 deg F higher than the test temperatures used at Marysville. This is a valuable supplement to the data submitted by the authors.

Results of the test presented by Mr. Fairchild indicate that the salts present in feedwater may have a very profound effect on the rate of corrosion-erosion attack of metals. Previously it was commonly believed that pH and dissolved oxygen were the most important factors. If the concentration of sodium chloride in the tests at Marion and Essex stations influenced the test results so greatly, it is conceivable that the presence of other salts may also greatly influence corrosion-erosion rates. This opens a whole new field the investigation of which would provide valuable information, particularly where salt water is used for condenser cooling.

At Marysville the salt concentrations in the feedwater were very low and specific conductance records indicated that variations were small. Therefore it is doubtful if variations in concentrations from one test to another had much effect on the results obtained. Inasmuch as concentrations in many plants cannot be controlled closely, Mr. Godshall's statement that ". . . pump materials always should be selected for their ability to withstand any of the conditions likely to be encountered" is a good one.

The filter about which Mr. Penniman inquired was placed in the circuit to remove suspended iron oxide from the feedwater used in the test. The filter element is made of a spool wound with cotton cord. The authors have found these filters to be quite effective for this purpose in this and similar installations.

The authors have no data nor have they seen any which would prove or disprove that one alkali is better than another for increasing the pH for corrosion prevention. The authors are inclined to agree, however, that the means for varying this pH may be most important.

The static pressure at the inlet to the test specimens was maintained at 700 psi, and the outlet pressure was, correspondingly, 400 psi. The saturation pressure corresponding to 388 F is about 200 psi gage. It is the authors' opinion that cavitation was not a factor under these conditions, which is supported by the fact that the type of metal wastage resulting from cavitation was not found.

When referring to Mr. Luce's work at Ohio State University, the authors neglected to state that it was done in aerated distilled water. The type of corrosion-erosion equipment used by Mr. Luce, and the conditions under which his tests were made were so different from the tests conducted by the authors that no valid comparison can be drawn between them. The authors merely wished to point out that some evidence exists tending to support the unexpected increase in corrosion-erosion attack secured on increasing the pH. These results were reported solely to indicate that changes in the pH should be made with caution.

The authors wish to express their appreciation to all those who submitted comments and discussion on the paper.

The Forces and Moments in the Leg During Level Walking

By B. BRESLER[1] and J. P. FRANKEL[2]

The mechanism of normal level walking is presented in this paper in terms of the displacements of and the force systems at the leg joints. The data on four normal subjects were obtained from simultaneous recording of the positions of the leg in space and the floor reactions during level walking. The mass moments of inertia of the lower extremity were determined experimentally and the effects of gravity and inertia were included in the analysis. The forces and moments are presented in terms of the space components referred to a system of horizontal and vertical orthogonal axes.

Introduction

As a locomotive mechanism the human body is extremely complex. In order to perform the various operations of locomotion such as walking, running, climbing slopes and stairs, man has been provided with an articulating system of levers (the arms, torso, and legs) connected by "superuniversal" joints (the shoulder, hip, knee, and ankle joints, for example). These levers are powered with a multitude of motor units (the muscle fibers) and operated by an elaborate network of controls (the nervous system).

The human mechanism is one that operates in three dimensions—further complicating its analysis. It is true that the main effects of locomotion are evidenced in a single plane (the plane of progression), but this should not lead one to neglect the effect of lateral displacement on the mechanics of locomotion. This omission has been made by some previous investigators in order to simplify the mechanical aspects of the problem, but does not seem to be justified by the results of this investigation.

Unlike the inanimate machines, one human body varies greatly from another in build (mass distribution), musculature (power supply), and mannerisms of motion (controlled by the nervous system). The effect of these variables on the displacement and forces involved in the locomotion process introduces an additional complication into the analysis of the experimental data.

Before attempting to correct any mechanical deficiencies in the human body, the surgeon, limb and bracemaker, and physiotherapist must be well-acquainted with the mechanical functions of the affected parts of the body. The techniques and scope of orthopedic treatment and surgery, limb and brace fitting, and the like are seriously limited by the force and displacement characteristics normally involved in the damaged or missing members. Recognizing the need for a scientific analysis of the mechanical functions of the legs in walking, the Advisory Committee on Artificial Limbs of the National Research Council and the Veteran's Administration sponsored a research program of fundamental studies of locomotion at the University of California at Berkeley.

In view of the range of variables involved in the mechanics of human locomotion, a complete analysis of the problem is not possible at this time. Various phases of this problem have already been reported (1),[3] others are now under investigation at the University of California Artificial Limbs Research Project. The material presented herein is based upon the investigations carried out at the University of California, and will deal primarily with the force systems in and the displacements of the lower extremities during level walking of normal subjects.

Historical Background

The present-day knowledge of the mechanism of locomotion is due to the contributions of many scientists. Only a few of these contributions will be mentioned here to introduce to the reader the state of present-day knowledge in this field.

In 1836, Wilhelm and Eduard Weber (2) presented a theory of walking and running based on measurements on cadavers and tests on living bodies. From studies of pendulum motions of the leg in both living and anatomical specimens the brothers Weber reached the conclusion that leg motion during the swinging phase of gait, that is, the time when the leg is off the ground, is a pure pendulum motion and does not depend upon muscular action. The Weber pendulum theory gave rise to much discussion by subsequent investigators and was later repudiated by Fischer and others. The Weber book contains also a great deal of information on other various aspects of gait, including a mathematical analysis of the data collected. In another publication Eduard Weber discusses some fundamental aspects of muscle physiology wherein the tension that a muscle can develop is compared to the shortening it undergoes. The importance of muscles as the prime movers of the articulating levers of the body focuses great attention on the work of Eduard Weber in this regard.

E. J. Marey, Professor at the College of France, reported in 1873, and on later dates (3, 4, 5, 6, 7) tests performed to determine the locus of the center of pressure on the sole of the foot and the vertical displacement of the body during walking. In addition, his computations of energy output during locomotion are worthy of mention in any bibliography however brief it may be. Marey's greatest contribution to the study of locomotion is no doubt his development of chronophotography. Successive exposures were made on the same photographic plate by means of a rotating disk in front of the camera. The subject was dressed entirely in black on which brilliant metal buttons and shining bands were attached to represent joints and bony segments. The subject, illuminated by the sun, was photographed as he walked in front of a black screen. This method is known as geometric photography, since the pictures obtained show points and lines only. Variations of this method have been used in practically all subsequent investigations, including that reported herein.

Otto Fischer, whose six volumes of research (8) were published from 1894 to 1904, is best-known for his studies on human gait.

[1] Assistant Professor of Civil Engineering, University of California, Berkeley, Calif.

[2] Instructor in Engineering, University of California, Los Angeles, Calif.

Contributed by the Applied Mechanics Division, co-sponsored with Management and Aviation Divisions, and presented at the Annual Meeting, New York, N. Y., November 28–December 3, 1948, of The American Society of Mechanical Engineers.

[3] Numbers in parentheses refer to the Bibliography at the end of the paper.

These were based upon chronophotographic studies similar to that employed by Marey but with some improvements. Fischer, a mathematician, in co-operation with Braune, an anatomist, made detailed studies (9) of the kinetic properties of the different segments of the human body. To these men belongs the credit for the first rational scientific investigation of the problems in human locomotion; so detailed was their treatment of the subject that no later publication has superseded the works of Braune and Fischer and that of Fischer himself as the classical works on gait.

In Moscow, in 1935, was published a comprehensive volume (10) on research in the biodynamics of locomotion performed by N. A. Bernstein and his associates. In this study the accuracy obtained by Fischer was questioned and techniques were developed to improve on his accuracy. In all, the gait of 65 subjects was investigated. Many more photographs were taken of the subject during one complete cycle of walking. Further, the curves were not smoothed out, since Bernstein felt that the complexity of locomotion would preclude the smoothing out of any curves. Fischer's data for locations of the centers of gravity of the various segments, their radii of gyration, and their relative masses were used in this study. The experiments included investigation of normal walking of men both carrying weights, and unburdened, as well as an analysis of fatigue effects due to these conditions. Mention is made of a volume on the determination of the masses and centroids of the segments of the human body on live subjects, but at the time of this writing such information has not become available to the authors. Mention is made, however, of the fact that differences from Fischer's data were found.

Most recently, Elftman has reported in articles from 1934 to the present, investigations on locomotion including studies of the distribution of pressure in the human foot (11), the function of the arms in walking (12), the force exerted by the ground in walking (13), the rotation of the body (14), the forces and energy changes in walking (15), the function of the muscles in locomotion (16), and the action of muscles in the body (17).

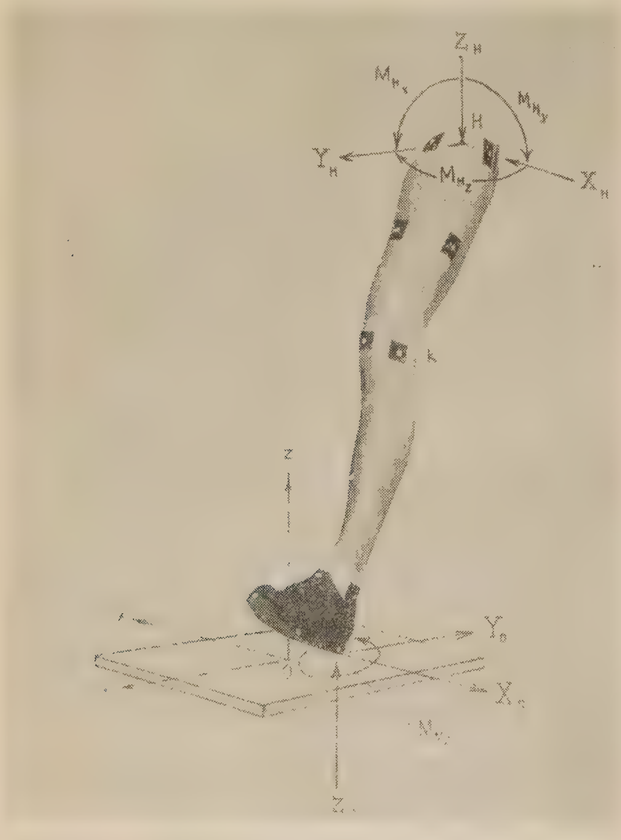

Fig. 1 Free-Body Diagram; Left Leg

Elftman has made a valuable contribution to the analysis of problems of locomotion even though he had a limited amount of experimental data at his disposal. Some of the results and conclusions presented were based partly on Fischer's classical experiments and partly on Elftman's direct measurements. The present investigation of locomotion, considered as a three-dimensional process, was undertaken at the suggestion of Elftman.

Theoretical Analysis

It has been felt by the authors that a knowledge of the positions of the joints of the lower part of the body and the internal force systems at these joints offer an adequate introductive description of the locomotive process of man.[4]

Fig. 1 is a free-body diagram of the leg during the stance phase of walking, i.e., when the foot is in contact with the ground. The reference (co-ordinate) axes are taken with the origin at the center of the force plate (described in the next section), and are designated by the lower-case letters x, y, and z. Postive co-ordinates denote inward (with respect to the leg investigated), forward, and upward directions. To define the position of a particular point of the leg, appropriate subscripts are used, e.g., x_A, y_A, and z_A are the three space co-ordinates of the ankle joint. The following subscripts are used throughout the paper

F = foot A = ankle
S = shank K = knee
T = thigh H = hip
O = center of pressure on the foot

The external forces acting on the body during walking are of only two types; (a) gravitational, due to the weights of the various parts of the body; and, (b) reactional, representing the ground forces acting on one or both feet.

The gravitational forces are considered acting at the centers of gravity of the leg segments, and are denoted by W with an appropriate subscript. Thus W_F denotes the weight of the foot, W_S denotes the weight of the shank of the leg, etc.

The ground reactions on the foot are obtained experimentally from a force-plate record and are considered to be applied to the foot at the center of pressure, which is also defined by the force-plate record. As shown in Fig. 1, X_0, Y_0, and Z_0 are the components of the ground reaction, and M_{0z}, is the torque in the plane of the force plate between the foot and the plate.

The internal forces acting at the leg joints are resolved into components parallel to the xyz reference axes and are denoted by X, Y, and Z, respectively. To define the force acting at a particular joint appropriate subscripts are used, e.g., Z_A denotes a vertical force at the ankle joint, Y_A denotes forward force at the ankle, etc. The sign convention used in the calculations of the joint forces is as follows:

X = inward force with respect to part of leg below joint.
Y = forward force with respect to part of leg below joint.
Z = compressive force (acting downward on part of leg below joint.

The internal moments acting at the leg joints are denoted by M_A, M_K, and M_H, at the ankle, knee, and hip, respectively. These moments are resolved into components about the xyz reference axes and are defined by appropriate subscripts, e.g., M_{Ax} denotes an internal moment at the ankle about the x-axis (a fore-and-aft moment), M_{Ay} denotes an internal moment at the ankle about the y-axis (inward-outward moment), etc. The sign

[4] A paper describing the energy and power aspects of locomotion is now in preparation.

convention used in the calculation of the internal moments is based upon the "screw" rule, the right-hand rule being used for the right leg, while, for the left leg, the left-hand rule is used, see Fig. 1.

By considering a free-body diagram of the leg below a section cut at a joint, one may state the equations of motion for the free body in terms of forces and accelerations. Using D'Alembert's principle of "equilibrium" of bodies in motion, the internal forces (or moments) at the joints can be expressed directly in terms of reaction forces (R), gravity forces (G), and "inertia forces" (I). Thus may be obtained the relations shown in Table 1. This table shows the reaction, gravity, and inertia terms in summary form for all force components at the joints of the leg. The symbols used in Table 1 and not previously explained are as follows:

g = acceleration due to gravity
$\ddot{x}, \ddot{y}, \ddot{z}$ = components of linear acceleration of centroid of segment
$\alpha_x, \alpha_y, \alpha_z$ = components of angular acceleration of segment
J_x, J_y, J_z = mass moments of inertia of segment about three axes through its center of mass

Experimental Methods and Reduction of Data

For a complete description of the behavior of the legs of the human mechanism in walking a knowledge of the forces and moments at the joints is essential. The determination of these forces and moments requires either measurement or calculation of the mass distribution of the leg, displacements and accelerations of the leg segments through one complete cycle, and the reactional forces of the ground on the foot.

Mass Distribution of Leg. The mass distribution of the leg is defined in terms of the weight (or mass), the location of the center of mass, and the mass moment of inertia about the center of mass. To date no adequate method has been presented whereby the numerical values of mass and inertia can be measured accurately from living subjects.[5] The most commonly used methods are the use of Fischer's coefficients and the Weinbach graphical method (19). Braune and Fischer (8, 9) established coefficients for expressing the relative masses of the segments as compared to the body as a whole, and the position of centers of mass and radii of gyration of the segments as proportional parts of the length of the segment. Although Braune and Fischer worked on a few frozen corpses their results have been accepted and used in most subsequent investigations. According to Fischer, the weight

[5] A reference to a Russian publication dealing with this subject has come to the attention of the authors, but this is not available in the United States at this time. The reference is given in the Bibliography as item (18).

TABLE 1 FORMULAS FOR JOINT FORCES AND MOMENTS

EFFECT OF:			FLOOR REACTIONS---R	GRAVITY---G	INERTIA --I
COLUMN:		(1)	(2)	(3)	(4)
ANKLE	FORCES	X_A	X_o	0	$\frac{1}{g}(W_F \ddot{x}_F)$ or X_F
		Y_A	Y_o	0	$\frac{1}{g}(W_F \ddot{y}_F)$ or Y_F
		Z_A	Z_o	$-W_F$	$-\frac{1}{g}(W_F \ddot{z}_F)$ or $-Z_F$
	MOMENTS	M_{Ax}	$Z_o(y_o-y_A)-Y_o(z_A)$	$-W_F(y_F-y_A)$	$Y_F(z_F-z_A)-Z_F(y_F-y_A)+J_{x_F}\alpha_{x_F}$
		M_{Ay}	$-Z_o(x_o-x_A)+X_o(z_A)$	$W_F(x_F-x_A)$	$-X_F(z_F-z_A)+Z_F(x_F-x_A)+J_{y_F}\alpha_{y_F}$
		M_{Az}	$M_{oz}-Y_o(x_o-x_A)+X_o(y_o-y_A)$	0	$X_F(y_F-y_A)-Y_F(x_F-x_A)+J_{z_F}\alpha_{z_F}$
KNEE	FORCES	X_K	X_o	0	$\sum_i^{F,S}\frac{1}{g}(W_i\ddot{x}_i)$ or X_F+X_S
		Y_K	Y_o	0	$\sum_i^{F,S}\frac{1}{g}(W_i\ddot{y}_i)$ or Y_F+Y_S
		Z_K	Z_o	$-W_F-W_S$	$-\sum_i^{F,S}\frac{1}{g}(W_i\ddot{z}_i)$ or $-Z_F-Z_S$
	MOMENTS	M_{Kx}	$Z_o(y_o-y_K)-Y_o(z_K)$	$-W_F(y_F-y_K)-W_S(y_S-y_K)$	$\sum_i^{F,S}[Y_i(z_i-z_K)-Z_i(y_i-y_K)+J_{x_i}\alpha_{x_i}]$
		M_{Ky}	$-Z_o(x_o-x_K)+X_o(z_K)$	$W_F(x_F-x_K)+W_S(x_S-x_K)$	$-\sum_i^{F,S}[X_i(z_i-z_K)-Z_i(x_i-x_K)-J_{y_i}\alpha_{y_i}]$
		M_{Kz}	$M_{oz}-Y_o(x_o-x_K)+X_o(y_o-y_K)$	0	$\sum_i^{F,S}[X_i(y_i-y_K)-Z_i(x_i-x_K)+J_{z_i}\alpha_{z_i}]$
HIP	FORCES	X_H	X_o	0	$\sum_i^{F,S,T}\frac{1}{g}(W_i\ddot{x}_i)$ or $X_F+X_S+X_T$
		Y_H	Y_o	0	$\sum_i^{F,S,T}\frac{1}{g}(W_i\ddot{y}_i)$ or $Y_F+Y_S+Y_T$
		Z_H	Z_o	$-W_F-W_S-W_T$	$-\sum_i^{F,S,T}\frac{1}{g}(W_i\ddot{z}_i)$ or $-Z_F-Z_S-Z_T$
	MOMENTS	M_{Hx}	$Z_o(y_o-y_H)-Y_o(z_H)$	$-W_F(y_F-y_H)-W_S(y_S-y_H)-W_T(y_T-y_H)$	$\sum_i^{F,S,T}[Y_i(z_i-z_H)-Z_i(y_i-y_H)+J_{x_i}\alpha_{x_i}]$
		M_{Hy}	$-Z_o(x_o-x_H)+X_o(z_H)$	$W_F(x_F-x_H)+W_S(x_S-x_H)+W_T(x_T-x_H)$	$-\sum_i^{F,S,T}[X_i(z_i-z_H)-Z_i(x_i-x_H)-J_{y_i}\alpha_{y_i}]$
		M_{Hz}	$M_{oz}-Y_o(x_o-x_H)+X_o(y_o-y_K)$	0	$\sum_i^{F,S,T}[X_i(y_i-y_H)-Y_i(x_i-x_H)+J_{z_i}\alpha_{z_i}]$

NOTE: COLUMN (1) · (2) + (3) + (4)

of a segment divided by the weight of the body is a constant C_1; the distance of the center of mass from the proximal joint divided by the length of a segment is a constant C_2, and the radius of gyration of the segment about the mediolateral centroidal axis divided by the length of segment is also a constant C_3. Thus

(a) Weight of segment $= C_1 \times$ weight of body
(b) Distance from proximal joint to center of mass of segment $= C_2 \times$ length of segment
(c) Radius of gyration, $\rho_x = C_3 \times$ length of segment; hence mass moment of inertia J_x = mass of segment $\times (\rho_x)^2$

The method proposed by Weinbach is based on the assumption that any cross section of a segment is elliptical and that the density of the body is uniform throughout. The masses, the locations of the centers of mass, and the radii of gyration of the leg segments may be determined by numerical or graphical integration of data obtained from front and side-view photographs of the leg. This method, proposed by Weinbach, is so tedious that in view of the questionable assumptions of ellipticity and uniform density, it was deemed adequate for the purpose of this paper to use Fischer's coefficients of location of centers of gravity, weights and masses, and the radii of gyration.

Calculations for the mass, centroid location, and moment of inertia of the combined shank and foot of one normal subject were made using both Fischer's and Weinbach's methods. All values as determined by Weinbach's methods were less than those by Fischer's method by about 10 per cent of the latter.

In the case of the location of the center of mass of the foot, Fischer's laborious graphical construction was replaced by an arbitrary coefficient. Table 2 shows the coefficients used in the calculations.

TABLE 2 ASSUMED COEFFICIENTS

Member	C_1	C_2	C_3
Body..........	1.0000	....	....
Thigh..........	0.1158	0.44	0.31
Shank..........	0.0527	0.42	0.25
Foot...........	0.0179	0.35	0.30

In order to check the accuracy of the coefficients listed in Table 2, a simple experiment was performed at the University of California.

A subject was seated so that one leg was supported only by a chair, as in Fig. 2. A cable connected to a proving ring was attached to the ankle. Mounted on the same ankle was an electrical accelerometer. The subject, by extending his knee joint, created a tension in the cable which was measured by the proving ring and a recording oscillograph. The moment of this force about the knee was thus determinable from the recorded force and the known distance of the cable from the knee joint. The cable was then cut, with the result that the shank and foot swung upward rapidly. The acceleration of the ankle was recorded on an oscillograph actuated by the accelerometer, and the angular acceleration of the foot and shank about the knee computed.

By assuming that the knee moment (M) supplied by the musculature was equal to the external moment before the cable was cut, the moment of inertia of the foot and shank about the knee J_x' was computed from the relationship

$$J_x' = \frac{M}{\alpha_x}$$

The results of the experiments on three subjects are presented in Table 3.

The fair agreement between the theoretical and experimental values shown in Table 3, together with the small effect of inertia

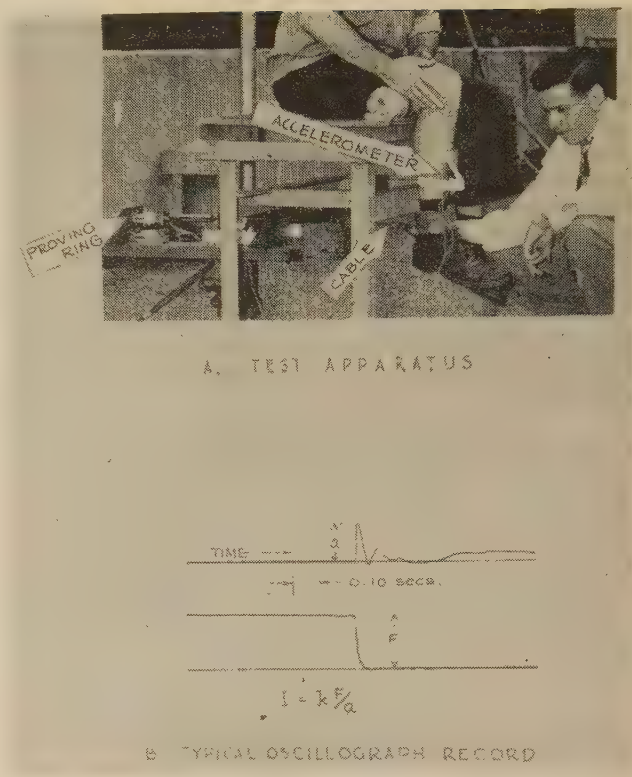

FIG. 2 MOMENT OF INERTIA DETERMINATION

(see "Results"), would seem to indicate that use of the coefficients shown in Table 2 is sufficiently accurate for purposes of comparison of several subjects.

TABLE 3 COMPARISON OF EXPERIMENTAL AND THEORETICAL VALUES OF MOMENT OF INERTIA OF LOWER LEG PLUS SHOE, ABOUT KNEE

Subject	Experimental J_x', slug-ft²	Theoretical J_x' (from Table 2), slug-ft²
1	0.28	0.274
2	0.20	0.265
3	0.24	0.258

Displacements and Accelerations. Several methods of defining the displacements, velocities, and accelerations of the joints of the leg were tried. The chronophotographic method of Marey, as improved by Fischer, was improved still further by substituting continuously lighted opthalmoscope bulbs at significant points on the leg, and taking all pictures in a darkened room. By exposing the film to the lights 30 times each second, a photograph containing many points of light was obtained. With the application of a suitable scale factor the co-ordinates of the lighted joints could be plotted, and graphic or arithmetic methods used to calculate velocities and accelerations. This method was useful only for the side view of the walking operation, since there was no gradual displacement of the body when viewed from the front to preclude overlapping of the point images on the film. In addition, the allowable magnification of the film was too limited to allow of accurate convenient reduction of the data.

For these reasons 35-mm motion-picture photography taken at 40 frames per sec from the front and side, while the subject was walking over a force plate, was used to obtain joint displacements. Targets were placed as close as possible to the most probable locations of the centers of the joints at the toe, ankle, knee, and hip of the leg nearest the side camera. Fig. 3 shows the positions of these targets. The use of targets taped to the skin involves

several limitations, namely, the movement of the skin over the bone causes some slight error in location, and due to the definite thickness of the limbs, the front and side targets will not be at the same elevation when the member, is inclined. Since the elevation in the frontal view figures in the determination of lateral movement, while that in the lateral view determines the fore-and-aft moment, small discrepancies will exist in a comparison of the two components of moment. The resulting film was projected to about one-half actual size and the co-ordinates plotted to a convenient scale. The origin of co-ordinates was taken as the center of the wearing surface of the force plate; the co-ordinate axes were z, positive upward; x, positive inward; and y, positive forward. Figs. 4 to 6, inclusive, show the displacements of the leg joints as obtained from the motion-picture records.

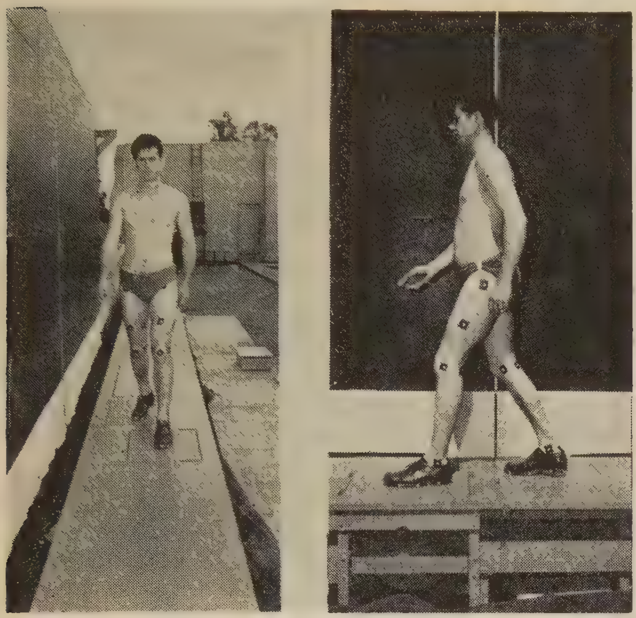

Fig. 3 Subject 4 on Force Plate

The x, y, z-components of the linear accelerations of the joints were obtained by differentiating twice the curves of the joint displacements with respect to time. In view of the accuracy of the motion-picture data, it was found that graphical differentiation was the best and quickest method and hence was used for determining accelerations.

The co-ordinates of the center of mass of each segment were obtained on the basis of the coefficients given by means of simple equations, for example (referring to Fig. 1 and Table 2)

$$x_S = x_K + 0.42\,(x_A - x_K) = 0.58x_K + 0.42x_A$$

where

x_S = x-co-ordinate of shank center of mass
x_K = x-co-ordinate of knee joint
x_A = x-co-ordinate of ankle joint

The linear accelerations of the center of mass of each segment were obtained in a similar manner, using the same form as the equations for center-of-mass location, but substituting accelerations for displacements in the foregoing equation.

In order to facilitate the calculations of the location of center of mass and corresponding linear accelerations simple nomograms were used.

The α_X and α_Y components of the angular accelerations of each segment were calculated from the linear accelerations of the two end points of the respective segment, as follows:

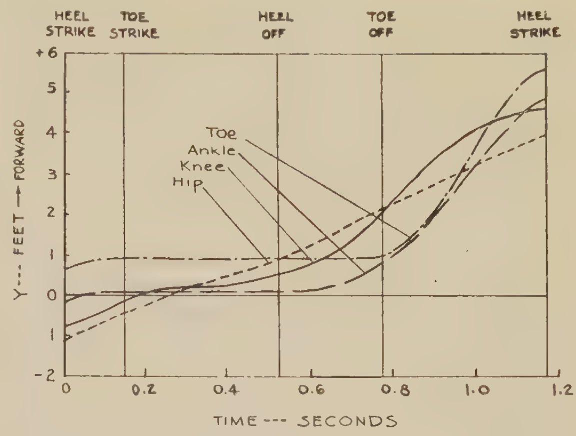

Fig. 4 Fore-and-Aft Displacement of Joints of Leg; Subject 1

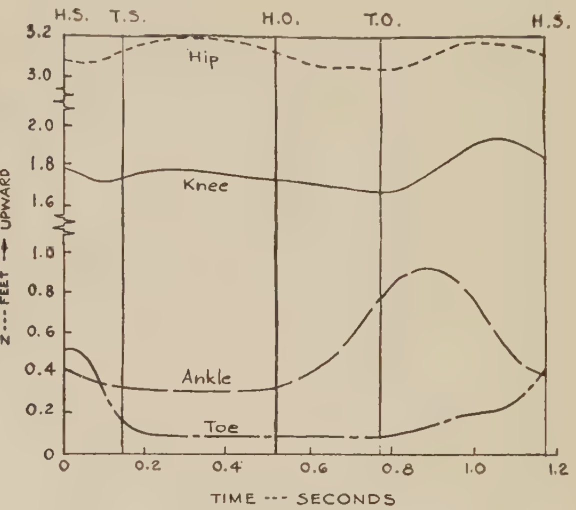

Fig. 5 Vertical Displacement of Joints of Leg; Subject 1

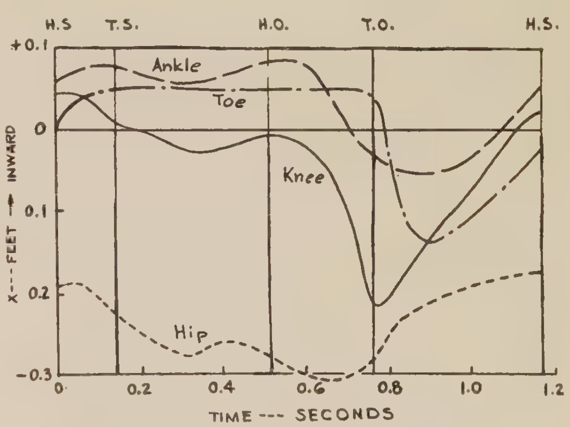

Fig. 6 Lateral Displacement of Joints of Leg; Subject 1

The tangential component of the relative acceleration of the upper joint with respect to the lower joint of a particular leg segment is equal to the product of the distance between the joints and the angular acceleration of the segment. The sign convention for the angular acceleration is the same "screw" rule convention as used for the moments.

The effect of the angular acceleration about the z-axis on the moments about the z-axis is very small, and hence was neglected in the calculations. Further, the angular accelerations about the z-axis could not be computed without the aid of measurements of the twists of the segments (21).

Reaction Forces. The reaction forces on the foot were measured on a force plate designed and manufactured under the supervision of Don M. Cunningham at the Artificial Limbs Research Project of the University of California. The lack of moving parts, and the recording of all measurements on an oscillograph tape made this force plate ideal for the problem at hand. The force plate determined the location of the center of pressure, the torque about z-axis, and the vertical and horizontal forces applied to the foot. A paper dealing with the details of the equipment and experimental procedures is now in preparation.

Data Reduction. The computations were set up in a tabular form but, nevertheless, constituted long and tedious procedure. The extent of the work involved in calculating the quantities for only one stride is indicated by the fact that approximately 14,000 numerical calculations were performed, 72 curves were plotted, and 24 curves were subjected to graphic differentiation. This work required approximately 500 man-hours at first but due to increased experience of the reduction personnel the computations for the fourth subject were completed in 250 man-hours.

Results

Displacements. While the subject is walking forward in a relaxed automatic manner, various segments of the body undergo displacements during different phases of a stride. The integrated result of these displacements is a stable, uniform, and mechanically efficient process of locomotion. Some displacements have a definite function in the process of locomotion—such as stabilizing the body during support on one foot, improving efficiency of muscle action, etc. Other displacements have no definite apparent function. A complete description of the kinematics of human locomotion will not be given here, since it is not necessary for analysis of the force system in locomotion. A few brief remarks about the displacement data used for force calculations are, however, in order.

Figs. 4, 5, and 6 show the components of the linear joint displacement of one subject in graphical form. A typical stride shown in these figures consists of a complete cycle of stance (foot in contact with the ground) and swing (foot off the ground) starting at heel strike of the left foot and ending at the next heel strike of the same foot. This cycle takes 1.18 sec, during which the subject moves forward through a distance of 5 ft.

It is apparent from examination of Fig. 4 that the hip moves through 5 ft at about a uniform rate during the entire cycle, while the toe and the ankle move through 5 ft only during 0.4 sec of the swing phase; thus the foot and ankle have larger accelerations than the hip.

Fig. 5 shows the vertical displacements of the leg joints. The rapid toe descent following heel strike, and the toe pickup during the swing phase are clearly apparent. The ankle starts rising just preceding toe-off, and starts descending just after toe-off. Little vertical motion takes place at the knee. The hip joint has a displacement pattern which is typical of joints lying closely to the torso: it has a period half that of the complete stride—the hip rises and falls twice during one complete stride.

The mediolateral displacements of the leg joints are shown in Fig. 6. These displacements are of relatively small magnitude but are of great importance for the stability of the body during normal walking. As the weight is transferred from one leg to the other, the body shifts toward the weight-bearing side. The lateral displacements of the hip joint, shown in Fig. 6, clearly indicate this motion. These data exhibited a large amount of scatter and the smooth curves representing joint-displacement variation are the best approximations. While the forward and vertical displacement patterns, shown in Figs. 4 and 5, are also represented by smooth curves, the amount of scatter for these data are definitely negligible. In comparing the character of data in Figs. 4, 5, and 6, however, it must be remembered that the displacement scales in these figures vary a great deal. The relative scales of the displacements are 20:4:1 for the forward, vertical, and lateral movements; thus any inaccuracy in the lateral-displacement data is much exaggerated.

It must be emphasized that locomotion involves a very sensitive balance on one foot—it has been previously described as a continuous process of fall and recovery—and therefore small displacements from the position of unstable equilibrium are to be expected. The stability of locomotion is preserved by muscle actions (controlled by nerve impulses) which tend to return the body to the equilibrium position. This results in minute jerkiness of motion which is not ordinarily apparent, but contributes to the scatter of the data. This "jerky" characteristic of locomotion is not reproducible, and the small deviations from the smooth process vary in each step even for the same subject. Since the purpose of this analysis is to consider the forces and displacements involved in a general reproducible pattern of locomotion, it was considered that smoothing out the displacement curves was justified.

Forces and Moments. The results of the computation of the forces and moments at the joints of the same subject are plotted in Figs. 7 and 8. To correlate the variation of the forces and moments with the position of the leg in space, the time of heel strike, toe strike, heel-off, toe-off, and the heel strike of the next stride are shown in the figures.

In order to obtain the over-all system of forces acting on the body, the forces acting on both legs must be considered. The total force on the body can be obtained by superposition of two curves, adjusting the time of beginning of each curve to correspond to the proper phase sequence of motion. This places the heel strike of the opposite leg little less than halfway between heel-off and toe-off of the given leg. (An accurate analysis of the forces acting on the body has been carried out at the University of California using data from two force plates. This analysis has not been included here).

The X-(lateral) components of joint forces shown in Fig. 7 have very small magnitudes. These forces are important, however, in providing the lateral stability in walking and contribute a large share of the lateral hip moment (M_{H_y}). As the body weight is shifted from one leg to the other the lateral force must be directed inward with respect to the body (negative X_H), in order to prevent the subject from falling sidewise. The magnitude of this force will depend largely upon the amount of lateral hip motion.

The Y-(fore-and-aft) components of joint forces shown in Fig. 7 have a typical shape approximating a full sine wave during the stance phase. During swing phase, the Y-forces are small and their variations are somewhat irregular. With the sign convention adopted in this analysis, a positive Y-force indicates an external force tending to retard the forward motion of the body. Thus it is apparent that the variation in Y-component of the force on the leg is due to the fact that upon heel strike the leg first must retard the forward motion of the body, and then a fraction of a second later must provide the "push-off" or forward acceleration necessary to continue the motion.

The Z-(vertical) components of joint forces shown in Fig. 7 have a typical double-peak shape; this is due to vertical upward and downward accelerations of the body. The difference between the vertical component of floor reaction Z_0 (very nearly equal to Z_A), and the body weight is proportional to the vertical accelera-

tion of the body. The first peak occurs shortly after heel strike, when the body rolls over the supporting leg, and the other peak occurs when the leg "pushes" the body up just before the other leg strikes the floor.

The differences between the forces at the ankle, knee, and hip joints indicate the effect of gravity and inertia at these joints. Thus the maximum vertical compressive force occurs at the ankle joint, while at the hip joint this force is reduced by the gravity and inertia effects of the shank and thigh. The variation in the X-

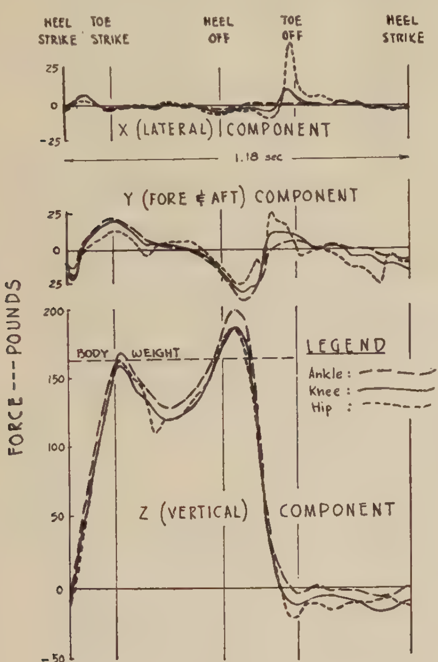

Fig. 7 Joint Forces; Subject 1
(Time for one complete stride, 1.18 sec.)

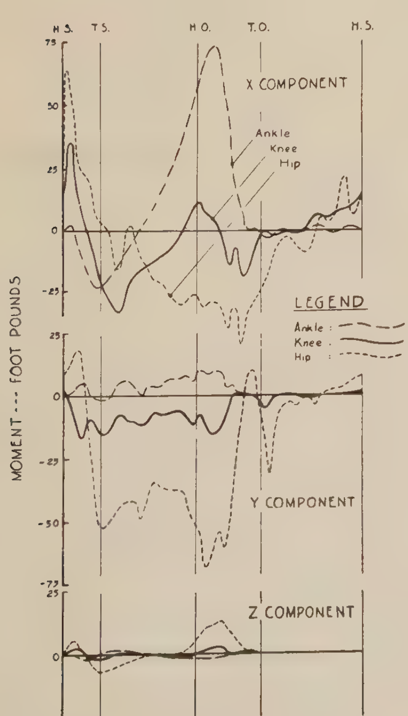

Fig. 8 Joint Moments; Subject 1

and Y-components of forces at the ankle, knee, and hip joints are due to inertia effects only, since gravity does not affect these components.

The X-component of moment shown at the top of Fig. 8 is that component tending to extend or flex the foot. From the adopted sign convention, a positive X-moment would be produced by the resultant force passing in front of the joint. Thus the negative X-moment occurring just after heel strike indicates that the resultant force passes behind the ankle at this time, when the toe is still being lowered. When the foot is flat the load shifts so as to pass ahead of the ankle, yielding positive moment which increases rapidly, reaching a maximum value at the time the subject pushes off on the foot. It is to be expected that the magnitude and timing of the negative moment, occurring when the foot is being lowered, would be a definite aid in diagnosis of such pathological conditions, as, for example, tabes dorsalis where the foot is allowed to slap down, possibly registering less negative moment over a shorter time than normal.

The X-component of the knee moment registers quite clearly a phenomenon of gait found in nearly all normal subjects to date. The sign of this component of the knee moment is such that, when negative, the resultant force passes behind the knee, tending to flex it (and therefore render it unstable), while a positive moment indicates that the knee is being moved into or held in a "locked" position (stable). Thus, from the curve, one may conclude that at heel strike the leg is quickly stabilized, then unlocked; and once again locked for the push-off phase of the step. This "double-locking" action permits the subject to move forward with a minimum raising of his center of gravity, and therefore with less expenditure of work.

The location of the resultant of the forces at the hip, as partially indicated by the sign and magnitude of the X-component of the hip moment, serves to demonstrate the precept of continual rotation of the body pointed out so clearly by Elftman (14). The initial positive moment at the hip indicates that the forward rotation of the torso is being retarded, while the later change to negative moment indicates the renewal of forward torso rotation.

The lateral components of moment reflect the requirements of bipedal walking on the joints of the leg. In shifting from leg to leg, the torso is shoved first one way then the other, and moments somewhat proportional to the elevation of the joint above the ground are recorded. This points out the relatively large magnitude of the Y-(lateral) component of moment at the hip, a factor beyond the analysis of investigations which have their attention confined to the plane of progression.

The Z-components of moment reflect the positioning of the shears in the leg, and therefore may be associated largely with the twist of the body as well as that of the segments of the leg. Of interest is the fact that the results of pin studies (21) on twist of the segments agree quite consistently in phasic nature with the M_Z-curves in Fig. 8.

Fig. 9 illustrates the significance of inertial and gravitational effects on the fore-and-aft moments at the ankle, knee, and hip. The contributions of reactions to these moments at the ankle, knee, and hip are compared to the total computed moments, so that the difference in ordinate between the total moment and the reactional moment represents the effect of gravity and inertia of the segments below the indicated joint. It is apparent from Fig. 9 that the effect of gravity and inertia on fore-and-aft moments is very small for the ankle and knee moments, and relatively small on the hip moments throughout most of the stance phase.

Since the computations of the moments about the joints due to these effects are the bulk of the calculations, a rapid first approximation to the magnitudes of moment and force may be made by considering only the moment due to the floor reactions. In

the case of the hip, however, considerable error may be introduced in such an approximation.

To serve as an indication of the general value of the results for one subject, comparisons of several characteristic joint forces and

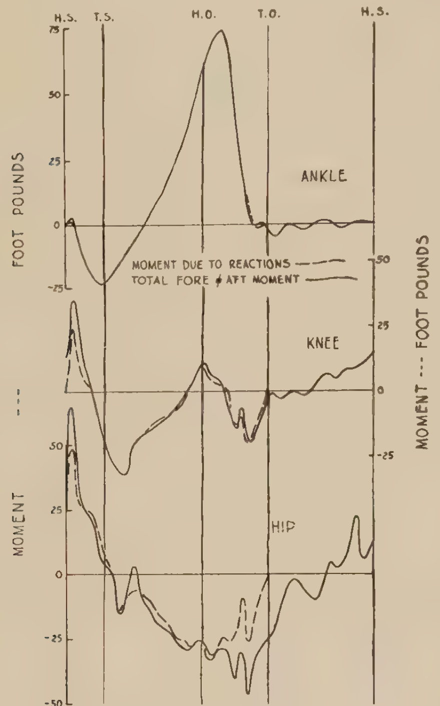

Fig. 9 Contribution of Reactions: Fore-and-Aft Moments; Subject 1

moments, computed for four subjects, are shown in Figs. 10 to 14, inclusive. The values plotted are the vertical force at the ankle (Fig. 10), fore-and-aft moments at the ankle, knee, and hip (Figs. 11, 12, and 13), and lateral moments at the hip (Fig. 14). These curves were selected as the most important ones, particularly from the point of view of magnitude. In these figures the time scale is plotted as per cent of the time for one complete stride, in order that the phasic activity of the four subjects can be most closely compared.

The examination of the comparison curves for four subjects illustrates the degree of variation between the individual subjects. Notwithstanding the large variations in magnitudes of the peak values and their phases relative to heel strike, the general patterns of the curves discussed with reference to Figs. 7 and 8 are apparent.

The curves shown are but one way of plotting the results of the calculations. If one chooses to ignore the inertial effects and the weight of the segments of the leg, a very convenient method of representing the results would be that employed by Elftman and his co-workers at New York University. This consists in plotting the positions of the segments in space as lines, and showing the accompanying floor reactions as vectors with the proper magnitude, direction, and point of application. By prolonging the line of action of this force vector, one may note by inspection the orientation of the joints of the leg with respect to the line of action of the ground force. One of the limitations of this method is that the walking cycle must be broken into many small intervals if one is to obtain a reasonable picture of the gait of the individual—a procedure of dubious economy, compared to the instantaneous indications of such curves as are presented herein.

No study of the mechanics of locomotion would be complete without the mention of the bone forces. Only the muscles at a joint can provide the moments, and since they act only in tension, the resultant force at a joint at the times when moment is evidenced can be compressive only if the bone forces are very high compressions themselves. Since muscles may also act to oppose each other at a joint so that there is no resultant moment, high compressive bone forces may be expected at times when there is no moment. It is not unreasonable to expect that at such times as push-off the bone forces may easily exceed twice the body weight. Inman (20) has investigated forces acting on the femur at the hip joint under several static conditions. He found that under these conditions the force on the femoral head is 2.4 to 2.6 times as great as the body weight, while the tension in the abductor muscles is 1.4 to 1.9 times the body weight. The magnitudes of the lateral hip moment used in Inman's investigation approach closely the peak values compute

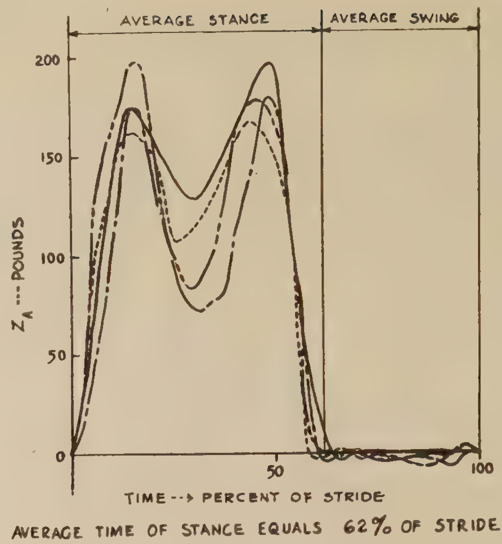

SUBJECT	CODE	HEIGHT	WEIGHT
1	———	6'-1"	165 lbs.
2	-----	5-8	153
3	—·—	5-8	140
4	—··—	5-11	161

Fig. 10 Vertical Ankle Force; Four Subjects

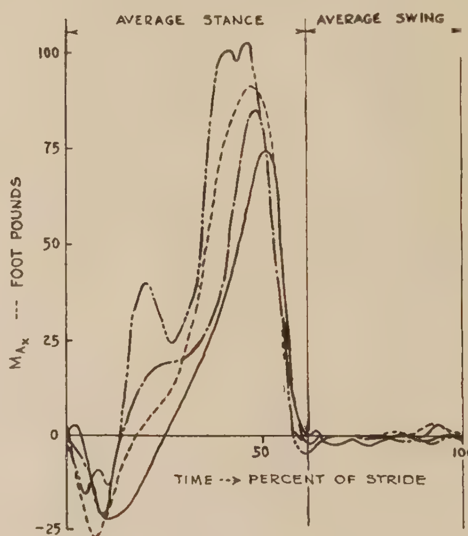

Fig. 11 Fore-and-Aft Ankle Moment; Four Subjects

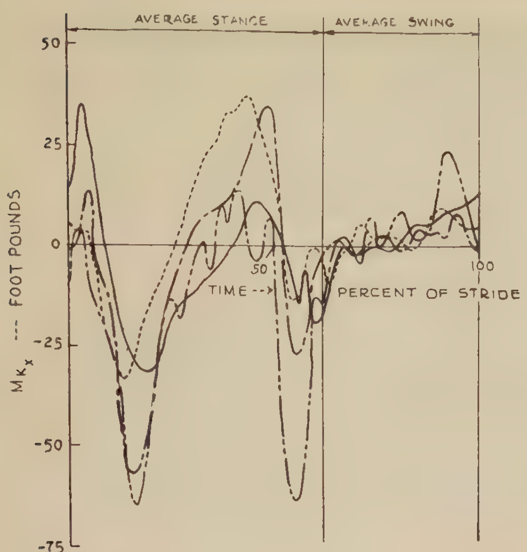

FIG. 12 FORE-AND-AFT KNEE MOMENT; FOUR SUBJECTS

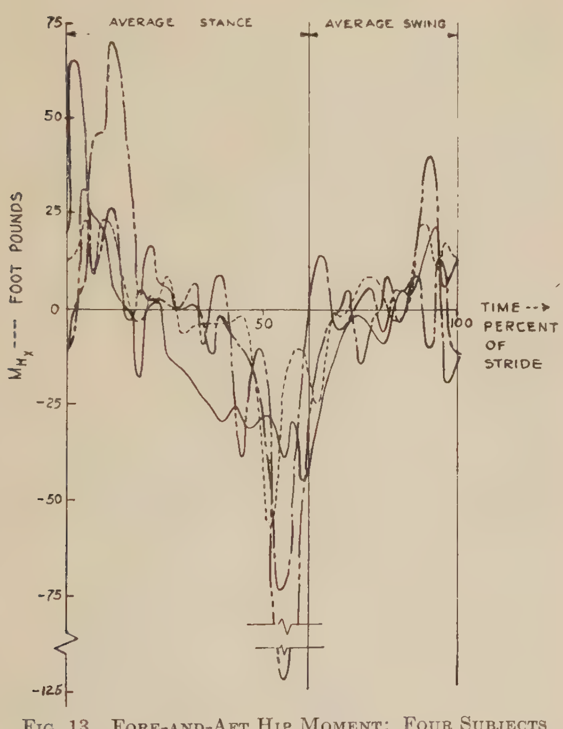

FIG. 13 FORE-AND-AFT HIP MOMENT; FOUR SUBJECTS

during level walking, and hence his results are indicative of forces acting at the hip joint during normal locomotion. Elftman (15) has made some computations of this nature, using such simplifying assumptions as the moment arms of the different muscles, and their time of action. Auxiliary studies of phasic activity of the muscles have shown, however, that any such calculations at this time would be, at best, first approximations.

It is apparent from the foregoing discussion that the variations of forces and moments in the leg joints are closely related to the mechanical functions of the leg in walking. These relationships, in addition to the studies of energy of human locomotion, investigations of the activity of different muscles of the leg, and the anatomical studies of leg-joint mechanisms (1) are necessary in order to solve the problems confronting the orthopedic surgeon and the designer of artificial legs and braces.

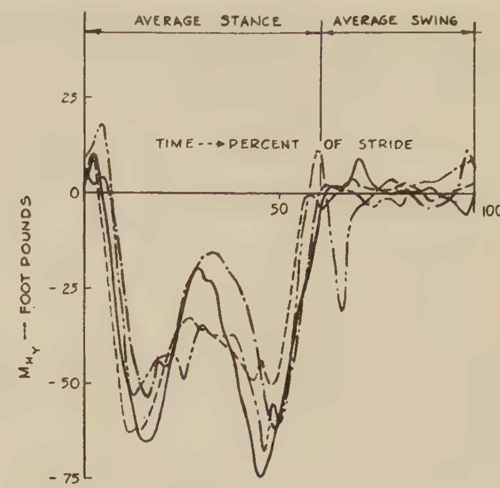

FIG. 14 LATERAL HIP MOMENT; FOUR SUBJECTS

BIBLIOGRAPHY

1 "Fundamental Studies of Human Locomotion and Other Information Relating to Artificial Limbs," Report to National Research Council, Advisory Committee on Artificial Limbs, vols. 1 and 2, June, 1947.

2 "Mechanik der menschlichen Gehwerkzeuge" ("Mechanics of Human Locomotion"), by Wilhelm and Eduard Weber, Göttingen, Germany, 1836.

3 "De la locomotion terrestre chez les bipedes et les quadrupedes" ("Terrestrial Locomotion of Bipeds and Quadrupeds"), by E. J. Marey, *Journal de l'Anat. et de la Physiol.*, vol. 9, 1873, pp. 42–80.

4 "Animal Mechanism: A Treatise on Terrestrial and Aerial Locomotion," by E. J. Marey, Appleton-Century-Crofts, Inc., New York, N. Y., 1874.

5 "La methode graphique dans les sciences experimentales" ("The Graphic Method in Experimental Sciences"), by E. J. Marey, G. Masson, Paris, France, 1885.

6 "Etudes experimentales de la locomotion humaine" ("Experimental Studies on Human Locomotion"), by E. J. Marey and G. Demeny, Comptes Rendus Acad. des Sciences, vol. 105, 1887, pp. 544–552.

7 "Movement," by E. J. Marey, D. Appleton Co., New York, N. Y., 1895.

8 "Der Gang des Menschen" ("Human Gait"), by O. Fischer, *Abhandlungen der Saechs, Gesellschaft der Wissenschaft*, vol. 21–28, 1898–1904.

9 "Über den Schwerpunkt des menschlichen Körpers mit Ruecksicht auf die Aursruestung des deutschen Infanteriesten" ("Concerning the Center of Gravity of the Human Body With Reference to the Equipment of the German Infantryman"), by W. Braune and O. Fischer, *Abhandlungen der Koenigl. Saechs. Gesellschaft der Wissenschaft*, vol. 15, 1872.

10 "Biodynamics of Locomotion," by N. A. Bernstein, et al, VIEM, Moscow, USSR, vol. 1, 1935.

11 "A Cinematic Study of the Distribution of Pressure in the Human Foot," by Herbert Elftman, *Anatomical Record*, vol. 59, 1934, pp. 481–490.

12 "The Function of the Arms in Walking," by Herbert Elftman, *Human Biol.*, vol. 2, 1939, pp. 529–535.

13 "The Force Exerted by the Ground in Walking," by Herbert Elftman, *Arbeitsphysiologie*, vol. 10, 1939, pp. 485–491.

14 "The Rotation of the Body in Walking," by Herbert Elftman, *Arbeitsphysiologie*, vol. 10, 1939, pp. 477–483.

15 "Forces and Energy Changes in the Leg During Walking," by Herbert Elftman, *American Journal of Physiology*, vol. 125, 1939, pp. 339–356.

16 "The Function of the Muscles in Locomotion," by Herbert Elftman, *American Journal of Physiology*, vol. 125, 1939, pp. 357–366.

17 "The Action of the Muscles in the Body," by Herbert Elftman, *Biol. Symposia*, vol. 3, 1941, pp. 191–209.

18 "Determination of Masses and Centroids of Segments of Human Body on Live Subjects," by N. A. Bernstein, et al, VIEM, Moscow, USSR, 1936.

19 "Contour Maps, Center of Gravity, Moment of Inertia and Surface Area of the Human Body," by A. P. Weinbach, *Human Biology*, vol. 10, Sept., 1938, pp. 356–371.

20 "Functional Aspects of the Abductor Muscles of the Hip," by V. T. Inman, *Journal of Bone and Joint Surgery*, vol. 29, July, 1947.

21 "Transverse Rotation of the Segments of the Lower Extremity in Locomotion," by A. S. Levens, V. T. Inman, and J. H. Blosser, *Journal of Bone and Joint Surgery*, October, 1948, pp. 859–872.

Report on Graphitization Studies on High-Temperature Welded Piping of The Philadelphia Electric Company

By J. B. ABELE[1] and A. E. WHITE[2]

Summaries of the work which has been done by and for the Philadelphia Electric Company in ascertaining the degree of graphitization in the piping system in the Chester, Schuylkill, and Richmond Stations since the fall of 1946, are reported in this paper. The results of a full-size pipe tension test on a graphitized weld section are reported. Solution treatment for removal of graphitization is described with some physical test results.

SECTION 1 By J. B. ABELE

THIS report is a supplement to one presented in 1946, by Hopping and White,[3] and gives results of further studies and investigations covering a period of approximately 2 years. The conclusions of the previous report, based upon the work done up to that time, led to a decision to continue the use of the pipe, and periodically to examine the welds further as a means of comparison and determination of increases, if any, in the formation of graphite. Such findings were to be used as a basis for a decision either to continue the use of the piping in its existing condition or to take appropriate steps to remedy this condition. The piping under investigation was as follows:

Chester Station. Operating since 1941 at a pressure of 1250 psi and 925 F; carbon-moly pipe, killed with $^1/_2$ lb of aluminum per ton of steel.

Schuylkill Station. Operating since 1938 at a pressure of 1250 psi and 900 F; carbon-moly pipe, killed with 1.8 lb of aluminum per ton of steel.

Richmond Station. Operating since July, 1943, at a pressure of 400 psi and 850 F; carbon-steel pipe. From 1935 to July, 1943, the operating temperature was 875 F with occasional swings to 900 F.

Operating Results at Chester and Schuylkill Station

Since the previous report, samples have been removed from all three stations for investigation.

At Chester Station, where approximately 20,000 service-hours have been added since the previous report, no appreciable amount of graphite has formed on either side of the welds in the heat-affected zones or in the pipe metal. Previous examinations of samples from the same welds showed no graphite in either the heat-affected zones or the pipe metal. Samples, however, have been removed from other welds where small amounts of nodular graphite were found. The conclusion, therefore, up to the present time and after 50,000 hr of service, is that very little graphite will form in the welds at Chester Station; however, occasional check examinations will be made in the future.

At Schuylkill Station the situation is somewhat different. Since the previous report, additional samples have been removed. They were taken from welds previously sampled and represent an additional 25,000 hr of service. In two of the samples examined, the amount of graphite in the heat-affected zones appeared to be somewhat greater and more continuous than was found in samples previously examined from the same welds. In another sample, the graphite did not appear to be quite as severe as that found in the sample previously examined from the same weld. In view of these findings, it is intended to remove completely one of these welds for mechanical tests, since metallographic examination does not give a quantitative measure of the degree of deterioration of the properties due to the presence of graphite.

The indicated increase in severity of graphite may be evidence of increased graphitization since the last examination, but this is not conclusive because previous work has shown that the amount of graphite varies considerably around the circumference of the weld. It can be stated, however, that the added graphite, if any, is quite small for the added service period of approximately 25,000 hr. At present, therefore, it is believed that, while there are indications of a slight increase in graphite in the welds at Schuylkill Station, it has not progressed to a point where continued use of the pipe in its present condition would be unwise. The results of future examinations will determine the action to be taken at Schuylkill Station.

It is thought that the small amount of aluminum used in killing the steel for the piping at Chester Station, as contrasted with the larger amount used for the Schuylkill Station piping, is the reason for the difference in the amount of graphite found in the welds at the two stations.

Details of Tests at Richmond Station

At Richmond Station a full section of 20-in-OD carbon-steel pipe was removed for a tension test. The section was approximately 3 ft long with a weld in the center and was tested on the 4,000,000-lb tension testing machine at the shops of the American Bridge Company, Ambridge, Pa. Fig. 1 shows the specimen before testing. It consisted of the section of pipe, two internally tapered transition rings, and two massive pulling heads. Twelve Baldwin Southwark SR-4 strain gages were used to measure strain. Four gages were placed on the weld, 90 deg apart and 4 gages were placed on the pipe 90 deg apart on each side of the weld.

The cross-sectional dimensions of the pipe, the data developed from the test loading and the strains measured with the SR-4 gages are given in Table 1. Yielding of the steel in the pipe metal on one side of the weld occurred at a load of 1,200,000 lb, which is

[1] Senior Engineer, Philadelphia Electric Company, Philadelphia, Pa.

[2] Director of Engineering Research Institute, University of Michigan, Ann Arbor, Mich. Fellow ASME.

[3] "Report on Graphitization Studies in High-Temperature Welded Piping of the Philadelphia Electric Company," by E. L. Hopping and A. E. White, Trans. ASME, vol. 69, 1947 (see "Graphitization of Steel Piping," special pamphlet).

Contributed by the Joint Committee on Effect of Temperature on the Properties of Metals and Power and Metals Engineering Divisions and presented at the Annual Meeting, November 28–December 3, 1948, of The American Society of Mechanical Engineers.

 Paper No. 48—A-94.

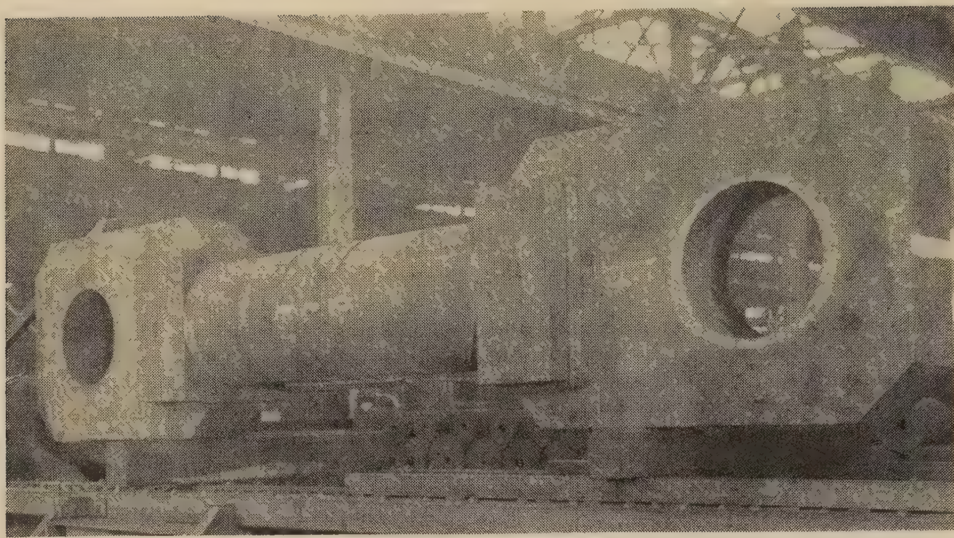

Fig. 1 Specimen Before Testing

TABLE 1 DIMENSIONS, TEST LOADING, AND MEASURED STRAINS FOR WELDED JOINT IN 20-IN. PIPE FOR PHILADELPHIA ELECTRIC COMPANY

Outside diameter of pipe	20.00 in. Nominal
Inside diameter of pipe	18.188 in. Nominal
Wall thickness	.906 in. Nominal
Cross-sectional area of pipe	54.35 sq.in. Nominal

Load		Strains Measured with SR-4 Gauges (Micro-inches per inch)											
Total Load	Stress on Nominal Cross-sectional Area of Pipe	Gauges on Weld				Gauges on Pipe							
						Northerly Half				Southerly Half			
(lb)	(psi)	BT	BB	BE	BW	AT	AB	AE	AW	CT	CB	CE	CW
0	0	0	0	0	0	0	0	0	0	0	0	0	0
250 000	4 600	73	51	90	64	108	89	90	74	102	95	143	90
500 000	9 200	206	118	213	160	283	211	258	253	246	262	305	189
1 000 000	18 400	483	251	460	412	616	491	583	501	575	578	687	470
1 200 000	22 080	Yield point in weld				-	-	-	-	Yield point in south half			
1 250 000	23 000	636	339	594	532	774	641	766	581	763	767	1 139	600
1 500 000	27 600	948	571	811	717	765	818	988	791	3 617	3 397	*	1 061
1 750 000	32 200	1 761	924	1 463	1 302	970	957	1 155	881	*	*		*
		-	-	--	-	Yield point in north half							
2 000 000	36 800	2 746	1 496	2 561	2 529	1 149	1 141	1 352	1 101				
2 250 000	41 400	4 085	3 550	*	*	*	1 443	*	1 486				
2 545 000	46 830	Pipe fractured at heat affected zone along south side of weld.											

* Gage yielding or fractured.

TABLE 2 ELONGATION MEASUREMENTS FOR WELDED JOINT IN 20-IN. PIPE FOR PHILADELPHIA ELECTRIC COMPANY[a]

Gauge Lines		Northerly Half				Southerly Half			
		1	2	3	Av.	4	5	6	Av.
Length before test	(ft)	.998	1.001	1.000	-	1.000	1.001	1.000	-
Length after test	(ft)	1.018	1.018	1.010	-	1.044	1.041	1.045	-
Elongation after fracture	(ft)	.020	.017	.010	-	.044	.040	.045	-
	(%)	2.0	1.7	1.0	1.6	4.4	4.0	4.5	4.3

[a] Fracture was outside both sets of gage lines.

equivalent to a stress of 22,080 psi. The strains measured by the SR-4 strain gages on the weld indicate that the weld metal also yielded at this load which is equivalent to a stress of about 19,280 psi in the weld metal. The yielding of the steel in the pipe metal on the other side of the weld occurred at a load of 1,750,000 lb which is equivalent to a stress of 32,200 psi. The elongation measurements are listed in Table 2. It is to be noted that neither set of measurements listed in Table 2 encompass the fracture of the specimen.

The fracture occurred in the weld-heat-affected zone and had three zones of distinctly different appearance; an outer zone of black and gray conchoidal fracture which is identified as graphitized steel extending in varying widths all around the fracture; a zone of a dark fine granular fracture extending around one-quarter of the pipe; and an inner zone, the largest, of a normal-appearing white fine granular fracture. Fig. 2 is a general view of the fracture, and Figs. 3 and 4 are detail views of a portion of the fracture.

From Table 1 it will be noted that the specimen broke in the weld at a load of 2,545,000 lb, equivalent to a fiber stress of 46,830 psi. The original tensile strength of the steel as reported by the mill was 70,900 psi. Probably half of the reduction in strength is due to the annealing effect from a service of 92,000 hr at temperatures ranging from 850 to 875 F, with occasional swings to 900 F. The balance of the reduction to 46,830 psi is due, without doubt, to graphitization. While a stress of 46,830 psi provides an ample factor of safety in a sound weld, resistance to thermal shock is of great importance and provision for this in a weld of this kind is none too good.

The appearance and nature of this fracture led to a decision to correct the condition at the earliest convenient time. Consideration was given to replacement of all the affected piping. An investigation, however, of the steel a short distance from the welds showed that the mechanical properties and the structure of the steel had not been unduly impaired, although the tensile strength had dropped to about 54,000 psi through normal service conditions but with no loss in ductility. It seemed inadvisable therefore to remove the pipe, and consideration was given to the replacement of the welds or to a solution treatment of the welds to disperse the graphite.

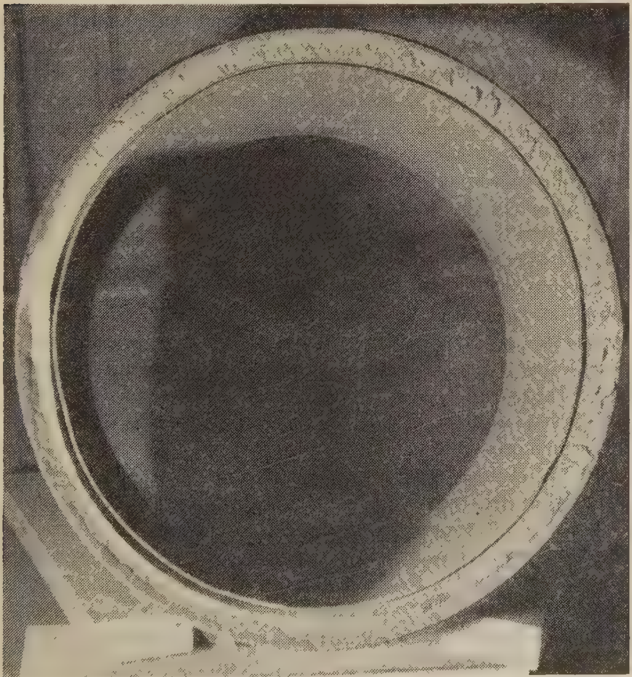

Fig. 2 General View of Test Specimen After Fracture

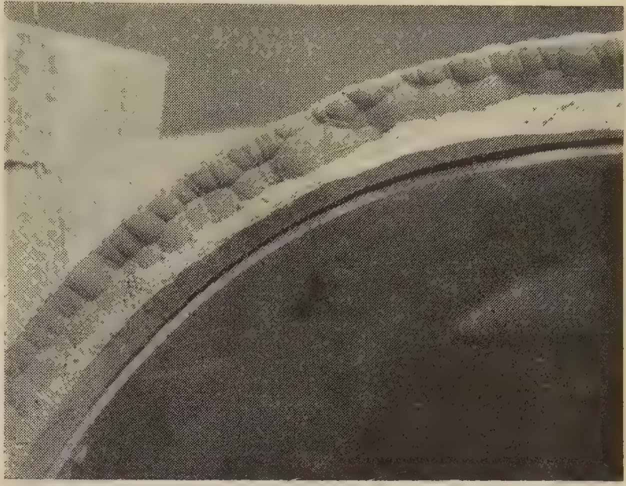

Fig. 3 Detailed View of Test Specimen After Fracture

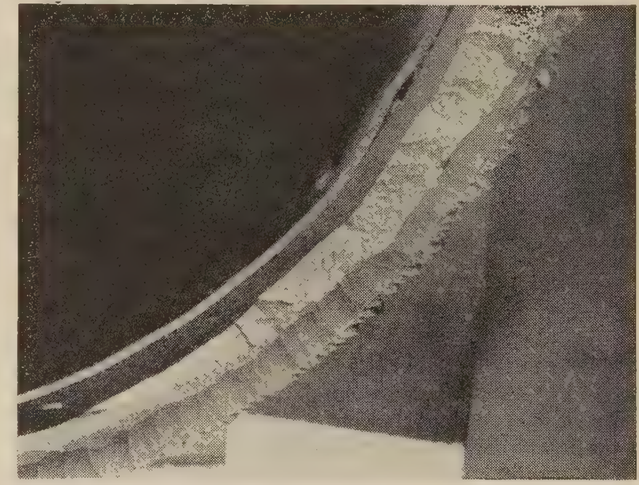

Fig. 4 Detailed View of Test Specimen After Fracture

Earlier work in normalizing at 1700 F at the University of Michigan together with more recent work at the same institution convinced us that this method offered a possible effective means of restoring graphitized welds.

Solution Treatment to Disperse Graphite

Investigation by A. E. White at the University of Michigan, discussed later on, disclosed the fact that solution treatment, followed by proper stress relief placed the graphitized metal in a safe state of strength and ductility. Therefore, it was decided to repair the pipe by this method rather than replace the welds. The latter method would require more time and involve greater cost.

A careful investigation of the practical application of solution treatment of welds in the field also indicated that the work could be speedily and successfully done.

The procedure finally agreed upon was as follows: Heat to 1700 F at a rate not to exceed 300 deg per hr from 1000 F to 1700 F. Hold at 1700 F for 2 hr. Control cooling from 1700 F to 1200 F at a rate not to exceed 100 deg per hr. Allow to cool, uncontrolled, from 1200 F to approximately 700 F. Stress-relieve by raising temperature to 1275 F at a rate of 400 deg per hr. Hold at

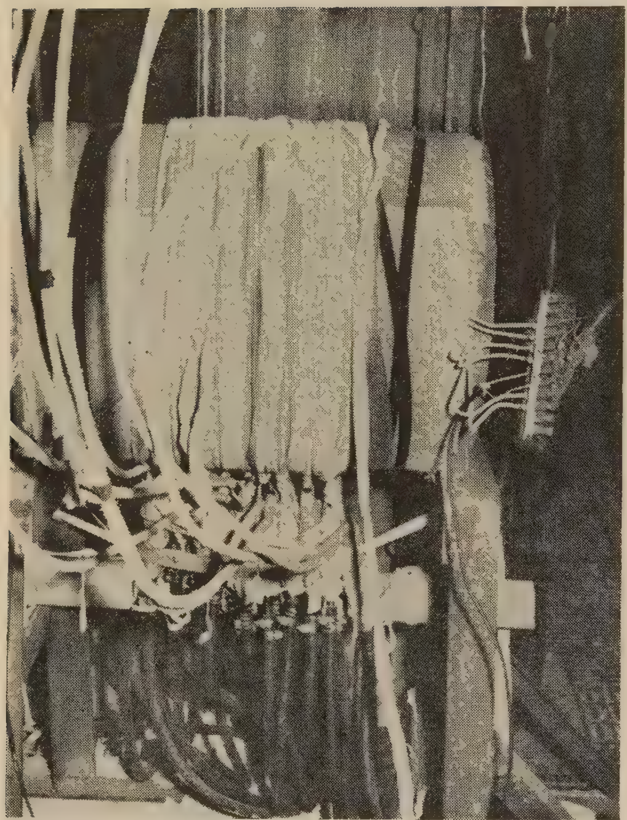

Fig. 5 Heating Arrangement on Experimental Piece

1275 F for 1 hr per in. of thickness. Cool to 700 F at a rate of 200 deg per hr. Allow to cool uncontrolled from 700 F.

A method of electronic heating was discussed with the engineers of the Radio Corporation of America. This method, however, was not practical because of the mass of metal involved. Calculations indicated that approximately 40 kw of radio-frequency power would be required to maintain a band 6 in. wide at 1700 F in the 20-in-OD pipe. While it is true that their 75-kw generator would produce enough heat to perform the normalizing treatment, it was felt that the portability and the relatively great expense of the equipment made its use impractical.

Heating with gas was considered, but this too was thought to be impractical since it was felt that it would be difficult to maintain a uniform heat around the entire circumference unless an oven or muffle was built around the pipe. Because of insufficient clearances and other interferences in many cases, such a muffle could not be used.

Induction Method of Heating Pipe. It was finally decided that the induction method was the most logical one to use and, accordingly, experimental tests were run on a short length of 20-in-OD pipe. Because of the extreme temperature and high amperage required, water-cooled coils were used.

Twelve turns of $^3/_8$-in-OD 0.035-in-wall copper tubing were used on each side of the welded joint (24 turns total). The turns were arranged so that the cooling water was discharged and fresh water was admitted for each 3 turns around the pipe. Four 60-kva stress-relieving transformers were used, making a total of 240 kva available. They were connected, two in series, to each heating coil with a separate control cabinet for each set of transformers. A water relay was used with each cabinet to shut the power off automatically in case the cooling-water supply failed. The leads between the transformers and heating coils were made up of four welding leads in parallel 100 ft long. Fig. 5 shows the setup on the experimental piece.

Experiments were also conducted in an effort to determine whether or not scale formation could be prevented or at least minimized. The amounts of scale formed were compared for (1) open-ended pipe with a free circulation of air, (2) dead air by blanking each end of the pipe, and (3) by the use of inhibitors such as helium, nitrogen, and CO_2. While the amount of scale varied between methods, the total in no case was considered great enough to warrant the use of any of the special methods; the conclusion being that there would be no more scale than is found in the welded joints of a new installation.

Formulating the Solution Treatment. In formulating a program for the solution treatment of the welds at Richmond Station, it was decided to remove additional boat samples from welds representing the various materials and combinations of materials. Samples were removed from pipe to pipe joints both in the 16-in. and 20-in. seamless pipe, and from pipe to pipe joints as well as from longitudinal welds in the 24-in. fabricated pipe. While graphite was found in the 16-in. and 20-in. welds, no graphite was found in the 24-in. fabricated piping, due, we believe, to the high silicon content of the plate material.

In passing, it will be of interest to note that a gas shop weld in the 20-in. pipe was examined and no graphite or other detrimental structural alterations were found in it. It would be unwise, however, to draw too general conclusions from the examination of a single weld.

Material for the castings for the gate and nonreturn valves contained approximately 1.00 per cent nickel, 0.70 per cent chrome and 0.50 per cent molybdenum. No samples were removed from the welds at these valves since it was reasonable to assume that little or no graphite exists on the valve side because of their high chromium content. Also, these welds were to be safeguarded by a solution treatment.

Valve Tests. It was feared that some valve distortion might occur with the 1700 F temperature heat, making it necessary to repair or reseat the valves; therefore, temperature measurements were taken in the castings to provide data for future temperature applications to valve welds. The nonreturn valves are Schutte & Koerting 16-in. double inlet, 20-in. single outlet. Thermocouples placed on the body at the center of the valves during solution treatment of the weld on the 20-in-diam outlet, which was 28 in. away from the center line of the weld, indicated a temperature of approximately 575 F. Removal of the bonnets of these valves after solution treatment and an examination of the trim, and a subsequent pressure test, showed that there had been no distortion of the seating surfaces. Similarly, thermocouples placed on the body of the 20-in. gate valves, 12 in. from the weld showed a temperature of 800 F. It is evident, therefore, that a temperature of 1700 F at the welding ends of valves of comparable size will not affect the trim of valves adversely.

Some thought was given to adequate bracing of the piping during solution treatment because of the plastic condition of the weld metal and of possible strain in the piping. It was finally decided that no elaborate means of bracing need be used, a decision which proved to be correct.

Electrical Energy for Solution Treatment. Electrical energy for the solution treatment at Richmond Station was delivered through a 600-kva temporary power bank, installed to provide 440-volt 3-phase power from the 2300-volt bus. Temporary feeders were installed to the distribution center located in the vicinity of the work to be performed. The stress-relieving transformers were placed at a central location and connected to the distribution center in such a manner that all transformers on any one joint were all on the same phase. The data in Table 3 show the requirements for heat-treatment.

TABLE 3 HEAT-TREATMENT DATA

Actual kva required to normalize 20-in. pipe.........	175
Average primary voltage required..................	445–450
Average secondary voltage required at pipe..........	62–65
Average secondary voltage required at transformer...	70–72
Average secondary amperage.......................	1100–1200
Water flow through 1 coil (3 turns), gpm, approx.....	1-$^3/_4$
Water flow through 8 coils (24 turns), gpm, approx...	15
Water pressure at header, psi......................	24
24 turns of $^3/_8$-in-OD, 0.035-in-wall, copper tubing insulated with woven asbestos.....................	
Pipe insulated with 4 layers of $^1/_8$-in. × 10-in. asbestos paper.	

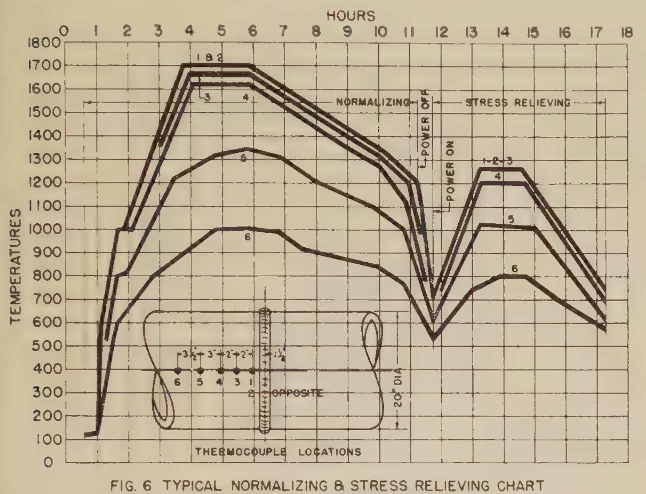

Fig. 6 Typical Normalizing and Stress-Relieving Chart Showing Temperature at Weld and at Various Distances From Weld

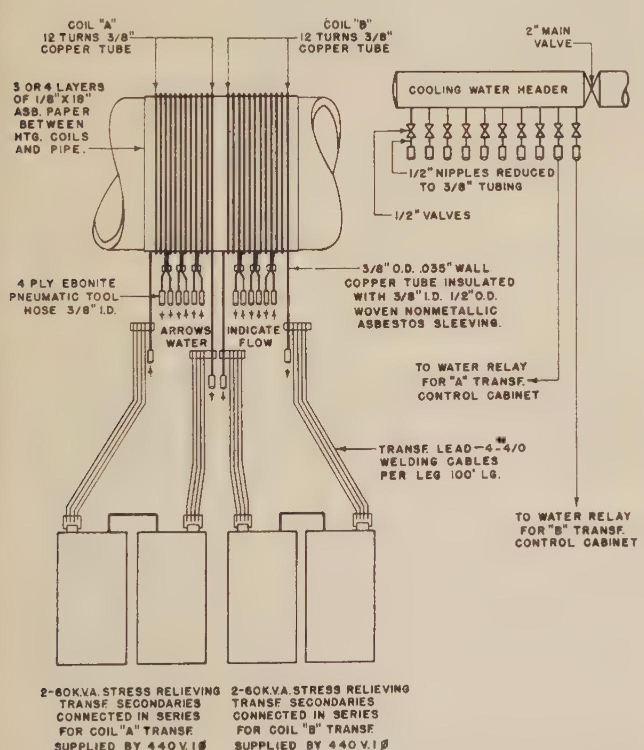

Fig. 7 Diagram of Normalizing and Stress-Relieving Equipment

Fig. 6 is a typical time-temperature chart showing the temperatures at the weld and at various distances from the weld during the solution and stress-relieving treatment. Fig. 7 is a schematic layout of the equipment used.

All welds in the high-pressure piping system at Richmond Station were solution-treated with the following exception: The 24-in. fabricated pipe where no graphite was found, and the pipe from the superheater header to the nonreturn valve on one boiler, which was replaced with one-half chrome and one-half moly pipe left over from Southwark Station.

Twenty-Nine Welds Treated. Twenty-nine welds were solution-treated and the work was completed in nineteen 24-hr working days, thus effecting a material time-saving over and above that which would be required were the graphitized welds cut out and replaced with new welds. It is felt, however, that the treatment has removed a latent critical condition, either temporarily or permanently, and substantially prolonged the useful life of this pipe, although it is not necessarily to be construed that this method should be used if graphitization has advanced to an undue degree.

Later samples will be removed from time to time and a future course of action will depend upon the findings.

SECTION 2 By A. E. White

Restoration of Properties of Graphitized Weld Sections by Heat-Treatment

Mr. Abele has pointed out that this author would deal with the subject of the restoration of the properties of graphitized weld sections by heat-treatment at the Richmond Station of the Philadelphia Electric Company.

The restoration of graphitized weld sections was advanced by the author in 1943, and a report covering some preliminary work in this field was given to the Philadelphia Electric Company on February 5, 1944. The restoration procedure, from a laboratory standpoint, is simple. It merely involves heating graphitized sections above the upper critical temperature for a sufficient time so that all of the graphite will go back into solution, with a time interval at this temperature sufficient to provide for the best possible dispersion of the resultant carbide. In this connection, a temperature of 1700 F continued over a period of 2 hr has been found adequate for graphitized-pipe weld sections.

No claim is advanced that the restoration of graphitized welds by solution treatment, which is the term commonly used to describe the heat-treatment, can be employed successfully in all cases. If the graphitization is too pronounced, some claim small disconnected sections or cavities might remain where the graphite had been, even though the conversion of graphite to carbon was complete. Also, there is a possibility that, due to location, not all types of graphitized welds might lend themselves to a solution treatment. A weld adjacent to a valve might be a case in point. However, as the technique of solution treatment advances, it is expected that less and less difficulty will be encountered in this respect.

With this background, serious consideration was given to restoration of the graphitized welds at the Richmond Station by solution treatment. This was because of the marked degree of graphitization found in a full-size pipe section that was broken at Ambridge, as well as the evidence of considerable graphitization obtained from boat samples and full-size pipe sections which had been removed from service for purposes of investigation.

Prior to the adoption of the solution treatment for the removal of graphite from many of the welded pipe sections, numerous solution treatments were run on small samples to show that the graphite could be put into solution. This was then followed by laboratory solution treatments on tensile specimens, accompanied, in some cases, by stress relief.

A summary of some of the most important of these tests is given in Table 4. It should be noted that the test sections removed early in 1948, for which figures are given in this table, were

TABLE 4 ROOM-TEMPERATURE TENSILE PROPERTIES FROM PREVIOUS TESTS ON 20-IN-DIAM WELDED CARBON-STEEL PIPE FROM RICHMOND STATION

Location of Test Section	Heat Treatment	Tensile Strength (psi)	0.2% Offset Yield Strength (psi)	Elongation in 2 In. (%)	Reduction of Area (%)	Location of Fracture	Year of Removal of Weld Section
(The Gage Section of the Samples Was 0.750-Inch Thick, 1.25-Inches wide and 3-Inches Long)							
Across weld	As removed from service	51,300	* ______	12.0	11.4	Graphite concentration	1945
Across weld	As removed from service	57,700	______	12.0	17.5	Graphite concentration	1945
Across weld	As removed from service	48,900	______	10.0	5.4	Graphite concentration	1945
Across weld	As removed from service	51,900	______	11.0	6.5	Graphite concentration	1945
Pipe metal	As removed from service	51,650	______	41.0	66.1	______	1945
Pipe metal	As removed from service	51,125	______	35.5	58.3	______	1945
Across weld	As removed from service	57,140	37,700	34.0	50.5	Pipe metal	1948
Across weld	As removed from service	60,000	37,900	25.4	47.1	Weld metal	1948
Across weld	As removed from service	58,200	35,400	14.0	10.6	Graphite concentration	1948
Across weld	As removed from service	60,600	36,000	17.0	16.0	Graphite concentration	1948
Across weld	1600°F, 2 hr, A.C.	66,600	44,000	23.5	32.8	Weld metal	1948
Across weld	1700°F, 2 hr, A.C.	65,760	41,600	19.0	28.8	Weld metal	1948
Across weld	1700°F, 2 hr, A.C.	64,630	40,800	13.0	22.0	Weld metal	1948
Across weld	1700°F, 2 hr, A.C. + 1 hr at 1200°F	62,700	39.400	31.0	39.2	Weld metal	1948
Across weld	1700°F, 2 hr, A.C. + 1 hr at 1200°F	55,200	39,300	29.0	47.5	Weld metal	1948
Across weld	1700°F, 2 hr, A.C. + 2 hr at 1275°F	58,500	36,000	33.5	56.8	Weld metal	1948
Across weld	1700°F, 2 hr, A.C. + 2 hr at 1275°F	58,100	34,800	33.0	54.6	Weld metal	1948

* Yield strengths were not obtained on these samples because at the time the tests were made interest centered only on tensile strength, elongation, and reduction of area.
NOTE: A.C. = air cooled.

from a weld which was graphitized to approximately the same degree as existed in the weld broken at Ambridge, which is illustrated in Figs. 2, 3, and 4. These results, together with the complete lack of evidence of graphite in the solution-treated samples, showed this treatment to be so promising that it was adopted as a method of restoring many of the graphitized sections in the carbon-steel pipe at the Richmond Station. The word "many" is used because a few of the graphitized welds, due to location, or some other cause, were removed and replaced by new welded sections.

It will be noted that greater ductility was found in the sample solution-treated at 1600 F than in the samples solution-treated at 1700 F. It was felt, however, that a solution treatment at 1700 F would be preferable to a solution treatment at 1600 F because of greater assurance of a more complete dispersion of the carbides. However, the greater ductility found with a 1600 F solution treatment led this author to suspect that a stress relief would improve the ductility of the metal which had undergone a 1700 F solution treatment. When tried, this proved to be the case and, because a stress relief of 1275 F gave superior ductility to the metal to a stress relief of 1200 F, the former was adopted. The procedure finally adopted, therefore, was to give the graphitized welds a solution treatment at 1700 F for 2 hr, followed by a stress relief of 1275 F for 1 hr per in. of metal thickness.

In the investigation weld-prober samples were taken from two graphitized weld sections and examined at the University to determine which one of the two sections contained the greater amount of graphite. These sections were designated as weld A and weld B. From the graphitization standpoint, little difference was found in the two sections and was less than had been found in other sections previously examined, although weld A appeared to have slightly more graphite than weld B. Weld A, therefore, was the section selected for a solution treatment, with a subsequent stress relief. Both sections were removed from the pipe line and, after weld A was given the solution treatment, followed by stress relief, at the Richmond Station, they were shipped to the University of Michigan for examination.

Test Material

The pipe was purchased to ASTM Specification A-106-33T Grade B. The samples were 16 in. diam with wall thickness of 0.745 in. and were 18 in. long with the weld in the center.

The mill analysis was reported as follows:

	Per cent
Carbon	0.23
Manganese	0.93
Phosphorus	0.014
Sulphur	0.03
Silicon	Not given

The physical properties, as reported by the mill, are as follows:

Tensile strength, psi	70900
Elongation in 2 in., per cent	35

The average operating temperature of the pipe sections since July, 1943, was 850 F, although from 1935, to July, 1943, the operating temperature was 875 F, with momentary swings to as high as 900 F. The pipe sections had been in service 92,000 hr.

Properties of Weld B Pipe

The room-temperature tensile properties of the welded carbon-steel pipe known as weld B are given in Table 5. It will be noted that, although the test specimens included the weld sections and the heat-affected zone sections wherein the most graphite would be found, the specimens all broke in the unaffected-pipe-metal sections. The values in the table, therefore, are more indicative of the values that would be found in the pipe metal than of the values that would be found in the metal in the weld or in the heat-affected zone. Attention is called to the fact that, although the pipe metal was reported as having a tensile strength of 70,900 psi, the tensile strength of the pipe metal after 92,000 hr of service averaged 56,375 psi.

Properties of Weld A—Solution-Treated

By far the larger amount of this particular investigation re-

TABLE 5 ROOM-TEMPERATURE TENSILE PROPERTIES OF WELDED CARBON-STEEL PIPE FROM THE RICHMOND STATION AS REMOVED FROM SERVICE

(Intermediate field weld between pieces MS-12 and MS-43 in the 16-inch down-river superheater piping of No. 66 boiler. Weld prober samples 16R, 17R, 21R, and 22R had previously been removed from this weld.[a])

Sample	Location of Gage Section	Tensile Strength (psi)	0.2% Offset Yield Strength (psi)	Elongation in 2 In. (%)	Reduction of Area (%)	Location of Fracture
(The gage section of the samples was 0.50-inch thick, 1.25-inch wide, and 3-inches long.)						
B1-1	Across weld	56,200	35,500	40.0	68.0	Unaffected pipe metal
B2-1	Across weld	56,800	35,200	40.0	67.0	Unaffected pipe metal
B3-1	Across weld	56,400	36,000	39.0	67.0	Unaffected pipe metal
B4-2	Across weld	56,100	32,900	38.0	69.1	Unaffected pipe metal

[a] The degree of graphitization was not severe as is shown in Report No. 39.
NOTE: The samples were taken from four quadrants of the pipe, 90 deg apart.

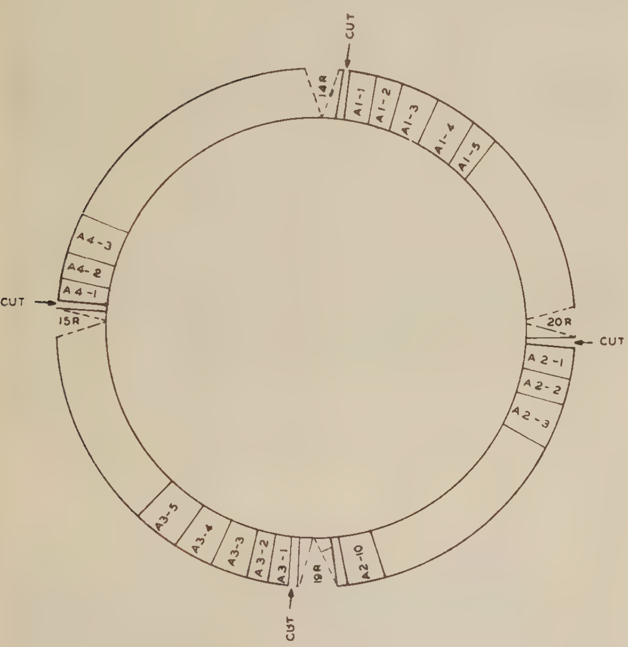

FIG. 8 SKETCH SHOWING LOCATION OF TEST SAMPLES IN PIPE CIRCUMFERENCE

(Weld-prober samples had been removed from locations labeled 14R, 15R, 19R, and 20R.)

lated to the studies which were made on the section of the welded carbon-steel pipe which was given a solution treatment, followed by a stress relief, at the Richmond Station of the Philadelphia Electric Company. Details with regard to the heat-treatment given this pipe section are covered in the portion of the paper by Mr. Abele.

Test Procedure. The test procedure which was followed in the examination of this pipe at the University was as follows:

1 The section of the pipe was cut into longitudinal strips to supply samples for macro- and microexaminations and for tensile tests, as indicated in Figs. 8, 9(*a*), and 9(*b*).

2 Strips from four quadrants were macroetched the full length of the pipe sample to check the structure at the weld and at the heat-affected zone resulting from the solution treatment.

3 Metallographic examinations were made to determine if the graphite at the heat-affected zone of the original weld had been dissolved and to show the microstructure resulting from heat-treatment.

4 Tensile tests were conducted at room temperature to establish the physical properties of the metal in the weld area and through the adjacent pipe metal following the solution treatment. The locations of the tensile test sections are shown in Fig. 9(*b*). Attempts to force fracture at the outside of the original weld-heat-affected zone, where the concentrated graphite had dissolved, were not successful.

Wherever possible, rectangular test specimens with a gage section 0.50 in. × 1.25 in. × 3 in. were used. The pipe sample was so short that it was necessary to use 0.505-in-diam test specimens when testing the material heated between the critical temperatures during the solution treatment.

GENERAL RESULTS OF STUDY

Physical Tests. The results of the tensile tests on the solution-treated pipe given in Table 6 indicate that the solution treatment and stress relief produced a material with satisfactory strength and ductility. The following additional comments are offered:

1 When the gage section of the test specimens was placed across the weld, the weld-deposited metal was the weakest, and fracture occurred at that point. The area where graphite had originally been concentrated, the coarse-grained area, had the higher strength.

2 When samples were machined (A2-10D and A3-3U) which covered the zone from the weld to a point where the temperature reached the upper critical temperature during solution treatment, the strength and ductility were both higher than that in the weld metal. It was not possible to force fracture at the region of graphite concentration before solution treatment in order to determine the ductility at that point.

3 The metal heated between the critical temperatures had strength about the same as the weld metal and somewhat lower elongation. This comparison is not to be interpreted too literally because, in order to test this section, it was necessary to use 0.505-in. test bars, whereas the other test bars were 0.50-in. × 1.25 in. × 3 in. The important point is that this portion of the solution-treated pipe had adequate strength and ductility.

4 Test data are not available for pipe metal heated at the lower critical temperature or the pipe metal not affected by the solution treatment, as the length of pipe supplied was cut just beyond the point where the temperature reached the lower critical.

As removed from service, there was very little difference in the amount of graphite in the two weld sections submitted for this investigation. Weld A had, at most, only slightly more graphite than weld B. Therefore the graphitization in weld A before solution treatment can be inferred to be about the same as that in weld B. The results of the tensile tests as given in Table 5 for weld B, therefore, can be assumed to be representative of what the tensile tests would show for weld A before solution treatment.

Although none of the samples broke in the heat-affected zone in any of the tests reported in Tables 5 and 6, it is evident

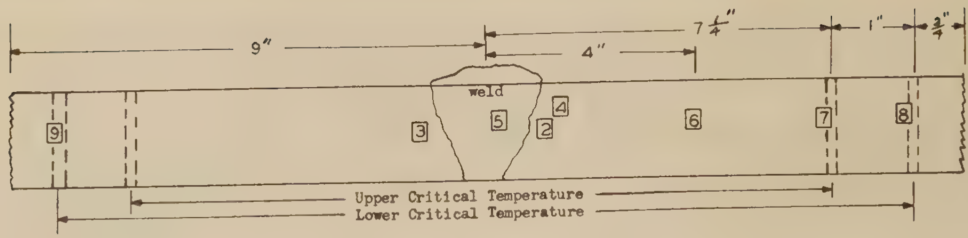

Fig. 9(*a*) Location of Photomicrographs of Pipe Section
(□ Refers to plate numbers)

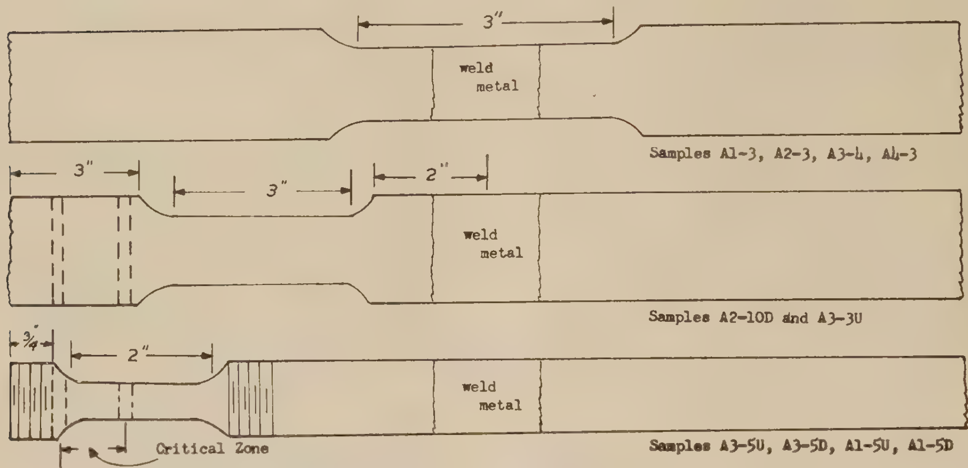

Fig. 9(*b*) Location of Gage Section of Tensile Specimens of Pipe Section

TABLE 6 ROOM-TEMPERATURE TENSILE PROPERTIES OF WELDED CARBON-STEEL STEAM PIPE FROM THE RICHMOND STATION AFTER FIELD HEAT-TREATMENT TO DISSOLVE GRAPHITE

(Center of weld heated to 1700 F for 2 hr, slowly cooled, and stress-relieved at 1275 F. Fig. 2 shows location of test coupons with position of gage section shown in Fig. 3.)

Sample	Location of Gage Section	Tensile Strength (psi)	0.2% Offset Yield Strength (psi)	Elongation in 2 In. (%)	Reduction of Area (%)	Location of Fracture
	(The gage section of the samples below was 0.50-inch thick, 1.25-inch wide, and 3-inches long.)					
A1-3	Across weld including original weld heat-affected zones	56,700	30,100	33.0	60.9	Weld metal
A2-3	Across weld including original weld heat-affected zones	54,700	32,100	31.0	56.5	Weld metal
A3-4	Across weld including original weld heat-affected zones	50,700	34,300	27.0*	36.1*	Weld metal
A4-3	Across weld including original weld heat-affected zones	55,900	31,300	32.0	54.9	Weld metal
A2-10D	Downstream pipe metal heated above upper critical temperature	58,000	37,500	43.0	59.9	————
A3-3U	Upstream pipe metal heated above upper critical temperature	59,600	35,300	43.0	59.8	————
	(The gage section of the samples below was 0.505-inch diameter and 2-inches long.)					
A3-5U	Upstream pipe metal across upper critical temperature zone	56,400	30,000	30.5	64.5	Pipe metal heated to temperature between upper and lower critical temperature during solution treatment.
A3-5D	Downstream pipe metal across upper critical temperature zone	56,900	30,500	28.0	64.0	
A1-5U	Upstream pipe metal across upper critical temperature zone	54,300	27,900	28.0	65.2	
A1-5D	Downstream pipe metal across upper critical temperature zone	56,800	30,500	29.5	64.0	

* Sample A3-4 fractured through a flaw in the weld metal.

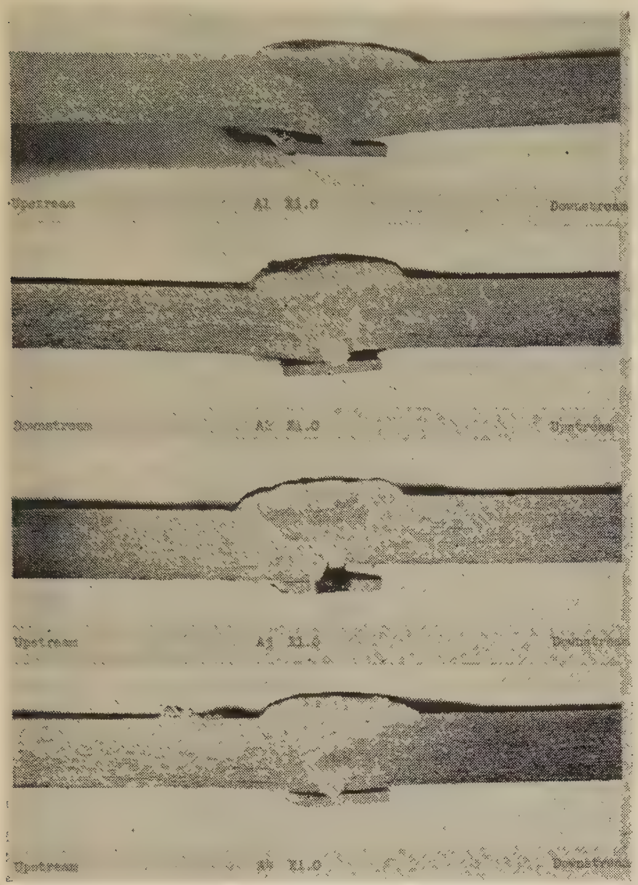

Fig. 10 Photomacrograph of Weld Section of Macroetched Samples From Four Quadrants of Pipe Section A

structure would have resulted as has been the case in all of the samples which were laboratory solution-treated.

Macrographic and Metallographic Studies. Macroetching of samples from quadrants of the pipe section known as weld A give the results shown in Fig. 10.

Metallographic examination of this same weld area gave the following results:

1 No graphite could be found at the location of the original heat-affected zone. Slow cooling during the solution treatment produced annealed types of structures.

2 A band of comparatively coarse grains was located parallel to the weld and at a location believed to be that of the outside edges of the heat-affected zones of the original weld where the more concentrated graphite had formed during service. Fig. 11 is representative of both the upstream and downstream weld-heat-affected zones of all four quadrants of the solution-treated pipe. Fig. 12 is fairly representative of all of these sections before solution treatment.

The band of comparatively coarse grains shown in Fig. 11 is believed to be due to the slow cooling to which this pipe was subjected following its heating to 1700 F. Had the rate of cooling been more rapid, equivalent to that used in normalizing, it is believed that a normal fine-grained structure would have resulted.

Naturally, during the solution treatment, a temperature gradient would exist from the center of the weld along the pipe in both directions. The zones in these different gradients were examined but nothing of moment was found, although mention is made of a graphitelike substance found about 1 in. from the heat-affected zone which showed slight discontinuities.

Conclusions

The field solution treatment resulted in the metal in the weld zone having the same strength and ductility at room temperatures as was found in the original pipe metal after it had been subjected to service for 92,000 hr. As was expected, the weld-

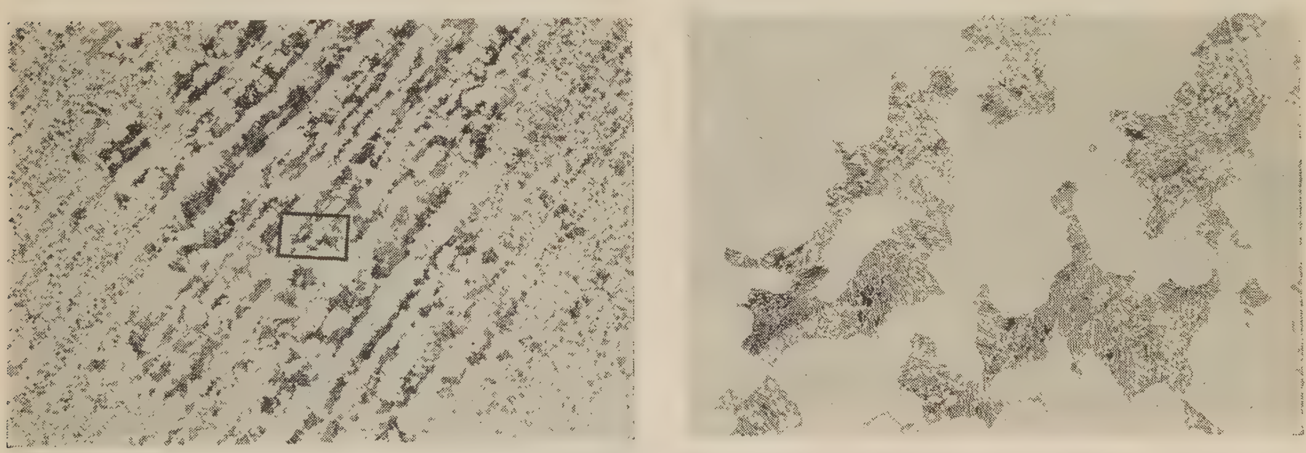

×100 ×1000

Fig. 11 Representative Photomicrographs of Upstream and Downstream Weld-Heat-Affected Zone of All Four Quadrants of Solution-Treated Pipe Section

that the solution treatment did not affect the properties of the metal adversely in the weld areas as a result of the conversion of the graphite in the heat-affected zone. This statement is made in spite of the rather large grains found in the heat-affected zones, which resulted from the very slow cooling of the metal during the solution treatment, as shown in Fig. 11.

It is believed that if a more rapid rate of cooling from the solution-treatment temperature had been adopted, a fine-grained

deposited metal was the weakest. The strength values were somewhat lower than those which previously have resulted from laboratory normalized samples because the heat cycle of the field solution treatment involved cooling rates slow enough to anneal the metal.

Graphitization during service had not been severe enough to affect the strength of the welded section given a solution treatment.

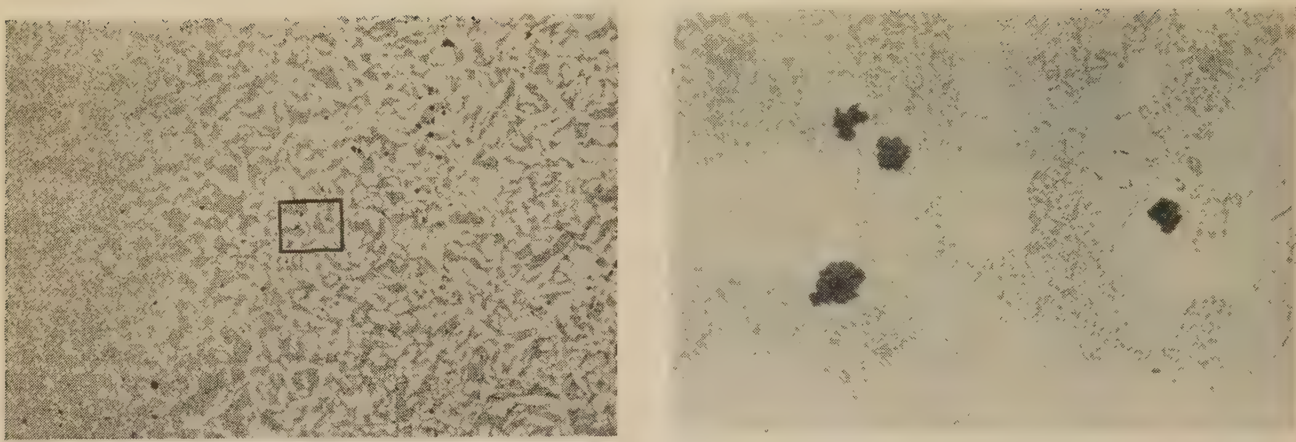

×100 ×1000

FIG. 12 MICROSTRUCTURE OF UPSTREAM AND DOWNSTREAM HEAT-AFFECTED ZONE OF WELD-PROBER SAMPLE 15R
(Sample removed prior to field solution treatment. Sample fairly representative of all four quadrants.)

No evidence was observed to indicate that the solution treatment had increased the amount of graphite in the pipe metal.

Finally, although the physical properties of the solution-treated weld section were not materially different from those in the untreated weld section, because the amount of graphite in the untreated weld section was not sufficiently great to have any influence on the properties of the sections in question, yet, it is believed that the treatment was worth while in that it converted any possible concentrated graphite to a carbide, with a resultant good dispersion of the carbide, and thus would restore any badly graphitized sections to a serviceable condition.

In conclusion, it should be pointed out that this treatment is not one which will effect a cure, but one which will permit the continued use of the pipe for possibly as long as it had been used previously. As stated by Mr. Abele, however, in his portion of the paper, these solution-treated sections, as well as all welded sections, should undergo inspection at suitable intervals in the interest of safety.

ACKNOWLEDGMENTS

The authors wish to express their appreciation to Mr. E. L. Hopping, Consulting Engineer, Philadelphia Electric Company, for his counsel, encouragement, and continued support to this program. Also, grateful acknowledgment is made to the field organizations of both the United Engineers and Constructors Inc., and the Philadelphia Electric Company for the constructive work done in the development of field methods which made the heat-treatment procedure so successful. Acknowledgment is further made to Dr. J. W. Freeman, research engineer, Mr. J. J. Heller, and others of the Engineering Research Institute, for their co-operative services.

Discussion

F. EBERLE.[4] This paper is of considerable practical importance in that it shows a possibily effective procedure of solution-heat-treating weld joints which are not too severely graphitized, thereby giving them, so to speak, a new lease on life. The authors used room-temperature tensile tests in conjunction with microscopic examination to evaluate the existing degree or extent of graphitization, low elongation and reduction of area plus failure in the zone of graphite concentration being the indicator of a potentially hazardous condition. This method of examination undoubtedly will reveal whether there is any danger to be expected due to shock, as illustrated by the original Springdale failure; but one may question whether it will also indicate the further behavior of such a graphitized weld joint at operating temperature when it is not exposed to shock. Therefore, it may be of interest to present here the result of a creep test which was made with a specimen containing a graphitized carbon-molybdenum pipe weld in the center of the gage length.

Fig. 13 of this discussion shows the condition in the weld-affected zone of the sample prior to creep testing. This pipe joint had been in service for $5^1/_2$ years at a temperature of 930–950 F. Graphitization, though discontinuous, was considered at that time severe enough to remove this joint from service. The specimen prepared from it was tested at 1000 F under a load of 5000 psi, which is the maximum allowable working stress given by the

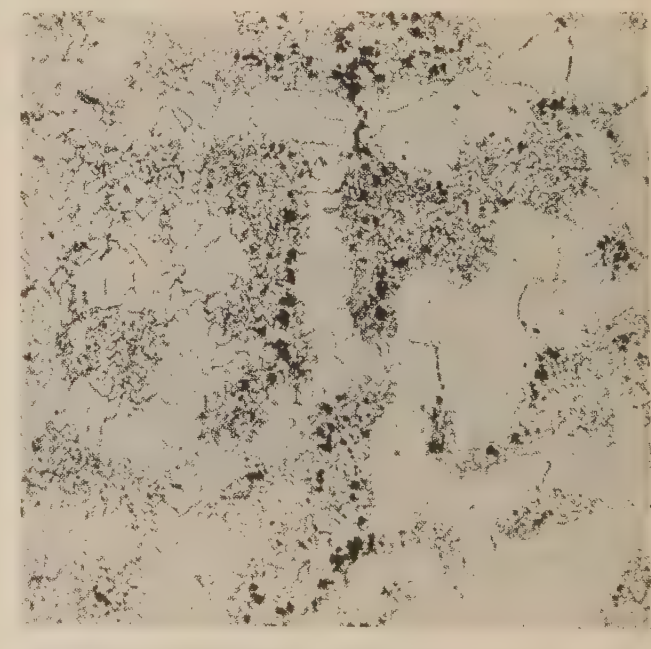

FIG. 13 WELD-HEAT-AFFECTED ZONE OF CREEP-TEST SPECIMEN PRIOR TO CREEP TESTING
(Nital etch; ×100)

[4] Chief Metallurgist, Research and Development Department, The Babcock & Wilcox Company, Alliance, Ohio.

Boiler Code. We kept this specimen under test for 40,200 hr, during which it displayed the following rates of creep, expressed in per cent per 100,000 hr:

	Per Cent
0 to 15000 hr	0.7
15000 to 31000 hr	0.8
31000 to 40200 hr	0.5

Fig. 14 shows the condition of the weld-affected zone after termination of the test. It will be observed that the manner and extent of graphitization is now in every respect as severe as it was in the original failed Springdale pipe. The graphite is seen to be almost totally concentrated in the grain boundaries, forming a continuous chain through the entire cross section of the specimen. One cannot help wondering why the latter did not rupture. It certainly would appear from this example that there is little likelihood of immediate danger at operating temperatures for weld joints in which graphite is present in a discontinous manner, provided of course that they are not exposed to shock.

It may be necessary sometimes to make a decision as to whether a weld joint may be permitted to continue in service for a certain length of time before remedial measures are taken. To our knowledge, there are no means or methods of predicting safely if and within what length of time a discontinuously graphitized weld-affected metal will develop dangerous graphite concentration

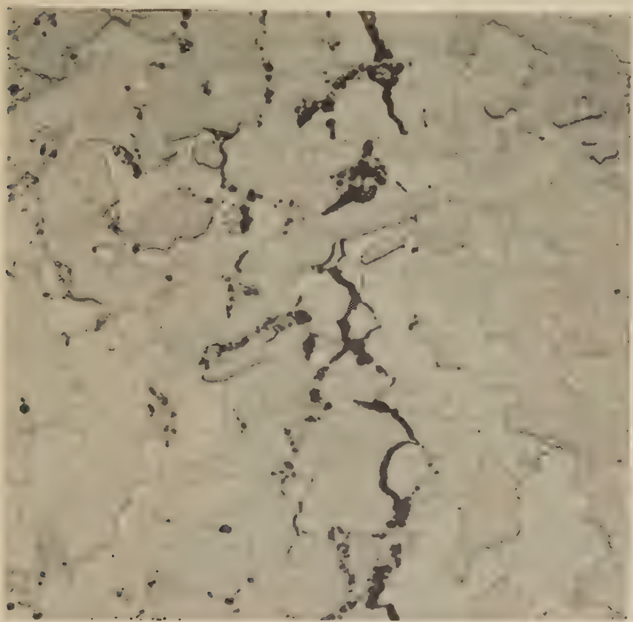

FIG. 14 WELD-HEAT-AFFECTED ZONE OF CREEP-TEST SPECIMEN AFTER 40,200 HR AT 1000 F UNDER 5000 PSI
(Nital etch; ×100.)

FIG. 15 WELD-HEAT-AFFECTED ZONE OF CREEP-TEST SPECIMEN AFTER 2-HR SOLUTION TREATMENT AT 1700 F, FOLLOWING TERMINATION OF CREEP TEST
(Light nital etch; ×100.)

(a)

(b)

FIG. 16 UNDISSOLVED GRAPHITE AND MICROFISSURES IN WELD-AFFECTED ZONE OF SOLUTION-TREATED CREEP-TEST SPECIMEN
(a, Unetched section; ×500. b, Lightly etched section; nital etch, ×500.)

or continuous grain-boundary chain graphite. The authors of the paper have observed that graphitization in some field welds was found to have increased very little, if at all, when checked again after 25,000 hr.

Our own graphitization studies have led us to believe that stress is one of the most important factors in promoting graphitization, and the outstanding factor in causing the formation of grain-boundary chain graphite. We are of the opinion that the graphitized weld from which the previously discussed creep-test specimen was prepared would not have deteriorated to the same extent as the latter if it had been exposed to the same temperature and for the same length of time in the unstressed condition. Elimination of stress concentrations in the weld-heat-affected metal, therefore, appears to be of paramount importance if the formation of dangerous graphite concentration or of grain-boundary chain graphite is to be avoided. A normalizing treatment followed by thorough stress-relieving would appear to be a step in this direction.

It seems to us that the effectiveness of restoring graphitized weld joints by this method will depend not only upon the complete solution of the existing graphite but also upon the effective dispersion of the locally dissolved carbon by diffusion.

Figs. 15 and 16 show the weld-heat-affected zone of the previously described creep-test specimen after a 2-hr solution heat-treatment at 1700 F, following termination of the creep test. It will be noted that some graphite remained undissolved throughout the entire cross section and, more important yet, that microfissures formed at locations where massive graphite went into solution. These microfissures were identified as such by the seepage of drying alcohol, and the resulting staining during microscopic examination. We are presenting this extreme case as a matter of general interest only.

H. J. Robar.[5] Early in the investigation of graphitization of welded pipe sections we, among many others, considered solution of the graphite by heat-treatment as a means of restoring ductility to severely graphitized zones in the C-Mo pipe and castings. In 1944 H. Weisberg reported that normalizing at temperatures up to 2200 F did not materially improve the ductility of the graphitized zone in the Springdale pipe or in a 12-in. cast valve, both of which were severely graphitized. Additional data, summarized in Table 7 (page 49), have been obtained since that time, and indicate that when the graphite is of the chain type or when the nodules are closely spaced, normalizing or normalizing and tempering does not improve the ductility appreciably. The ductility of more mildly graphitized sections, however, is considerably improved.

A miniature bend test was used in determining ductility, for

[5] Metallurgist, Testing Laboratory, Public Service Electric and Gas Company, Maplewood, N. J.

TABLE 8 SOLUTION HEAT-TREATMENT AND REGRAPHITIZATION OF SAMPLES FROM SERVICE

Spec. No.	C-Mo Material	Service Hr	Degree of Graphitization in Service	Graphite Solution Heat Treatment	Degree of Regraphitization in 6000 hr at 1000 F
28DN	Pipe	24636	Medium	1700 F for 2 hr, air cool.	To same degree, but in narrower zone and larger flakes than before heat treatment.
28DA	"	"	"	1700 F for 2 hr, furnace cool 300 F/hr to 1000 F.	Zone is narrower, flakes larger and fewer in number than before heat treatment.
47UN	"	45972	Mild	1700 F for 2 hr, air cooled.	To slightly lesser degree but in slightly larger nodules than before heat treatment.
48DA	"	"	"	1700 F for 2 hr, furnace cool at 300 F/hr to 1000 F.	To slightly greater degree than before heat treatment.
50.1DN	Casting	29000	Heavy	1700 F for 2 hr, air cooled.	To same degree as before heat treatment.
50.1DA	"	"	"	1700 F for 2 hr, furnace cool at 300 F.hr to 1000 F.	To same degree, but in slightly larger nodules than before heat treatment.

(a) (b) (c)

Fig. 17 Regraphitization of Carbon-Moly Steel, ×500
(a, Graphite formed in service; b, same as a after normalizing at 1700 F for 2 hr; c, regraphitization of b after 6000 hr at 1000 F.)

TABLE 7 EFFECT OF SOLUTION HEAT-TREATMENT ON DUCTILITY OF GRAPHITIZED WELDED JOINTS

Spec. No.	C-Mo Material	Degree and Type of Graphitization	Graphite Solution Heat Treatment	Bend Test Results
4-6 AR	Pipe (Springdale)	Heavy chain	None	Cracking started at 1% elongation.
4-6 NA	"	" "	1700 F for 2 hr in N_2, furnace cooled 300 F/hr in N_2 to 1000 F.	Cracking started at 1% elongation.
4-6 X9	"	" "	2200 F for 5 min., air cooled.	Cracking started at no measurable elongation.
4-6 X 10	"	" "	2200 F, compressed 4%, held 5 min. at 2200 F, air cooled.	½" long crack at 6% elongation.
50.3D	Valve casting	Heavy; closely spaced large nodules.	None.	Cracking started at 7.7% elongation, at 11.5% elongation crack was 0.3" long.
50.3DNA	" "	Same as 50.3D.	1700F for 2 hr in N_2, furnace cooled 300 F/hr in N_2 to 1000 F.	Cracking started at 16% elongation, at 20% elongation crack was 0.3" long.
50.1D	" "	" " "	None	Cracking started at 1.96% elongation.
50.1DN	" "	" " "	1700 F for 2 hr, air cooled.	0.18" long crack at 6% elongation.
50.2D	" "	" " "	None	Cracking started at 3.8% elongation, at 5.7% elongation crack was 0.25" long.
50.2DA	" "	" " "	1700 F for 2 hr, furnace cooled 300 F/hr to 1000 F.	0.06" long crack at 14.3% elongation.
99.2U	Pipe (Essex)	Medium; scattered medium size nodules.	None	Three small fissures at 20% elongation.
99.2UN	"	Same as 99.2U	1700 F for 2 hr, air cooled.	No cracking at 24% elongation.
99.2D	"	Medium; medium size nodules, scattered and in short chains.	None	0.3" long crack at 8% elongation, at 16% elongation crack was 0.6" long.
99.2DN		Same as 99.2D.	1700 F for 2 hr, air cooled.	No cracking at 30% elongation.
102.2U	"	Heavy; medium size nodules, scattered and in short chains.	None	0.58" long crack at 4% elongation.
102.2UN	"	Same as 102.2U	1700 F for 2 hr, air cooled.	0.1" long crack at 11.5% elongation, 0.5" long crack at 17.3% elongation.
102.2D	"	Medium; scattered medium size nodules.	None	0.05" long crack at 21.6% elongation, no change at 33.3% elongation.
102.2DN	"	Same as 102.2D	1700 F for 2 hr, air cooled.	No cracking at 32% elongation.
106.2U	"	Medium; scattered medium size nodules	None	Slight fissures at 6% elongation, no change at 31% elongation.
106.2UN	"	Same as 106.2U	1700 F for 2 hr, air cooled.	No cracking at 32% elongation.
106.2D	"	Medium to heavy; scattered medium size nodules.	None	0.2" long crack at 8% elongation, 0.34" long crack at 16% elongation.
106.2DN	"	Same as 106.2D	1700 F for 2 hr, air cooled.	No cracking at 30% elongation.
138.2U	"	Medium; scattered medium size nodules in narrow zone.	None	At 7% elongation specimen was cracked completely across its width.
138.2UN	"	Same as 138.2U	1700 F for 2 hr, air cooled.	Cracking started at 11% elongation, at 22% elongation crack was 0.3" long.
138.2UNT	"	Same as 138.2U	1700 F for 2 hr, air cooled, 1275 F for 2 hr, air cooled.	Cracking started at 6% elongation, at 20% elongation crack was 0.08" long, no further cracking.
138.2D	"	Heavy; medium size nodules as short chains and aggregates.	None	0.3" long crack at 6% elongation.
138.2DN	"	Same as 138.2D.	1700 F for 2 hr, air cooled.	Cracking started at 11.5% elongation, at 15.4% elongation crack was 0.38" long.
138.2DNT	"	Same as 138.2D.	1700 F for 2 hr, air cooled, 1275 F for 2 hr, air cooled.	Cracking started at 10% elongation, further bending increased extent of cracking.

the only available material was small boat-shaped probes cut out of pipe joints. The test specimens, $^1/_8$-in-thick center sections of the probes, were bent in a guided-bend test jig along the zone of graphitization. Fiber elongation was measured on a $^1/_2$-in. gage length.

Heat-treatment does not restore ductility to all graphitized zones, because a residue of unknown composition remains after the solution of the graphite. When the graphite is of the chain type, the residue exists as an irregular fine line; if the graphite is nodular, the residue is nodular, annular, and/or crescent-shaped. It is because of this similarity in form between the residue and the graphite that the ductility of severely graphitized sections is not restored by solution heat-treatment.

Concomitant with the foregoing study, the possibility of regraphitization after solution heat-treatment was investigated. Specimens of varying degrees of graphitization were solution-heat-treated, as shown in Table 8 (page 48) of this discussion, and then maintained in an oven at a temperature of 1000 F for 6000 hr. Subsequent metallographic examination disclosed that all specimens had graphitized again and to approximately the same degree that existed before solution treatment. Fig. 17 herewith illustrates the degree of graphitization before heat-treatment, after solution treatment and degree of regraphitization in the 6000-hr period.

Based upon these results, we have not resorted to solution heat-treatment as a means of rehabilitating graphitized welded sections. Our practice has been to cut out and reweld those joints that are severely graphitized and of poor ductility. All welded sections in old specification pipe and all castings are of course probed at suitable intervals.

I. A. Rohrig.[6] The authors are to be commended for the information they have contributed on the subject of heat-treatment of welded joints in high-temperature main steam piping. Their method of accomplishing the heat-treatment has been outlined clearly, and their test data show that graphitized welded joints can be reconditioned suitably for further service, provided the graphitization has not become critical.

Work of the same nature has been done by the writer's company, and the results are in general agreement with those presented by the authors. An account of this study has been given by D. H. Corey and the writer.[7] By the use of this method normalizing of graphitized welded pipe joints while in position has been carried out by the writer's company since early in 1947.

The tensile-test data given in the paper show that the ductility of the graphitized welded joints used for test was improved markedly by heat-treatment. The data, however, apparently do not reveal the ductility of that part of the sample which is of greatest importance, namely, the graphitized zone. The paper states, "Attempts to force fracture at the outside of the original weld-heat-affected zone where the concentrated graphite had dissolved were not successful." What is required, therefore, is a test that can be applied to the graphitized zone.

The bend test mentioned by Mr. Weisberg in his discussion of an earlier paper[8] meets this requirement reasonably well. That test indicates in a quick and simple manner the relative bend ductility of the graphitized zone. It has been used in the Research Department of The Detroit Edison Company with satisfactory results in evaluating the condition of graphitized welded joints. The apparatus used in the Research Department in performing the bend test consists of two dies, similar to those

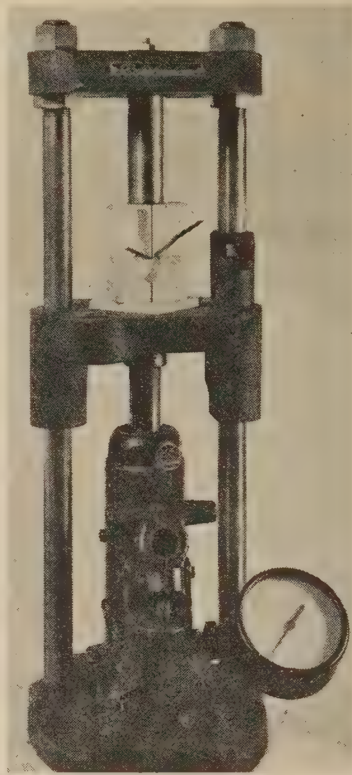

Fig. 18 Bend-Test Dies in Use in Metallographic Specimen-Mount Press

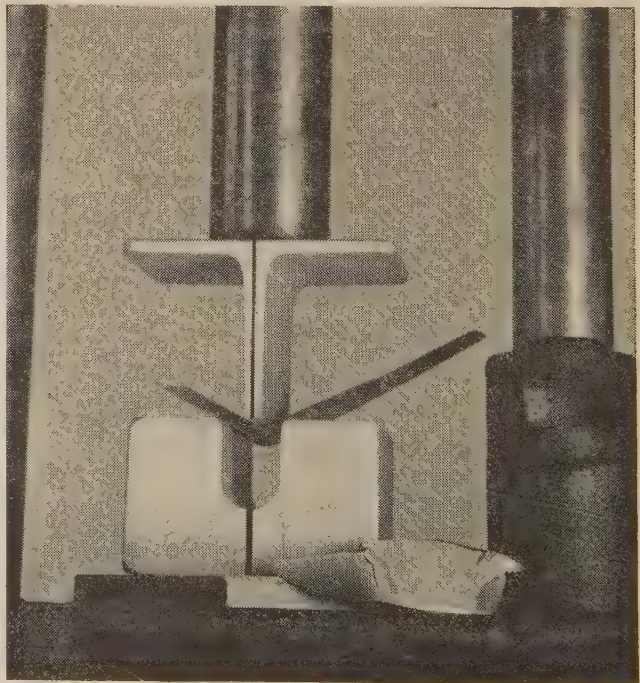

Fig. 19 Close-Up View of Bend Test Dies in Use in Metallographic Specimen-Mount Press and of Graphitized Weld Sample After Bending

[6] Research Dept., The Detroit Edison Company, Detroit, Mich.

[7] "Normalizing of Welds in Carbon-Molybdenum Steel Pipe by 60-Cycle Induction Heating," by D. H. Corey and I. A. Rohrig, Welding Research Supplement of *The Welding Journal*, vol. 24, January, 1945, pp. 1-s–6-s.

[8] See pamphlet, "Graphitization of Low-Carbon and Low-Carbon-Molybdenum Steels," by H. J. Kerr and F. Eberly, bound with Trans. ASME, vol. 67, 1945, pp. 1–45; discussion by H. Weisberg, pp. 35–39.

used by Mr. Weisberg, and mounted in a metallographic specimen-mount press, as shown in Fig. 18 of this discussion. A close-up view is shown in Fig. 19. Pressure is applied by a hydraulic jack, manually operated. A specimen after bending is shown adjacent to the lower die in Fig. 19. Note that the specimen which was cut from a weld-prober sample removed from a graphitized welded joint has cracked badly in the graphitized zone.

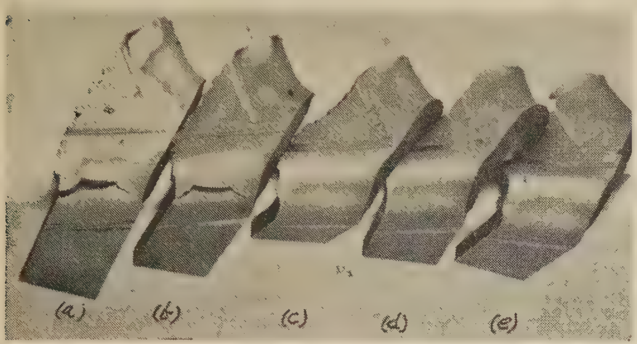

Specimen (a) As removed from service after 64,000 hr at 825 F
(b) Heated at 1700 F for 2 hr, cooled in still air
(c) Heated at 1700 F for 2 hr, furnace-cooled to 800 F, then cooled in still air to room temperature
(d) Same as (c), followed by a draw at 1200 F for 1 hr
(e) Same as (c) followed by a draw at 1275 F for 1 hr

Fig. 20 Bend-Test Specimens From a Welded Joint in Medium-Carbon-Steel Pipe

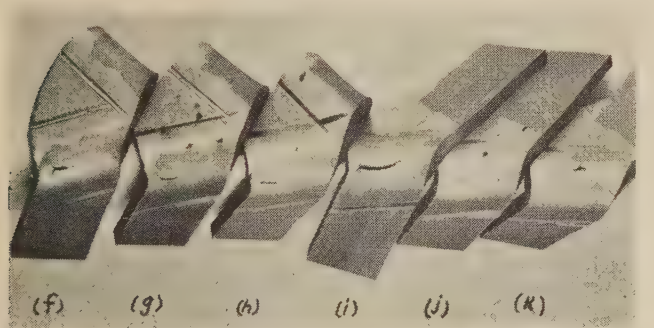

Specimen (f) As removed from service after 59,000 hr at 825 F
(g) Heated at 1700 F for 2 hr, cooled in still air
(h) Heated at 1700 F for 2 hr, furnace-cooled to 800 F, then cooled in still air to room temperature
(i) Same as (h), followed by a draw at 1100 F for 1 hr
(j) Same as (h), followed by a draw at 1200 F for 1 hr
(k) Same as (h), followed by a draw at 1275 F for 1 hr

Fig. 21 Bend-Test Specimens From Welded Joint in Medium-Carbon-Steel Pipe

The specimens shown are $^1/_8$ in. thick and are finish-ground on both faces. Slight etching before test readily reveals the outline of the weld and facilitates positioning of the specimens in the dies so that the bending can be made to occur in the graphitized zone. The results obtained by means of the bend test may be stated in terms such as, length and width of cracks after bending, angle of bend, elongation of the bent area, or gage pressure. Some of the results obtained from this test may be of interest. Bend-test specimens of medium-carbon steel representing various conditions of heat-treatment are shown in Fig. 20.

Severe cracking occurred in the graphitized zone of specimen (a) and in the formerly graphitized zone of specimen (b), when bent. Specimen (c) which had been furnace-cooled, exhibited satisfactory ductility as did specimens (d) and (e), which had been drawn at 1200 F and 1275 F, respectively.

The bend-test specimens shown in Fig. 21 also were taken from a medium-carbon-steel welded joint removed from service.

Although specimen (h), which had been furnace-cooled after 2 hr at 1700 F, had much better bend ductility than specimens (f) and (g), it exhibited a crack in the formerly graphitized zone. Specimen (i), which had been drawn at 1100 F, cracked badly in the affected zone. This fact indicates that a draw treatment at 1100 F may cause brittleness in the formerly graphitized zone. Samples (j) and (k), which had been drawn at 1200 F and 1275 F, respectively, did not crack even when bent 110 deg. The single heat-treatment, consisting in heating at 1700 F for 2 hr, followed by slow cooling, produced good improvement in ductility as determined by the bend test. Further improvement in ductility of joints so treated could be expected as a result of the annealing effect of service at 800 to 900 F.

The results of the bend test, which was made on the samples described herein, are in agreement with the tensile-test results given in the paper, in that the best ductility was obtained by employing a draw treatment at 1275 F, following the 1700 F solution reatment.

The primary purpose of this discussion, however, is to point out that the bend test has the advantage in that the testing force can be applied to the significant area, i.e., the graphitized zone.

Authors' Closure

The authors are grateful to Messrs. Eberle, Robar, and Rohrig for the contributions made to their paper through their discussions.

They are in agreement with the thought expressed by Mr. Eberle, that stress concentration in weld-heat-affected zones appears to be of paramount importance in the formation of dangerous graphite concentrations or of grain-boundary chain graphite. They have never found in their examinations of graphitized metal, after a solution treatment, as large an amount of what we may speak of as "constituent X"—that is, voids, graphite, inclusions, or occlusions, as shown in Fig. 15. As a matter of fact, they have not found any evidence of constituent X in any of the heat-affected zones following solution treatment in the plain carbon steel reported in this paper. They have found constituent X in the carbon-moly steel, in the heat from which the 12-inch pipe was made in the main steam line in the Schuylkill Station, though it was smaller in amount and in particle size than that shown in the photomicrographs in Fig. 16 of Mr. Eberle's discussion. The evidence of constituent X at the time the paper was given was not pronounced. Also, the constituent X was not of a chain-like type.[9]

The authors are grateful for the valuable contribution of Mr. Robar. They recognize that solution treatments would not materially improve the ductility of graphitized zones in pipe as severely graphitized as was the case with the Springdale pipe. Also, they have found that the graphite has a tendency to return to the locations in which it was found after several thousand hours of heating. They have never held that solution treating was a cure, but a method which might be employed for prolonging the useful life of graphitized pipe, provided the graphitization has not developed to too great a degree.

The authors also appreciate the contribution of Mr. Rohrig which so completely described the bend test procedure used by The Detroit Edison Company.

[9] A recent further examination of carbon-moly welded pipe which had been solution treated, that was made nine months after this paper was presented, shows in one of the quadrants of a heat-affected zone a constituent X somewhat similar to that shown in Fig. 16 of Mr. Eberle's discussion.

The authors' feeling with regard to the solution treatment is summed up by Mr. Abele in his statement to the effect that "The treatment has removed a latent critical condition, either temporarily or permanently, and substantially prolonged the useful life of the pipe." This statement, of course, relates to the pipe that had undergone graphitization at the Richmond Station. It does not necessarily hold, however, for all graphitized plain carbon pipe.

Also, the feeling of the authors is covered in the statement by A. E. White to the effect that "No claim is advanced that the restoration of graphitized welds by solution treatment can be employed successfully in all cases."

Development of the Hydraulic Design for the Grand Coulee Pumps

By CARL BLOM,[1] LOS ANGELES, CALIF.

The Grand Coulee pumping plant has been the subject of an extensive hydraulic research program. The first part of this program was conducted at The California Institute of Technology for the Bureau of Reclamation from January, 1938, to July, 1940. Some of the results of this program have already been published (1 to 4),[2] and other papers (5, 6) describe the different features of this project. This paper presents some of the results of continued experimental research of the author's company from 1943 to 1946. The investigation covered the effects of various diffuser-type pump cases and impellers on the pump characteristics of the Grand Coulee model. The paper concludes with the description of the final test of the contractor's model completed in July, 1947.

Preliminary Investigations and Operating Requirements

In a paper by E. B. Moses (5) is described the development of the Grand Coulee Project in detail. A brief summary of the pumping plant will be reviewed here for ready reference. The pumping plant is situated at the Grand Coulee Dam on the Columbia River in the State of Washington. This huge pumping plant will consist of twelve vertical single-stage pumping units. Each unit will be driven by a 65,000-hp motor, or a total of 780,000 hp for the complete pumping plant. The pumps will have a wide operating head range, from 365 to 270 ft, with a corresponding capacity of 1100 cfs to 1650 cfs, when operating at the constant speed of 200 rpm. The pumps will be of the vertical single-stage single-suction type, with 12-ft-diam discharge, and a 14-ft-diam suction.

The Grand Coulee Project makes one feel the daring of its conception, the overwhelming grandeur of its size and power, and last but not least the painstaking care given to the investigation of all its details. In order to obtain strict and exacting final specifications, a research program lasting $2^1/_2$ years was conducted at the Hydraulic Machinery Laboratory of the California Institute of Technology (later called Cal Tech), sponsored by the Bureau of Reclamation (later called The Bureau), and carried through with the co-operation of three pump manufacturers.

The foregoing program was considered necessary even though the investigations and test results of the large pumping units (7, 8) for the Metropolitan Water District of Southern California were available. No part of the research program mentioned would have been effective in detail without the development of Cal Tech Hydraulic Machinery Laboratory (9), with its precision instruments and exact measurements to aid in securing the effect of small design changes.

The final specifications called for a minimum flow rate of 1350 cfs at a rated total dynamic head of 310 ft, and a minimum warranted pump efficiency of 87 per cent at this point. Furthermore the specifications require a minimum flow rate of 800 cfs at a total dynamic head of 365 ft, and a maximum load not to exceed 65,000 hp at 270 ft total dynamic head. The great variations of head and flow rate had to be obtained at a constant speed of 200 rpm. The specifications also prescribe that the head-capacity curve shall be relatively steep, and the pump efficiency as high as possible over the entire range of operation. The pump shall have stable operation free from cavitation within the full range of operating heads.

Pumping-Plant Layout and Head Variation

Each pumping unit will pump through separate piping systems (see Fig. 1). Each system consists of the trash rack, intake structure, a 90-ft-long 14-ft-diam suction pipe and elbow, and an 850-ft-long 12-ft-diam discharge pipe. The water surface at the intake to the pumping plant will fluctuate from a maximum elevation of 1290 to a minimum of 1208, that is, a total difference of 82 ft. At the same time the water surface at the outlet will vary between the elevations of 1571 and 1557, a difference of 14 ft.

The foregoing head variations, and the pipe-friction loss, also shown in Fig. 1, and the static water-surface elevation from the intake to the outlet lead to a variation of total dynamic heads from a minimum of 270 ft to a maximum of 365 ft, or an operating range from 100 to 135 per cent. The most severe suction conditions occur at low capacities when the water surface at the intake is at an elevation of 1208. The center line of the pump is located at an elevation of 1203, which provides only a 5-ft submersion for pumping heads from 365 ft down to 350 ft.

Need for Further Investigations

Difficulties were encountered when the former test results were applied to our investigation of a pumping unit of minimum weight and cost. Early weight calculations eliminated the most attractive case type, that is, the double-volute case. This type satisfied all the requirements of the specifications. However, the weight became excessive because of the heavy reinforcing needed to maintain permissible stresses in the open section. Unlike this, the diffuser-type case, in which the diffuser vanes act as connecting members between the two side walls, leads to a lighter pump case and thereby to the most economical unit.

In the original model study, pumps with diffuser cases gave a very unstable performance near the 365-ft operating head. The problem therefore was to design a diffuser-type case which would meet all the hydraulic requirements and particularly have stability of performance near the high operating head. This unstable portion of the pump characteristics was greatly affected by the pump-case design and had not been overcome satisfactorily by the preliminary experiments with diffuser-type cases.

Further investigation was also necessary owing to the wider operating head range given in the final specifications. The original model study conducted at Cal Tech from 1938 to 1940, was based upon a total head variation from 295 to 365 ft, or a total operating range from 100 to 125 per cent, while the final specifications call for an operating range of from 100 to 135 per cent.

---

[1] Chief Engineer of Byron Jackson Co. Mem. ASME.

[2] Numbers in parentheses refer to the Bibliography at the end of the paper.

Contributed by the Hydraulic Division and presented at the Semi-Annual Meeting, San Francisco, Calif., June 27–30, 1949, of The American Society of Mechanical Engineers.

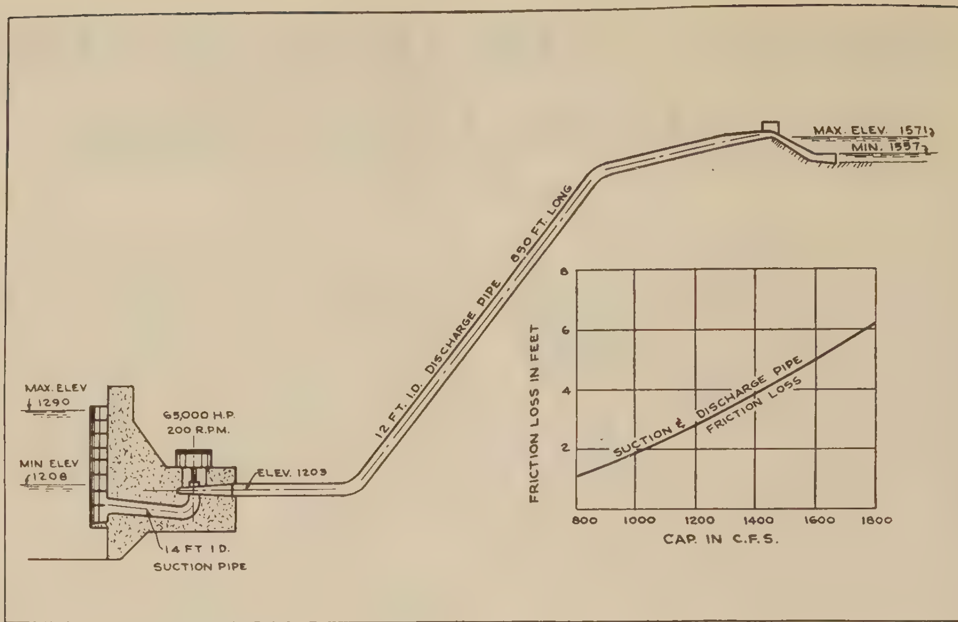

Fig. 1 Sectional Elevation of Grand Coulee Pumping Plant

As these and other problems became more evident soon after Byron Jackson Co. and The Pelton Water Wheel Company decided to make a joint bid, they initiated in 1943, a program of development. This program assigned to Byron Jackson Co. the task to design, build, and test models in order to develop the final hydraulic lines of the pump. The investigation was conducted at Byron Jackson Co.'s plant from 1943 to 1946, and carried to a successful completion in spite of war and postwar difficulties.

At the end of the investigation a bid was submitted and resulted in the award of a contract to build six pumping units. After the award the research program was continued at Byron Jackson Company's plant and, at the same time, it was decided to conduct the final acceptance test at Cal Tech. It was deemed advisable to take advantage of the precision test facilities at Cal Tech because of the magnitude of the project and the desirability of having impartial observers. Also, the big prototype-to-model ratio of 13 to 1 made it imperative that tests should be conducted with the greatest possible accuracy.

Presentation of Test Data

Before going into the details and comparisons of test results at the different stages of development, the following differences of presentation are noted. The preliminary tests at Cal Tech and some of the tests by the author's company were made with model units of greater size than the final ones used for acceptance tests. The reason for this was that the horsepower available at Cal Tech was not sufficient to run the original model at speeds corresponding to the operating heads in the field. The specifications called for tests at field heads. Furthermore, in the final model the casing was built with sectional breaks in curvature, corresponding to the welded structure of the prototype case. This was a deviation from the earlier models which were all furnished with smooth pump cases and were of a larger size. Unfortunately, time did not permit us to duplicate the final model with a smooth casing so that the friction losses in the two cases might have been compared.

In the original testing program from 1938 to 1940, the suction-head reading was taken at the suction flange, and the discharge head reading 10 diam beyond the end of the discharge

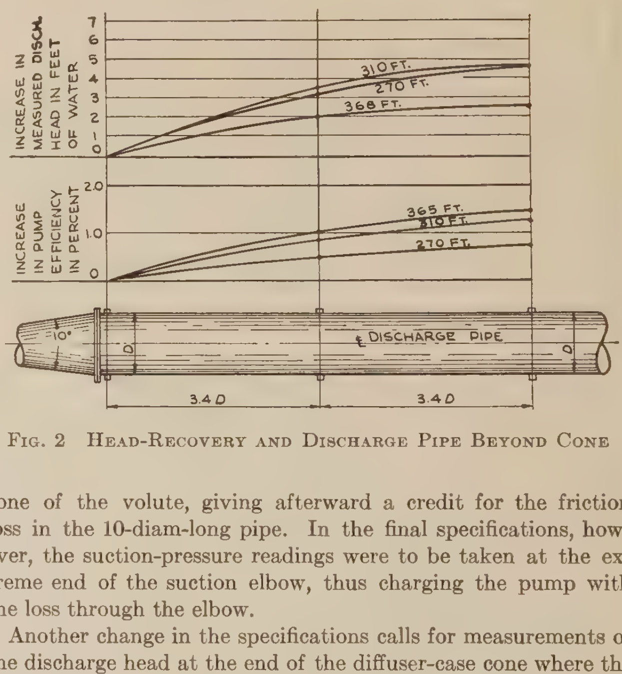

Fig. 2 Head-Recovery and Discharge Pipe Beyond Cone

cone of the volute, giving afterward a credit for the friction loss in the 10-diam-long pipe. In the final specifications, however, the suction-pressure readings were to be taken at the extreme end of the suction elbow, thus charging the pump with the loss through the elbow.

Another change in the specifications calls for measurements of the discharge head at the end of the diffuser-case cone where the velocity distribution is far from uniform, while the velocity head is figured from a uniform velocity arrived at by dividing the capacity with the area. That there is an apparent gain in discharge head further downstream figured on this basis is shown in Fig. 2.

To determine the amount of this gain in discharge head, a set of readings was taken on a model with a 10-deg-discharge cone at the end of the cone, and 3.4 and 6.8 diam beyond the cone. These readings showed a substantial gain at 6.8 diam beyond the end of the cone, and so justify the Hydraulic Institute's recommendation of measuring the head at a point 10 diam beyond the cone. However, the specifications permitted lengthening of the discharge cone by reducing the total cone angle, thereby obtaining much more uniform velocity distribution at the end of the cone.

In the last models a discharge cone with a 3-deg total cone

angle was used, and head readings obtained at the end of this cone were slightly lower than readings obtained with a 10-deg cone at a point 6.8 diam beyond the end of the cone.

Owing to these different definitions and measurements of total head, the different performance curves are not directly comparable. No attempt was made to recalculate the performance curves and bring them to the same basis, but performance curves shown on any one figure were obtained with the same test procedure and are directly comparable.

For convenience of comparison, most of the model test data were converted into prototype values at an operating speed of 200 rpm. Also, it was found most practical to compare the pump characteristics at an operating point of 1450 cfs at 310 ft. This point gave the same percentage of safety above the minimum required capacity of 1350 cfs at 310 ft as the power percentage safety below the maximum permissible power requirement of 65,000 hp at 270 ft.[3]

For better understanding of the various performance curves, the main dimensions for the various model impellers and pump cases referred to in the various figures are given in Table 1. All models were mounted horizontally and were of a construction as shown in Fig. 15.

Following is a description of the step-by-step development of various pump cases and impellers to arrive at the smallest pump size and highest pump efficiency unit having a stable noncavitating performance curve under all operating conditions.

Pump-Casing Study

The pump casing represents a high percentage of the total pump weight and, as previously mentioned, the diffuser-type casing proved to be lighter than the single- and double-volute case. However, the pump characteristics with a 12-vane diffuser-type case had not proved satisfactory. Therefore, a continued study of various types of diffuser cases was necessary.

The effect of the pump-casing type on the head-capacity characteristics is shown in Fig. 3. Here the same impeller was tested in two pump cases, a double-volute case with a volute area of 21 sq in. and a 12-fixed-vane diffuser case with a diffuser entrance area of 20.8 sq in. The double-volute-case performance meets all the requirements with a stable head-capacity curve over the operating range, and also exceeds the minimum pump efficiency of 87 per cent at the 310-ft operating point. The 12-vane diffuser case, however, has an abrupt drop in head near the 365-ft head, and the pump efficiency at the 310-ft operating point is

[3] To permit simplified test procedure and also to eliminate the possibility of cavitation, all performance tests were run with a constant net positive suction head of 115 ft.

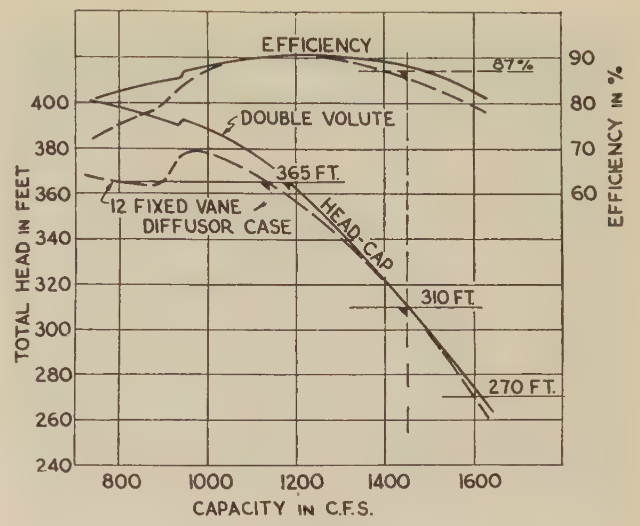

Fig. 3 Effects of Casing Type on Pumping Characteristics

below the minimum 87 per cent required. This drop in head also affected the brake horsepower, and this unstable portion of the performance curve was considered too close to the 365-ft head for safe operation. The foregoing performance curves indicate that the lower number of diffuser vanes would give a more stable and, in general, a more satisfactory performance.

In order to determine the influence of diffuser-case entrance area on the pump characteristics, a series of tests were run with a gradual increase of diffuser-case entrance areas, using the same impeller for all tests. In Fig. 4 is shown the effect of diffuser-vane inlet area on pump characteristics for model pumps using the same impeller and the same 12-fixed-vane diffuser case as described and illustrated in Fig. 3. The diffuser-case inlet area was changed from A to B, which latter is 18 per cent larger than A. Alternating the diffuser-vane inlet area also affects the diffuser-vane entrance angle, but experiments have shown that the area affects the pump performance to a much greater degree than the diffuser-vane angle. The increased diffuser-vane entrance area improved by several points the pump efficiency at 310-ft head, but the head-capacity curve dropped below the 365-ft head. Therefore this performance curve was not acceptable, and further study of the 12-fixed-vane diffuser case was abandoned.

Next a design study was made of fixed-vane diffuser cases with 3, 4, 5, and 6 diffuser vanes, in order to analyze the practical

TABLE 1 IMPELLER AND CASING DIMENSIONS OF MODELS

		Fig. 3	Fig. 4	Fig. 5	Fig. 6 Fig. 8 Fig. 9	Fig. 10	Figs. 11, 12, 13 Final model A	B
Impeller	Outlet diam, in.	14 9/16	14 9/16	14 9/16	12 7/8	14 9/16	12 7/8	12 7/8
	Outlet width, in.	1 5/8	1 5/8	1 5/8	1 1/2	1 5/8	1 1/2	1 1/2
	Eye diam, in.	7 1/2	7 1/2	7 1/2	6 7/8	7 1/2	6 3/4	6 7/8
	Outlet vane angle, deg	23 1/2	23 1/2	23 1/2	24	Fig. 10 8	23 1/2	24
	Number of vanes	8	8	8	7	7 6	8	7
Diffuser case	Entrance area, sq in.	21 (volute) 20.8	20.8 24.0	20.8 21.0	18.7	22.0	18.7	18.7
	Outlet area, sq in.	44.0	44.0	44.0 36.0	28.0	36.0	28.0	28.0
	Vane lip diam, in.	15.5	15.5 15.6	15.5 15.6	13 3/4	15.6	13 3/4	13 3/4
	Vane lip width, in.	2 7/8 (volute) 1 21/32	1 21/32	1 21/32 1 3/4	1 5/8	1 3/4	1 5/8	1 5/8
	Number of vanes	2 12	12	12 6	6	6	6 with rib	6 with rib
Model size		11.5	11.8	11.8	13.0	Fig. 10	13.1	13.0
Factor		11.8	11.5					

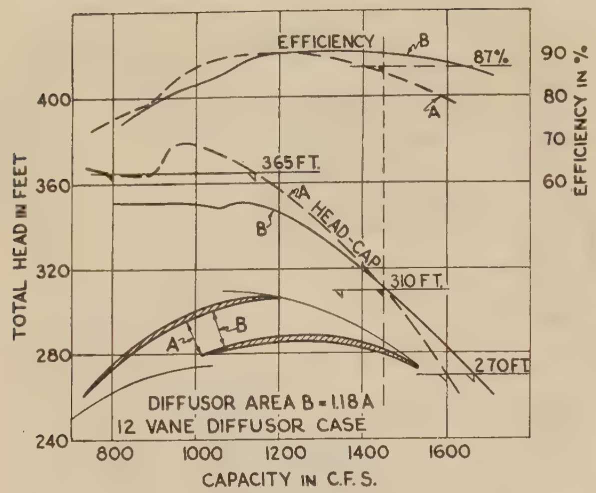

Fig. 4 Effects of Diffuser-Inlet Area on Pump Characteristics

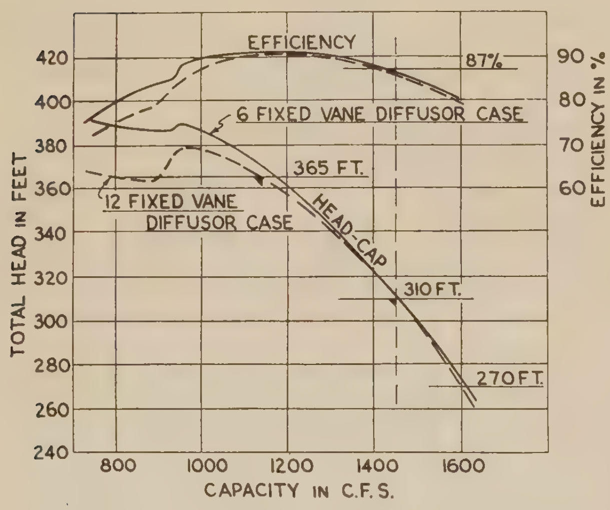

Fig. 5 Effects of Number of Diffuser Vanes on Pump Characteristics

minimum number of vanes which would give sufficient strength and allow a substantial weight saving and still meet all requirements. This study proved that the 6-vane diffuser case was the most satisfactory.

Fig. 5 shows comparison of pump characteristics for 6 and 12-fixed-vane diffuser cases. Here the same impeller was tested in the two diffuser cases, both having practically the same diffuser-vane inlet area but different diffuser-vane outlet areas as shown in Table 1. The 6-vane diffuser case improved noticeably the head-capacity performance near the 365-ft head and materially reduced the dip in the unstable range. The pump efficiency at the 310-ft operating point for the 6-vane diffuser case showed only a slight gain over the 12-vane diffuser case. However, the pump efficiency at that point was later improved. This was accomplished partly by increasing the diffuser-case inlet area which was permissible with the 6-vane diffuser casing, as this casing still gave a stable characteristic at the 365-ft head.

Next, the change of performance with increased outlet area of the diffuser cases was determined. As might be expected, the larger diffuser cases with lower velocities permitted a greater head recovery at the end of the diffuser vanes and therefore showed some improvement in the pump efficiency. However, this would have resulted in too large a pump case, and therefore further study was continued in order to improve the pump efficiency with the small diffuser case.

New-Type Diffuser Case. By studying the flow distribution in the outlet of the pump-discharge cone for a 6-vane diffuser case, it was found that the higher velocities crowded toward the outside of the pump casing. To obtain a more uniform flow at the end of the discharge cone, several ribs were tried in the pump casing. The best result was obtained when using one rib dividing the flow in a diffuser case into two separate streams similar in principle to a double-volute case. This rib design is shown in Fig. 6. The location of the dividing rib may also be seen in Fig. 7 which shows the final model on its base in the laboratory with the front half of the case removed but with impeller diffuser ring and dividing rib in place.

The velocity distribution at the end of a 3-deg discharge cone for a 6-vane diffuser case, with and without a dividing rib, is shown in Fig. 8. The effect of this dividing rib on the pump characteristics, resulting in increased head and higher efficiency, is shown in Fig. 9.

The same tests were repeated on 6-vane diffuser cases, with and without dividing rib, the cases having a total cone angle of 10 deg, and the results were relatively the same. In the two sets of tests, the gain in pump efficiency and head for the case, with a dividing rib as against the case without this rib, was greater than the energy difference calculated by the integration of the velocity heads corresponding to the different velocity distributions, Fig. 8.

It will be noted that the first three diffuser vanes remain the same in the two pump cases with and without the dividing rib. The difference in performance obtained by these two pump cases therefore can only be the result of what happens beyond the outlet of the third diffuser vane. From this point on, in the case without the dividing rib, the streams from the 4th, 5th, and 6th diffuser vanes flowing into the stream from the first three diffuser vanes must introduce shock and mixing losses which are greater than the friction loss from the two separate streams in the case with a dividing rib. This result was somewhat surprising, since the dividing rib decreases the hydraulic radius of the case.

By continued use of this reasoning, the best results should perhaps be obtained by separating all the streams coming from the diffuser vanes. But such a diffuser case would become impractical to manufacture and, undoubtedly, the further decrease of the hydraulic radius would result in greater friction losses which would offset the gain in reduced mixing and shock losses.

No further tests were made to clear up this point. The improved efficiency in the larger diffuser case previously mentioned, undoubtedly was the result of longer diffuser vanes, although in that case we dealt with diffuser cases with lower velocities. Hence the results are not directly comparable.

Effects of Impeller-Discharge Vane Angle on Pump Characteristics and Pump Size

Three impellers, having the same profile but with $26^1/_2$, $23^1/_2$, and $18^1/_2$ deg discharge vane angles were tested in a 6-fixed-vane diffuser case. The pump characteristics of these three impellers are shown in Fig. 10. In this particular case, it was more advantageous to present the actual model performance curves, as they more clearly indicate the spread in the head-capacity performance.

The impeller with the $26^1/_2$-deg discharge vane angle will require a multiplying factor of 11.4, while the impeller with an $18^1/_2$-deg angle requires a multiplying factor of 12.3 of this larger model, or, converted into weight, the impeller with the lower

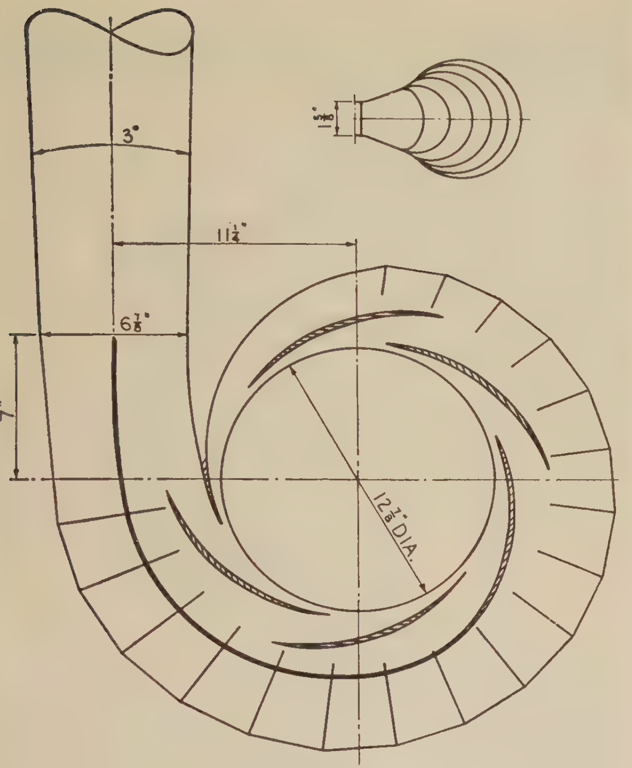

Fig. 6 Diffuser Case With Separating Rib for Grand Coulee Model Pump

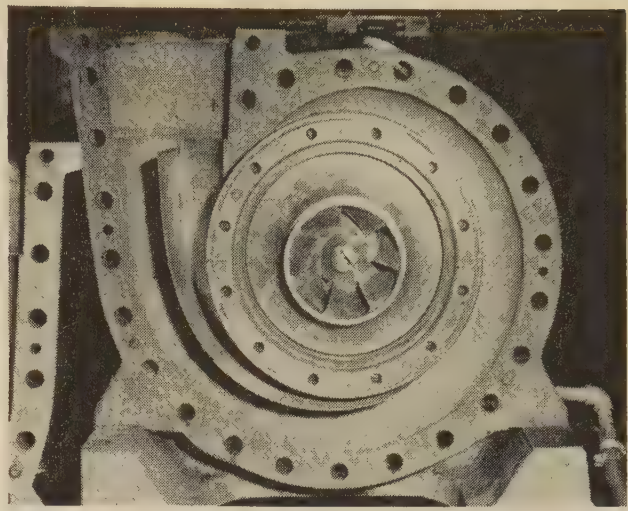

Fig. 7 Grand Coulee Model Pump With Half of Casing Removed Showing Impeller, Diffuser Ring, and Separating Rib

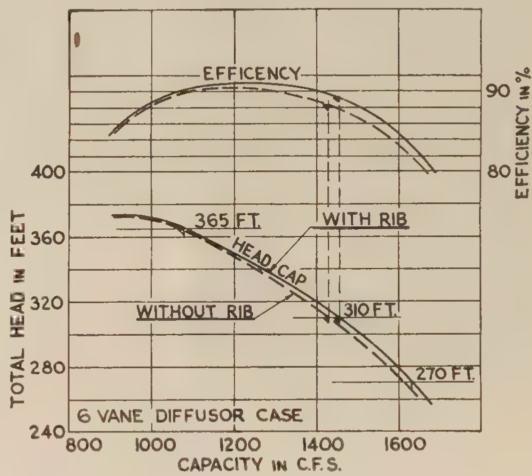

Fig. 9 Effects of Casing Separating Rib on Pump Characteristics

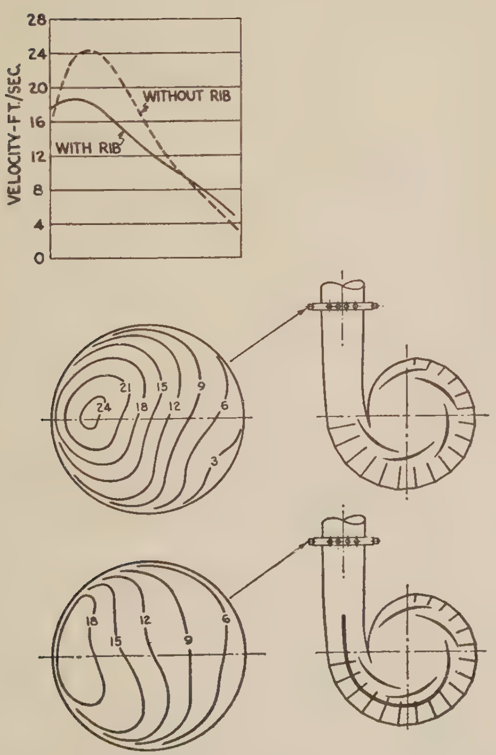

Fig. 8 Velocity Distribution in Pump Discharge for 6-Vane Diffuser Case With and Without Separating Rib

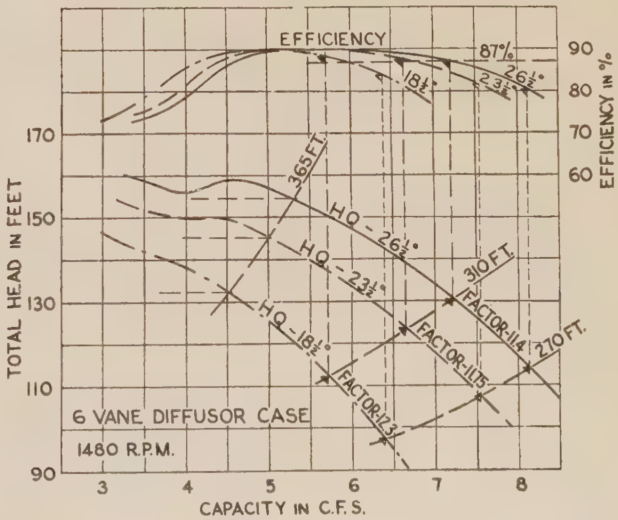

Fig. 10 Effects of Impeller-Outlet Vane Angle on Pump Characteristics

angle would result in a 25 per cent heavier pump case than an impeller with the steeper angle.

However, the head-capacity performance near the 365-ft head became more unstable for impellers with steeper vane angles. The unstable part of the curve for the $26^1/_2$-deg vane angle was considered the upper safe limit for an impeller with this profile. Therefore, to allow for a certain margin of safety in the unstable range, the final model pump was designed with impellers having outlet discharge vane angles of 24 deg. Also, impellers with wider profiles were tested in wider diffuser cases, but these casings had the same diffuser inlet area as the narrow diffuser casings. The wide-profile impeller gave the same type of performance as a narrow-profile impeller with steeper vane angle. No noticeable gain in pump efficiency was obtained with the wider impellers.

Effects of Impeller-Vane Entrance Angle on Cavitation Performance and Pump Characteristics

Impellers with different impeller-eye profiles were designed and tested to determine the effect of the ratio between radial and peripheral eye velocities on the cavitation performance. In this study it was found that the information given in C. A. Gongwer's paper (2) was very useful, and the best cavitation performance was obtained with an impeller-eye profile which agreed with the formula recommended in that paper.

The effect of the impeller-entrance vane angle on the cavitation performance and pump characteristics is demonstrated by two impellers, A and B, tested in the same 6-vane diffuser case with a separating rib. The two impellers have practically the ame profile and outlet vane angle (see Table 1). The main differences in design are the impeller-entrance vane angles as shown on the diagrams in Fig. 11.

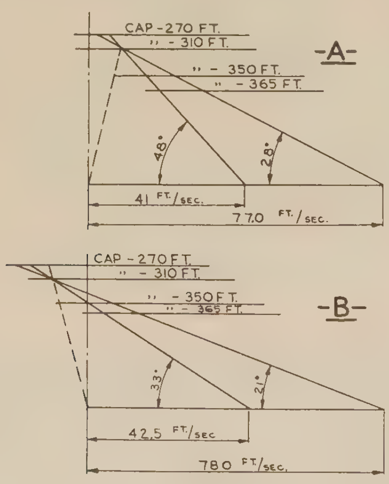

Fig. 11 Entrance Velocity Triangles for Impellers A and B

Impeller A, with entrance vane angles 28 deg at the eye and 48 deg at the hub, favor shock-free operation at the larger capacity, while impeller B, with vane entrance angles of 21 deg at the eye and 33 deg at the hub, will give shock-free operation at lower capacities.

Fig. 12 shows the result of cavitation tests for these two impellers. Impeller A does not satisfy the minimum σ requirement for the lower capacities at 365 and 350-ft head but, as expected, gives ample safety at the larger capacities, particularly for the capacity at 270 ft. Impeller B, however, satisfies all requirements, but the amount of safety of course is less at the larger capacities.

The pump characteristics of the two impellers are shown in Fig. 13. A comparison of these two pump characteristics shows that the impeller-vane entrance angle also has an amazingly great effect on the pump performance. The lower impeller-vane en-

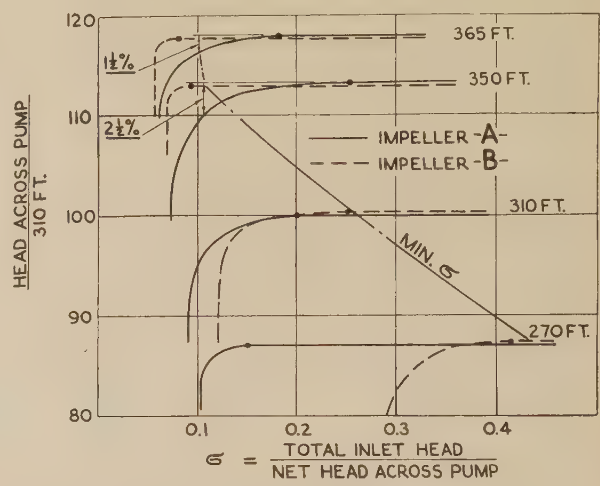

Fig. 12 Effects of Impeller-Entrance Vane Angle on Cavitation Characteristics

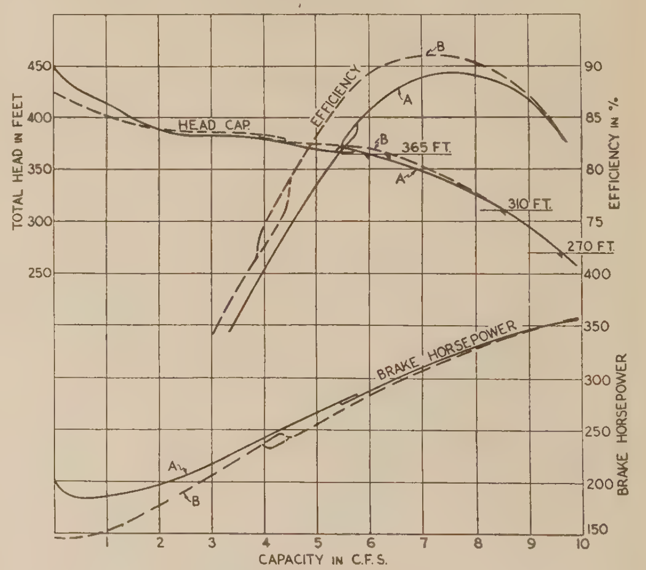

Fig. 13 Effects of Impeller-Entrance Vane Angle on Pump Characteristics

trance angles on impeller B have also several beneficial results on the pump characteristics, as follows:

1 Lower head and brake horsepower at the closed valve, which latter would result in less starting-torque requirement for the motor if started under shutoff conditions. The lower head may be the result of less back pressure created by the lower vane angle at zero and low capacities.

2 The unstable portion of the head-capacity curve and brake horsepower moves to a lower capacity with a flatter impeller-entrance vane angle and allows for greater safety of stable operation near the 365-ft head. It is interesting to note in the previous figures shown that the unstable performance caused by the pump casing remains at the same capacity from one type of pump case to the next, and the case design affected only the magnitude of the dip in the head-capacity curves. This also held true in the unstable portion of the brake-horsepower curve. As the lowering

of the impeller-entrance vane angles moved the unstable portion of the head-capacity curve as well as the brake-horsepower curve to a lower capacity, this would indicate that the unstable portion in the performance is the result of flow conditions in the impeller eye.

3 The improved pump efficiency over the operating range, particularly at the lower capacities, gives a strong indication that for pumps designed for a definite operating point, in this case, for instance, 310 ft, the impeller should have vane entrance angles giving a velocity diagram similar to impeller B, rather than the conventional diagram as obtained by impeller A. The suction approach and the NPSH available must of course also be given consideration in the selection of the impeller-entrance vane angles. For commercial pumps, however, which must cover a wide range of capacities it probably will be found necessary to use impellers with vane entrance angles similar to those used in impeller A, as this steeper vane entrance angle has a greater σ safety against cavitation at the larger capacities.

The final model used for acceptance tests incorporated all the improvements mentioned, and the following résumé will give the results of the final acceptance tests.

Model-Pump Tests

Final model tests were conducted by the Cal Tech Hydrodynamics Laboratory. Laboratory equipment, except for slight modifications, was the same as previously described in detail (9).

Specifications No. 1128 of the United States Department of the

Fig. 14 Grand Coulee Model Pump Installed in Cal Tech Lab

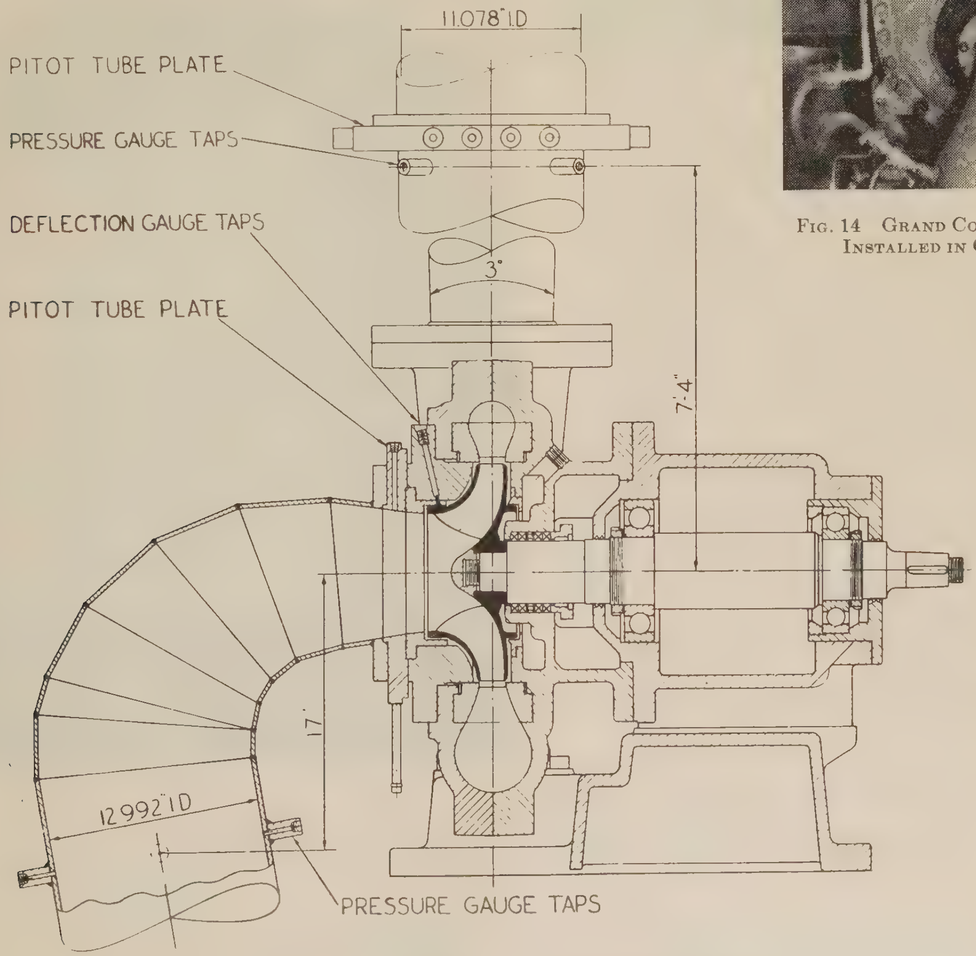

Fig. 15 Assembly, Grand Coulee Model Pump

Interior, Bureau of Reclamation, under which the contract for the six 65,000-hp pumps was awarded, required, in addition to characteristic and cavitation tests, the determination of the following:

1 Amount of unbalanced side thrust on the impeller.

2 Distribution of flow and amount of prerotation at the eye of the impeller.

3 Velocity distribution at the end of the casing extension diffuser.

4 Pressure variations near the periphery of the impeller in both the top and bottom covers.

The final model, set up for test in the Cal Tech Hydrodynamics Laboratory, is shown in Fig. 14. The long stainless-steel casing extension diffuser is shown, with discharge piezometer connections at the upper end. A portion of the converging-cone suction elbow, together with one of the balance lines from the back of the impeller to suction pressure, also will be noted in this illustration.

Fig. 15, the model pump assembly, shows the location of both suction and discharge piezometer connections and also the Pitot-tube plates used in the determination of velocity distribution. Piezometer connections, as shown, are located in accordance with the specifications.

From Figs. 14 and 15 it may be seen that the heads and efficiencies obtained in these tests, and reported herein, are not those of the model pump alone but include losses in the suction and discharge piping between the piezometer connections and the pump.

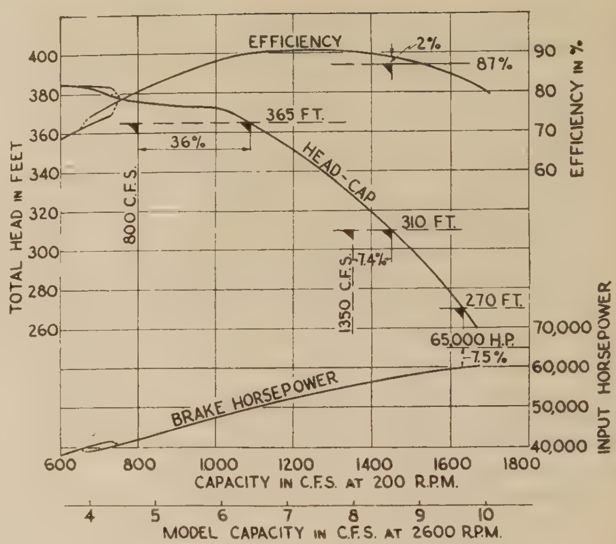

Fig. 16 Model Pump Characteristics

Characteristic and Cavitation Tests

All testing was performed at heads equal to those of the prototype, necessitating operation at 2600 rpm, i.e., prototype speed of 200 rpm multiplied by the model ratio of 13. Results of characteristic tests are plotted in Fig. 16 on which a scale has been added for prototype capacity, obtained by multiplying model capacity by the cube of the model ratio, and the inverse ratio of the operating speeds. In accordance with the specifications, the efficiencies shown are those obtained by the model and include losses in suction and discharge piping between piezometer connections. Furthermore, model efficiencies are shown as applying to the prototype, unlike turbine practice wherein an increase is permitted due to decreased relative roughness and clearances.

The test installation included a scale model of the trash rack and inlet structure of the prototype, enclosed in a pressure tank to permit varying the suction pressure (see Fig. 17). The width of the channel ahead of this trash rack was restricted by side plates to that equivalent to one bay in the Grand Coulee wing dam. Water flowing into this channel was passed through a gravel-bed filter having sufficient resistance to insure uniform flow, in an effort to duplicate, as nearly as possible, suction conditions obtaining in the prototype. The entire suction from the trash-rack structure to the pump duplicated that of the prototype to a model ratio scale of 1 to 13.

Table 2 is a comparison of model test results with specification requirements.

The minor discontinuity in the head-capacity curve, indicating unstable operation, falls well outside the operating range of the prototype.

The test results show the model ratio of 13 to be ideal in that it permits minor variations, either smaller or larger, due to manu-

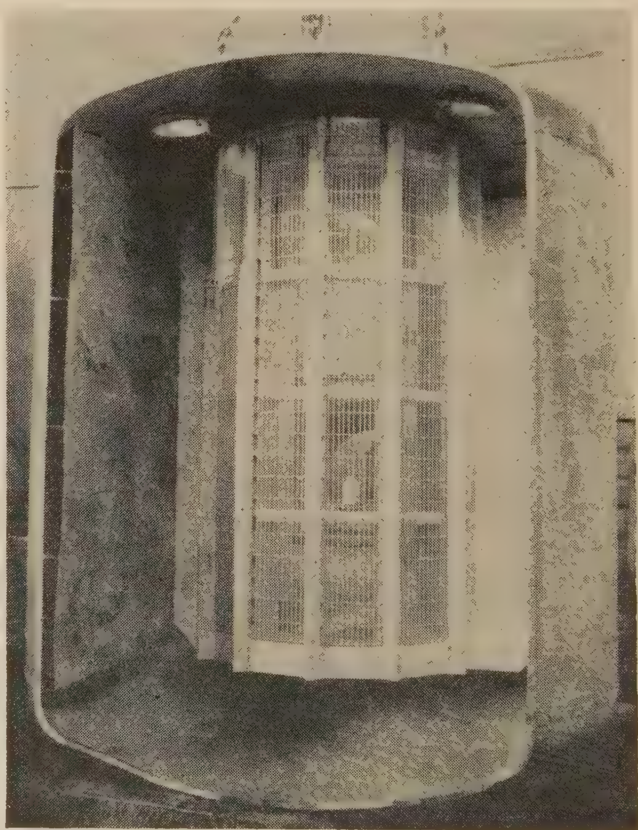

Fig. 17 Model of Inlet Trash Rack

TABLE 2 COMPARISON OF MODEL TEST RESULTS WITH SPECIFICATION REQUIREMENTS

	From Fig. 16	Required by specifications	Safety above requirements, per cent
Cap. at 365-ft head.......	1087 cfs	800 cfs (min)	36
Cap. at 310-ft head.......	1450 cfs	1350 cfs (min)	7.4
Eff. at 310-ft head........	88.9 per cent	87 per cent (min)	2
Bhp at 270-ft head........	60100	65000 max	7.5

facturing tolerances in the prototype, without falling short of the minimum required capacities or exceeding the maximum permissible horsepower.

Cavitation performance is shown in Fig. 18 for each of four operating conditions, i.e., the maximum head, the minimum head, the normal (or warranted) head, and a head corresponding to low water in both the lake and the discharge canal. The operating range shown is based on prototype performance, lake levels on the suction side, discharge canal levels, and anticipated conduit and entrance and exit losses. Upper and lower limits of this operating-range area are based upon high and low water

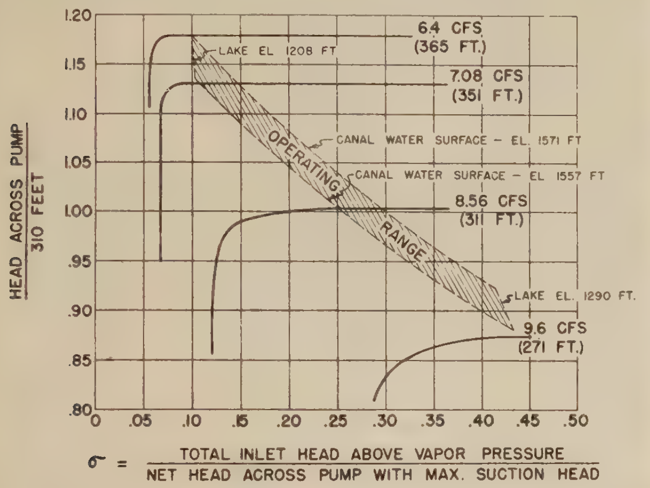

Fig. 18 Cavitation Characteristics of Final Model

in the discharge canal, and right and left limits are based on high and low water in Lake Roosevelt. These tests show a margin of safety between the operating range and the inception of cavitation sufficient to exclude the possibility of cavitation damage.

Unbalanced Side Thrust on Impeller

The direct measurement of the amount of unbalanced side thrust on the impeller of a pump, operating at 2600 rpm and 355 bhp, presents numerous difficulties, aggravated by the requirement to make the measurements on a model which in its final form had only 0.007-in. diametral clearance between the rotating and stationary seal rings. Therefore it was decided that the deflections of the pump shaft during operation would be measured; which, combined with the spring constant of the shaft determined at rest, would permit accurate calculation of the forces causing the deflection.

To measure the deflection of the shaft during operation, two insulated metal probes were inserted at points 90 deg apart through holes in the suction cover. A suitable bracket was provided for each probe to hold it in position and at the same time permit fine control of its movement, toward or away from the impeller seal ring. A dial indicator reading to 0.0001 in. was rigidly mounted on each bracket and used to determine the location of each probe. Contact with the impeller seal ring was determined by neon bulbs operated by transformers through a low-voltage trip circuit (see Fig. 19).

It was possible accurately to locate the center position of the impeller with the pump filled with water and slowly rotating so that side thrust was negligible. Then, with the model operating at full speed, deflection readings were taken at various capacities. The resultants of these readings, at the proper angle with the model center lines, are plotted in Fig. 20.

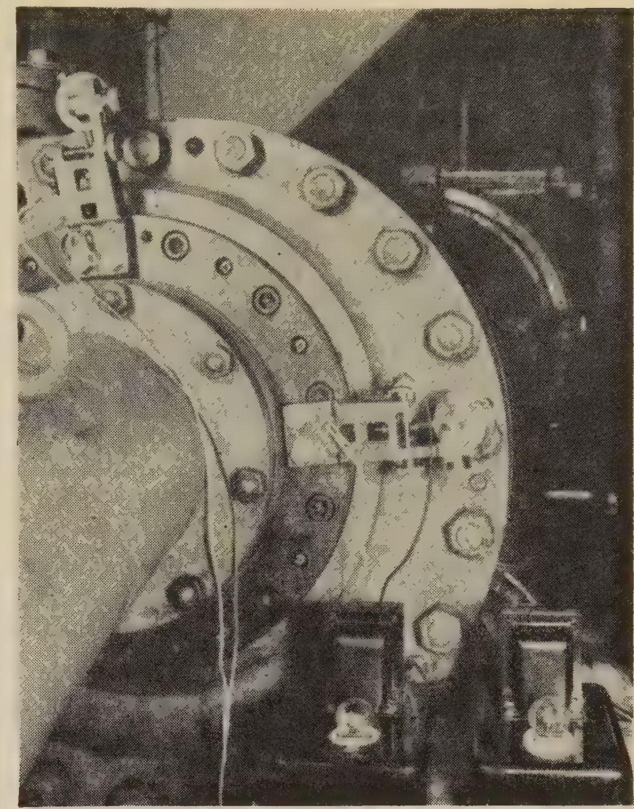

Fig. 19 Setup for Measuring Deflection at Impeller, Grand Coulee Model

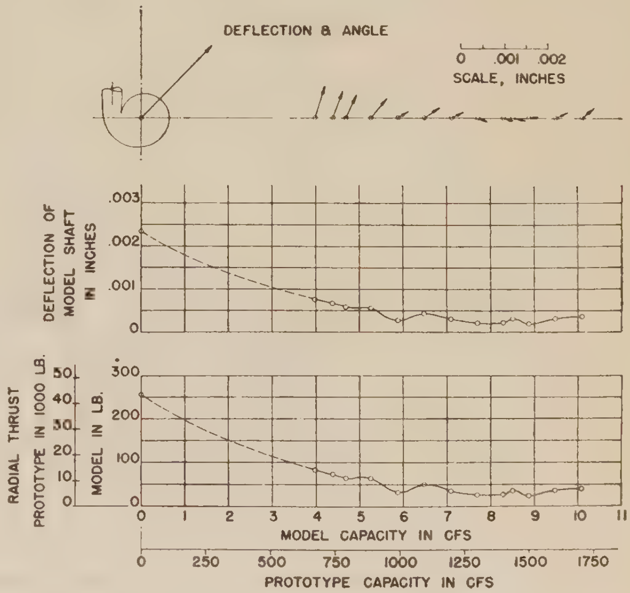

Fig. 20 Deflection and Radial Thrust of Final Model

Determination of the spring constant of the model shaft, while at rest, with a beam and weights, permitted the calculation and plotting of the lower curve in Fig. 20, radial thrust versus capacity. The radial-thrust scale for the prototype was obtained by multiplying the model thrust scale by the ratio of areas, that is, the square of the model ratio.

From this curve it may be seen that the maximum radial

thrust under any operating condition, to be encountered in the prototype, is less than 9000 lb and the maximum at shutoff head is only 43,000 lb. This is considered insignificant in a unit of this size having a shaft nearly $2^1/_2$ ft diam and an impeller which weighs nearly 30 tons.

Distribution of Flow and Amount of Prerotation at Eye of Impeller

The velocity and direction of flow of the water entering the impeller were determined by a direction-finding Pitot tube inserted into a plate located approximately 2 in. ahead of the impeller, as shown in Fig. 15. Five traverses were made in each direction. Readings were taken through the entire cross section and results plotted. Numbers on the isovelocity diagrams in Fig. 21 indicate velocity in feet per second.

Velocities on these diagrams are unusually uniform and corroborate the wisdom of The Bureau in the choice of a converging-cone elbow for the pump suction. There is no backflow and consequently no prerotation within the normal operating range for the prototype.

Velocity Distribution at End of Casing-Extension Diffuser

Velocity and direction of flow of the water leaving the casing-extension diffuser were determined by a direction-finding Pitot tube inserted in a plate similar to that used on the suction side, except that four traverses instead of five were made in each of two directions at 90 deg. The plate used is illustrated in Fig. 22 with a Pitot tube inserted through one of the holes. Note the circular scale with a vernier to determine accurately the direction in which the impact hole in the tube is pointed. A scale on the mounting head permits determination of the location of the impact- and static-pressure holes with respect to the center of the pipe. This plate may be seen installed in the discharge line at the end of the upper casing-extension diffuser in Fig. 14.

Results of readings taken at the highest head, normal or guaranteed head, and lowest head, are shown in Fig. 21. Numbers indicate velocity in feet per second.

At the guaranteed point of 310-ft head, the unit produces approximately 0.6 ft more head than it can be credited with owing to additional kinetic energy available in excess of that based on uniform velocity. This may be proved by integration of the velocity-distribution chart for 310-ft head.

Pressure Variation Near Periphery of Impeller in Both Covers

Pressures were taken at 12 piezometer connections in each cover (see Fig. 23), at operating heads of 365 ft, 310 ft, and 270 ft, and results plotted in Fig. 24. Velocity and direction of flow were not measured. However, the result of the change in the absolute angle of the water leaving the impeller is clearly indicated by the reversal of high- and low-pressure points between the maximum and minimum head conditions.

Conclusions

The pump-casing type has a great influence on the pump performance, as pumps with single-volute, double-volute, and

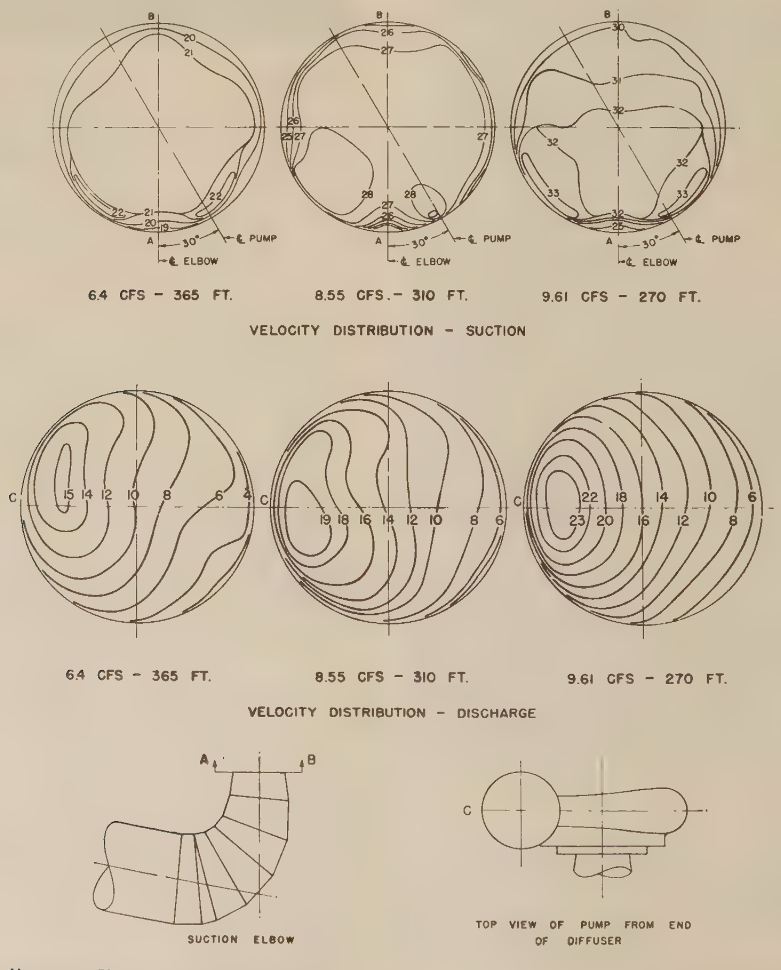

Fig. 21 Velocity Distribution in Suction and Discharge of Final Model

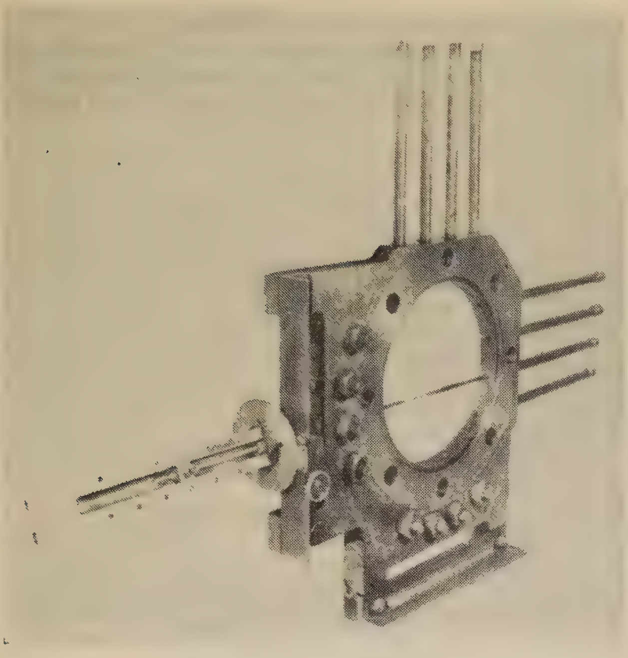

FIG. 22 PITOT-TUBE PLATE FOR DISCHARGE PIPE

diffuser casing designed on the same basis will give different performances. Furthermore, the number of diffuser vanes in the diffuser case has a definite influence on the unstable portion of the performance curve. Fewer diffuser vanes reduce the magnitude of the dip in the head-capacity curve. The diffuser-case inlet area affects the shape of the head-capacity curve and also the pump-efficiency curve. Six diffuser vanes seem to be the minimum number for practical design of a welded pump-diffuser-casing structure, which will give the casing sufficient strength and also allow a substantial reduction in weight. A dividing rib in the diffuser case gives better velocity distribution and improves the pump efficiency.

Impellers with the same profile, but with different impeller-outlet vane angles, materially affect the pump size and weight. The steeper vane angle gives a flatter performance curve and produces a more pronounced dip in the unstable head-capacity range.

The impeller-inlet vane design has a great influence on the cavitation characteristics and also affects the unstable portion of the head-capacity and horsepower curves. A flat entrance vane angle reduces the head and horsepower at closed valve and also improves the pump efficiency at lower capacity.

The unusual performance of the Grand Coulee pumps was a challenge to existing knowledge and techniques. To obtain the desired results, careful testing was required, and the use of the latest testing equipment was necessary. It is hoped that the work presented will be useful and will be followed by detailed disclosures in similar pump studies.

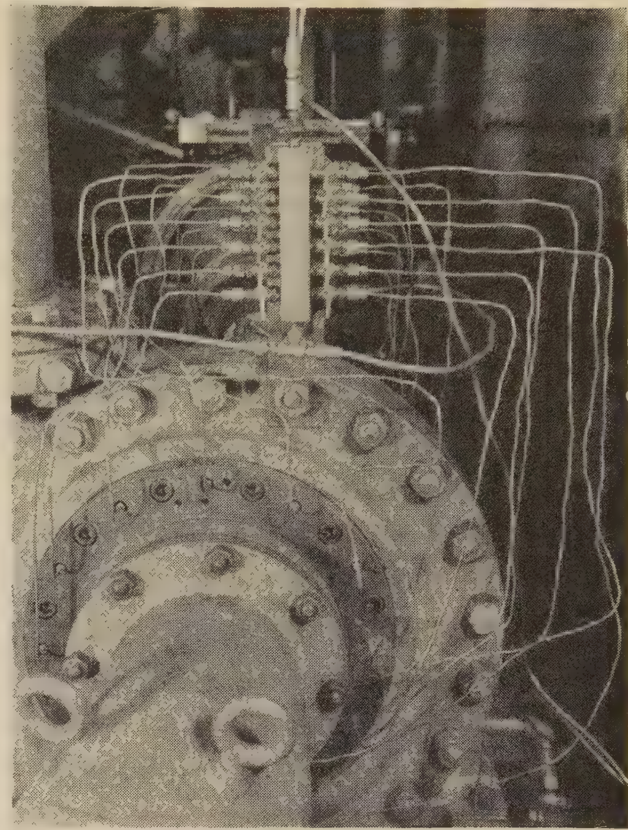

FIG. 23 SETUP FOR MEASURING PRESSURES AROUND PERIPHERY OF IMPELLER IN BOTH COVERS

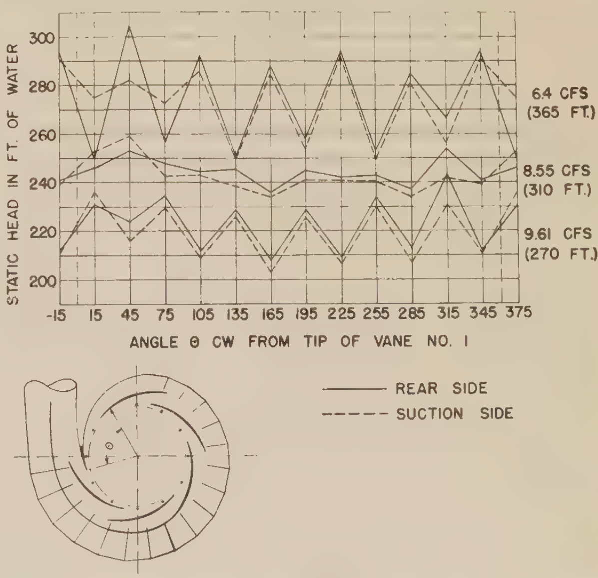

FIG. 24 PRESSURE DISTRIBUTION NEAR PERIPHERY OF IMPELLER OF FINAL MODEL

ACKNOWLEDGMENT

The Bureau of Reclamation started the Grand Coulee model test study which was conducted at The California Institute of Technology. Without this basic study the final results of the model would not have been possible.

The author is indebted to Mr. L. N. McClellan, Chief Electrical and Mechanical Engineer of the Bureau of Reclamation, and to Mr. I. A. Winter, Senior Engineer of the Bureau of Reclamation, for technical advice and assistance, as well as to Mr. E. B. Moses, who represented The Bureau at the acceptance tests.

The close collaboration between Byron Jackson Co. and The Pelton Water Wheel Company, particularly the co-operation of Mr. M. White, its Chief Engineer, made the results presented possible.

Special acknowledgment is due Mr. A. Hollander, Associate Professor of Mechanical Engineering, California Institute of

Technology, who took an active part in the original model study and followed the design progress of the final model as technical consultant of Byron Jackson Co.

The final model testing was conducted at the California Institute of Technology under the direction of Prof. R. L. Daugherty and the Director of the Hydraulic Laboratory, R. T. Knapp, who also assisted with valuable suggestions.

The model testing technical staff was in charge of Mr. E. Lindros, Assistant Chief Engineer, Byron Jackson Co., who also worked out the data on the final model test presented in this paper.

BIBLIOGRAPHY

1 "Cavitation Characteristics of Centrifugal Pumps Described by Similarity Considerations," by G. F. Wislicenus, R. M. Watson, and I. J. Karassik, Trans. ASME, vol. 61, 1939, pp. 17–24.

2 "A Theory of Cavitation Flow in Centrifugal-Pump Impellers," by A. Gongwer, Trans. ASME, vol. 63, 1941, pp. 29–40.

3 "Centrifugal-Pump Performance as Affected by Design Features," by R. T. Knapp, Trans. ASME, vol. 63, April, 1941, pp. 251–260.

4 "Test Characteristics of a Combined Pump-Turbine Model With Wicket Gates," by R. V. Terry and F. E. Jaski, Trans. ASME, vol. 64, 1942, pp. 731–744.

5 "History and Development of the Grand Coulee Pumping Plant," by E. B. Moses, for presentation at the Semi-Annual Meeting, San Francisco, Calif., June 27–30, 1949, of The American Society of Mechanical Engineers.

6 "The Mechanical Design and Manufacturing of the Grand Coulee Pumps," by I. M. White, for presentation at the Semi-Annual Meeting, San Francisco, Calif., June 27–30, 1949, of The American Society of Mechanical Engineers.

7 "Experimental Determinations of the Flow Characteristics in the Volutes of Centrifugal Pumps," by R. C. Binder and R. T. Knapp, Trans. ASME, vol. 58, 1936, pp. 649–661.

8 "Complete Characteristics of Centrifugal Pumps and Their Use in the Prediction of Transient Behavior," by R. T. Knapp, Trans. ASME, vol. 59, 1937, pp. 683–689.

9 "The Hydraulic Machinery Laboratory at the California Institute of Technology," by R. T. Knapp, Trans. ASME, vol. 58, 1936, pp. 663–676.

Discussion

I. A. Winter.[4] This paper presents some of the outstanding results of experimental research as applied to the development and construction of large centrifugal pumping units. It is of particular interest to the utility engineer since it presents basic research data on construction features related to the pump-impeller design. The importance of the hydraulic designs of the inlet and discharge to the pump casing, and to the casing itself, are presented in the text of the paper and in the comprehensive list of illustrations. The continuity of the presentation is excellent and the material selected is pertinent.

The difficulty of obtaining a satisfactory mechnical design of pump casing of the size and for the pressure required for the Grand Coulee development indicated that some form of diffuser casing would offer the most economical construction. The testing program of the Bureau was directed toward establishing the feasibility of such a design. It had been the general policy of the pump designers of this country to consider the turbine or diffuser casing detrimental to the performance of the pump, although, until recently, it had received wide application in important European installations. It was generally believed that the introduction of vanes in the line of flow opposite the impeller discharge would result in a loss of from 3 to 5 per cent in pumping efficiency. The initial tests at the California Institute of Technology on diffuser casings resulted in the development of designs which gave efficiencies and capacities equal to and exceeding, in some cases, the performance of single-volute casings.

Further development work, as will be noted by comparing the curves shown in Figs. 25 and 26 of this discussion, resulted in obtaining performance with the diffuser casing equal in all practical

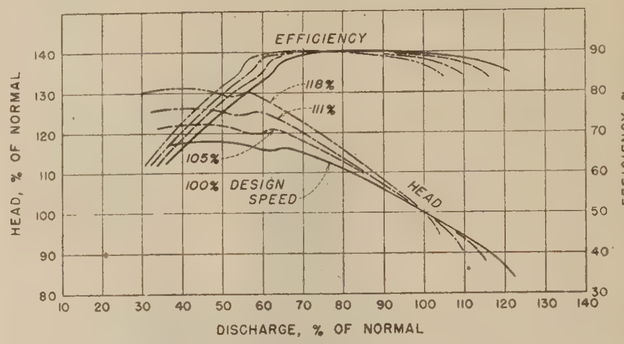

FIXED-VANE DIFFUSOR CASING

Fig. 25

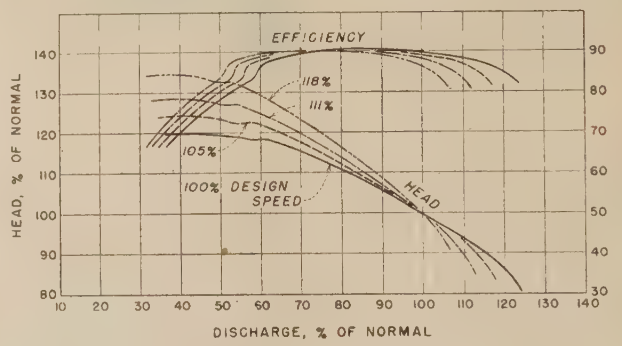

DOUBLE VOLUTE CASING

Fig. 26

respects to the performance of the double-volute casing without the use of an auxiliary splitter as described by the author. The difference in performance between the double-volute casing and the 12-fixed-vane casing, as shown in Fig. 3 of the paper, undoubtedly could be considerably reduced by the use of a larger casing, which would provide for greater expansion in the first stage of diffusion. The author's study and development have been quite properly directed toward obtaining the maximum performance for the minimum mechanical equipment. It is likely that any appreciable improvement in pump performance above that presented by the author would be obtained at an increase in cost inherent with the construction of larger equipment.

The development of a satisfactory recovery of velocity head within a diffuser casing requires two separate and distinct stages. The first stage is developed within the diffusers opposite the periphery of the impeller and provides an outflow area 2.4 of the inflow area as described later. The second and final stage is in the conventional conical discharge nozzle also having an outflow area 2.4 of the inflow area for optimum performance. The casing channel at the end of the diffusers, because of the transfer of momentum opposite each diffuser, collects the fluid into a stream having a velocity distribution at the end of the last diffuser vane favorable to the recovery of pressure head in the expanding diffuser of the pump discharge nozzle. Experiments have indicated that the efficiency of a straight conical diffuser is greatly influenced by the distribution of flow at its inlet, and the best design of casing would have a well-distributed velocity relation

[4] Head, Hydraulic Machinery Division, Branch of Design and Construction, Bureau of Reclamation, Denver, Colo.

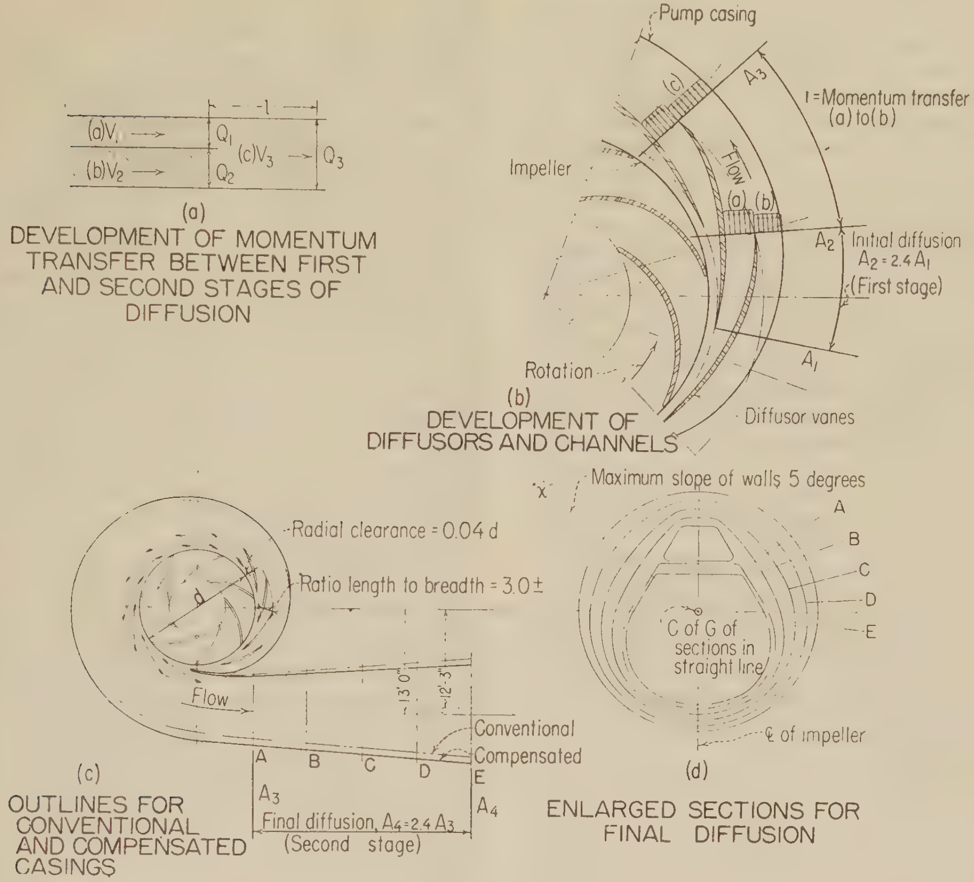

Fig. 27 Design Details

at this point. The diffuser-type casing offers the best possibilities in this regard.

The initial design of diffuser casing prepared by the Bureau was on the basis of turbine draft-tube practice utilizing the principle shown in (*b*) of Fig. 27 herewith. The basic diffuser for both casings had a nominal outflow area of 2.4 of the inflow area which represents the optimum amount of negative acceleration which can be obtained in a single stage of diffusion, as determined when the change in momentum of the stream within a closed conduit exactly equals the change in pressure. The number of vanes placed around the casing was selected to obtain an optimum ratio of height to breadth of water passage at the outflow in conformance with the best practice in fluid mechanics.

Two methods of balancing the pressure and discharge throughout the 360 deg of impeller periphery were investigated. The first casing provided for a variable amount of expansion in the diffuser ring with the greatest rate of expansion in the diffuser immediately following the tongue of the casing, because of the greater amount of friction head developed beyond this point. The estimated loss of pressure throughout the entire casing at rated capacity was approximately 2.20 ft, and therefore it was necessary to provide 2.20 ft greater recovery of velocity head in the first diffuser, as compared to the last diffuser. These adjustments were made on all vanes in a manner which would produce the same effective pressure around the periphery of the impeller thereby minimizing the amount of unbalanced hydraulic side thrust and creating substantially a uniform rate of flow through the various passages of the impeller.

It is possible that the sudden change in pressure within the passages of an impeller, as the vanes pass the tongue of the pump casing, may be one of the contributing factors to excessive cavitation and vibration. A sudden change in velocity of flow through a pump impeller when created by a change in pressure would have a cavitational effect because of the presence of inertia similar to that of a vibrating column as used in commercial cavitation-testing apparatus. The favorable sigma value obtained with the 12-vane diffuser casing in the initial tests, where the pressure around the impeller was substantially uniform, lends support to this concept.

Further investigations of the optimum design of diffuser casings resulted in the development of the method shown in Fig. 27(*a*). The purpose of this design is also to compensate for the losses in pressure head around the periphery of the impeller due to friction. The equalizing effect is accomplished within the casing proper by the transfer of momentum from the relatively higher velocity jets issuing from each consecutive diffuser to the slower moving fluid having been discharged into the casing from previous diffusers. This method may be compared to the transfer of momentum and conversion to pressure of fluids as utilized in jet-pump designs whereby the momentum of one mass is transferred to a second mass having a lesser velocity in accordance with basic laws. The momentum theory states that $M_1 + M_2 = M_3$ or $Q_1 V_1 + Q_2 V_2 = Q_3 V_3$, that is, the velocity after mixing

$$V_3 = \frac{Q_1 V_1 + Q_2 V_2}{Q_3}$$

is illustrated in Fig. 27(*a*).

The momentum transfer design of casing requires that the difference in velocity head, as represented by the momentum and

pressure formula between each adjacent vane, will be equal to the friction head developed in the distance corresponding to l, as shown on the diagram of Fig. 27(a). This procedure differs from the one previously described in the respect that the recovery of velocity head required to compensate for the loss of friction head in the corresponding section is created in the casing, whereas in the first design, the recovery was effected within the first-stage diffuser ring.

After completion of the tests on the vanes with varying clearances between the impeller and diffuser entrances, the vanes were cut off at the discharge edge until the outflow area of all diffusers were equal. The test on the altered diffuser ring did not result in any noticeable change in pump performance, and it is concluded that the refinement resulting from variable length diffusers is not justified. The author has apparently come to the same conclusion as the illustrations indicate that all six diffusers of the final design are identical. Initial results did not indicate that the principle of the first design was important and the second lacks experimental confirmation. The proposed methods, however, serve the purpose of arriving at a design of casing based on sound engineering principles.

A casing designed to equalize the pressures around the pump impeller, independently of the friction developed within the casing, has been designated as a "compensated" casing and differs from the conventional casing without a diffuser ring approximately as shown in Fig. 27(c). Comparing the compensated casing, having an optimum amount of diffusion in the first stage with the casing described by the author, indicates that a proper design of 12-vane diffuser ring would require a somewhat larger casing than the conventional casing. It is likely that the difference in performance between the 6 and 12-vane diffusers, as shown in Fig. 5 of the paper, may be the result of an inadequate amount of diffusion in the first stage, and to the small hydraulic channels external to the diffusers. Early experiments with rings of various diameters would indicate this possibility.

The author refers to the difficulty of developing the desired pumping capacity under the wide range of effective heads required for the Grand Coulee development. During the early stages of the preliminary investigations conducted by the Bureau, it was realized that this objective may not have been possible of attainment. Accordingly, the prime movers for the Grand Coulee pumps were purchased with provisions for variations in speed of 15 per cent above and below normal so that the best speed for pump operation could be obtained. Results of the investigations made to determine the effect of a change in speed of the pumping unit on the steepness of the head-discharge curve are presented in Figs. 25 and 26 herewith. These data show that the steepness of the head-discharge curves may be affected appreciably by changing the speed of the unit.

On the basis of the preliminary experiments, the specifications for the pumps required that satisfactory operation be obtained at constant speed throughout the full range of pumping heads. It was contemplated that the successful bidder would select characteristics whereby the rated speed of the unit was increased above the normal optimum speed in an amount which would result in the desired operating characteristics within the specified range. It was realized that the required performance would be obtained at an increase in cost of the pumping equipment since the capacity of the pump is lessened as its speed is increased. This, however, was considered to be a proper approach to the problem since it offered means of operating the pumps at synchronous speeds from commercial electrical distribution systems at all times. This flexibility was highly desirable because of the possibility of utilizing excess energy for pumping which might be available from associated generating plants. It was also realized that some doubt would develop regarding the hydraulic performance obtainable over such a wide range of head, and the minimum acceptable warranty of efficiency was lowered accordingly.

The author has further explored the possibility of increasing the steepness of the head-capacity curve, as shown in Fig. 4 of the paper, where it is evident that an adjustment at the entrance edge of the diffuser considerably affects the steepness of the head-capacity curve. Some of the differences shown in this curve may be due to an increase in radial clearance between the periphery of the impeller and the entering edge of the diffuser vanes.

In turbine practice it has been established that the clearance between the movable and stationary vanes should not be less than 4 per cent of the diameter of the runner at the vane tips. In the experiments conducted by the Bureau, a similar relation was found to exist for pumps. The first model tested used a diffuser vane having a clearance at the periphery of the impeller of approximately 3 per cent of the impeller diameter. The performance was erratic and generally unsatisfactory. The vanes were then cut back until a clearance of approximately 4 per cent of the impeller diameter was obtained, and satisfactory performance resulted. Further cutting of the vanes resulted in a loss in pump performance.

The difference in the slope of the head-capacity curves shown in Fig. 3 of the paper, may be due in part to the influence of the volute and diffuser vanes upon the characteristics of the flow as it leaves the pump impeller. It will be noted that the slope of the curve for the double-volute casing is somewhat more favorable than that of the fixed-vane diffuser casing. Best results are obtained with a fixed-vane diffuser if velocity traverses are first made to determine the exact angle of discharge from the impeller while it was being operated in a single-volute casing and the entrance to the diffusers designed to accommodate the actual measured angle of flow. It is not believed that the calculated angle is sufficiently accurate for the purpose of designing the entrance to the diffusers.

The wide range of development work described in the paper is the result of an interest in the Grand Coulee pumps and related engineering development work considerably beyond the requirement for the manufacture of adequate pumping equipment. The author and his associates are to be highly commended for the professional attitude manifested in this important undertaking and the industry, as a whole, is indebted to this symposium for the presentation of the engineering problems and their solution in connection with the world's outstanding pumping development.

R. T. Knapp.[5] This is an exceptional paper, not only because it presents the performance of an exceptionally good pump, but also because it gives in detail the steps taken and the reasons for taking them in the design and development program that led to this very successful result. Both the author and his company are to be congratulated on their achievement and their farsightedness in making this technical information available to the engineering profession. The writer is confident that this policy of free exchange of knowledge will prove to be of benefit not only to the engineering profession at large, but also to the individual organizations contributing to it.

The writer would like to emphasize one point brought out by the paper. It should be remembered that the diffuser-case design was selected for the Grand Coulee pumps, not for hydraulic reasons but to secure greater mechanical strength and lower cost of manufacture. These factors were of major importance in this installation, both because of the tremendous size of the pump units and also because of the exceptionally low cost of electric power for their operation. From an hydraulic point of view, it is nearly certain that if the double-volute design could have been

[5] Director, Hydrodynamics Laboratory, California Institute of Technology, Pasadena, Calif. Mem. ASME.

used, somewhat better performance characteristics would have been obtained; specifically, the head-capacity characteristic would have been somewhat steeper, and the average efficiency would have been slightly higher. Therefore, although this design of the Grand Coulee pump represents a sizable step forward in the development of the diffuser-case volute pumps, it does not mean that it will now become the cure-all for all pump problems. Diffuser-case pumps now simply join the ranks of good design, superior for some applications, of equal merit with different types for other installations, and inferior to other designs for still other requirements.

It is interesting to note that the Grand Coulee pump departs quite radically from all previous diffuser-case designs employed in American and European practice. Although this design is described as a diffuser-case pump, it is truly a cross between the normal fixed-vane diffuser design and double-volute case. As such, it has some of the merits of both. One of the fundamental virtues of the double-volute type of design is that it establishes two symmetrical discharge zones around the periphery of the impeller, and thus creates automatically a balanced system of radial forces for all conditions of flow. The separating rib of the Grand Coulee pump divides the case very effectively into two symmetrical volutes, each containing two fixed diffuser vanes. This geometrical result is shown very clearly in Fig. 6 of the paper. Furthermore, Fig. 20 gives the measurements which show the effectiveness of this construction in securing low radial thrusts for all values of discharge.

There is another aspect of this pump that deserves emphasis. Up until very recently most pumps, large or small, have been purchased from specifications which required given performance characteristics at one operating point only. Specifications might also request a certain general shape of the head-capacity curve and describe other desirable operating characteristics. Contrast this to the requirements for the Grand Coulee machine. Here the minimum capacities are specified at two widely separated heads. The minimum efficiency is specified at one of these heads and the maximum brake horsepower is specified at still a third head. Furthermore, the pump must operate over this entire head range with complete freedom from cavitation. It would seem that this represents a definite trend for the future requirements which will be set up for large units. Such pumps are truly "tailor-made" to fit the measurements of the installation. The Grand Coulee pump is a fine example of how good a fit the manufacturer can obtain for his customer with the help of a well-planned and executed design and development program.

The writer must confess to some amusement concerning the dilemma in which both the manufacturer and the purchaser found themselves concerning the measurement of discharge head. The resulting solution might be called the triumph of specifications over good engineering judgment. As can be seen from the paper, the test results established quite clearly that for the velocity distribution existing in the diffuser a short 10-deg diffuser followed by a length of full-diameter pipe was a little more efficient energy converter than the long 3-deg diffuser. Nevertheless, to meet the specifications the manufacturer is required to furnish a long diffuser and the purchaser to install it even though he thereby secures a slightly less efficient installation than if he had accepted the original design. This minor incident does not detract from the remarkably fine co-operation between the purchaser, the manufacturer, and the laboratory that existed throughout this successful development program.

A. J. Stepanoff.[6] The testing program reported by the author was initiated with the intent to find a better type of pump to meet special conditions of one particular installation. However, the problems investigated are of general interest and deal with the most intimate design features for which it is possible to build up a theoretical background and in this way to make results applicable to different types.

The following points are of particular interest to the writer: The first deals with the moot question of the impeller-inlet conditions. In a great majority of existing designs the impeller-inlet angles are "exaggerated," or are considerably higher than those required for "shockless" entrance at the best efficiency point. The reason for such design can be traced to a quite common misconception that exaggerated inlet angles improve cavitation qualities of the impeller. Although a larger area for the relative flow accompanies higher inlet angles, this may not produce a greater flow for a fixed net positive suction head because a sizable portion of this area is not available to the flow on account of a bad (high) angle of attack. The author's tests prove this. This has been known for some time to the leading pump manufacturers.[7]

On the entrance-velocity triangles A and B, Fig. 11 of the paper, the author selects the vane-inlet angles for the impeller eye and hub diameters in such a way that the two lines intersect on figure A about 14 deg to the right and on figure B, 16 deg to the left of the vertical axis, both at capacities corresponding to the head of 310 ft. This latter is not a best efficiency or design point. The objection to such an arrangement is that by allowing the same linear prerotation or the same tangential component of the absolute velocity (c_{u1}) for two different diameters would require a different angular velocity for these two streamlines. Assuming the same pattern of flow will extend to the center of the eye, this would result in an infinite angular velocity there. This is hard to visualize in view of a constant angular velocity of impeller causing this prerotation.

A much simpler pattern of flow and a simpler rule for layout of impeller-inlet angles is obtained if the two lines representing the impeller vane angles are made to intersect on the vertical axis shown in Fig. 28 herewith. Then a desired degree of prerotation is obtained by moving point of intersection D, or changing the ratio P_{1s}/c_{m1}, where c_{m1} is the meridional velocity at the best efficiency point. This ratio can be established experimentally for different suction-nozzle designs. Thus for horizontally split double-suction pumps, this ratio, being a measure of the degree of prerotation, is within the limits 1.25 to 1.42. For pumps with end suction nozzle, like the author's pumps, lower values should be used. If the velocity triangles in Fig. 11 of the paper are redrawn to comply with the foregoing method, and keeping the same angles at the impeller eye (28 deg for A, and 21 deg for B), the ratio $P_{1s}/c_{m1} = 1.41$ for A, and 1.115 for B are obtained. The

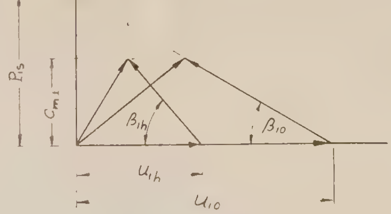

Fig. 28 Inlet-Velocity Triangle

[6] Development Engineer, Ingersoll-Rand Company, Phillipsburg, N. J. Mem. ASME.

[7] The National Transit Pump and Machine Company, in its Bulletin 6000, 1947, p. 4, states that the minimum net positive suction-head requirement is accomplished by "using lowest practical impeller-vane inlet angles" and maximum impeller eye area.

angle at the hub will change from 48 to 44 deg for A, and from 33 to $34^1/_2$ deg for B. The effect of such change on performance, if any, will be insignificant, but the method has the advantage of simplicity and a better theoretical reasoning.

The physical meaning of the ratio P_{1s}/c_{m1} is the ratio of "shockless" capacity to the normal or design capacity Q_s/Q_n. The writer has shown in a previous publication[8] that the best efficiency point always occurs at a capacity lower than the shockless capacity. The pattern of flow following from the described method of inlet-vane layout requires a constant angular velocity of prerotation at any capacity, which is the easiest thing to imagine and natural to expect.

It should be realized that the impeller-inlet conditions play only a minor part in comparison to the impeller discharge in locating the shockless and normal capacity of the pump.

A study of the discharge conditions from the impeller also is interesting and instructive. For this the writer has plotted the best efficiency points of the tests from Figs. 10 and 13, on the writer's chart of centrifugal-pump characteristics[9] (Fig. 29 of this discussion). On this, heads and capacities appear in dimensionless form, (points E, F, G, H), and actual discharge-velocity triangles are obtained by joining these points with points A and O. All velocities appear on this chart as ratios to the impeller peripheral velocity at discharge. From inspection of this figure the following can be stated:

1 The points plot very closely on the respective lines of the discharge angle β_2, the two high angle points fall slightly above their respective lines. The latter could be expected as the performance of the author's pumps is better than those for which the chart was intended (best commercial pumps).

2 The absolute discharge velocity angle α_2' measures 13 deg. As far as can be ascertained from the small-scale drawings of the paper, the angle of the mean line of the diffuser vanes in B of Fig. 4 is approximately 13 deg.

3 Note that all points fall on the same line of c_2' (13 deg from the axis of heads), indicating that the peak-efficiency point is determined by the pump casing, which was the same for three impellers. If the casing were to be changed to suit the impeller-discharge angles, points would follow the constant specific-speed line, which is associated with a given impeller profile.

4 The absolute velocity at the impeller discharge for the point G (test Fig. 13) scales 0.525, which corresponds to $0.525 \times 146.3 = 76.8$ fps absolute velocity ($u_2 = 146.3$ is the peripheral velocity at discharge). The average velocity at the diffuser inlet is calculated to be $c_3 = 54.8$ fps. Some time ago the writer had prepared a curve, reproduced in Fig. 30 herewith, of what was called "volute velocity distribution factor" $c_3/c_2' = R_{c3}$. For the point G this factor is $54.8/76.8 = 0.713$ which falls on the curve in Fig. 30.

[8] "Centrifugal and Axial Flow Pumps," by A. J. Stepanoff, John Wiley & Sons, Inc., New York, N. Y., 1948, p. 173.

[9] Ibid., footnote 1, p. 184.

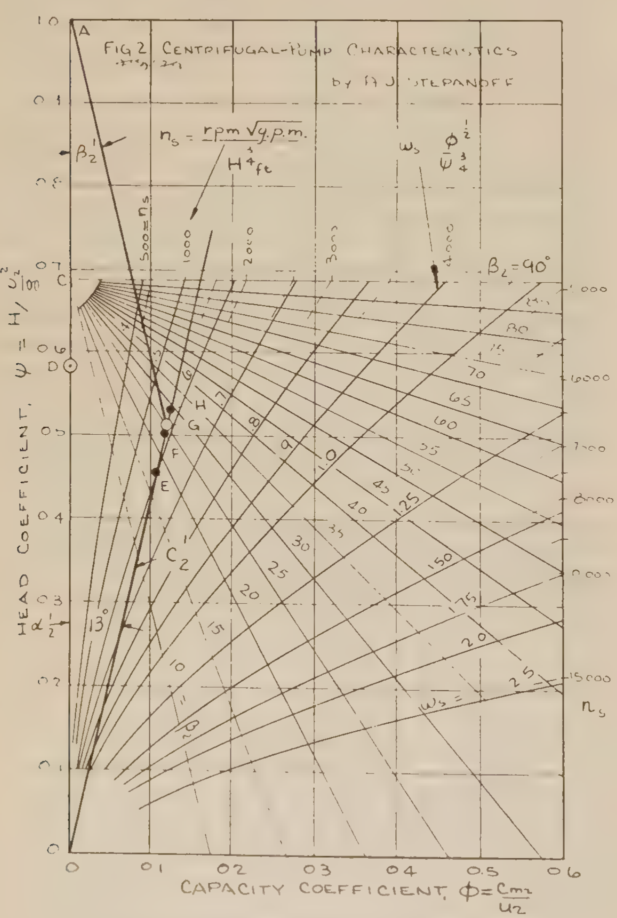

Fig. 29 Centrifugal-Pump Characteristics

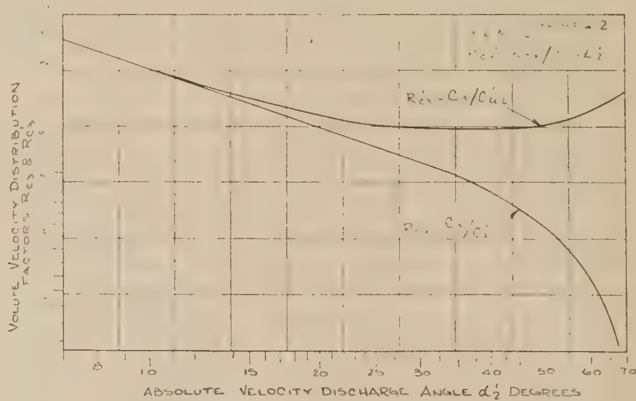

Fig. 30 Volute Velocity-Distribution Factors

The casing velocity-distribution factor represents the ratio of the average velocity in the volute or diffusion-vane casing to the maximum velocity at the impeller discharge. This latter is given approximately but very accurately by the writer's chart, Fig. 29.

The pump casing as finally adopted, with 6 vanes, was intended to provide mechanical strength to the casing and thus reduce its size and weight. Hydraulically the casing is equivalent to a double volute—with an addition of 4 guide vanes. With a diffusion angle of 40 deg in the radial plane (profile) and a small vane overlap, the 6-vane casing does not make a good diffuser.

The beneficial effect of the "rib" on the velocity distribution, Fig. 6(a), and efficiency, Fig. 7, can be observed on any double-volute pump as compared with single volute. In other words, hydraulically the 6-vane casing has no advantage over a double volute.

B. L. VanderBoegh.[10] The extensive and painstaking research necessary to design pumps of this magnitude becomes evident when the testing-program results are released. The author is to be commended for his clear presentation of valuable data.

Comments by the author on several points would be enlightening. It would be interesting to compare tests made with the

[10] Hydraulic Division, Newport News Shipbuilding and Dry Dock Company, Newport News, Va. Mem. ASME.

smooth pump casing with those of the segmented casing to learn of the degree of difference in frictional losses between the two.

It is noted the specifications permitted lengthening the pump-discharge nozzle beyond the original location, with a resulting gain in efficiency and head when pressure readings were taken farther downstream. This increased length was not allowed in testing the Granby pump models, and so, with due allowance for the difference in specific speeds and casing design, a comparison of test results is difficult. It is strongly urged that the recommendations of the Hydraulic Institute be followed in locating discharge piezometer connections. Pumps then would be allowed to develop their full heads and test results would be comparable.

In Fig. 6 of the paper the overlap of the diffuser vanes appears to be about 25 per cent of the vane length. This is a relatively short distance to allow for diffusion, and the reasoning that the water is more guided than diffused seems proper, for the figure also shows a rather rapid enlargement between vanes. Comments as to the percentage of velocity decrease in this diffusion area would be of interest.

It is noted in Fig. 16 of the paper that the point of discontinuity lies outside the operating range. This instability occurs at about 2 per cent above the high head condition and extends over a fairly broad range. A margin of 2 per cent appears relatively slight when it is considered that a surge of approximately 200 cfs is involved.

It is believed that data were taken well below the 270-ft head condition, but the H-Q test curves are not completely shown. Perhaps the author will describe the shape of the H-Q curve below 270 ft head and mention where cutoff occurred.

Author's Closure

The Bureau of Reclamation took an active part in the preliminary Grand Coulee model-testing program and also developed the first diffuser-type casing, so Mr. Winter's comments are therefore of particular interest and his discussion a valuable addition to this paper.

Mr. Winter suggests that a larger diffuser case with a greater diffuser expansion should reduce the unstable portion of the performance curve near the high-head condition shown in Fig. 3 of the paper. The author ran performance tests with the same impeller in two 6-vane diffuser cases, which had the same diffuser-vane entrance area but different ratio of the diffuser-vane inlet-to-outlet area. This ratio was 1.5 for a small case, the same as used in the final model for Grand Coulee, and 2.5 for a large case. The performance with the large case did not show any noticeable improvement in the unstable head-capacity range over the small case. The pump efficiency, however, as mentioned in the paper, was slightly higher for the pump with the large case than for the small case, and about equal to the pump efficiency obtained with the small case furnished with the separating rib. However, the weight of the large case was 25 per cent heavier than the small case.

The two types of diffuser-vane designs, investigated by Mr. Winter, to develop even pressure distribution around the impeller periphery have a great deal of merit. His reasoning, however, is based upon the assumption that the outlet velocity from the diffusers and the velocity in the volute sections are uniform. Actual measurements show uneven velocity distribution at the end of the volute discharge cone (see Fig. 8 of the paper), and the velocity distribution between the diffuser vanes shows a greater variation. It is therefore difficult to suggest a diffuser-vane design which will give balanced pressure distribution around the periphery before this uneven velocity type of flow has been further explored.

The effect of change of speed on the steepness of the performance curves, shown in Fig. 25 and Fig. 26, gives the misleading impression that the slope of the performance curve could easily be changed. These curves are calculated from the same model performance by changing the size model ratio, which means operating the model at different speeds to meet the same operating point. This, in reality, is nothing more than moving the operating point up and down the same performance curve. The smaller pump at higher speed would move the operating point down on the performance curve and result in a steeper performance curve, but with reduced pump efficiency at the 310-ft operating point (see Fig. 16). A larger pump at lower speed would move the operating point up on the performance curve and improve the pump efficiency at the 310-ft operating point, but the high-head point would move closer to the unstable portion of the head-capacity curve.

The author agrees with Dr. Knapp that the Grand Coulee type diffuser casing has no hydraulic advantage over the double-volute case, but is hydraulically inferior. Unquestionably, the double-volute case will remain the practical and best solution in most pump designs, and the division line between it and the Grand Coulee type case will be determined by various factors, such as, size, test pressure, number of units involved, and others. Dr. Knapp's complimentary remarks, which clear up further some of the problems posed by the condition of operation of these pumps, are greatly appreciated.

Dr. Stepanoff shows a suction-vane layout, which has a better theoretical background than the one used by the author, if we suppose uniform radial velocity approach in the impeller eye at all capacities. In the design of entrance-velocity diagrams, consideration should be given to the uneven flow distribution in the impeller eye, which is of greater variation than measured at the suction flange, shown in Fig. 21 of the paper. The author agrees that the minor differences in vane angle arrived at by Stepanoff's and the author's procedure will have no significant effect on the performance.

The author feels gratified that the model-test results and pump proportions are in agreement with Stepanoff's excellent charts. The author objects to the quotation that the minimum suction-head requirements are obtained by using lowest practical impeller-vane inlet angles and maximum impeller-eye area. While the word, "practical" somewhat excuses the statement, it is well known to designers that the cavitation depends on the absolute inlet velocity which is the vector sum of peripheral and radial velocity, and that there is a ratio of these two velocities at which the cavitation will occur at the minimum head.

The pump casing as finally adopted is not equivalent to a double-volute case with additional guide vanes as claimed by Dr. Knapp and Dr. Stepanoff, but must be considered as a diffuser-type case with a dividing rib. The main purpose of a double-volute-case design is to balance the radial forces acting on the impeller, and therefore all volute sections 180 deg apart in a double-volute case are identical in area and shape. In the separating-rib-type case, however, the final volute sections 180 deg apart differ materially in shape with a half-circle shape in one, and a trapezoid shape in the other.

The last paragraph in Dr. Knapp's discussion is an excellent answer to Mr. VanderBoegh's remark regarding the length of the discharge cone. The author strongly supports Mr. VanderBoegh's recommendation that pump specifications should be based upon the Standards of the Hydraulic Institute and no deviations allowed.

The diffuser-vane length is determined by the chosen pump-case size or the ratio of diffuser-vane inlet-to-outlet area. A ratio of 1.5 was used in the diffuser-case design finally adopted, and the total diffuser-vane cone angle in the direction of flow was 12 deg, which is somewhat larger than the 8 deg recommended for uniform flow. In pump cases where the flow is far from uniform,

tests with cases having a total discharge-cone angle of 15 deg, have given the same pump efficiency as cases with 8 deg.

The instability in the head-capacity curve is admittedly close to the high-head operating point, but it is difficult to determine the percentage of safety required to guard against surges. The model development accomplished two major improvements in this respect: (1) It moved the unstable portion of the horsepower curve further away from the high-head point. (2) It eliminated the dip in the head-capacity curve, and thereby prevented the pump from passing over a hump in the performance in case of a major surge.

Test data were taken for heads as low as 200 ft with 145 ft NPSH at the pump suction, and the head-capacity curve continued on the smooth curve without a sign of instability or cutoff.

In conclusion, the author wishes to thank the discussers for their encouraging comments and valuable contributions to this paper.

Heat-Conduction Errors in Temperature Measurements

By L. E. SMITH,[1] WATERBURY, CONN.

In practical applications of temperature measurements where the temperature-sensitive bulb assembly is fastened rigidly to a containing vessel, heat-conduction errors must be considered in order to determine the accuracy of the indicated or recorded temperature. This paper presents for various thermometer-bulb assemblies, the experimental magnitude of the heat-conduction error possible in a medium with a low heat-transfer coefficient (air), and in a medium with a high heat-transfer coefficient (water). The effect of heat-conduction error on the over-all response in simulated practical installations is discussed. It is shown that comparative information on response action of any type of temperature-sensitive element necessitates careful considerations of the condition of attaching the element to a wall or vessel, where heat-conduction effects are present.

Practical Considerations

In practical applications of temperature-measuring instruments, it is desirable that the temperature of the medium be indicated or recorded accurately and promptly, despite variations of the temperature outside the vessel containing the medium. In many applications, the measuring bulb, by means of a union connection, is fastened rigidly into a threaded bushing which is attached permanently to the containing wall. A supporting nonsensitive extension for the bulb usually separates the sensitive portion from the union connection, Fig. 1. For other applications, the bulb is inserted into a protecting well, Fig. 2, and for convenience of removal it is necessary that the bulb be smaller than the inside diameter of the well, resulting in an air gap between the bulb and the well. A liquid or metallic filler may be interposed between them, but in all cases, the transfer of heat from the medium to the sensitive portion of the bulb is retarded.

The primary requirement in measuring temperature is to transfer heat from the measured medium to the fluid inside of the sensitive portion of the bulb in the shortest possible time. It is also required that a minimum amount of the heat available from the measured medium must be lost to the union connection and vessel walls by way of the bulb extension. Where a well is used, the condition is aggravated because heat will also escape by way of that portion of the well which surrounds the bulb extension. The accuracy of measurement for a given application under a steady state of heat flow will be dependent upon the amount of heat lost to the union connection and the well head in a unit time. In the majority of cases, the temperature around the thermometer head will change with time, causing a change in the rate of heat loss. This change in heat flow will also influence the indicated temperature reading, an effect particularly emphasized in installations where the measured medium has a low heat-transfer value, such as flowing gas or air. Here, too, the over-all rate of response of the thermometer bulb will be seriously affected.

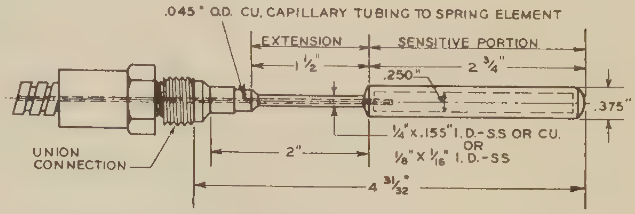

Fig. 1 Union-Connected Bulb

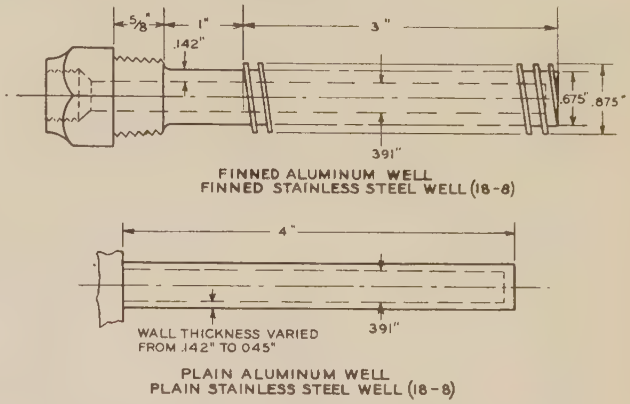

Fig. 2 Various Wells Used With Union-Connected Bulbs

Others have written papers on response characteristics of thermometer elements (1, 2, 3)[2] and heat-conduction effects (4, 5). The object of this paper is to present experimental data simulating practical applications, to indicate the magnitude of heat-conduction errors, and to show how heat conduction influences the response time of thermometer bulbs. Means for improving the over-all performance of an installation are studied. Filled-system thermometer assemblies are utilized in this investigation, but similar results will be obtained with resistance-bulb or thermocouple assemblies.

Test Equipment

The thermometer system used in the tests was liquid-filled, and consisted of a union-connected bulb, Fig. 1, which was connected to the recording Bourdon-spring element by 10 feet of capillary tubing. The spring element was installed in a regular recording-thermometer case, and readings recorded on a 12-in-diam chart driven by a clock mechanism. This system was of the fully compensated variety, so that changes in ambient temperature of the capillary tubing or spring element had no effect on the recorded reading.

In the case of the union-connected bulb with bushing, all heat-conduction loss is through the extension, and the factors which affect the rate of heat loss from the sensitive portion of the bulb to the head and bushing for a given application are as follows:

---

[1] Development Engineer, The Bristol Company.

Contributed by the Industrial Instruments and Regulators Division and presented at the Spring Meeting, New London, Conn., May 2–4, 1949, of The American Society of Mechanical Engineers.

[2] Numbers in parentheses refer to the Bibliography at the end of the paper.

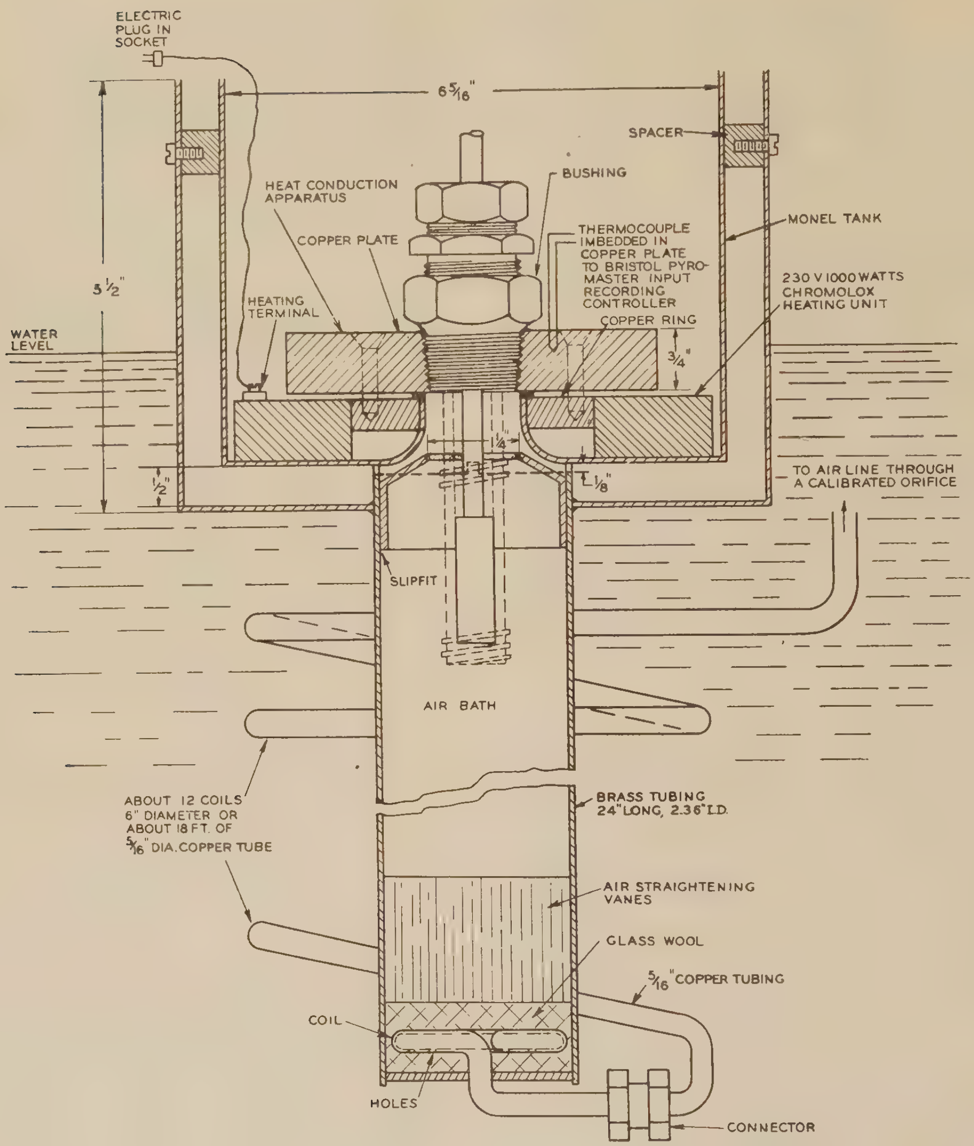

Fig. 3 Heat-Conduction Apparatus Installed in Air Bath

(*a*) The thermal conductivity of the material of the extension; (*b*) the cross-sectional area of the extension; (*c*) the length of the extension. In the tests, the following combinations of bulb and extension were used (extension was $1^1/_2$ in. long in all cases; see Fig. 1, for actual dimensions):

1 Copper bulb, with $^1/_4$-in-OD × 0.155-in-ID copper extension.

2 18-8 stainless-steel bulb, with $^1/_4$-in-OD × 0.155-in-ID 18-8 stainless-steel extension.

3 18-8 stainless-steel bulb, with $^1/_8$-in-OD × $^1/_{16}$-in-ID 18-8 stainless-steel extension.

When the bulb is installed in a well, the heat loss is the total through the portion of well surrounding the extension, and that through the extension. The design factors which affect the rate of heat loss from the body of the well surrounding the sensitive portion of the bulb are the same as for the bulb extension. In the design of the well it is possible to increase the external area of the surface exposed to the medium to improve the rate of heat flow. The following combinations were used to determine the effect of the various factors (see Fig. 2 for well designs):

1 Copper bulb with $^1/_4$-in-OD × 0.155-in-ID copper extension in (*a*) a finned aluminum well with 0.142-in. wall; (*b*) a finned 18-8 stainless-steel well with 0.142-in. wall.

2 18-8 stainless-steel bulb with $^1/_4$-in-OD × 0.155-in-ID 18-8 stainless-steel extension in (*a*) a finned aluminum well with 0.142-in. wall; (*b*) a plain aluminum well with 0.142-in. wall; (*c*) a plain aluminum well with 0.045-in. wall; (*d*) a finned 18-8 stainless-steel well with 0.142-in. wall; (*e*) a plain 18-8 stainless-steel well with 0.142-in. wall; (*f*) a plain 18-8 stainless-steel well with 0.045-in. wall.

3 18-8 stainless-steel bulb with $^1/_8$-in-OD × $^1/_{16}$-in-ID 18-8 stainless-steel extension in (*a*) a finned aluminum well with 0.142-in. wall; (*b*) a plain aluminum well with 0.142-in. wall; (*c*) a finned 18-8 stainless-steel well with 0.142-in. wall; (*d*) a plain 18-8 stainless-steel well with 0.142-in. wall; (*e*) a plain 18-8 stainless-steel well with 0.045-in. wall.

The heat-conduction apparatus used to determine the performance of the bulb and well assemblies is shown in Fig. 3. It consists essentially of a copper plate provided with a pipe thread for holding the well or the bushing for the union-connected bulb. A

thermocouple was imbedded in the copper plate, the temperature of which was recorded continuously and controlled by a recording-potentiometer input controller. Heat was supplied by a resistance coil, and the temperature of the plate was varied by adjusting the set point of the controller. The plate-and-coil assembly was fastened rigidly inside of a monel tank. The complete unit could be handled easily and moved from one water bath to another, or quickly placed in the air chamber, as shown in Fig. 3.

The air chamber was used for studying response action and heat-conduction errors of the various thermometer-bulb assemblies in a flowing air medium. It consisted of a long piece of brass pipe connected rigidly to an upper chamber which housed the heat-conduction apparatus. The air chamber was heated to a constant temperature by first passing the air through $^5/_{16}$-in-diam coiled copper tubing submerged in a controlled water bath and then bleeding it into the chamber through a number of small holes in the tubing. The flow rate was controlled by measuring the pressure drop across a calibrated orifice, and the velocity of air past the inserted bulb or well in the chamber was calculated.

Air chambers were installed in each of two adjacent water baths, one bath being held at 70 F, the second bath at 120 F.

Experimental Procedure

The tests were conducted in water, a medium with high heat-transfer coefficient, and air, a medium with low heat-transfer coefficient. In the water-medium tests, the heat-conduction apparatus was placed in the cold bath with the monel tank partly submerged. Sufficient time was allowed for the heat-conduction plate and bulb to reach their equilibrium temperature conditions. The apparatus was then transferred quickly to the hot bath, and equilibrium conditions again reached. Time-temperature curves of the bulb-assembly response were obtained on the recording thermometer, and similar curves for the copper conduction plate were obtained on the recording-potentiometer controller. The temperature of the heat-conduction plate was then raised about 50 deg F by connecting the heating unit to the controller, and equilibrium conditions were again reached. The recorded change in the temperature of the bulb assembly was noted for the temperature change of the heat-conduction plate. The change in bulb temperature due to 1 deg change in plate temperature is called the "extension conduction error," a term which will be used throughout this paper.

In the air-medium tests, the heat-conduction-plate apparatus with bulb assembly, installed in the air-chamber unit, was located in the cold-water bath. Response of the bulb assembly in air at a given velocity was determined by transferring the heat-conduction-plate apparatus from the cold-air chamber to the hot-air chamber. The procedure was identical with that in the water-bath tests, except that the temperature of the heat-conduction plate was raised in 20 F intervals to provide additional points on the extension conduction-error curve.

In addition to the foregoing tests, the response of the various bulb and well combinations in the water bath and air bath was obtained in the usual way without the heat-conduction apparatus, that is, by moving the unattached bulb assembly from one bath to the other. In the air bath, a third method of obtaining response was utilized. The heat-conduction plate was heated up to the hot-air temperature prior to the insertion of the heat-conduction apparatus from the cold-air chamber to the hot-air chamber. It remained in the cold-air chamber until temperature equilibrium was obtained. Extension conduction effect on the response action was thus obtained from heat flowing into the sensitive portion of the bulb.

Data Derived From Tests

Water-Bath Tests. The response time for a 63.2 per cent change (1) (called time constant or time lag), a 90 per cent change, and the heat-conduction factor are tabulated in Table 1 for an agitated water-bath medium. The complete response actions of the bare bulb and the various bulb and well combinations are shown in Fig. 4. It should be noted that data include tests made both with the assembly attached and not attached to the heat-conduction plate. In all these tests a stainless-steel bulb with a $^1/_4$-in-OD × 0.155-in-ID stainless-steel extension was used.

TABLE 1 PERFORMANCE OF UNION-CONNECTED BULB ASSEMBLIES IN AGITATED WATER[a]

Well used	Response time, sec: 63.2 Per cent change	Response time, sec: 90 Per cent change	Extension conduction error	Heat-conduction apparatus
None	14	31	0.010	Yes
	14	31		No
Finned aluminum	63	132	0.050	Yes
	57	120		No
Plain aluminum, 0.045-in. wall	63	132	0.056	Yes
	57	120		No
Plain stainless steel, 0.045-in. wall	78	175	0.059	Yes
	71	152		No

[a] $^1/_4$-in-OD × 0.155-in-ID stainless-steel extension.

It is seen that with a bulb assembly immersed in a fluid with a high heat-transfer coefficient such as water:

1 The heat-conduction plate has no effect on the response of

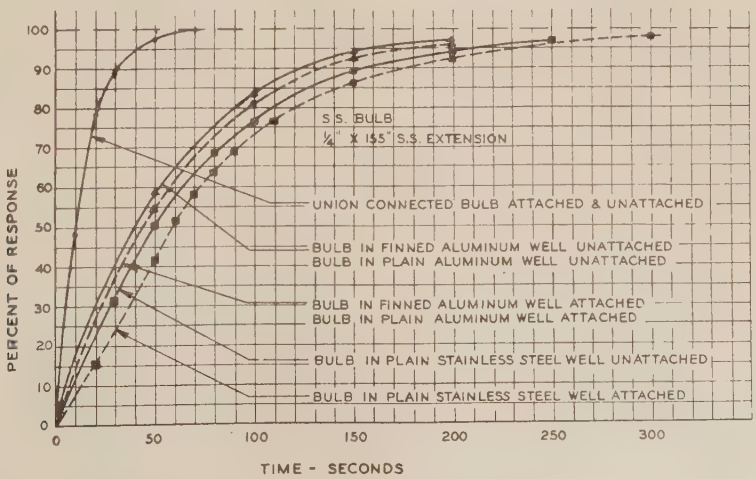

Fig. 4 Response in Water With and Without Heat-Conduction Apparatus

the union-connected bulb assembly with bushing whose extension-conduction error was very low.

2 The heat-conduction plate has only a small effect on the response of the union-connected bulb assembly with well. The response action is slowed down about 10 per cent when the heat-conduction apparatus is used.

3 The material of the well has some effect on the response, the response depending upon the thermal conductivity and heat capacity of the well material.

4 The use of fins on a well, as applied and designed here, does not improve the response or materially affect the conduction error.

5 The use of a well produces an extension conduction error which is practically independent of the material of the well.

6 Extension conduction errors are negligible for a bulb with a stainless-steel extension immersion of $1^1/_2$ in. installed in a bushing.

In order to check the extension conduction effects obtained with the heat-conduction apparatus, a separate installation was made by inserting the well in a bushing welded into the sheet-metal side of the water bath used for the tests. With the bulb installed in any of the listed wells, the recorded reading after equilibrium conditions were obtained was $^3/_4$ F lower than the reading with the bulb suspended at the same position in the bath, but not rigidly connected to the metal side. The temperature of the exposed head of the well was 105 F, while the water bath itself was 120 F. This gave an extension conduction error of 0.05, which agreed with the results obtained with the heat-conduction apparatus.

It is thus apparent that even in the best of heat-transfer media, the bulb assemblies must be considered carefully. In applications where the length of the extension is shorter, the cross-sectional area of the extension is greater, or the extension material has a higher heat conductivity than the design tested, the extension conduction error will be greatly increased. This condition will be greatly aggravated in poor heat-transfer media, as shown in the following discussion on results in the air bath.

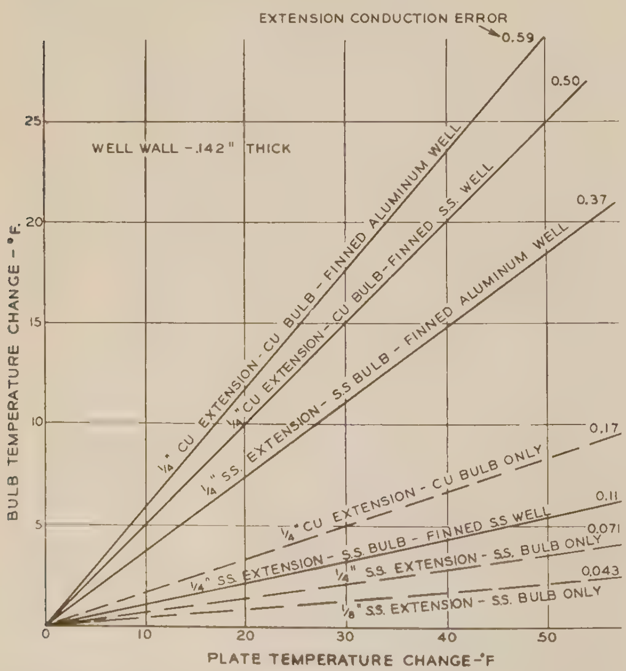

Fig. 5 Extension Conduction Error of Various Union-Connected Bulb Assemblies With Bushing and With Wells (Air velocity, 250 fpm.)

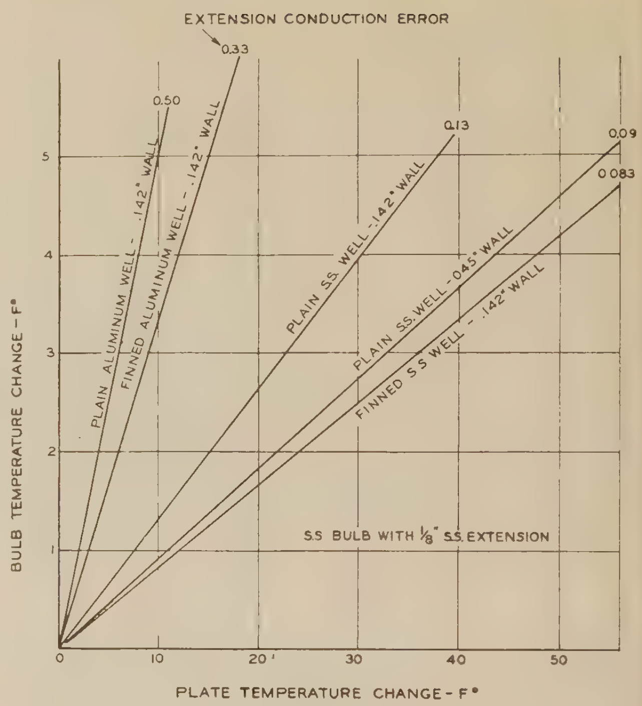

Fig. 6 Effect of Fins on Well and of Well Thickness (Air velocity, 250 fpm.)

Air Bath Tests. The extension conduction errors obtained with different union-connected bulb assemblies and varying plate temperatures are shown in Fig. 5, for an air velocity of 250 fpm. The relationship between plate temperature and extension conduction error is found to be linear. The following conclusions are possible for the various bulb assemblies with well:

1 The worst combination is a bulb with a good conducting extension (copper) and a good conducting well (aluminum). A 1.7 F change in the plate temperature causes a 1 F change in bulb reading, or 0.59 extension conduction error.

2 If the well material only is changed to a less conducting material (stainless steel) a small improvement is noted; 0.50 extension conduction error.

3 If the extension material is changed to a less conducting material, the improvement is more marked; 0.37 extension conduction error.

4 If both the extension and well materials are changed to less conducting materials, the improvement is outstanding, with the extension conduction error decreased to 0.11. This combination would be a desirable one for practical installations.

In considering bulb assemblies with bushing, in which the bulb is directly exposed to the air medium, the following is observed from Fig. 5:

1 With the $^1/_4$-in. copper extension, the extension conduction error is 0.17. Thus this bulb alone produces a greater error than that obtained with the best bulb assembly with well combination in item 4 of the foregoing conclusions.

2 If the extension is changed to $^1/_4$-in. stainless steel, the extension conduction error is decreased to 0.071.

3 If the cross-sectional area of the stainless-steel extension is decreased by use of $^1/_8$-in-OD $\times$ $^1/_{16}$-in-ID instead of $^1/_4$-in-OD $\times$ 0.155-in-ID material (area ratios of 1 to 3), the extension conduction error can be reduced to 0.043.

A series of tests were made on wells to study the effect of fins, and also of the thickness of the well wall on the extension con-

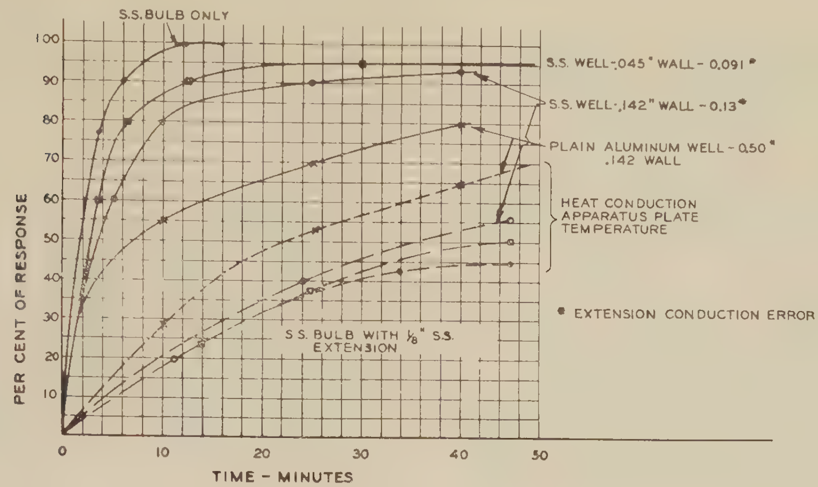

Fig. 7 Response of Union-Connected Bulb Assembly With Bushing and With Well Attached to Heat-Conduction Apparatus

duction errors (see Fig. 6, for data.). The following conclusions can be made:

1 Removal of the fins from the well increases the extension conduction error. In the case of the aluminum well, the extension conduction error is increased from 0.33 to 0.50; for the stainless-steel well, from 0.083 to 0.132.

2 A decrease in the wall thickness of the stainless-steel well from 0.142 to 0.045 in. decreased the extension conduction error from 0.132 to 0.091.

It should be mentioned that a change in the cross-sectional area of the stainless-steel extension from $^1/_4$-in-OD × 0.155 in. ID to $^1/_8$-in-OD × $^1/_{16}$-in-ID produces a decrease in the extension-conduction error from 0.11 to 0.083, when the bulb is used with the stainless-steel finned well.

Response in Air. In Fig. 7 the response of the union-connected bulb assembly with bushing and wells is shown. A bulb extension of $^1/_8$-in-OD × $^1/_{16}$-in-ID stainless-steel material was used in all cases. The actual temperature of the heat-conduction-apparatus plate is also plotted with time for the given response runs. In this part of the test, the plate was allowed to heat up from the natural flow of heat from the well and bulb.

In Table 2, data taken from Fig. 7, are tabulated. Also shown is the 90 per cent response time of the same assemblies obtained with the heat-conduction-apparatus plate heated initially to the temperature of the hotter air bath before beginning the response test, and with the bulb assembly being moved from one chamber to the other without the use of the heat-conduction-apparatus plate.

From Fig. 7 and Table 2 it is seen that:

1 The less the extension conduction error, the better is the response action.

2 The greater the extension conduction error, the faster does the heat-conduction-apparatus plate heat up. This is to be expected, as more heat flows up the well wall and the extension per unit time.

3 The response of a bulb assembly when immersed directly from one bath to another is much better where heat conduction can be disregarded than where heat conduction can function. The divergence between the two methods of obtaining response action is more marked for a poorly designed bulb assembly.

Conclusion

This paper has attempted to show the advisability and the necessity of considering the complete design of any type of a temperature-measuring bulb from the viewpoint of extension conduction errors, rather than from the response action of a bulb or bulb-and-well combination, as ordinarily obtained by simply moving the bulb or bulb assembly from one bath to another.

TABLE 2 PERFORMANCE OF UNION-CONNECTED BULB ASSEMBLIES IN AIR AT 250 FPM[a]

Well used	Response time, min: 63.2 per cent change	Response time, min: 90 per cent change	Extension conduction error	Heat-conduction apparatus
None	2.5	5.7	0.043	Yes
		6.0		Yes—Heated
		5.8		No
Plain aluminum, 0.142-in. wall	16	58	0.50	Yes
		5.6		Yes—Heated
		15		No
Plain stainless steel, 0.142-in. wall	5.3	25	0.13	Yes
		11		Yes—Heated
		15		No
Plain stainless steel, 0.045-in. wall	3.5	13	0.091	Yes
		9		No

[a] $^1/_8$-in-OD × $^1/_{16}$-in-ID stainless-steel extension.
Note: Under heat-conduction apparatus, "Yes—heated" refers to the condition where the conduction apparatus was heated before moving the assembly from the cold bath to the hot bath.

In the case of a measured medium with a good heat-transfer coefficient, this common way of obtaining the response characteristic is generally acceptable. However, designs are possible where there may be considerable heat transfer, resulting in large extension conduction errors. This is true in a design with no extension between the sensitive portion of the bulb and the union connection, or where a short extension has a large cross-sectional area and is composed of a good heat-conducting material.

In a poor heat-transfer medium, the usual way of obtaining the response characteristic is not advisable, unless one knows that heat-conduction effects are negligible. Extension conduction errors may be very large in many industrial applications, particularly where it is necessary to use a protecting well. Comparative response actions in practical applications may be entirely different from those obtained by the customary laboratory methods.

In general, it is recognized that the lowest extension-conduction error can be realized by the proper selection of material, a minimum cross-sectional area of the well and the connecting extension of the bulb, and a maximum length of the extension between the sensitive portion of the bulb and the union connection to the well.

Too often, a thermometer system is condemned as having calibration error, or not being propertly compensated for ambient-temperature changes. This observation may be based upon a check with a mercury-in-glass test thermometer placed in another well with an extension conduction error which may be much differ-

ent from that of the recording thermometer bulb-and-well installation. The discrepancy noted may be the result of extension conduction errors, and will vary with the ambient temperature. On the other hand, an agreement between the mercury-in-glass thermometer and the tested thermometer system does not necessarily mean accurate calibration, as they may possess similar extension conduction errors. It is necessary to know the magnitude of the extension conduction error of the test thermometer in order to determine the exact performance of the measuring-thermometer system.

The best way to overcome the effects of heat conduction is the familiar method of covering the thermometer head and its containing vessel with insulation so that the head remains at the approximate temperature of the measured medium and will not change measurably with ambient-temperature changes.

This paper has touched upon the high lights of the variables which result in heat-conduction losses, and has not attempted to consider errors due to other effects such as radiation. Such errors would be added to those from heat conduction to give the over-all errors. Also statements made are based upon a given immersion assembly; for a different immersion, the relative performance may be altered.

BIBLIOGRAPHY

1 "Thermometric Time Lag," by Rudolph Beck, Trans. ASME, vol. 63, 1941, pp. 531–543.

2 "Response Time and Lag of a Thermometer Element Mounted in a Protecting Case," by W. N. Goodwin, Trans. AIEE, vol. 64, 1945, pp. 665–670.

3 "Response Characteristics of Thermometer Elements," by A. J. Hornfeck, Trans. ASME, vol. 71, 1949, pp. 121–133.

4 "Heat-Flow Effects in a Resistance-Type Thermometer," by N. P. Millar, Trans. AIEE, vol. 64, 1945, pp. 678–685.

5 "Temperaturmessfehler in Gasen und uberhitzten Dampfen Durch Warmeableitung von der Mass-stelle," by Von H. Reiher and K. Cleve, *Archiv. für Warmewirtschaft und Dampfkesselwesen*, vol. 7, October, 1926, pp. 273–279.

Fatigue Tests on Flanged Assemblies

By A. R. C. Markl[1] and H. H. George,[2] Louisville, Ky.

Qualitative differences between the various types of pipe flanges in common use have long been recognized, but their quantitative evaluation in terms of rules, formulas, or ratings which could be used as a guide by the practicing engineer has been accomplished only partially. Two problems are involved, i.e., the determination of the strength and tightness of a flanged assembly under internal pressure, and the other the effects of the variable bending moments associated with mechanical vibrations or temperature fluctuations of the flowing medium or surrounding atmosphere. The present investigation is intended to contribute toward an understanding of the latter phase; stress-intensification factors are reported which have been obtained from fatigue tests of full-scale assemblies of 4-in. flanges of the 300-lb ASA pressure class and hence are directly applicable to piping flexibility calculations.

Introduction

Of late, a growing demand for a more complete understanding and detailed evaluation of the components entering into the design of pressure containers and piping has made itself felt. In the pressure-vessel field, this has led to the formation of the Pressure Vessel Research Council which already has produced valuable information on the magnitude of local stresses at shell-to-head junctions and other related problems. In the piping field, evidence of the same trend is to be found in the efforts of a special subgroup of Subcommittee 3 of ASA Sectional Committee B16 to define more closely the limitations of the commonly used types of pipe flanges and to differentiate between their pressure ratings.

The pressure-vessel flange problem is primarily one of statics and involves an evaluation of the interaction of bolt extension, gasket compression, and flange rotation under the effects of an applied bolt load and internal pressure, as it affects flange stress and, perhaps more significantly, joint tightness. For flanges forming part of a piping system, an additional, dynamic problem arises, namely, that of evaluating the useful life of assemblies subject to cyclic bending moments caused by mechanical vibrations or thermal changes.

Scope of Tests

The investigation reported herein relates to the latter aspect of the problem. While it has been initiated with the express purpose of assisting ASA Committee B16 in its difficult task of defining the proper uses, ratings, and limitations of different flange types, at the same time it is to be considered as part of a comprehensive fatigue-testing program on full-scale piping assemblies undertaken by the authors' company as a service to the industries which use its products.

Cyclically reversed bending tests were carried out on assemblies involving the following types of commonly used flanges:

(A) Slip-on flanges.
(B) Socket-welding flanges.
(C) Welding-neck or butt-welding flanges.
(D) Ring flanges.
(E) Lap-joint flanges.
(F) Threaded flanges.

Wherever different methods of attachment could be visualized, their influence on the life of the assembly was explored separately. For instance, in the case of slip-on flanges, not only were two types of double-welded designs tested, but separate runs were made with a hub weld only and a face weld only, to determine their relative contributions to the endurance strength of the assembly. In the case of socket welding flanges, similar investigations were carried out and, in addition, an attempt was made to evaluate the effect of the relative proximity of front and back welds; also to find out whether any significant differences in strength are evident where the pipe is butted against the bottom of the socket as compared with a loose assembly leaving a gap at the end of the pipe. In the case of threaded flanges, some assemblies were made up with normal thread engagement, and others with the pipe threaded through the flange and refaced. Every one of the basic variants is illustrated in Fig. 1.

All the assemblies involved in the main test series were made using 4-in. carbon-steel flanges of the 300-lb ASA pressure class and standard weight (Schedule 40) pipe, all welding being done by the Heat and Power Corporation, Baltimore, Md., employing welders qualified by The Hartford Inspection and Insurance Company.

Supplementary tests were run with some of the same types of assemblies, but using ordinary experienced welders who had been instructed expressly to deposit the minimum amount of welding which might be considered as passing the requirements of Section VIII of the ASME Boiler Construction Code, the express purpose being to widen the range of the test data and assure that any values derived for design use would be reasonably conservative.

A further supplementary test series, restricted to slip-on and welding neck flanges, was run with pipe of 0.080 in. wall thickness to obtain an idea of the size effect; this test series, besides providing direct information on assemblies involving 4-in. light-wall pipe, also might be considered as a model test of, say, a 12-in. flange attached to standard-weight pipe.

Materials and Preparation

All assemblies were of 4-in. nominal size, the flanges being made of forged steel and conforming to the 300-lb American Standard, and the pipe and lap-joint stub ends to standard weight (except for the supplementary tests on lightweight pipe referred to previously). Dimensional and materials information on these components is compiled in Table 1.

Through-threaded bolt studs of $^3/_4$ in. diam and SAE 4140 material were used to attach the test flanges to the mating flanges on the adapters, which were designed to be slightly stiffer to assure that flange failure, if encountered, would occur in the test specimen rather than the adapter. The physical properties of the studs conformed to the requirements of ASTM Specification A193, Grade BC. The semifinished hexagon nuts conformed to the heavy series of ASA Standard B18.2.

Gaskets were $^1/_{16}$ in. thick × 4 in. ID × $7^1/_8$ in. OD asbestos

---

[1] Chief Research Engineer, Tube Turns, Inc.
[2] Research Engineer, Tube Turns, Inc.

Contributed by the Power Division and presented at the Spring Meeting, New London, Conn., May 2–4, 1949, of The American Society of Mechanical Engineers.

Note: Statements and opinions advanced in papers are to be understood as individual expressions of their authors and not those of the Society. Paper No. 49—S-6.

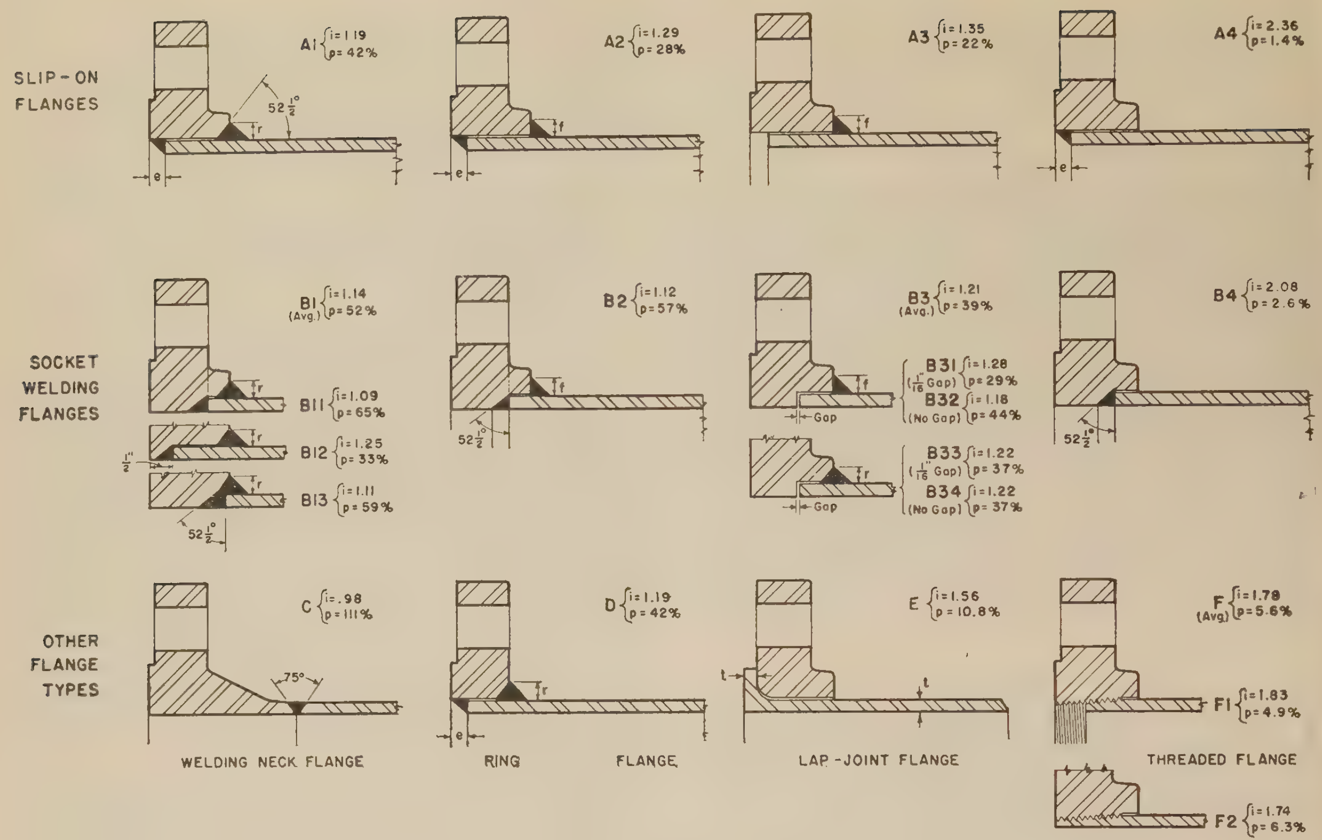

Fig. 1 Details of Flanges and Variants of Flange Attachment Tested in Main Series

The hub welds were specified to be $^3/_8$-in. leg size or approximately 15 per cent heavier than required by the Code for Pressure Piping; the deposited welds actually ranged from $^7/_{16}$ to $^{11}/_{16}$ in. Symbol r denotes weld deposited against a $52^1/_2$-deg recess, while symbol f denotes an ordinary fillet weld. The end welds for the slip-on flanges were full-fillet welds, the dimension e from the end of the pipe to the flange face being held to approximately $^3/_8$ in. The values i and p marked opposite each variant, respectively, denote the stress intensification factor and percentage of fatigue life in terms of that of straight pipe. The values noted opposite B1, B3, and F represent averages, weighted by the number of tests, of the subvariants shown thereunder.)

TABLE 1 DIMENSIONAL AND MATERIALS DATA

	Dimensional standard	Materials specifications	Range of physical properties, from tensile tests: Ultimate tensile strength, psi	Yield point, psi	Elongation per cent in 2 in.
Flanges[a]	ASA B16e	ASTM A-181, Gr. I	70250 to 74750	39500 to 41000	27.5 to 31.0
Pipe	ASA B36.10	ASTM A-106, Gr. B	69200 to 70600	39880 to 47500	37.0
Lap-joint stubs	ASA B16.9	ASTM A-106, Gr. B	62865	38600	39.0

[a] The ring flanges were machined from forged flanges.

composition, manufacturer's designation "Tenax." A new gasket was used for each assembly; it was applied dry, without prior wetting or the use of a gasket compound.

The welds made in joining certain flange types, notably the slip-on and socket welding variants, were of two markedly different qualities. All the welding for the main test series was carried out by ASME Code qualified welders; while not strictly code welds (since they were not code-inspected or chipped to the extent customary when preparing for code inspection), the welds may be considered representative of good commercial practice; they were generously proportioned (the fillets attaching the flange hubs were practically full size) and presented a smooth, somewhat concave contour. By contrast, the welds prepared by welders of the research department of the authors' company for the supplementary tests, which were meant to represent the least weld size and quality compatible with code requirements, were small (the weld size on hub fillets was of the order of $^5/_{16}$ in. to $^3/_8$ in.) and of a beadlike, unfinished appearance.

Incidentally, no difficulties were encountered by the fabricator's welders in welding any of the flange types, except that the face welds on slip-on flanges were found to chill rather quickly, resulting in an occasional poor weld which had to be machined out and redone.

The threaded flanges were made up with machine-threaded pipe to ASA Standard B2.1. In one set of tests, they were pulled up with 2000 ft-lb torque for normal thread engagement; in the second set, where the pipe was threaded through the flange and refaced, a 4000 ft-lb torque was applied. A liquid thread compound, sold under the name "Copaltite," was used on the threads in both cases.

Test Equipment

A specially designed fatigue testing machine of the specific-strain reversed-bending type, as described in an earlier paper by the senior author,[3] and illustrated in Fig. 2, was used. The test principle is a simple one, as becomes evident from the diagram in Fig. 3; the assembly presents a cantilever beam fixed at one end, with a cyclically reversed load being applied at the other. The specimen proper is located close to the fixed end, where the bend-

[3] "Fatigue Tests of Welding Elbows and Comparable Double-Miter Bends," by A. R. C. Markl, Trans. ASME, vol. 69, 1947, pp. 869–879.

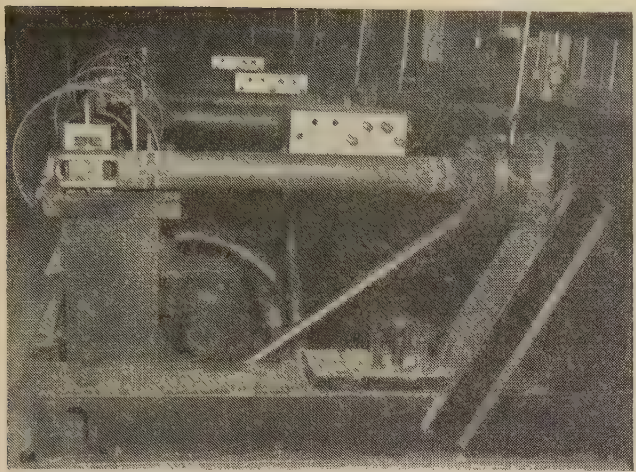

Fig. 2 Fatigue-Testing Machine

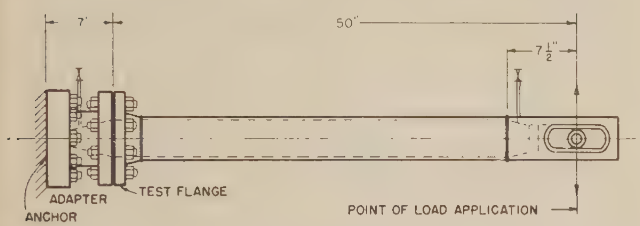

Fig. 3 Diagram of Test Assembly

ing moment is a maximum. In the main test series, an adapter was used to approach the condition of two mating flanges of equal stiffness; in the supplementary tests no adapter was used, the test flanges being bolted directly to the anchor plate.

Test Procedure

Prior to mounting the specimens, each assembly was inspected and subjected to a pressure test of 600 psi, which is the service pressure at atmospheric temperature set up in ASA Standard B16e for flanges of the 300-lb-pressure class. Leakage was encountered in a single instance, this being a slip-on flange attached by a face weld only; the defective fillet was machined out, the specimen rewelded and retested with satisfactory results.

In mounting the specimens, careful attention was given to alignment and uniformity of bolt pull-up. The $^3/_4$-in. bolts were pulled up incrementally with a torque wrench, using a predetermined sequence. The torque was set at 2000 in-lb, which corresponds to approximately 40,000 psi bolt stress, as determined with SR-4 strain gages. Originally it was planned to apply only 1200 in-lb, but this led to early gasket leakage of the specimens subjected to high deflections.

In the next step, each specimen was cycled at a low deflection amplitude about 20 times to "iron out" mounting irregularities; specimens were then realigned, where necessary, and the bolts rechecked with the torque wrench.

A load-deflection calibration of each specimen was next carried out, and the results were plotted as curves; the variation between individual specimens belonging to any one series being of the order of only a few per cent, an average or typical curve, such as is plotted in Fig. 4 for the welding neck type, was considered as adequate for all tests of one type. Using these data and the anticipated stress intensification factors, amplitudes of deflection were selected so as to spread failures evenly within the range from 1000 to 1,000,000 cycles.

Some of the large displacements required for the short-life

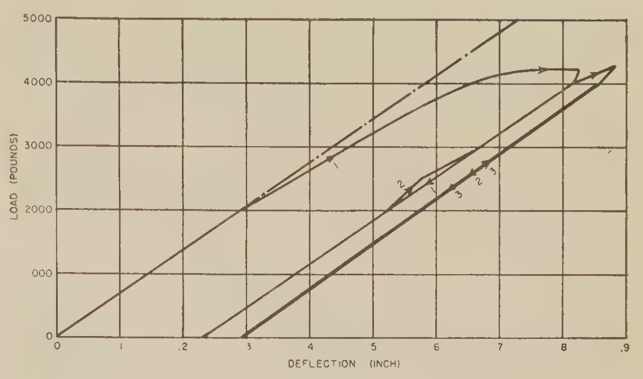

Fig. 4 Typical Load-Deflection Calibration Curve for Welding-Neck Flange Assemblies

(Note that yielding occurs at appreciably higher load in the repeat calibration as compared with the first load application. The value S used in plotting the S-N curves, Figs. 7, 8, and 9, is based upon the dash-dot extrapolation of the straight portion of the calibration curve.)

specimens fall onto the curved part of the load-deflection curve, denoting a stress high enough to produce more than local yielding. In the conversion of these displacements into loads, moments, and ultimately, stresses, the load-deflection curve, however, was considered as a straight line, i.e., the loads in the yield zone were obtained by an extrapolation from the elastic zone. A justification of this procedure, which, while not strictly correct, offers practical advantages, is given later under "Numerical Evaluation of Test Results."

In order to ascertain whether the originally applied load was maintained throughout the cyclic tests, a representative number of tests were interrupted for making check determinations of the load-deflection ratio. On flanges with wide gasket faces, no change in flexibility could be detected as the fatigue test progressed, and hence the stress conditions could be assumed as constant. The same was not true of the lap-joint flanges, specifically those under a high load. For example, in one specimen subjected to a load of 2350 lb (corresponding to failure in less than 3000 cycles), the load was reduced by about 3 per cent at 40 per cent of the total life of the assembly, by 10 per cent at 60 per cent, and by 16 per cent at 80 per cent of the life. After the stub end had cracked, the load was found to be 20 per cent lower than that originally applied. Inspection after disassembly led to the definite conclusion that the loss in load was attributable to progressive destruction of the gasket; the tops and bottoms at the inner circumference, which were alternately subjected to very high and low compressive stresses, were badly "chewed up." This was not the case for the lap-joint assemblies subjected to low moments, nor for any of the other assemblies, the gaskets invariably being found in good usable condition on taking the flange apart after failure.

All specimens were filled with water; a 25-in. head was held on those not under pressure to serve as a means for recognizing failure promptly. In order to find out whether the face weld cracked before the hub weld in double-welded slip-on or socket welding assemblies, a $^1/_8$-in. hole was drilled through the hub at an angle of 45 deg from the bottom.

After all preliminaries were completed, the machine was started up and kept under constant observation. Where leakage appeared (or, in rare instances, a crack was noted shortly before leakage became apparent), the cycles which the unit had run were recorded. However, the test in nearly all cases was continued for at least 20 per cent more cycles to confirm failure and give information on the direction of crack propagation. Tests where no failure occurred within one or two million cycles were abandoned. In the case of threaded flanges, a slight seepage

along the threads, unaccompanied by a crack, often became evident early in the tests; by comparison, the later actual failure of threaded assemblies was always heralded by a sudden flow.

After completion of the test, the specimen was removed and photographed; a quarter section was cut out, with one of the saw cuts going through the center of the initial crack, and this was then etched and photomacrographed to record the type and location of failure. An occasional micrograph was made for more detailed study.

Visual Test Evidence

For various types of bolted flanged connections, tested with a given gasket and a uniform bolt pull-up, the tests established what type of failure is encountered under conditions of cyclic bending, where it occurs, and how many reversals are necessary to bring it about.

A joint could be rendered unsatisfactory by the occurrence of either of two things, i.e., it could leak, or some component could break. Leakage across the gasket to the outside of the flange or through the bolt holes did not occur in a single instance under the test conditions. A possibility of such leakage was approached, however, in the case of lap-joint assemblies where alternating overcompression of the gasket and release of most of its load resulted in deterioration of a large part of the gasket area in contact with the lap face. Another type of leakage, in the form of a persistent seepage along the threads, was encountered with threaded flanges. Even with only 25 in. head of water, this occurred long before structural failure, and with 600 psi pressure and some of the higher bending moments, around 100 reversals were enough to start a dribble of water.

In general, apart from the threaded joints, the usefulness of all flange types was terminated by structural failure, not of the flange proper or the bolts, but invariably of the pipe, or, where a single attachment weld of small cross section or poor contour was used, the weld. All of these failures occurred as circumferential cracks and started on the outside of the pipe at or near the top or bottom of the assembly where bending stresses were highest. Fig. 5, reproducing representative photomacrographs taken of failed specimens of the main test series, will be used to comment more in detail on the nature of the failures.

The top line in Fig. 5 shows variants of slip-on flange attachment in the order of decreasing strength; the first three photographs, identification A1, A2, and A3, reveal identical failures, at the toe of the hub weld, whether a face weld was used in addition to it or not, and whether the hub weld was deposited against a square hub face or a reverse bevel or recess. In the last photograph, identification A4, which represents the obviously weak and hence unusual construction, where a face weld only is applied, failure occurred across the throat of the fillet weld. The middle line of photographs, in which the four basic variants of socket-welding flange attachment are assembled, presents almost identical evidence and requires no individual comment.

Referring to the bottom line, the butt-welding flange, shown at the left, designation C, shows failure at the edge of the weld overlay away from the flange, the crack remaining entirely within the pipe, as is also evident from the photomicrograph in Fig. 6. This is typical also of the cracks at the toes of fillet welds. The ring flange, designation D, failed at the extreme edge of the weld, as in the case of hub welds of slip-on or socket welding flanges. The lap-joint assembly, designation E, cracked across the stub end, close to the tangent point with the fillet radius. The threaded flange, designation F2 (and likewise F1, which is not shown)

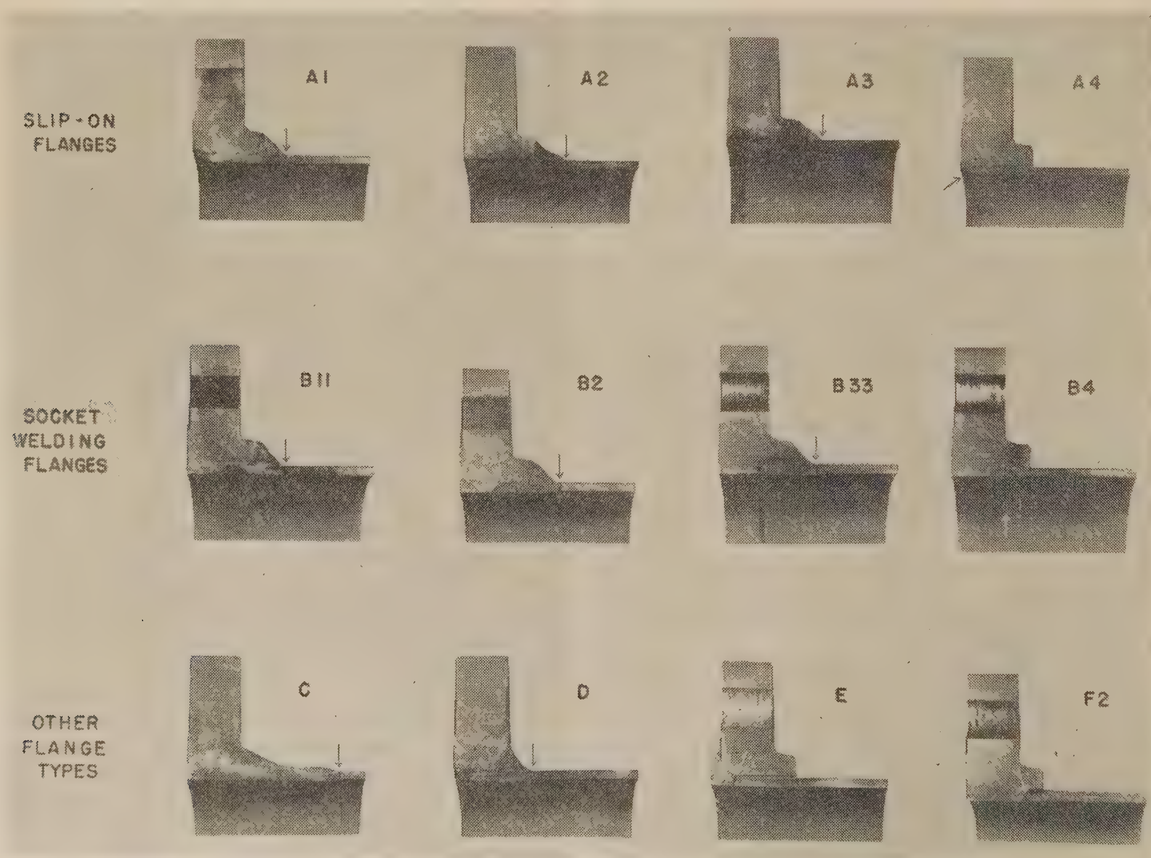

Fig. 5 Photomacrographs of Representative Failed Specimens
(Arrows indicate location and approximate direction of cracks.)

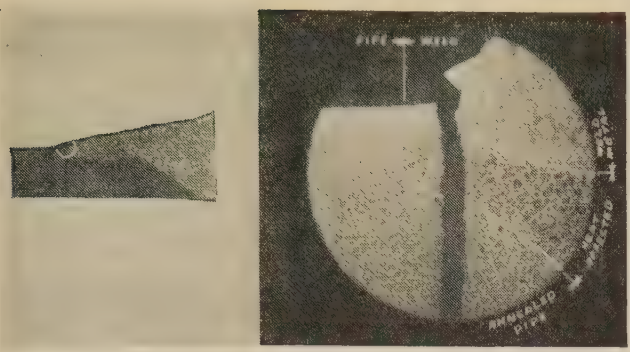

Fig. 6 Photomacrograph and Photomicrograph of Crack in Welding Neck Flange Assembly

(Micrograph covers circled—1/8-in. actual diam—area of macrograph. Crack starts in edge of weld and propagates through pipe. Fracture is cross-crystalline.)

cracked through the root of one of the first three engaged threads.

Of the two supplementary series, the few exploratory runs of butt welding and double-welded slip-on flanges with lightweight pipe gave the same kinds of failure as the main test series. The other series, in which small and poorly contoured welds were used with standard-weight pipe, differed in only one respect; where flanges were attached by a single fillet weld at the hub, the weld itself failed in three out of four specimens.

The following conclusions can be drawn from visual observation during and after test:

1 Flanges of the size and types investigated, with the given gasket material and size, and using an amount of bolt pull-up in line with common practice, are stiff enough to avoid leakage across the gasket and strong enough to prevent failure of the flange proper under its maximum rated service pressure and a superimposed bending stress of appreciable magnitude.

2 The welds customarily deposited by experienced welders are more than adequate to prevent failure of welded joints, this being true even of single-fillet welded construction; not included in this statement, however, are slip-on and socket welding flanges with weld attachment of the pipe end only, these constructions not being found in common usage.

3 Caution is in order when using lap-joint flanges with laps of a thickness of the same order as the pipe wall in locations of high bending moments, since the lap apparently rocks back and forth on the gasket, and tends to destroy it.

4 Threaded flanges are unsatisfactory for any but the mildest cyclic services; the threads constitute not only a structural weakness, but are prone to open up under bending and cause leakage.

5 Structural failure appears associated entirely with contour, the crack invariably appearing at a location of marked change in section adjacent to the flange. For welded joints, this is the edge of the weld, for lap joints the start of the fillet, and for threaded joints the notch formed by the root of the thread.

Numerical Evaluation of Results

Fatigue data are usually reported in the form of so-called S-N curves, and where the tests performed involve a comparison of a part in which a stress raiser is present with a similar part with undisturbed stress flow, it is convenient to interpret the results in terms of a stress-intensification factor.

For practical piping design, the properties of straight pipe offer the most satisfactory reference medium, since the bulk of piping is straight pipe. For this reason, the endurance strength of an assembly, involving a flange and straight pipe of a certain size and wall thickness, will herein be referred to the endurance strength of the same kind of straight pipe by itself. In an earlier paper by the senior author,[3] the endurance strength S of commercial straight Grade B carbon steel pipe between limits of 500 to 500,000 cycles of stress reversal was tentatively expressed in terms of cycles-to-failure N by the equation[4]

$$S = 245{,}000\,N^{-0.2} \qquad [1]$$

To make possible the construction of an S-N curve for the recording of the present tests, it becomes necessary to translate the applied deflections into nominal stresses. In so far as the stresses caused by the deflections imposed upon the test cantilever remain within the elastic limit, the load-deflection calibrations of the different assemblies made preparatory to these tests serve to establish the loads corresponding to any specific deflection; by multiplication by the lever arm from the point of load application to the point of starting failure, the controlling moment is obtained, and this, divided by the section modulus of the pipe used, gives the nominal stress. In the present tests, however, the larger displacements applied in the short-life runs definitely caused more than local yielding. It would have been entirely possible to establish the corresponding load, and therewith the stresses, from the applicable load-deflection curve. However, in view of the fact that the results of this investigation are primarily intended for use in the flexibility analysis of piping systems (where the displacement is given and the loads or reactions are solved for), and since such calculations are commonly based upon the elastic theory, it has been considered preferable to extrapolate the straight-line portion of the load-deflection curves (see Fig. 4 for an example) and plot the cycles-to-failure against a fictitious stress thus obtained, which, obviously, is higher than the actual stress.

This last is the basis upon which the median lines given as the S-N curves for different assemblies in Figs. 7, 8, and 9, have been derived. They are all drawn parallel to the S-N curve for straight pipe expressed by Equation [1] and go through the computed center of the respective group of test points obtained from the main series; the results of the supplementary tests series (shown by symbols of reduced size, but otherwise identical with those used for recording the results of the main tests) have been ignored in drawing the median lines. The justification for using a constant slope for all median lines resides in the advantage this offers of representing the stress-intensification factor as a constant, which would not otherwise be possible. A study of the charts indicates that this arbitrary adjustment is accomplished without violating the test evidence seriously. To avoid undue reliance on the median lines in the low-cycle range, in view of the liberties taken in extrapolating the load-deflection curve beyond the elastic range, these median lines have been cut short at a stress level roughly corresponding to definite yielding.[5]

The test results as reduced to these median lines are readily interpreted in either of two ways. To derive the stress intensification factor i for any particular assembly, the nominal stresses applicable to straight pipe and the assembly in question are read at the intercepts of the two corresponding median lines with any one ordinate, and these divided by each other. To determine the comparable life of any assembly in relation to that of straight

[4] Results obtained by this formula should not be confused with results of fatigue tests on polished bars, since commercial straight pipe involves certain inherent stress raisers in its surface condition, and additional stress raisers are introduced by any form of clamping or joining, mechanical or by welding, regardless of the amount of care taken to avoid notch effects. This should be well understood in view of possible future attempts at a rigorous mathematical analysis of the shapes involved in the present test.

[5] It will be noted by reference to Fig. 4 that the departure from a straight-line law occurred much earlier in the first load application, as compared with subsequent retests; the latter only have been considered significant in the present investigation.

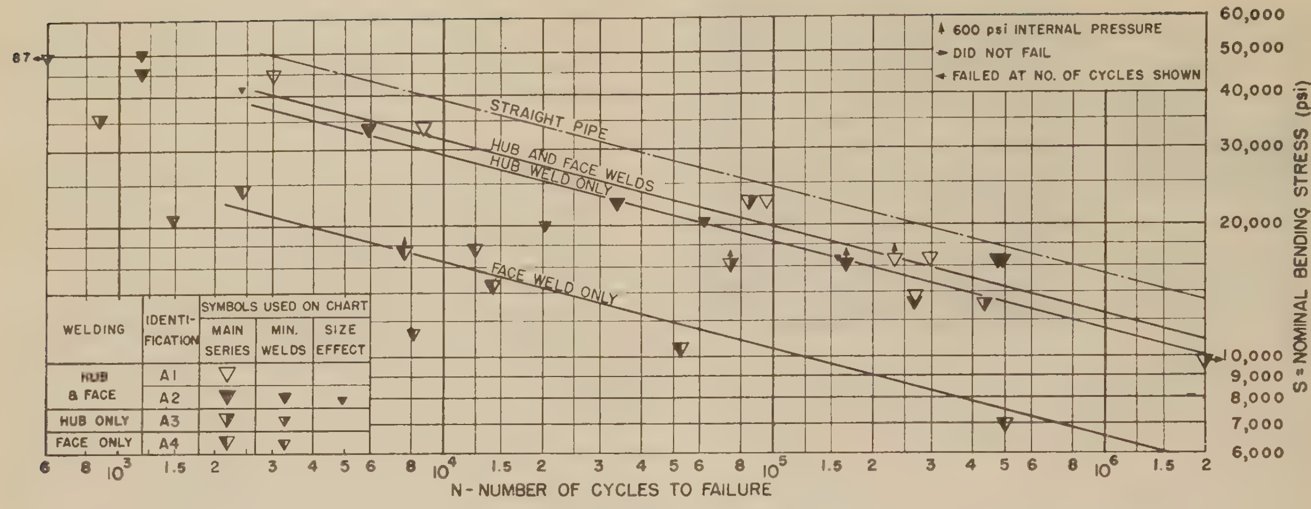

Fig. 7 *S-N* Curves for Slip-On Flanges

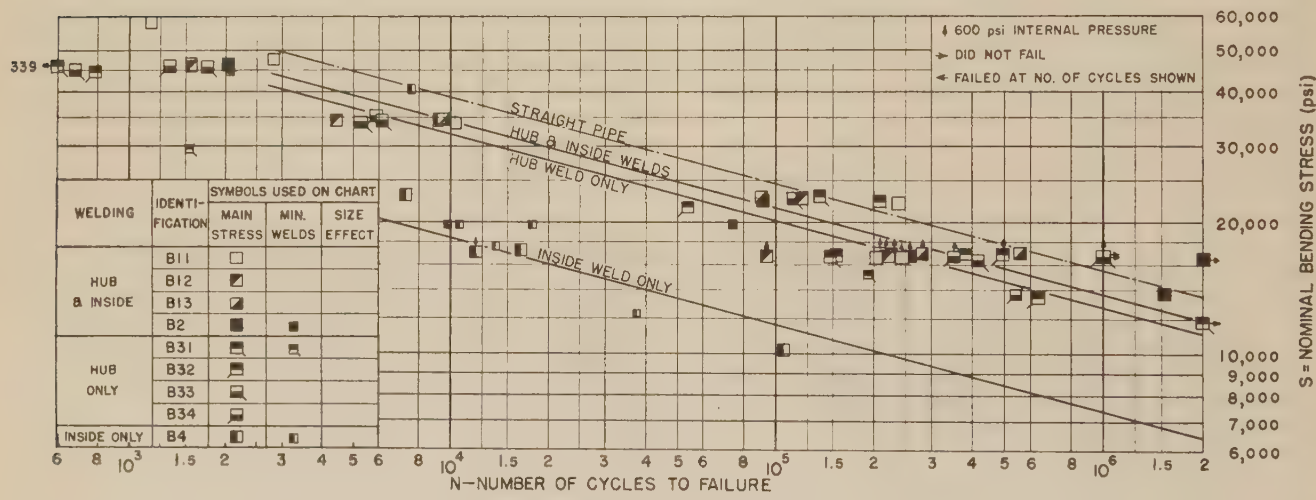

Fig. 8 *S-N* Curves for Socket Welding Flanges

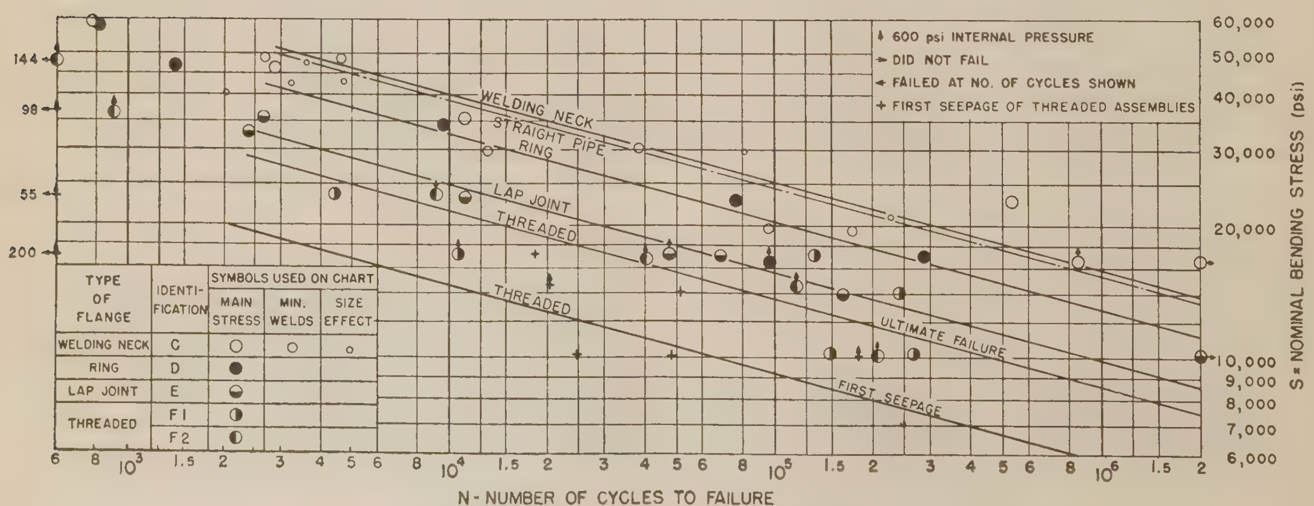

Fig. 9 *S-N* Curves for Flanges Other Than Slip-On or Socket Welding

TABLE 2 DETAILED EVALUATION OF TEST RESULTS

Flanges and variants of flange attachment	Identification	Main series: No. specimens	Main series: i	Main series: p, per cent	Supplementary series, Minimum welds: No. specimens	Minimum welds: i	Minimum welds: p, per cent	Supplementary series, Size effect: No. specimens	Size effect: i	Size effect: p, per cent
Slip-on flanges with double welds (average)		12	1.24	34						
Recessed hub and fillet face welds	A1	6	1.19	42						
Fillet hub and face welds	A2	6	1.29	28	2	1.26	32	2	1.30	27
Slip-on flanges with single fillet hub weld	A3	5	1.35	22	2	1.84	4.7			
Slip-on flanges with single inside fillet face weld	A4	6	2.36	1.4	2	3.14	0.3			
Socket welding flanges with double welds (average)		21	1.14	52						
Recessed hub and inside butt welds (average)	B1	16	1.14	52						
Same with butt weld in line with back of flange	B11	6	1.09	65						
Same with butt weld 1/2 in. from face of flange	B12	5	1.25	33						
Same with butt weld made as through weld with hub weld	B13	5	1.11	59						
Fillet hub weld and inside butt weld	B2	5	1.12	57	2	1.25	33			
Socket welding flanges with single hub welds (average)	B3	25	1.21	39						
Fillet welds (average)		13	1.21	39						
Same with 1/16-in. gap between end of pipe and bottom of socket	B31	4	1.28	29	2	1.64	8.4			
Same with no gap; pipe bottomed in socket	B32	9	1.18	44						
Recessed welds (average)		12	1.22	37						
Same with 1/16-in. gap between end of pipe and bottom of socket	B33	7	1.22	37						
Same with no gap—pipe bottomed in socket	B34	5	1.22	37						
Socket welding flanges with single inside butt weld	B4	4	2.08	2.6	6	1.78	5.6			
Welding-neck flanges	C	5	0.98	111	6	1.09	65	6	1.06	75
Ring flanges	D	6	1.19	42						
Lap-joint flanges	E	6	1.56	11						
		6	1.65[a]	8.2[a]						
Threaded flanges (average)	F	12	1.78	5.6						
		12	2.65[b]	0.8[b]						
Same, with normal make-up	F1	6	1.83	4.9						
		6	2.48[b]	1.1[b]						
Same, with pipe threaded through and refaced	F2	6	1.74	6.3						
		6	2.83[b]	0.6[b]						

[a] Value corrected for loss in load observed during course of test.
[b] Value based upon first appearance of seepage whether accompanied by crack or not (i here is not strictly a stress-intensification factor, but may be applied as such for design purposes).
i = stress intensification relative to straight pipe.
p = life of assembly relative to straight pipe.

pipe, the cycles-to-failure are read for the assembly in question and for straight pipe along any abscissa denoting constant nominal stress, and the one is then expressed as a percentage p of the other. Both the i and p values for all variants tested in the main series are recorded against each type in Fig. 1 and compiled in Table 2 for ready comparison. The table also includes the results of the supplementary test series and gives the number of specimens tested of each variant.

It may be noted that a single median line has been drawn for all double-welded slip-on flanges, and the same has been done for the socket welding flanges. While these group averages are helpful in an over-all appraisal of the effect of the major design characteristics, a more detailed study of each individual variant in relation to others will be found worth while, inasmuch as it gives an idea of the contribution of minor details to the endurance strength of an assembly; while the differences between variants to be commented upon appear of a low order and well within the range of scatter of the test results, some of them are entirely too consistent and logical to be ignored, as will be shown. All comparisons will be made on the basis of the stress intensification factors developed, but it should be remembered that relatively small differences in this factor connote appreciable differences in fatigue life, i.e., the anticipated number of cycles to failure. As an example, a 10 per cent increase in stress-intensification factor is equivalent to a reduction in useful life under cyclic bending of over 40 per cent.

Single Welds. As expected, the butt weld used for attaching a welding-neck flange, test series C, was found vastly superior to any other form of attachment; it is equivalent to any butt weld between pipe, and practically as good as straight unwelded pipe. Even in an unfavorable location at the junction between two parts of greatly differing stiffness, as in socket welding variant B4, this form of weld gave a 13 per cent improvement over a similarly located fillet weld, as used in slip-on variant A4. As far as the two types of hub welds are concerned, i.e., the regular fillet weld and a weld deposited against a 52 1/2-deg reverse bevel or recess, neither the comparable single-welded variants (B31 versus B33, and B32 versus B34), nor the double-welded ones (A2 versus A1 and B2 versus B11) show any consistent differences. Apparently, where both welds are of adequate size, the pipe failure is influenced solely by the contour at the toe of the weld, which is the same for both types.

Bottoming of Pipe in Socket. Having just mentioned variants B31, B32, B33, and B34, it may be opportune to cover briefly the second objective of this particular subproject, which was to discover whether butting the pipe solidly against the face of the recess in a socket-welding flange improved resistance to cyclic bending. From a comparison of the values of i, given for the condition with no gap with those for that with a 1/16-in. gap, it would appear that forcible contact of the end of the pipe with the socket face is helpful, but that the benefit is minor. Incidentally, the result of the slip-on flange series A3 would tend to confirm the results obtained on socket welding flanges with a definite gap.

Single Versus Double Welds. Three directly comparable groups of test series are available to evaluate the beneficial effect of the weld at the end of the pipe when used in conjunction with a hub fillet weld: Series A2 can be compared with series A3; series B31 and B32 with B2; and series B33 and B34 with B11. From such a study it may be concluded that the added welds produce an improvement in endurance strength of the order of 8 or 10 per cent.

Weld Proximity. There are indications that the distance between welds in double-welded flange attachments is not without significance. Below are listed the seven different variants of double-welded constructions tested, together with their stress-intensification factors; the order is from the closest spaced welds to those most widely separated:

B13:	1.11	close (avg. 1.11)
B11:	1.09	
B2:	1.12	
D:	1.19	intermediate
B12:	1.25	apart (avg. 1.24)
A1:	1.19	
A2:	1.29	

Considering the two bracketed groups listed, it will be noted that a weld spacing not exceeding the height of the hub of a slip-on or socket welding flange on the average produces a 12 per cent higher endurance strength than a wider spacing, of the order of the flange thickness. Omitting test series B12 from the foregoing comparison, it will be seen that the two groups are directly representative of socket welding and slip-on flanges, and hence the former, when used with shallow sockets, can be pronounced about 12 per cent stronger against cyclic bending as compared with the latter.

The results for lap-joint and threaded-flange assemblies, as plotted in Fig. 9, and averaged in Fig. 1 and Table 2, require modification before they can be applied to piping design. It has been mentioned already that a slight loss in applied load was encountered in the case of lap-joint assemblies under high loadings; the plots are based on the initial loading (or strictly, the applied deflection), and adjustment to the approximate average loading over the test duration would raise the stress-intensification factor from 1.56 to 1.65, or reduce the life from about 11 per cent of that of straight pipe to only 8 per cent. In the case of threaded assemblies, seepage through the threads on the average occurred in one seventh of the time it took to produce structural failure. If we expand the definition of the "stress intensification factor" so that, for any given cyclic life, it expresses the relation between the stress producing fracture in a straight pipe and the stress producing failure from whatever cause in a comparative assembly (including the same kind of pipe), or in other words, if we consider leakage on equal terms with failure, this premature loss of serviceability of threaded flanges would have to be compensated by applying an "effective" stress intensification factor of 2.65 rather than 1.78 as obtained using cracking as the sole criterion of failure.

A few brief comments on the findings of the two supplementary test series included in Table 2 appear in order before going on to the conclusions. The one series, in which weld size effects were explored, indicated that it might be advisable for design purposes to increase the stress intensification factors obtained from the main test series somewhat for flanges involving attachment by fillet welding. The second series, involving thin-wall pipe, may be considered as providing a certain measure of assurance that, within the more common range of pipe sizes, the effect of the pipe-wall thickness and size or series of the flange is not overly significant.

Conclusions

The tests established that, even under unusually severe bending stresses, flange assemblies do not fail in the flange proper, or by fracture of the bolts, or by leakage across the joint face. Structural failure occurs almost invariably in the pipe adjacent to the flange, and in rare instances, across an unusually weak attachment weld; leakage well in advance of failure is observed only in the case of threaded flanges.

While it is the pipe that fails, the type of flange is influential in determining the endurance strength of the assembly, largely by the way in which it affects the stress transfer at the joint. The smooth tapering transition, afforded by a welding-neck flange, provides an endurance strength of the assembly equivalent to that of a butt-welded joint between two pieces of pipe, which itself is not greatly different from that of unwelded straight pipe to judge from indications obtained from tests in such pipe conducted by the authors. A fillet weld presents less favorable conditions owing to the sharp change in cross-section and stress-flow direction. In the case of lap-joint flanges, the transition would not appear unfavorable, but the lap apparently lends inadequate support to the neck of the stub end. Finally, in the case of threaded flanges, the reduced pipewall thickness and notch effect, caused by the threading, constitute weaknesses which become even more apparent under cyclic loading than under static conditions.

In order to provide a quantitative measure of the relative endurance strength of different common flange assemblies, Table 3 has been prepared by the authors, using all the evidence produced in these tests, including the supplementary series and giving weight to any tendencies which may have been present of premature loss of serviceability prior to ultimate fracture. It is thought that the stress-intensification factors given may find direct use in flexibility calculations following the rules of the Code for Pressure Piping, and that the parallel information on relative fatigue life, as more descriptive, may be helpful in setting limitations on flange types, depending upon the service involved.

TABLE 3 PROPOSED STRESS INTENSIFICATION FACTORS AND COMPARATIVE FATIGUE LIVES FOR DESIGN

Type of assembly	Stress-intensification factor, i	Relative fatigue life, p, per cent
Welding-neck flanges....................	1.00	100
Socket welding flanges (double-welded, with inside butt weld approximately in line with back of flange)...............	1.15	50
Double-welded slip-on or forged ring flanges	1.25	33
Single hub-welded slip-on or socket welding flanges............................	1.30	27
Lap-joint flanges (with standard lap-joint stub ends)............................	1.60	10
Threaded flanges........................	2.30	1.5

Acknowledgment

The authors desire to acknowledge the co-operation of the management of Tube Turns, Inc., whose generosity in placing the facilities and personnel of its Research Department at their disposal made possible the investigation herein reported. The assistance in preparing the test assemblies, by welding the flanges to the pipe, rendered by Mr. John H. Zink, is also gratefully acknowledged. Mr. Zink, president of The Heat and Power Corporation of Baltimore, Md., is a member of the Subgroup on Flange Limitations of Subcommittee No. 3 of ASA B16, for the benefit of which the present investigation was conducted. Mr. Zink must also be given credit for proposing the design of the internally welded socket-weld flange which was included in the tests reported herein.

Discussion

H. F. Moore.[6] Full-size fatigue tests of structural and machine parts are always preferable to tests of small polished specimens when such full-size tests are feasible. Hence this paper is very welcome as it describes such full-size tests for flange-pipe assemblies.

The fatigue-testing machines used are of the simplest type—the type which measures directly the deflection of the specimen and the number of cycles of stress to cause fracture. The stress pattern, the load, and the bending moment are then measured from the deflection, using the specimen itself as the dynamometer. The authors determined the stress range from the deflection of the specimen, stopping the machine at various stages of the test to determine the steady value to which the stress range "settled down."

The authors carried out their tests to a maximum of about 2,000,000 cycles of reversed flexure. As is the case with railroad rails and with many structural parts, repeated-stress tests to 2,000,000 cycles are sufficiently long to cover the customary period of use. The results, plotted on log-log stress-cycle (S-N) diagrams show no sign of "flattening out," and show a con-

[6] Research Professor of Engineering Materials, Emeritus, University of Illinois, Urbana, Ill. Mem. ASME.

siderable, although not too serious, scatter of test results. It is probable that longer tests would show a flattening out of the S-N diagrams. In that case extrapolation of the authors results to 10,000,000, or even to 100,000,000 cycles might be expected to give results "on the safe side."

The writer is especially impressed by the poor showing made by the threaded flanges. Screw threads in any structural or machine part constitute one of the most dangerous of stress raisers, especially if the rod or pipe is screwed in as far as the thread will allow.

Attention is also called to the tabulation in Fig. 1 and Table 2 of both i, the effective stress-intensification factor, and to p, the ratio of length of endurance (number of cycles of stress) of a flanged assembly to that of the straight pipe. Thus the assembly can be judged on the basis either of comparison of stress range for a given endurance or of comparison of endurance for a given stress range of a straight-pipe specimen.

J. J. Murphy.[7] The authors are to be congratulated on having made a valuable contribution of test data on the performance of various flange types, on the organization of the tests, and presentation of the results for handy reference. There has been too little information available on this subject, and the paper is a fitting supplement to the senior author's previous paper.[3]

The role of fatigue-test data as an index to the relative serviceability of flange types is difficult to assess, and the authors have been careful not to draw any unwarranted conclusions. Data such as these are, nevertheless, quite valuable, and the order of performance of the various types fits in well with what would be expected, with the exception that the relatively poor performance of lap-joint flanges is somewhat surprising. While service experience with all types of flanges has been generally good, slip-on, lap, and threaded flanges are used normally only in the less severe services.

The tests provide excellent comparative data for the various weld details for slip-on and socket welding flanges. The ASME Boiler Code Subcommittee on Bolted Flanged Connections already has recognized a socket welding detail similar to B11 except that the inner weld is located at the mid-point of the flange thickness. The data here presented provide valuable information for permitting the weld to be located near the hub. The authors' opinion that the pipe failure is influenced solely by the contour at the toe of the weld appears logical, and it would be interesting to see if the performance of flange attachment B13 could be made to more closely approach butt-welded flange construction by modifying the fillet-weld contour as indicated in Fig. 10 of this discussion.

Also, it would be interesting to have comparative test data on threaded flanges with a seal weld, a construction which is widely used. The test data obtained in the supplementary tests provide valuable information on the possible effect of variations in weld quality and size to be expected in actual applications. It is noted that the performance of welding-neck flanges in the supplementary tests in Table 2 of the paper is the same as the main tests on flanges B11. The authors may wish to comment on this.

The bending moments applied in these tests simulate those which might be caused by mechanical vibrations or changes in temperature of the pipe line. Fluctuating pressures or cyclic temperature changes which cause the pipe locally to run cooler or hotter than the flange would impose a different-type loading on the attachment welds in that the shear and moment would be uniform around the circumference. It is possible that the performance of the various details would react somewhat differently to this type loading.

[7] The M. W. Kellogg Company, Jersey City, N. J.

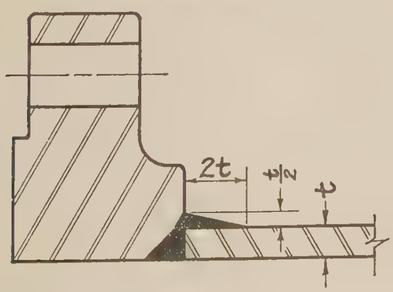

Fig. 10

E. C. Petrie.[8] In interpreting the results of the authors' research investigations, the designer must consider the piping system as one integrated structure. In other words, it would be inconsistent to demand of a flanged assembly, resistance to fatigue of a much higher order than that required for another part of the piping system. Due precaution should be exercised, therefore, in attempting to draw all-inclusive conclusions from the results of a series of tests on only one size and class of product.

In order to illustrate this point, let us compare the test results obtained in the earlier Markl paper[3] with those published in the present paper. The writer has combined these results in graph form in Fig. 11 of this discussion.

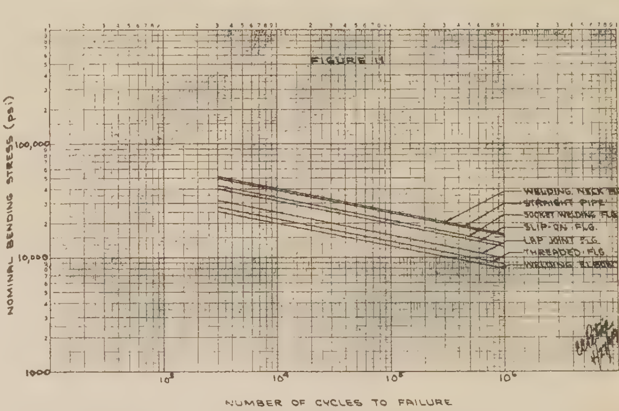

Fig. 11

It will be noted from this graph that the number of cycles to cause complete failure of the conventional and acceptable types of flange assemblies fall between those given for straight pipe and welding elbows. One exception is the welding-neck flange, which is slightly higher than that of straight pipe.

While it is a well-known fact that fatigue failures occur under certain conditions of severe stress in some threaded assemblies, there has been no indication, to the writer's knowledge, of failure in the side of a welding elbow due to fatigue as illustrated by the tests in the previous paper. The type of end fixation, notch effect in threads, clearances in flange assemblies, total resisting moment developed by bolting, are all important factors in an investigation of this type, and tests under various combinations may produce results which differ considerably from those presented in this paper. It is suggested, therefore, that more extensive investigations be made before arriving at any definite comparative values of fatigue life of elements which are component parts of a piping structure.

Another point mentioned in the paper being discussed is that the results obtained for lap-joint flanges indicate that "caution

[8] Engineering and Research Division, Crane Company, Chicago, Ill. Mem. ASME.

is in order when using lap-joint flanges with laps of a thickness of the same order as the pipe wall in locations of high bending moments, since the lap apparently rocks back and forth on the gasket and tends to destroy it," but that "this was not the case for the lap-joint assemblies subject to low moments." Apparently the high moments referred to by the authors are not encountered in a properly designed piping system due to the fact that, to the writer's knowledge, this damage to the gasket has never been found under actual service conditions.

E. O. Waters.[9] Static stresses in piping and piping connections always have been given due respect. Somewhere along the road of acquiring knowledge of piping design, the effect of live loads caused by temperature differentials, and those due to rigid end connections and intermediate supports, were taken into account as a matter of course. However, even here the results of tests and theoretical analysis are mainly applicable to the pipe alone, and much still remains to be learned about the effect of live loads on flanged or other forms of piping connections, and on the vessels to which piping is attached. Most recently, the question of the endurance of piping systems subjected to dynamic loading has come to the fore, the chief reason for its importance doubtless being due to the substitution of welding for what might be termed "semipermeable" forms of pipe connection which always could be counted upon to leak profusely long before any structural failure took place.

The authors have made a factual statement of their findings without attempting any extensive analysis, and the question arises as to how best to interpret the results. In so far as the welding-neck type of joint is concerned, behavior was exactly as would be predicted; in this case, there are no sudden transitions in size of cross section, and no sharp re-entrant corners, the weld is inherently superior, and the flow of stress from flange to pipe follows comparatively straight lines and easy curves. At the other end of the scale, the poor showing of the single inside welds (series A4 and B4) was to be anticipated. However, there are several intermediate cases which give rather unexpected results, calling for further explanation. For example, the general setup in Fig. 1 of the paper would lead a superficial reader to conclude that socket-welded connections are, as a class, superior to slip-on connections. However, a closer inspection of the sketches in line 2 in Fig. 1 reveals that the quality of these connections is very sensitive to inside and outside weld proximity. In fact, the authors call attention to this point. This at once raises the question: If close proximity improves the performance of socket welds, would it not be possible to improve the slip-on group by inserting the pipe only part way into the flange? Also, from a comparison of series B11, B12, and B13, it appears that there is an optimum proximity beyond which a closer weld spacing impairs the fatigue life of the connection. This would seem to make further detailed study desirable, including if possible an investigation of the actual stresses at points of concentration, before truly quantitative conclusions can be drawn.

In conclusion, the writer would call attention to one feature wherein the tests showed remarkable consistency, namely, the location of the point or region of failure. This is consistent with static tests and theoretical stress analyses based on static loading, which always indicate a relatively high bending stress in the pipe that is intensified by a sudden transition from a comparatively thick flange to a thin-walled pipe. The inclusion of this stress as one of the criteria for the design of flanges has at times been a bone of contention among users of the ASME Unfired Pressure Vessel Code, on the ground that it imposed an unnecessarily severe restriction. However, the results of these fatigue tests, as here reported, indicate that the existence of this stress, even though it is highly localized, cannot safely be ignored, at any rate when dynamic loads must be provided for.

[9] Professor of Mechanical Engineering, Mason Laboratory, Yale University, New Haven, Conn. Mem. ASME.

Authors' Closure

The authors are appreciative of the lively interest exhibited in the tests reported by them, and value particularly those comments which raise the issue how the test data relate to service experience and what their significance is with respect to future piping design.

As has been pointed out in the discussion, there has been no published record of stress failures in service of the types shown in this and the senior author's earlier paper[3], although failures in screwed joints, at branch connections and other points involving major stress raisers have been recognized as due to fatigue. One explanation, as inferred by Mr. Petrie, is that high sustained bending stresses, say, of 24,000 psi or over, are not encountered in properly designed piping systems; a second factor is that major stress cycles much in excess of 1000 over the life of a system are confined to the process industries, are not too frequent even there, and usually receive special consideration. Close inspection of Figs. 7, 8, and 9 reveals no stress failures of commonly used flanges within the quadrant defined by these limits, except in the case of threaded flanges, with lap-joint flanges coming close.

Accordingly it would seem that the tests and experience are in good accord. But, while experience proves that all but the two last-mentioned types of flanges will survive the conditions to which an average piping system is subjected, the tests are able to distinguish between the merits of the different types and thus offer an indication of how many more reversals at a given stress, or how much more stress at a given number of cycles, a welding-neck flange, for instance, can support with reference to any other variant. This is important in view of the trend toward more severe services in the process industries and the accompanying desire to liberalize allowable stresses; this latter objective can be accomplished, without reducing the true safety factor, only if our understanding of stresses improves so as to take part of the "ignorance component" out of the safety factor.

It is recognized that tests on a single size, class, and material of flange, with a specific type of gasket and bolting under a specific pull-up cannot be expected to form the basis for broad conclusions embracing the entire field of flanged connections. The authors, as some of the discussers noted, were careful to avoid such an impression. On the other hand, they feel that, considering the confirmation obtained from the supplementary test series, the results are suitable for engineering application to a somewhat broader range of conditions; in a way, there would seem to be no other alternative pending further experimental or analytical progress in this field.

A note of caution is in order with respect to comparisons of the type drawn by E. C. Petrie in Fig. 11. While the results of the flange tests might be applied with reasonable accuracy to a fairly wide range of sizes and thicknesses, those obtained for welding elbows are restricted to one specific size and thickness and can be extrapolated to other conditions only through the medium of a theoretical analysis, such as Beskin's development.[10] Furthermore, moments due to expansion vary from zero to a maximum over the length of a line, so that a piping component with a lower stress-intensification factor situated at a location of high moment will often control even though other parts with higher factors are present in the line. The critical condition can only be properly evaluated by multiplying the stress at each significant location by the applicable stress-intensification factor.

[10] "Bending of Curved Thin Tubes," by Leon Beskin, *Journal of Applied Mechanics*, Trans. ASME, vol. 67, 1945, p. A-1.

Many additional investigations have been proposed, and the authors would have wished to have been able to conduct these, but due to press of other work must confine themselves to giving answers which are no more than opinions.

J. J. Murphy's design, Fig. 10, might be expected to approach the welding-neck flange in performance, or at least equal the ring flange which behaved surprisingly well. A threaded flange with seal weld would probably be the equivalent of a single-hub-welded slip-on flange with minimum welding.

Professor Water's question, whether slip-on flanges would benefit from weld proximity to an equal extent as socket welding flanges is difficult to answer; the authors feel confident that they would benefit, but perhaps not quite to the same extent as the socket welding type which can be reasoned to provide a somewhat better stress flow. No doubt there is an optimum distance between the front and back welds, but it is doubtful whether this can be determined from tests on commercially fabricated joints; a photoelastic analysis of models probably would furnish an answer.

Regarding J. J. Murphy's comment on the similarity in fatigue life of group B-11 and the supplementary welding-neck flange assemblies, no explanation can be offered except to point out that the results show a fair amount of scatter and hence overlapping between flange types of similar endurance strength.

Modern Mercury-Unit Power-Plant Design

By H. N. HACKETT[1] and DWIGHT DOUGLASS[2]

This paper outlines briefly the general theory of mercury-binary cycle efficiency, how it works, and the more usual types of applications where it may be used. The use of the mercury-steam cycle as applied to topping plants is explained more completely with the relative capabilities of 140 psig mercury and 2300 psig steam for such service specifically compared. As a typical, as well as the most recent application of a mercury topping unit, the new 15,000-kw mercury-unit power-plant equipment recently installed at the South Meadow Station of the Hartford Electric Light Company is dealt with in considerable detail. In the manufacture of the mercury-boiler parts, factory prefabrication of relatively large mercury-furnace wall sections was successfully done for the first time. The new 15,000-kw mercury plant has been in operation since February 1, 1949, and for the month of February produced 20,000,000 kwhr of electric power at an average fuel rate of 10,200 Btu per net kwhr.

Cycle Efficiency

The efficiency of a vapor cycle is determined largely by the saturated-temperature range through which it operates—the greater the range, the higher the efficiency of the cycle. This may be expressed by the equation, efficiency

$$E = \frac{T_1 - T_2}{T_1}$$

when T_1 and T_2 represent the saturated-temperature range through which the cycle operates, in degrees absolute.

The mercury cycle, superimposed on a steam cycle, boosts the efficiency of the resulting cycle because of the high boiling temperature of the mercury. For example, at 140 psig, mercury boils at 975 F, whereas at 1250 psig, water boils at 575 F.

With 975 F mercury and a proper selection of steam and fuel conditions, thermal efficiencies of from 34 to 38 per cent can be attained.

How the Mercury-Steam Power Cycle Works

Fig. 1 shows a typical flow diagram of the mercury-steam cycle.

Heat from the burning fuel is absorbed by liquid mercury within the tubes of the mercury boiler to form mercury vapor, which passes from the boiler to the mercury turbine where it releases a portion of its energy to produce electric power. The vapor from the turbine is exhausted to the vacuum shell of the mercury-condenser boiler. There it condenses and releases its heat of vaporization to water within the tubes. The liquid mercury is returned from the sump, or hot well, to the boiler by a mercury feed pump, or by gravity, as the case may be.

The feedwater which absorbs heat from the condensing mercury vapor is boiled into steam at any desired pressure. This steam is then superheated in tubes located in gas passages of the mercury boiler. This superheated steam is then available for driving a steam turbine, or may be put to other desired uses.

It is of interest to note that the steam thus produced by the binary cycle is only slightly less in amount than it would be if the equivalent fuel were burned directly in a steam boiler.

Types of Application

A heat cycle or a power cycle upon which a higher-temperature heat cycle has been thermodynamically superposed may be said to have been topped. Hence a power plant composed of the higher-temperature cycle equipment may be known as a "topping plant." In reality, all power plants where binary cycles or superposed steam cycles are used, fall into the general class of topping applications. However, for the sake of simplicity, as well as for the purpose of easy identification, the types of applications for mercury-unit power plants have been divided into three general classes, i.e., topping plants, process or heating steam plants, and condensing plants.

A topping plant is one in which relatively high-pressure steam is desired, usually to be used in existing steam turbines.

A "process," or "heating steam plant" is one in which relatively low-pressure steam is required. If the steam is desired at a pressure below the minimum limit set for operation of the mercury-condenser boilers, it is then desirable to include a noncondensing steam turbine having its exhaust shell designed to exhaust the steam at a pressure suitable for the proposed application.

A "condensing plant" is one in which electric power only is produced. In this case, a condensing steam turbine of suitable size and design is included as a part of the mercury power plant.

The initial steam pressure and temperature for each of the three types of applications may be varied as dictated by existing steam conditions, or by the power-plant designer as he finds necessary in his effort to produce the most useful and economical over-all power plant.

Ratio of Mercury Topping Kilowatts to Steam Output

A by-product kilowatt produced from a high-temperature topping cycle is obtained at nearly the mechanical equivalent of the thermal energy.[3]

Because of boiler and other machine efficiencies, by-product kilowatt output, as such, requires the expenditure of approximately 4000 Btu per hr from the fuel, regardless of whether the topping kilowatthour is produced by a steam topping turbine or a mercury topping unit.

Another way of indicating this situation might be to say, that whenever a heat power plant or a portion of a heat power plant is credited with heat rejected, then the net heat consumption of the kilowatts generated in that portion of the power plant is equal to heat put in minus heat rejected to the next portion or system, divided by the kilowatts produced; and that this is usually in the neighborhood of 4000 Btu per kwhr.

Mercury topping plants as generally applied, will produce about twice as many 4000-Btu kw per 1000 lb of high-pressure steam as can be secured from other topping cycles. Furthermore, a mercury topping plant, designed originally to produce, say, 400-psig steam, may be used if desired to top 850-psig steam, or higher, merely by altering the size of the steam superheater and changing the steam safety valves, if allowance has been made in the design

[1] Construction Engineering Division, General Electric Company, Schenectady, N. Y. Mem. ASME.

[2] Superintendent of Power, Hartford Electric Light Company, Hartford, Conn. Mem. ASME.

Contributed by the Power Division and presented at the Spring Meeting, New London, Conn., May 2–4, 1949, of The American Society of Mechanical Engineers.

 Paper No. 49—S-17.

[3] "Mercury for the Generation of Light, Heat, and Power," by H. N. Hackett, Trans. ASME, vol. 64, 1942, pp. 647–656.

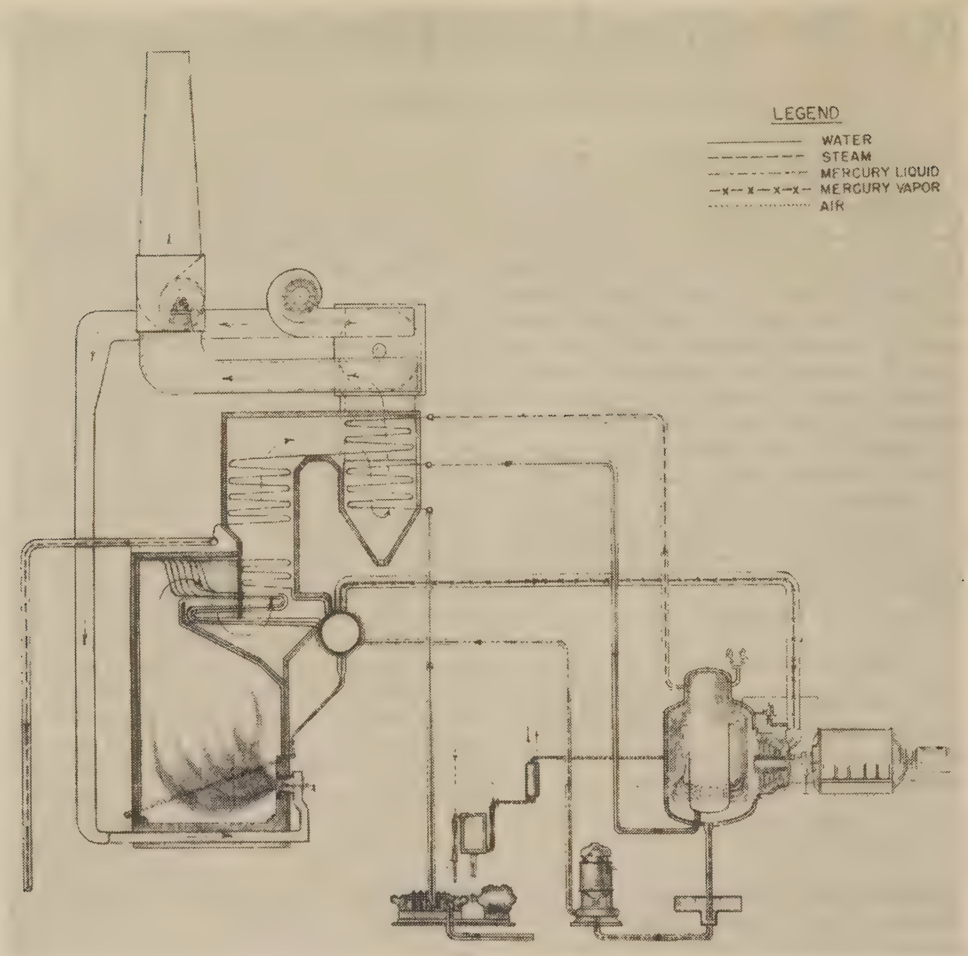

Fig. 1 Typical Flow Diagram of Mercury-Steam Cycle

for the stresses which will be encountered at the desired pressure.

Fig. 2 gives a clue as to why mercury-topping power ratios are so high. In this comparison, the total heat of the mercury vapor and its competitor, high-pressure steam, have been corrected to the same total heat as is contained in 1 lb of 2300-psia 1050-F total temperature steam, or to 1497 Btu. For this total heat, 9.7 lb of mercury vapor must flow through a mercury turbine for each pound of 2300-psia steam flowing through a 2300-psi steam turbine.

As a basis for comparing the topping capabilities of these two cycles, the upper curve is a plot of the available energy of approximately 9.7 lb of mercury vapor when used to produce topping steam at various pressures in the mercury-condenser boilers. The lower curve is a plot of the available energy of 1 lb of 2300-psia steam used in a turbine, exhausting at the indicated back pressures. The steam pressures thus indicated by the abscissa are the back pressures of the steam expansion from the 2300-psi noncondensing steam turbine, or the pressure of the steam made in the mercury-condenser boilers. In keeping with present design practices, a 30-deg F terminal difference between the condensing mercury vapor from the mercury-turbine exhaust, and the boiling water was taken into account when establishing the mercury-vapor available-energy figures.

It will be noted on the chart that at 400-psia steam pressure, the available-energy ratio of mercury to steam is 442/220, or almost exactly 2 to 1, and, at 1250 psia, the ratio is 320/87 or almost 3.7 to 1.

The fact that the available energy of mercury vapor varies only some 27.5 per cent when generating steam in the mercury-condenser boilers at pressures varying from 400 psig to 1250 psig, makes it possible to design standard mercury units for wide ranges of by-product-steam pressures with a relatively small change in mercury-turbine output.

Over the same back-pressure range, the available energy of a 2300-psig noncondensing topping turbine varies about 60 per cent.

Further, the mercury power plant may be used effectively operating in conjunction with 850-psig or even 1250-psig steam turbines to increase greatly the over-all plant capacity and efficiency.

A steam-turbine plant capacity may be increased some 60 per cent for the same quantity of condensing water by mercury topping. For example, the new Schiller Station at Portsmouth includes a 25,000-kw steam turbine which, in effect, is topped with 15,000 kw of mercury capacity. For the 40,000 kw total capacity, only 25,000 kw are affected by the usual condenser losses. This saving in condenser-cooling-water requirements may become very important in localities where cooling water is scarce, although this was not the case at Portsmouth.

Mercury Topping at South Meadow

The South Meadow Station of the Hartford Electric Light Company was the first steam-generating plant to use a mercury-vapor cycle to top existing steam-generating units as a commercial undertaking. This original 10,000-kw mercury topping plant was

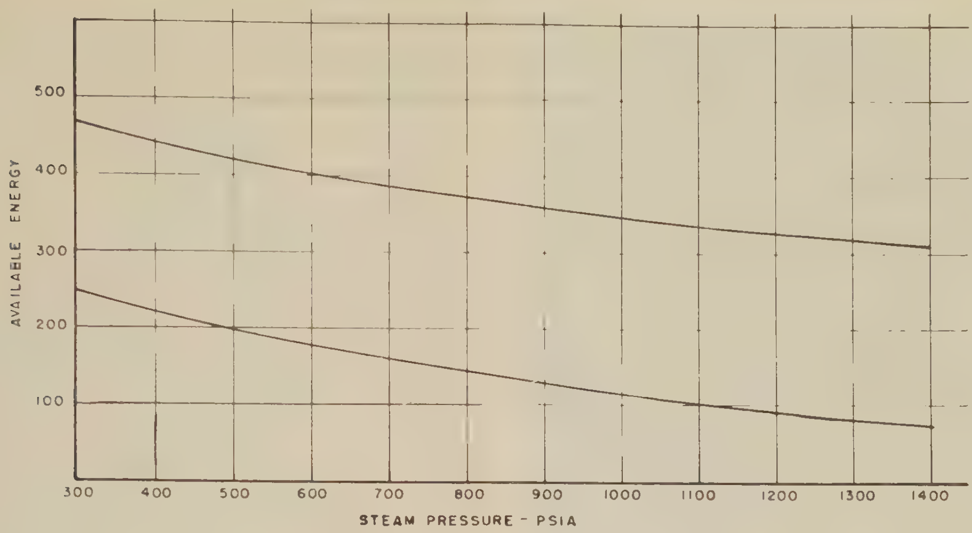

FIG. 2 AVAILABLE-ENERGY CURVES FOR MERCURY VAPOR AND STEAM

(The available energy of 155 psia 975 F total temperature mercury vapor and 2300 psia 1050 F total temperature steam have been corrected to the same total initial heat of 1497.1 Btu. The curves are then plotted with actual available energy of the two corrected fluids as the ordinate with the abscissa representing the back pressure of steam expansion of a 2300-psia noncondensing steam turbine, or the steam pressure generated in the mercury-condenser boilers. The mercury-turbine exhaust pressure has been corrected to include a designed drop of 30 deg F terminal difference in the mercury-condenser boilers.)

put into service in 1928, superposed on 250-psig 700 F total temperature steam-generating equipment installed in 1921. The design margin in the steam portion of this first mercury installation was ample to permit the raising of its operating pressure to 400 psig 700 F total temperature early in the 1930's simply by changing the safety valves.

In the 19 years between 1928 and 1947 this first commercial mercury topping plant operated on line for some 119,000 hr, producing a net output of more than 1.7 billion kwhr of electric power.

It was evident prior to 1946 that the original installation, constructed from materials available in 1927, was coming to the end of its economical life owing to the metal fatigue at the associated high operating temperatures. The Hartford Electric Light Company made an economic study of the value of a 50 per cent larger-capacity unit in the same building with the result that it was decided later in 1946, to proceed with active engineering of a modern replacement for the 1928 unit and its associated equipment.

The removal of the old equipment was started in the summer of 1947, to make the building area available for the installation of an entirely new design of mercury plant having a capacity at full load of 15,000 kw, and a steam output from the condenser boilers of 210,000 lb per hr at 400 psig 700 F total temperature.

NEW 15,000-KW MERCURY-UNIT POWER-PLANT EQUIPMENT

The mercury-unit power-plant equipment now in operation is entirely new except for the condenser-boiler steam drums and vacuum shells, the mercury-turbine generator, and a portion of the mercury-turbine exhaust shell. In order to assure reliable operation of the condenser boilers, new steam-generating tubes with water circulators were installed. Because of the ample size of the 10,000-kw generator stator frame and rotor, these parts were rewound to give maximum output of 15,000 kw at unity power factor.

Most of the existing building steel, as well as certain of the old boiler supporting members, were usable with the new equipment. However, as might be expected, the major portion of the equipment structural supports had to be replaced to meet the new design conditions.

Fig. 3 shows a schematic arrangement of the main equipment as it is now installed in the South Meadow Station.

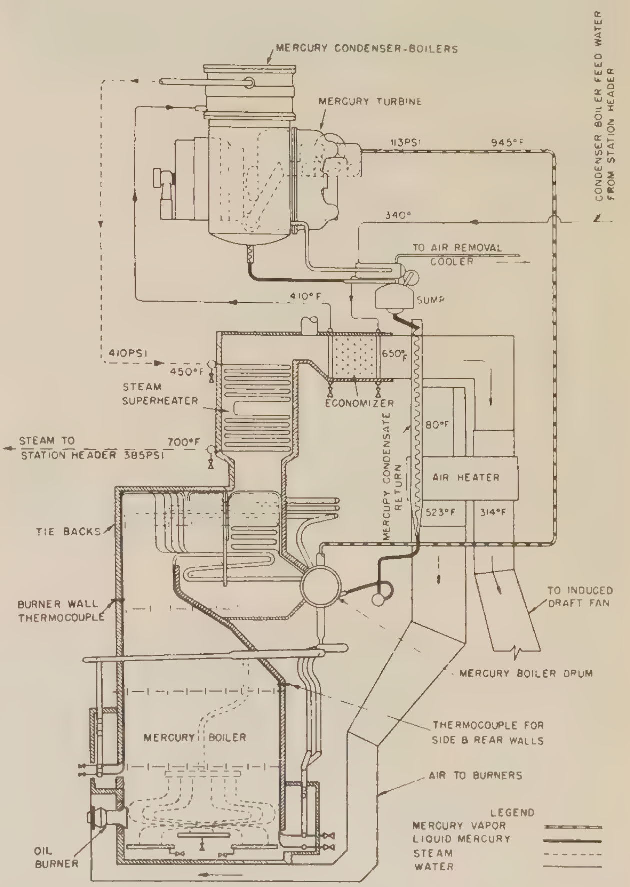

FIG. 3 SCHEMATIC ARRANGEMENT OF 15,000-KW MERCURY-UNIT POWER PLANT AT SOUTH MEADOW STATION

The oil-fired mercury boiler is of the latest design, having completely mercury-cooled furnace, slag screen, and mercury fog-convection surfaces. The steam superheater, water economizer,

and regenerative-type air preheater are of conventional design, as are the forced and induced-draft fans.

Mercury vapor is generated within the tubes of the mercury boiler at a pressure of 130 psig and at a saturated temperature of 964 F. The mercury vapor thus produced flows upward through four 12-in. vapor pipes to the five-stage single-flow mercury turbine located in the turbine room above the mercury boiler. Suitable mercury stop and throttle valves are attached directly to the mercury-turbine high-pressure shell for controlling the mercury-vapor flow to the turbine. Likewise, two 14-in. mercury-boiler relief valves are mounted out from the inlet end of the turbine stop valve to protect the mercury boiler from overpressure. When operating, these two relief valves discharge into the condenser-boiler vacuum shell where the energy from the overpressure mercury vapor is absorbed to produce steam which may then be used by the steam-turbine units, or exhausted to atmosphere through the condenser-boiler steam safety valves, depending upon the station load conditions.

The mercury turbine exhausts into two vertical-type side-mounted mercury-condenser boilers at an exhaust pressure of 1.5 psia 480 F. In condensing, the exhaust mercury vapor releases its heat of vaporization to water within the tubes of the condenser boilers to produce steam at 410 psig. The condensed mercury liquid then flows by gravity through a cleaning sump and suitable piping system to the mercury boiler where it is again evaporated at 130 psig.

The steam generated in the condenser-boiler tubes is superheated by the boiler flue gases to 700 F total temperature in the steam superheater mounted directly above the mercury boiler. The steam thus superheated is piped to the 385-psig station steam header for use in the 385-psig steam turbines.

When desired, steam may be generated for use with the 250-psig steam turbines. No equipment alterations are necessary as the change-over may be made from one station steam pressure to the other merely by valving the steam superheater-outlet pipe to the desired steam header.

The condenser-boiler feedwater is taken from the station feedwater header at 340 F, pumped through the cooling coils of the primary air-removal cooler and into the water economizer, where it is heated by the boiler flue gases to 410 F. The heated feedwater then flows into the condenser-boiler steam drums where it is boiled into steam by the condensing mercury vapor.

In order to assure satisfactory over-all power-plant combustion efficiency, a large regenerative-type air preheater heats the air used for combustion from 80 F to 523 F. The resulting exit-gas temperature with 15 per cent excess air leaving the furnace is expected to be 300 F, when corrected for air leakage through the air preheater.

Mercury Boiler

A mercury-furnace tube operated with properly treated mercury is capable of pumping large quantities of liquid mercury and vapor through long flow circuits located considerably above the liquid level in the boiler drum. This action is produced by the relatively high pumping head of the down-flowing liquid column supplying the lower feed headers of the furnace tubes, as well as from the proportionately high available energy in the expanding mercury vapor as it flows upward through the boiler tube. The release of energy is brought about by the large change in pressure throughout the tube from where boiling first occurs in the lower portion of the furnace to where the tube enters the boiler drum at operating pressure. In a very high boiler this pressure head may be 100 psi or more.

As heat is applied to the boiler tube, generating more and more vapor, the theoretical density of the flowing mixture may change from solid liquid, weighing approximately 778 lb per cu ft, to a lean mixture having a weight of approximately 2.5 lb per cu ft, before decrease in heat-absorbing ability of the tube occurs. In actual mercury-boiler designs, such as the 15,000-kw Hartford boiler, the mixture discharging into the boiler drum from the fog-convection tubes is designed to be in the order of 13 lb per cu ft for the heaviest loaded circuit. Such a mixture contains approximately 1 lb of vapor for each 7 lb of liquid mercury circulated, or may be said to have a circulation ratio of 7:1.

The economic advantage of such circuit design is immediately apparent as great savings in total boiler mercury are possible, since it is only necessary to fill the furnace tubes with mercury to a minimum depth with no liquid mercury in the fog-convection portions of the circuits at starting. The liquid portions of the tubes can be of small internal diameter while the fog section tubes may be much larger.

A mercury boiler usually requires some 70 to 80 per cent of the total heat-absorbing surface in the convection regions, and if it were necessary to use all liquid-filled tubes, the quantities of mercury required might be prohibitive. This theory of mercury-boiler design was first used successfully in 1940 in the 20,000-kw mercury boiler at Kearny where many of the fog circuits are some 250 ft long from end to end with approximately 40 ft of the furnace portion of the tubes liquid-filled at starting.[3,4]

These simplifications and economies are possible because the titanium-magnesium-treated mercury in the boiler circuits produces intimate and perfect contact between the metal of the tubes and the flowing mercury. The treated mercury has lost its spheroidal properties and spreads in a tenacious film over the inside walls of the tubes, forming a "wetted" surface from which evaporation of the mercury occurs.[3]

The tenacity of the wetted film is such that it is not destroyed when superheated upward to 200 F above the temperature of the saturated-vapor-liquid mixture flowing in the circuit, as long as treated mercury is supplied to the heated film as rapidly as evaporation occurs. By maintaining suitable velocities of the flowing mixture in the tubes, the required "make-up" supply of mercury droplets is available over the extremely wide range from solid mercury liquid to the approximately low density of a 1.2 parts by weight of liquid mercury to 1 part vapor.

The extensive use of mercury-fog-convection surface throughout the entire boiler reduces the maximum pressure at any point in the tube circuit, which subsequently reduces the boiling temperature of the mercury and the metal temperature of the tube steel. This allows added protection against oxidation of the tube metal on the fire side of the tubes, as well as increases the allowable working stress of the material.

Our standard-design, mercury-unit-power-plant mercury boilers, of which the 15,000-kw Hartford unit and the three 7500-kw units for Pittsfield and for the Schiller Station are typical examples, all utilize the well-proved principle of fog-circuit design.

The Hartford Mercury Boiler

Fig. 4 is a cross section of the Hartford boiler. The flow of mercury in the various boiler circuits is simple and direct. The operating liquid level is maintained at or near the inside bottom of the boiler drum. With the boiler in operation, the fluid mercury flows from the drum downward through suitable downcomer supply pipes to the various lower headers, and then upward to the drum, as required, to provide coolant for the furnace tubes and fog-convection circuits.

Owing to the simplicity of the mercury-boiler design, only four basic types of tube-flow circuits were required.

The tubes covering the two furnace side walls are simple

[4] "The Mercury-Vapor Process," by A. R. Smith and E. S. Thompson, October, 1942.

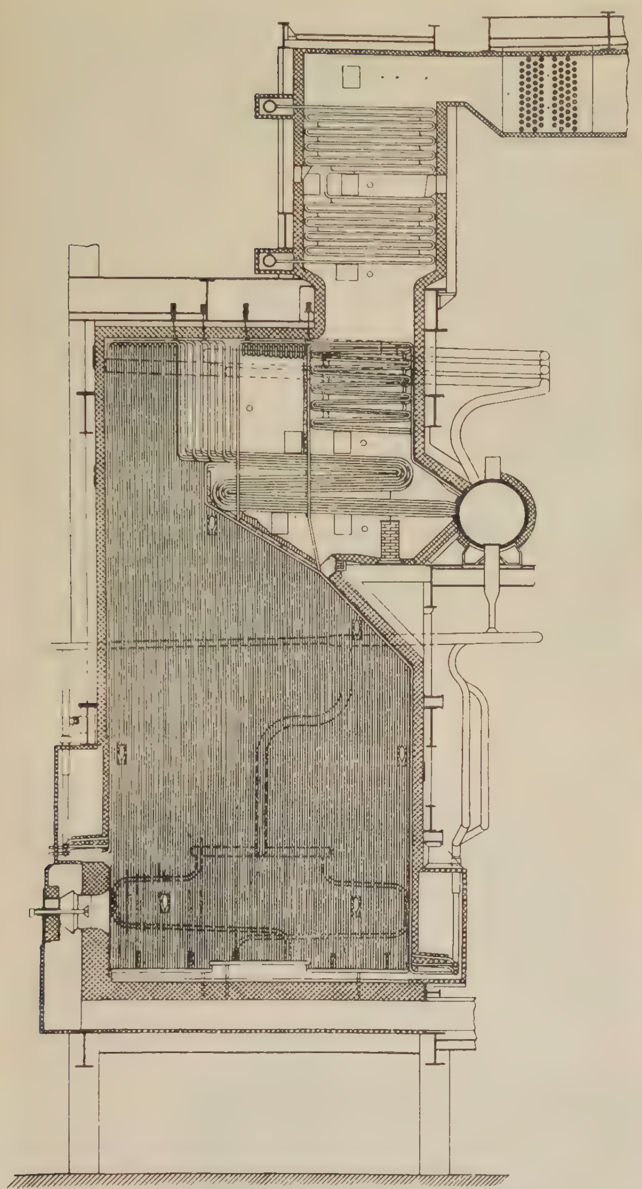

FIG. 4 CROSS SECTION OF 15,000-KW MERCURY BOILER
(Portion of furnace tubes, downflow slag screen, fog-convection tubes, drum and downcomer supply system, as well as steam superheater and water economizer are shown.)

straight-through elements receiving mercury from bottom headers and discharging into vapor headers at the top. Each of the six vapor headers connects to the mercury-boiler drum through a vapor discharge pipe. The side-wall furnace tubes are $1^1/_2$ in. OD $\times$ $^7/_8$ in. ID for the lower 16 ft and are 1 in. ID for the remaining 30 ft of their length.

The burner-wall or front-wall tubes supply mercury to the roof section of the furnace vestibule, the vertical downflow slag-screen tubes, the first and second passes of the horizontal fog-convection tubes, and finally discharge into the drum. These tube circuits are stepped in size from $^7/_8$ in. ID, where they leave the lower headers, to $2^1/_8$ in. OD $\times$ $1^3/_4$ in. ID, where they form the first-pass fog bank.

The rear-wall furnace tubes also form the sloping roof section under the fog-bank assemblies. A number of the roof tubes are directed upward and function as the two mercury-cooled supports for the fog circuits. These tubes then continue on to form the

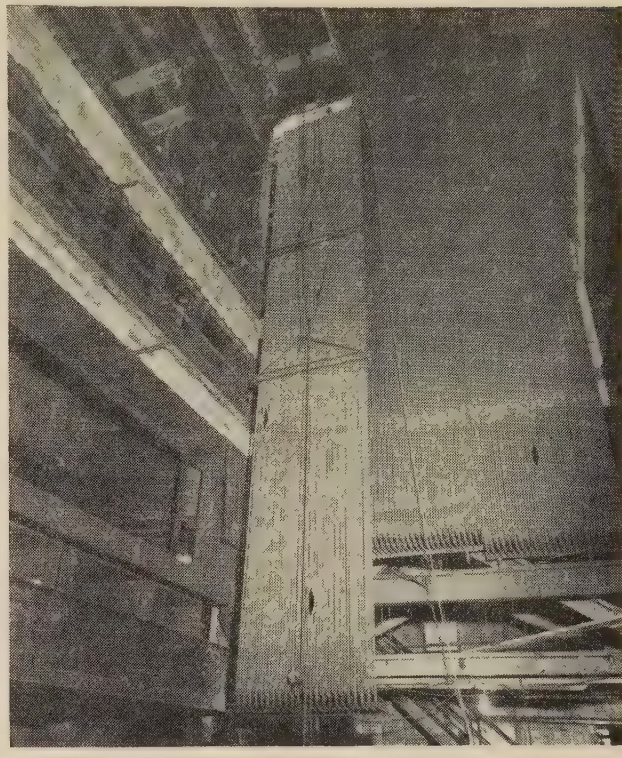

FIG. 5 15,000-KW MERCURY FURNACE SIDE-WALL ASSEMBLY BEING HOISTED INTO POSITION
(Showing sections already in place, a third section being hoisted into position to complete east furnace wall.)

third-pass fog circuits. The remainder of the roof tubes protect the nose of the furnace arch and then turn back and become a portion of the first and second-pass fog banks. The tube sizes vary from $1^1/_2$ in. OD $\times$ $^7/_8$ in. ID at the bottom to $2^1/_2$ in. $\times$ $1^3/_4$ in. where they form the fog circuits.

In an effort to reduce over-all costs as well as to reduce the time required to complete field assembly of the boiler units, factory fabrication of the furnace tubes with their liquid and vapor headers was tried for the first time. Fig. 5 shows one of the furnace-side-wall subassemblies of which there is a total of six, three for each side wall. These are approximately 7 ft wide $\times$ 46 ft long. Some 47 tubes are completely assembled with their upper and lower headers, tiebacks, and supports ready for placing in position in the boiler-supporting steel. Similar but small subassemblies of the front and rear-wall tubes likewise were made at the factory and shipped ready for field erection. The fog tubes, slag-screen tubes, and the upper portions of the front and rear-wall tubes were handled as individual pieces in the field. However, the apparent savings in erection time and over-all cost seemed to be sufficient to warrant further development of factory prefabrication of mercury-boiler parts. Therefore similar but more complete subassemblies were manufactured for the three 7500-kw units now in the process of being erected.

Fig. 6 shows the upper portion of the completed Hartford furnace.

Fig. 7 shows the six horizontally mounted fuel-oil burners. These six burners are mounted under the front-wall tube headers near the bottom of the refractory furnace bottom.

MERCURY-BOILER DESIGN AND MANUFACTURE

The three 7500-kw boilers for Pittsfield and the Schiller Station are of identical design and are being manufactured by the Babcock & Wilcox Company from identical blueprints. The Hart-

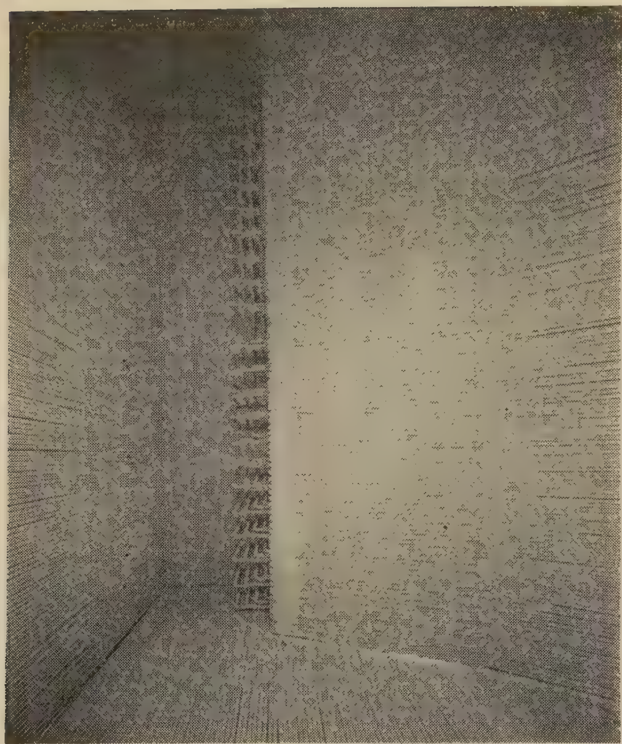

Fig. 6 View Taken From Inside Completed Furnace of the 15,000-Kw Mercury Boiler, South Meadow

(View shows upper portion of furnace walls, sloping arch and furnace roof. Downflow screen tubes are also shown above sloping roof sections.)

ford boiler, manufactured and installed by the Foster-Wheeler Corporation, differs somewhat from the 7500-kw boilers in that it was designed with a flat refractory-covered furnace floor for burning fuel oil only. The 7500-kw units have dry-ash mercury-cooled hopper-bottom furnaces for burning pulverized coal or fuel oil as desired.

Mercury-Turbine Generator

Fig. 8 shows the 10,000-kw Hartford turbine after 16 years' operation. This simple single-flow 720-rpm, five-stage turbine has run more than 116,000 hr since its last internal inspection. When finally dismantled in 1947 for replacement, the machine internals were found to be in unbelievably good condition for a unit that had operated without internal maintenance for such a period of time.

However, because of the design conditions at 15,000-kw output, requiring the use of higher pressure and temperature, it was necessary to replace the old mercury turbine completely, using the latest in materials and machine design. The new machine followed the general pattern of the original unit but included all of the modern improvements, such as mercury-sealed shaft seals, and vanadium-molybdenum alloy castings for the high-pressure turbine head, turbine control, and stop valves, and for the mercury-boiler relief valves. A complete new turbine-rotor assembly, having separately mounted split diaphragms, was provided. A new main bearing, incorporating a double-thrust-type thrust bearing, was also necessary. Because the unit was to be operated as a base-load machine, no speed governor was installed. Two emergency trips were provided, one on the hand-operated control valve, and one on the turbine stop valve.

Fig. 9 is a view of the mercury turbine with the four split diaphragms in place and the high-pressure head removed. The two wing-back-mounted condenser boilers have been placed in position ready for making the two large turbine-exhaust-shell welds.

Fig. 10 is a view of the exhaust opening of the east condenser boiler, showing the porcupine-type tube bundle.

Fig. 11 shows the completed assembly of the mercury turbine, condenser boilers, control and stop valves, and the mercury-boiler relief valves.

Hartford Electric Light Company Operating Experience

Previous Designs. The Hartford Electric Light Company operating experience with the mercury cycle for power generation covers the period beginning in 1923 up to the present date.

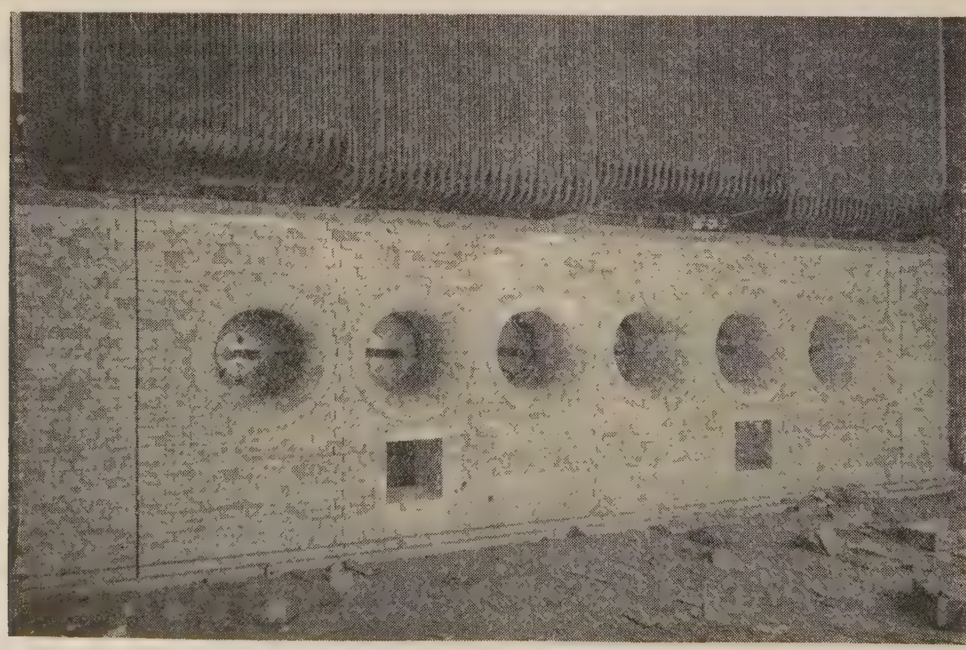

Fig. 7 Six Horizontally Mounted Fuel-Oil Burners

(Lower end of front-wall furnace tubes, refractory burner wall, and refractory furnace bottom are shown.)

Fig. 8 10,000-Kw Mercury Turbine Being Dismantled in 1947 After 16 Years of Operation in South Meadow Station

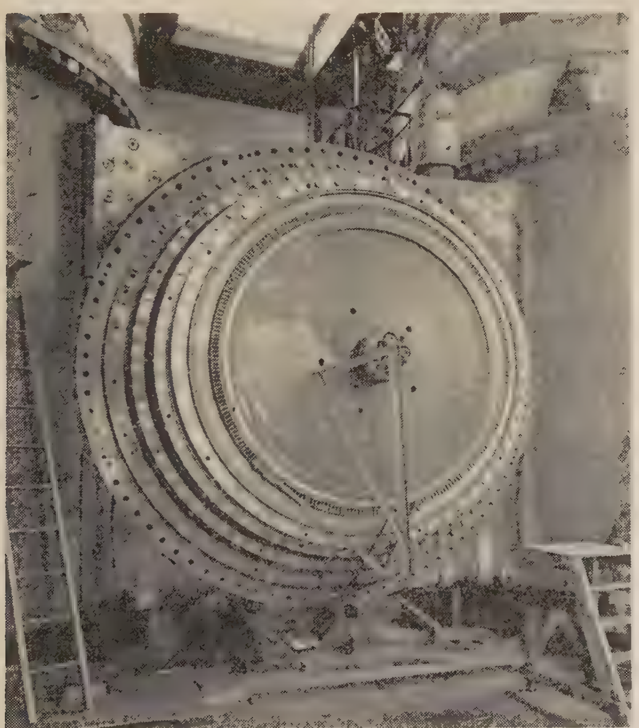

Fig. 9 15,000-Kw Mercury Turbine Being Assembled in 1948, South Meadow Station

(View shows portion of original 10,000-kw turbine-exhaust shell, original but newly retubed condenser boilers, and partial assembly of new wheels and new built-up diaphragms. Split interstage diaphragms were used in new machine rather than the old shell-supported solid-disk type shown in Fig. 8)

During the first 4 years it was a joint venture with the General Electric Company for the purpose of developing a design that would meet all the requirements of a central station from the

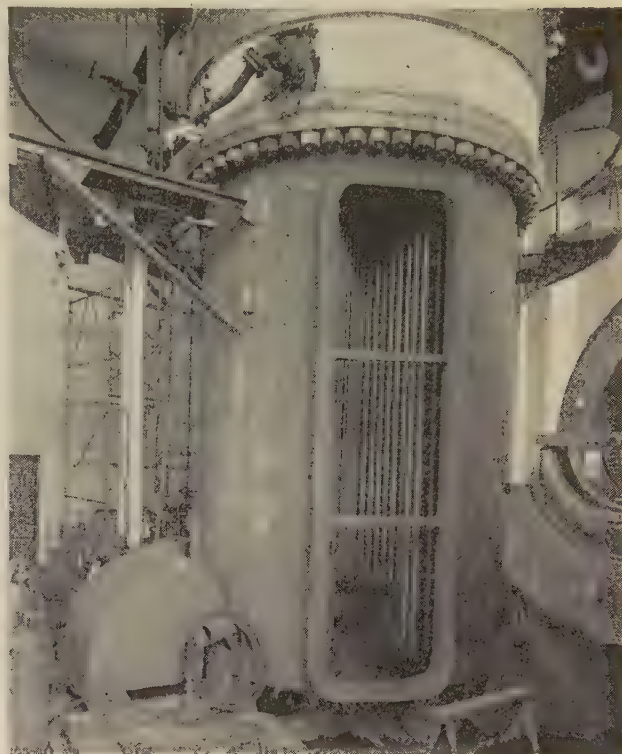

Fig. 10 Mercury-Condenser Boiler Showing Portion of Porcupine-Type Tube Bundle and Opening for Attaching to Mercury Turbine-Exhaust Shell

(Downflow water circulators were installed in each steam-generating tube to improve circulation.)

point of flexibility, dependability, and economy. This first topping unit was installed in the Hartford Electric Light Company's Dutch Point plant and consisted of a 1500-kw generator, driven by a mercury-vapor turbine exhausting to a condenser-boiler operated at 200 psig and 540 F total temperature, the conditions of the main steam header in the plant. Five entirely different designs of boilers were covered in this experience cycle.

In 1927 a 10,000-kw mercury-vapor unit was contracted for as a plant extension at the South Meadow Plant to top an existing 250-psig, 700 F total temperature steam unit installed in 1921. This design was proved by the Dutch Point experience but in the larger size developed several faults. Consequently it was 1932 before all defects had been eliminated and the plant could be considered as dependable central-station equipment.

From 1932, until its removal in 1947, the 10,000-kw South Meadow unit operation was quite satisfactory even though it was necessary to reduce top operating load progressively as metal fatigue progressed. By thus reducing load, and consequently stresses, we were enabled to produce the results given in the first section of this paper at an over-all plant availability in excess of 85 per cent. This availability includes outage time for steam-cycle equipment as well as that for the mercury cycle.

Operation of 10,000-Kw Unit. Operation of this 10,000-kw unit was extremely simple: Liquid mercury was returned by gravity to the boiler; there was no treatment of the liquid-mercury charge; no treating of the boiler feedwater was required; there was no complicated feed-heating cycle, and the pressures were low.

Mercury replacement, due to all losses, was low, averaging less than 2000 lb per year from all causes both avoidable and unavoidable.

Maintenance was variable. General maintenance was usual for

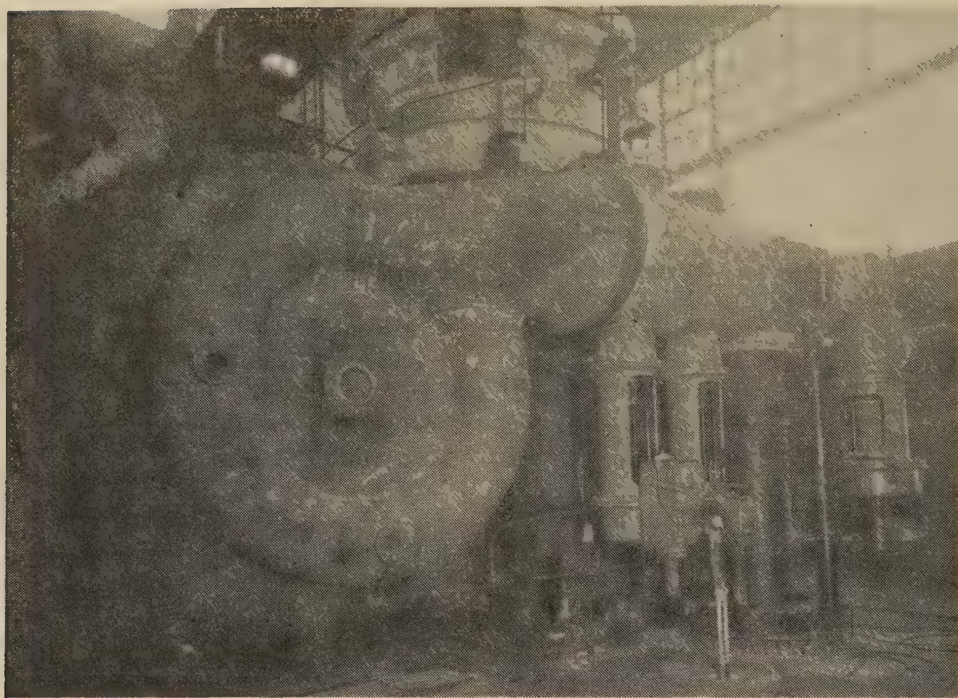

Fig. 11 Assembly of 15,000-Kw Mercury Turbine, South Meadow Station

(High-pressure shell control and stop-valve assembly with 26-in. mercury-vapor inlet pipe entering bottom of stop-valve casing. One of two 14-in. mercury-boiler relief valves with their 18-in. vapor-relief pipe is shown attached beyond vapor-inlet pipe. Boiler relief valves discharge their vapor, when operating, into west condenser boiler.)

TABLE 1 15,000-KW SOUTH MEADOW MERCURY UNIT[a]

Oil burned, lb	12,281,169
Steam generated at 260 psig and 700 FTT, lb	126,118,000
Gross output from vapor-driven generator, kwhr	10,048,000
Gross generated from steam, kwhr	11,387,000
Total auxiliary usage, kwhr	565,000
Net total unit output, kwhr	20,870,000
Fuel rate, lb oil/net kwhr	0.588
Heat rate, Btu/net kwhr	10,200

[a] Twenty-eight consecutive days' operation at full load.

all associated equipment and there was no maintenance on the mercury turbine from 1931 until it was dismantled in 1947. The mercury boiler required a major internal cleaning approximately once a year using acid, and external cleaning at the same intervals as a steam boiler. As a general statement, it should be said that average maintenance costs for this unit were slightly in excess of those for a comparable steam unit.

New 15,000-Kw Mercury Plant at South Meadow

While construction work had not been completed it had progressed to such a point that it was possible to light the first fire under the boiler on January 2, 1949. Preliminary operation consisting of boiling out, trying out all associated apparatus, and making indicated changes and adjustments had been completed by January 8, and the mercury-vapor-driven generator was phased in on the line. By February 1 construction work had been completed, the changes indicated by the first two runs had been made, and the unit phased for service the third time. The plant had been accepted for service with this third start and the results of this operating period are shown in Table 1.

All quantities shown in Table 1 are actual net figures, as all charges have been made to the mercury plant occurring from associated auxiliary equipment whether it is a part of the mercury plant directly or a part of the steam-turbine unit using the steam from the condenser boilers.

Shutdown of the unit at the end of 28 days of operation at full load was caused by a partial stoppage in the regenerative air heater. Thorough inspection, during this shutdown, indicated that all parts of the mercury cycle were in as good condition as at time of the start-up.

Conclusion

From the Hartford Electric Light Company's experience to date, no serious difficulty is anticipated with any part of the equipment covered by the new design. The plant forces are adequate to handle all phases of the new problems introduced by the necessary chemical treatment, the special metals used in fabrication, and the novel instrumentation.

The operating economies have been proved, and the design demonstrated as generally adequate.

Acknowledgment

In the Hartford boiler, and also the three 7500-kw units, the basic boiler design, the treatment of the boiler mercury, and the design and size of the boiler flow circuits is by General Electric Company. However, such problems as structural supports, fuel burning, and over-all boiler performance, as well as actual detail designs, manufacturing, and erection of the complete boiler units could best be done by the boiler manufacturers. Joint responsibility was shared by the General Electric Company and the boiler companies with regard to the materials used in the tubes and other pressure parts.

This broad division of responsibility has offered no problems whatsoever of customer relations between either the General Electric Company as principal contractor and the boiler companies or operating companies in carrying out the several projects now under way. The relationship has been most cordial and all parties concerned have spared no efforts in promoting vigorously their various portions of the work. We particularly wish to congratulate at this time those of the Foster-Wheeler Corporation who have worked with such diligence and painstaking care in making the Hartford boiler such an outstanding success.

Discussion

William Kowalsky.[5] Another step toward widespread commercial acceptance of the mercury-vapor steam cycle for power generation has been taken with the successful completion of the mercury power unit at the South Meadow Station of the Hartford Electric Light Company. The heat-rate data given in Table 1 of this paper will be a criterion against which other utilities may check their own plant performances.

For the writer's company, the work of planning, fabricating, and erecting the mercury boiler was an unusual and valuable experience. Each stage of development of the mercury boiler was preceded by exhaustive tests and investigations. No material or procedure was adopted until tried and proved. (It should be emphasized that this approach was used by General Electric Company from the very beginning of its experiments with the mercury-vapor process back in 1912. This step-by-step development can be pointed out as a classic example of the solution of an engineering problem in which there was no previous experience and where every item involved unknown elements.)

From a metallurgical standpoint, there were commercial alloys available for the furnace tubing which could withstand the 1100 F metal temperature and the 1000 F mercury temperature, but fabricating methods, welding, heat-treating, and stress-relieving procedures had to be developed. The difference between shop- and field-welding procedures had to be investigated. With the operating-temperature range mentioned, creep strength limited the design stresses, and considerable stress-analysis work was done to insure that the low permissible stresses were not exceeded. The boiler was designed to meet the requirements of the ASME Boiler Code in so far as possible.

Due to high metal temperature, it was necessary to select materials with high resistance to oxidation. High-silicon steels were selected. It is estimated that these superior materials give the mercury boiler the same economic life as a modern steam generator. The tube material for all of the furnace, slag screen, first-pass convection tubes, and eighteen rows of second-pass convection tubes, corresponded to SA-213-T13. The upper bank of second-pass convection tubes had a composition very similar to SA-213-T21. The mercury drum, downcomer system, upper and lower headers, conformed to SA-213-T12. Thus expensive alloys were used only where needed, as dictated by boiler conditions. Tube supports, fixed ties, and tie-back supports, when exposed to furnace or boiler temperatures, were normally of 25-20 alloy composition. The SA-213-T13 tubing (4 to 6 chrome, $^1/_2$ moly, 1 to 2 silicon) was welded by the atomic-hydrogen method, using a bare rod of the same composition as the tubing. The SA-213-T21 (2.75 to 3.25 chrome, 1 moly alloy) tubing was welded by electric arc with a 2 chrome 1 moly coated rod. The SA-213-T12 tubing (chrome-stabilized carbon-moly) was welded by electric arc with a $^1/_2$ chrome $^1/_2$ moly coated rod. Backing rings for all welded joints were of the integral type, machined right on the tube to form the male end, with a standard bevel machined in the matching tube for the female end. All welds in which SA-213-T13 material was involved, were ground and magnafluxed. Only random welds of the other compositions were ground and magnafluxed. A proof of the welding quality of the total volume under pressure or vacuum can be seen in the extremely low air leakage into the system.

The superheater is of the continuous-tube type of carbon-steel material. Because the superheater occupies the tail position in the boiler, and because of the variable mercury-pressure operation, the superheat characteristic drops very sharply as the load decreases. To get the maximum performance of the steam end at fractional loads, a group of parallel dampers have been installed to by-pass the upper second-pass convection surface, and thereby increase the heat available for steam superheating.

In order to save time and expense in the field, and in order to accomplish as much of the welding as possible under shop conditions, the mercury-cooled walls were assembled in fourteen sections in the shop. The elements were fabricated, welded into the headers, and then stress-relieved as complete units. This was the first time a boiler had been shipped in such large flexible prefabricated assemblies. Necessarily, this procedure involved solving numerous problems, such as handling methods, assembly jigs, railroad clearances, erection clearances in the building, and so on.

The mercury boiler is supported across the front and rear at the level of the bottom of the mercury drum and is allowed to expand up and down from that point. The side walls are supported at the top of the furnace. Vertical expansions are of the order of 3 in. and require provision for flexibility in connecting downcomer piping to the riser side, a problem which was complicated by the much colder mercury on the downcomer side. Tie-backs are spaced at approximately 10-ft intervals and arranged for each tube to move laterally and vertically, independently of its neighboring tube.

During the initial start-up of the mercury boiler, when all concerned were crossing fingers, praying to the "gods of kilowatts," and trying hard to look unconcerned (even though we knew that every care and precaution possible had been taken), it was a source of wonderment to the writer to find how correctly the General Electric Company designers had predicted the behavior of this mercury boiler. When circulation of mercury was still erratic and efforts to induce some kick-over of hot mercury into the drum and downcomer system to try to equalize temperatures and expansions were being made, the prediction was offered that, starting at 4000 kw output, there would be some audible thumping of slugs of mercury in the vapor tubing, and that this would quiet down at 6500 kw. It worked exactly as predicted. We knew that untreated mercury did not "wet" the inside tube surfaces and that this caused erratic heat-transfer rates. We also knew that mercury with small amounts of magnesium and titanium did wet the inside tube surfaces and allow a uniform heat flow into the mercury. Nevertheless, we had to rub our eyes when we actually saw this happen. When circulation was established, our thermocouple readings indicated wide variations in first-pass convection-tube temperatures. Within a few minutes after the treating chemicals had been injected into the mercury feed lines, the temperature of these tubes dropped approximately 100 deg F, and all reached a more-or-less uniform level. It was obvious that the heat-transfer rates had suddenly become dependable.

The early mercury-boiler designs were complicated, but now it is just like any steam generator in appearance, both from the outside and from the inside of the furnace. The low position of the mercury drum with relation to the top of the furnace tubes strikes one as unorthodox at first glance; moreover, there is no level of mercury in the drum, a condition in which steam boilers are shut down promptly. The unit is specially developed and designed to run on minimum mercury content, which is possible because of the ability of mercury vapor to entrain substantial amounts of mercury mist or fog of tremendous cooling effect. It is necessary of course to supply a liquid mercury fog to the upper tubes to keep the film of mercury, which coats the inside tube surfaces, supplied with chemically treated mercury to replace that which has been evaporated. Provided reasonable mixture velocities are maintained, there is no limitation in size or shape of the tube circuits. The length of the tube circuit could be considerable, depending on the available mercury-circulating head and heat input. As long as treated liquid mercury mist is carried by the vapor, there can be no overheating of the tubes.

[5] Project Engineer, Foster-Wheeler Corporation, New York, N. Y.

The Hartford mercury boiler was not built as another experimental attempt to improve the Emmet mercury-vapor process. It is just another boiler built on a purely commercial basis of sound economics, because the practicability of the system has been proved before.

H. Weisberg.[6] At the Kearny Station, Public Service of N. J., there is installed a 20,000-kw superposed mercury-turbine generator which has been in operation since 1933. The combined mercury-steam capacity is 45,000 kw. For the first 6 years this unit was in service 51 per cent of the time, and generated over 750,000,000 kwhr; the average output being 32,000 kw.

In 1940 the boiler was replaced with a more modern design, somewhat similar to the new Hartford boiler. In the 9 years since then, the unit has been in service 72 per cent of the time. It has generated over 2,100,000,000 kwhr, and has had an average output of 38,000 kw. The total generation for both installations has been about 3,000,000,000 kwhr.

At the present time the unit is in regular operation on the system at loads up to full rated capacity. Early next year rather extensive repairs are planned to the furnace tubes owing to wastage on the gas side. Also, the vapor piping and control valves, which are plain-carbon steel and operate at 970 F, will be replaced with alloy-steel parts. It is expected that as a result of this work, along with other improvements which have been made in recent years, the availability of the unit will approach that of steam units, which is better than 90 per cent.

The heat rate of the unit, combined with 1925 design, 355-psi, 725-F steam capacity, compares favorably with the most efficient steam units which we are installing today, and as a result, with the inflation that has taken place since 1933, the value of the unit on the system is about double the original cost.

We are often asked whether we would install another mercury unit, or why we are not installing mercury units now rather than steam. The answer is that the availability up to the present time has not been as good as that of steam. It is our belief that the troubles we have had are not inherent in the mercury cycle and have been overcome by operating experience and development. With the present state of development, however, it seems inadvisable to build mercury boilers in capacities of 125,000 to 150,000 kw, which size steam units can be utilized safely on a system as large as that of the Public Service. This results in considerable disadvantage in the first cost of mercury units when compared with steam.

The mercury cycle when combined with modern steam capacity is more efficient than any steam cycle currently practicable, and therefore it is attractive where fuel costs are high and a unit not over 45,000 kw combined capacity is needed. Larger units would require two boilers and would be less economical. For superposition in sizes not over 20,000 to 30,000 kw, the mercury cycle is even more advantageous. Here again, if any of the Public Service units were to be superposed now, considerably larger units could be considered, and the mercury cycle would be at a disadvantage compared to steam. For these reasons we have not been able to justify additional mercury capacity on recent installations.

Summing up, 16 years of experience with the mercury cycle indicated definite and continuing progress. Additional installations appear to be justified at this time in limited sizes and for special applications.

O. L. Wood.[7] There are many interesting details of the new mercury installation at Hartford which might be used to supplement the comprehensive paper presented by the authors. The writer, however, will discuss only some of the phases of installing the new equipment, which is of 50 per cent greater capacity and operating pressure, within the space occupied by the original unit.

The original operating boiler pressure of 85 psig 908 F saturation was increased on the new unit to 130 psig 964 F. This was done, as explained in the paper to obtain (1) greater cycle efficiency by having the total heat available at a higher initial temperature, and (2) more available energy per pound of vapor.

The increase in capacity, requested by The Hartford Electric Light Company, was based upon its studies of a replacement and the real economies obtained on the original unit.

A new mercury-boiler design had been developed based upon considerable investigation of comparable steam-boiler experience. It required fewer types of circuits and bends, reducing circulation studies and manufacturing costs. This design fitted nicely between the main building columns at South Meadow. A 29-ft width and $20^1/_2$-ft depth of furnace were obtained to give the low heat-liberation rate of 18,150 Btu per cu ft at full load. Since the vertical cross section of the new boiler had been established, this fixed the location of the boiler drum 47 ft directly below the original turbine and condenser boiler-room floor.

It was decided to use four 12-in. schedule 80 vapor pipes of SA-280 material for the full-load flow of 1,640,000 lb per hr. This decision was based upon holding 15-psi pressure drop from the boiler drum through the double-disk stop and control valves to the turbine bowl. These pipes also had to be of sufficient length to take care of a vertical temperature expansion of 4 in. with stresses within code limits.

The turbine, generator, and condensers were rebuilt, rewound, and retubed, respectively, and placed in their original positions on the turbine-room floor.

The gravity mercury-return system, which carries the condensed mercury back to the boiler, was designed to have as a part of it a new type sealed sump. This sump, located 9 ft below the turbine-room floor, removes large foreign matter by flotation in a low-velocity section. In addition, by producing a better vacuum in the sump than that in the condenser boiler, a portion of the cascading mercury in the sump is flashed into vapor. This vapor passes through a short connection from the top of the sump to a cooler where it is condensed and run into the system through a trap. By means of this vapor carrier, the light magnesium-oxide dust, which is the only oxide residue in a chemically treated mercury system, is taken out of the returning mercury continuously and deposited in the cooler. The residue formation in Hartford is extremely small because of the all-welded mercury system, bellows-sealed valves, and leakproof turbine-shaft seal. The total air leakage of less than 1 cu ft per hr into the 3000-cu-ft operating vacuum space causes a metallic-magnesium loss in the treated boiler mercury of less than $^1/_2$ lb per day.

Spiral ramps were designed to avoid shock from falling mercury in the gravity-return system. The largest of these ramps was calculated to carry the mercury down 24 ft vertically. The two elements required were to keep the mercury content in the flow circuit to a minimum and to hold the pressure drop within the limited head available. This head had been reduced by the increased boiler pressure of the new unit, which at 130 psi backs the liquid mercury 27 ft up the return line. Only a few feet are left above this to the sump outlet for additional pressure requirements for blowing the mercury safety valves and pressure drop through the return system at full load.

Other items, which were designed to a minimum size, but yet sufficiently large to meet the heat-balance requirements were (1) the water economizer, and (2) the air preheater. For the

[6] Mechanical Engineer, Electric Engineering Department, Public Service Electric and Gas Company, Newark, N. J. Mem. ASME.

[7] Construction Engineering Division, General Electric Co., Schenectady, N. Y. Jun. ASME.

economizer, the inlet water was increased 130 deg F over that used in the original unit by additional bleed-heating. A regenerative-type air heater was used instead of the tubular type used in the original installation.

Author's Closure

The modern-design fog-type mercury boilers such as the 15,000 kw Hartford Unit are in reality simple boilers offering no serious problems of design and manufacture although somewhat different procedures were necessary as compared to the present-day high-temperature steam generators. Operating problems appear to be quite similar particularly with regard to expansion and other temperature problems.

The problem of burning low-grade fuels may be somewhat more critical with the mercury units because of the higher metal temperatures encountered in the entire mercury boiler rather than in the high-temperature superheaters and their supports only.

As Mr. Weisberg mentioned in his discussion, furnace-tube wastage under certain conditions of coal or fuel-oil operation has been experienced in a greater or lesser degree at both Kearny and Hartford as has also been the case in certain of the newer high-pressure, high-temperature steam boilers and superheaters.

Corrective measures for this annoying problem are being vigorously pursued with extremely encouraging results already reported from Kearny and elsewhere. Surface coatings of fused 25-20 weld metal as well as likely silicon coatings and paints are now under test in various mercury and steam plants while various tests are in progress using additives in the fuel as corrosion preventives.

Standard design mercury-unit power plants of extremely high over-all efficiency up to 80,000 kw combined mercury-steam capacity are now available for general power applications.

At the present time, only the plants larger than 50,000 kw total mercury-steam capacity require two mercury boilers per mercury turbine although a twin-boiler combination of mercury boilers and turbine may be had if desired in all but the smallest plan sizes.

For example, the new 40,000 kw Schiller Station of the Public Service Company of New Hampshire utilizes two standard-design 7500-kw mercury-unit power plants to supply steam to one 25,000-kw steam turbine.